University of Bath

PHD

Impedance algorithm for distance protection of non-homogenous 33 kv power distribution systems

Hewett, Richard James

Award date:
1999

Awarding institution:
University of Bath

Link to publication

Alternative formats
If you require this document in an alternative format, please contact:
openaccess@bath.ac.uk

Copyright of this thesis rests with the author. Access is subject to the above licence, if given. If no licence is specified above, original content in this thesis is licensed under the terms of the Creative Commons Attribution-NonCommercial 4.0 International (CC BY-NC-ND 4.0) Licence (https://creativecommons.org/licenses/by-nc-nd/4.0/). Any third-party copyright material present remains the property of its respective owner(s) and is licensed under its existing terms.

Take down policy
If you consider content within Bath's Research Portal to be in breach of UK law, please contact: openaccess@bath.ac.uk with the details. Your claim will be investigated and, where appropriate, the item will be removed from public view as soon as possible.

Download date: 04. May. 2023

Impedance Algorithm for Distance Protection of Non-Homogenous 33kV Power Distribution Systems

Richard James Hewett

Thesis for the Degree of Doctor in Philosophy in Electrical Power System Protection

University of Bath

September 1999

UMI Number: U601863

All rights reserved

INFORMATION TO ALL USERS
The quality of this reproduction is dependent upon the quality of the copy submitted.

In the unlikely event that the author did not send a complete manuscript
and there are missing pages, these will be noted. Also, if material had to be removed,
a note will indicate the deletion.

UMI U601863
Published by ProQuest LLC 2013. Copyright in the Dissertation held by the Author.
Microform Edition © ProQuest LLC.
All rights reserved. This work is protected against
unauthorized copying under Title 17, United States Code.

ProQuest LLC
789 East Eisenhower Parkway
P.O. Box 1346
Ann Arbor, MI 48106-1346

70 14 JUL 2011
Ph.D.

Impedance Algorithm for Distance Protection of Non-Homogenous 33 kV Power Distribution Systems

Submitted by Richard James Hewett
for the degree of PhD
of the University of Bath
1999

Copyright Declaration

Attention is drawn to the fact that copyright of this thesis rests with the author. This copy of the thesis has been supplied on the condition that anyone who consults it is understood to recognise that its copyright rests with its author and that no quotation from the thesis and no information derived from it may be published without prior written consent of the author.

Restrictions of Use

This thesis may be made available for consultation within the University Library and may be photocopied or lent to other libraries for the purposes of consultation.

Synopsis

The work in this thesis proposes a novel impedance measuring algorithm suitable for application to the distance protection of power distribution composite circuits. The algorithm can be included in a microprocessor based protection relay. Composite circuits comprise cable and overhead line sections at typical voltage levels of 33kV. Environmental reasons are just one cause for the use of underground cable sections in distribution networks. Composite networks present a number of challenges to classical distance protection relays. Three of these are; high earth fault path resistance due to faults on the overhead line section, unpredictable grounding factors for cable sections, and significant shunt admittance per unit length compared with overhead lines (caused by inter-core capacitance of cable). The algorithm proposed addresses these issues and results presented indicate significant improvement over existing distance relaying techniques, when discriminating single phase to earth faults and phase faults clear of earth.

Acknowledgements

The author would like to thank the following institutions for their support during this work.

- University of Bath, School of Electronics and Electrical Engineering.
- EPSRC
- ALSTOM T&D P&C
- South Western Electricity Plc.

Further thanks are extended to the following individuals.

- Dr. Phil Moore for outstanding patience.
- Dr. Matt Chickensfield for always being right.
- Jane and Beth.
- Dr. Raj Aggarwal.
- Dr. Z. Bo.
- Mr. Geoff Weller, ALSTOM.
- Mr. Alex Wallis , SWEB plc.
- Prof. A. T. Johns.

Contents

Chapter 3 – Distance Protection

Chapter 4 – Digital Microprocessor Based Distance Protection & Distance Relay Test Harness Development

Chapter 6 – Power System Simulation

Chapter 7 – Results

Chapter 8 – Conclusion and Future Work

Tables

Figures

List of Abbreviations

Abbreviation	Meaning
UK	United Kingdom
USA	United States of America
PPS	Positive Phase Sequence
NPS	Negative Phase Sequence
ZPS	Zero Phase Sequence
HDC	Hard Drawn Copper
H	Hochstadter
M.I.N.D.	Mass Impregnated non draining
HSL	Hochstadter Single Lead
CAS	Corrugated Aluminium Sheath
CSA	Cross Sectional Area
SCL	Short Circuit Level
I.D.M.T.	Inverse definite Minimum Time
s.p.m.	Self Polarised Mho
f.c.p.m	Fully Cross Polarised Mho
DSP	Digital Signal Processing
DFT	Discrete Fourier Transform
PDE	Partial Differential Equation
SCADA	Supervisory Control and Data Acquisition
ADC	Analogue to Digital Convertor
RAM	Random Access Memory
ROM	Read Only Memory
ATP	Alternative Transient Simulation Program
CT	Current Transformer
VT	Voltage Transformer
AA	Anti Alias as in 'anti alias filters'
F77	FORTRAN 77

List of Symbols

Symbol	Meaning
R_{dc}	PPS conductor DC resistance per unit length in Ohms
R_{ac}	PPS conductor AC resistance per unit length in Ohms
ΔR	The variable value of resistance which when added to R_{dc} results in R_{ac} in Ohms
C_{01}	PPS operating capacitance per unit length in micro Farrads
I_{chg}	Charging current per unit length at nominal operating voltage in Amperes
R_1	Equivalent to R_{ac}
εr	relative permeability of cable insulation material
X_{c1}	PPS shunt capacitive reactance per unit length in Ohms
Y_{c1}	PPS shunt admittance per unit length in micromhos
$V_{ph\text{-}e}$	Voltage between phase conductor and earth in Volts
π	Pi
f	Frequency in Hz
Ω	Ohms
X_{l1}	PPS series inductive reactance per unit length in Ohms
X_{C1}	PPS shunt capacitive reactance per unit length in Ohms
R_2	NPS series resistance per unit length in Ohms
X_{l2}	NPS series inductive reactance per unit length in Ohms
X_{l0}	ZPS series inductive reactance per unit length in Ohms
R_0	ZPS series resistance per unit length in Ohms
R_s	PPS series resistance of the sheath per unit length in Ohms
X_{C0}	ZPS shunt capacitive reactance per unit length in Ohms
Y_1	PPS shunt admittance per unit length in micro mhos
Y_2	NPS shunt admittance per unit length in micro mhos
Y_0	ZPS shunt admittance per unit length in micro mhos
Rf	Earth fault path resistance in Ohms
X_R	Setting value of a reactance relay in Ohms
R_a	Arc Resistance as calculated using Van Warringtons equation in Ohms
L_{arc}	Length of arc in metres
I_{arc}	Current flowing in an arc in Amperes
Z_L	Line impedance in Ohms

Z_S	Source impedance in Ohms
$Z = Z_{L1}$	PPS line impedance in Ohms
Z_{L0}	ZPS line impedance in Ohms
Z_{S1}	PPS source impedance in Ohms
Z_{S0}	ZPS source impedance in Ohms
V_R	Voltage applied to a relay (can be line or phase as defined) in Volts
I_R	Current applied to a relay (can be line or phase as defined) in Amperes
V	Power system open circuit voltage
Z_R	Measured impedance by a distance relay in Ohms
I_N	Neutral current in Amperes
k	compensation factor applied to measured current when detecting earth faults
Z_0	ZPS impedance per unit length in Ohms per km
Z_1	PPS impedance per unit length in Ohms per km
R	Series resistance of a line in Ohms
L	Series inductance of a line in Henries
ΔT	ATP simulation time step in seconds
N	Number of samples in a discrete time input signal
f_s	Sampling frequency in Hz
V_x	Voltage calculated at distance x along a transmission line in Volts
I_x	Current calculated at distance x along a transmission line in Amperes
x	Distance along a transmission line in km
V_{Rec}	Transmission line receiving end voltage in Volts
I_{Rec}	Transmission line receiving end current in Amperes
Z_c	Line characteristic or surge impedance in Ohms
γ	Line propagation coefficient in ?????
V_{rel}	Single phase voltage at the relay point
I_{rel}	Single phase current at the relay point
ABCD	Hyperbolic line parameters single phase transmission line
$[A_x]$	3x3 matrix of hyperbolic line parameters replacing A for a three phase line length x
$[B_x]$	3x3 matrix of hyperbolic line parameters replacing B for a three phase line length x
$[C_x]$	3x3 matrix of hyperbolic line parameters replacing C for a three phase line length x
$[D_x]$	3x3 matrix of hyperbolic line parameters replacing D for a three phase line length x
[S]	Karrenbauer's modal transformation matrix
$[Z_c]$	Modal characteristic impedance 3x3 matrix

$[Y_c]$	Modal propagation coefficient 3x3 matrix
$_{1,2,3}$	Subscripts denoting modal quantities
V_{arel}	'a' phase complex voltage at relay point
V_{brel}	'b' phase complex voltage at relay point
V_{crel}	'c' phase complex voltage at relay point
I_{arel}	'a' phase complex current at relay point
I_{brel}	'b' phase complex current at relay point
I_{crel}	'c' phase complex current at relay point
V_{arp}	'a' phase complex voltage at reach point
V_{brp}	'b' phase complex voltage at reach point
V_{crp}	'c' phase complex voltage at reach point
I_{arp}	'a' phase complex current at reach point
I_{brp}	'b' phase complex current at reach point
I_{crp}	'c' phase complex current at reach point
L_{en}	Total length of a composite protected feeder in km
Z_{arp}	Reach point 'a' phase impedance in Ohms
R_{arp}	Reach point 'a' phase real component of Z_{arp} in Ohms
jX_{arp}	Reach point 'a' phase imaginary component of Z_{arp} in Ohms
SCL	Short circuit level in MVA
Z_{arel}	Relay point 'a' phase impedance in Ohms
R_{arel}	Relay point 'a' phase real component of Z_{arel} in Ohms
jX_{arel}	Reach point 'a' phase imaginary component of Z_{arel} in Ohms
X_{th}	Threshold reactance setting for earth fault element quadrilateral in Ohms
X_{thp}	Threshold reactance setting for phase fault element quadrilateral in Ohms
R_b	Earth fault quadrilateral resistive blinder setting in Ohms
R_{bp}	Phase fault quadrilateral resistive blinder setting in Ohms
Y_{al}	Pre fault 'a' phase remote end admittance seen from zone 1 reach point
Y_{bcl}	Pre fault 'b-c' phase remote end admittance seen from zone 1 reach point
I'_{arp}	Pre fault 'a' phase current at the zone 1 reach point in Amperes
I'_{brp}	Pre fault 'b' phase current at the zone 1 reach point in Amperes
I'_{crp}	Pre fault 'c' phase current at the zone 1 reach point in Amperes
V'_{arp}	Pre fault 'a' phase voltage at the zone 1 reach point in Volts
V'_{brp}	Pre fault 'b' phase voltage at the zone 1 reach point in Volts
V'_{crp}	Pre fault 'c' phase voltage at the zone 1 reach point in Volts
Y_{af}	a-earth fault admittance

Y_{bcf}	'b-c' fault admittance
Z_{af}	Post fault 'a' phase fault impedance in Ohms
R_{af}	Post fault 'a' phase fault impedance real component in Ohms
X_{af}	Post fault 'a' phase fault impedance imaginary component in Ohms
Z_{bcf}	Post fault 'b-c' fault impedance in Ohms
R_{bcf}	Post fault 'b-c' fault impedance real component in Ohms
X_{bcf}	Post fault 'b-c' fault impedance imaginary component in Ohms
Z_{bcrel}	'b-c' impedance at relay point in Ohms
R_{bcrel}	'b-c' impedance real component in Ohms
X_{bcrel}	'b-c' impedance imaginary component in Ohms
$[E_S]$	matrix of source three phase voltages at busbar S
$[E_R]$	matrix of source three phase voltages at busbar R
$[Z_S]$	Source impedance matrix at end S
$[Z_R]$	Source impedance matrix at end R
$[V_{sp}]$	Matrix of pre-fault three phase voltage at end S
$[I_{sp}]$	Matrix of pre-fault three phase current at end R
$[V_{FF}]$	Matrix of three phase voltage at an a-earth fault location distance l from busbar S
$[I_{FF}]$	Matrix of three phase current at an a-earth fault location distance l from busbar S
$[dV_s]$	Matrix of post fault three phase voltage at end S
$[dI_s]$	Matrix of post fault three phase current at end R
$[Z_{FA}]$	a-earth fault path impedance matrix
$[V_s]$	Matrix of three phase voltage at end S for resolved network subject to a-earth fault
$[I_s]$	Matrix of three phase current at end R for resolved network subject to a-earth fault

Chapter 1

Introduction

1.1 Power System Protection

Power systems must afford a level of protection against the occurrence of faults in order to maintain safety, security, system stability and minimise primary and secondary system damage. The degree to which a network may be protected is based on a consideration of the risk of damage or instability, consumer security requirements, safety and cost.

Any protection scheme first has to detect the presence of a fault and then act to disconnect only the faulted section of a network. This is generally achieved by measuring system voltage, current, phase angle and time. Any of these quantities alone or combined may be compared with a predetermined value and an operate or restrain decision made. A suitable point for disconnection is then found via a process of discrimination.

The general components of a protective scheme are; relay, current and voltage transformers, circuit breakers, tripping and auxiliary supplies, and a means of communication.

There are many varieties of protection scheme, but they may generally be divided into one of two categories, namely non-unit and unit protection.

1.1.1 Non -unit Protection

Distance, inverse definite minimum time overcurrent (IDMT) and the fuse are all forms of non-unit protection, relying on measurements made at the relaying point, and requiring no form of communication channel. They provide inherent backup protection for faults outside the protected zone.

Non-unit, is one of the most widely used protection schemes in the modern power system, with unit protection used where major loads with high security requirements exist. For the bulk of the United Kingdom (UK) 11kV system basic overcurrent and earth fault protection (IDMT) is utilised, with distance protection and overcurrent used on the 33kV system. Auto-reclose and sensitive earth fault protection will generally be applied to overhead circuits, in addition to that described above. High voltage HRC fuses are

generally found protecting ground mounted transformers from 100kVA to 1MVA, while overhead drop out fuses may be used to protect overhead spur lines and pole mounted transformers on main line poles (11kV).

1.1.2 Unit Protection

Unit protection such as current differential, phase comparison and several types of directional comparison, rely on measurements taken at the boundaries of the protected zone. Advantages are inherent restrain for faults outside the protected zone, and instantaneous operation. Disadvantages are no inherent back up facility for out of zone faults, and an increase in cost due to the requirement for several sets of matched transducers and a communication channel.

1.2 Distance Protection

In 1947 Lewis and Tippett [28] wrote on the fundamentals of applying distance relays to three phase systems. Their work stated that conventional impedance and reactance relays applied to three phase systems are subject to errors other than those caused by fault impedance. For three phase systems factors such as fault type, load and system configuration all contribute to the accuracy of impedance measurement. Reactive relays which may be assumed to be unaffected by resistive faults are subject to error from an apparent reactive component in the measured impedance at one end of a protected circuit which is fed from both ends. To overcome these inaccuracies the authors proposed that for relays protecting against phase faults delta current transformer connections should be used. For those relays protecting against earth faults compensation of measured voltage or current should be made to overcome inaccuracy. Once employed the limitation of application of distance protection is related to fault impedance with respect to the length of the protected circuit - impedance and reactance type relays being affected to different extents.

Since this definitive work, many authors have published results of research in the area of distance protection applied to multi phase power systems [11 - 32]. Directed towards transmission system applications (tower lines operating at >275kV) distance relaying principles have been developed and applied to power systems the world over. Distance relaying offers inherent back up for down stream faults while reducing the need for remote end relays, communications systems and matched current transformers such as required by line differential protection schemes.

Moore[32] models the protected system as a lumped series resistance and inductance; the effect of line shunt capacitance being ignored. A time spaced solution and difference

equation technique are used to solve the differential equation for the simple transmission line equation and thus estimate resistance R and inductance L of the protected circuit. A quadrilateral tripping characteristic is employed to allow the calculated values of R and L to be used to assess an in or out of zone fault and cope with the affects of fault path resistance. Simulation results presented by the author indicate that for a short transmission line (100km), algorithm operation times of the order of 8ms offer the possibility of sub-cycle fault clearance times. This time domain technique required additional digital filtering techniques to remove the effects of travelling wave noise, exponential offsets, harmonics and extraneous noise. Suitability for application to long transmission lines (>250km) or cable sections remains undefined due to the lack of consideration of shunt capacitance in the protected circuit model. This latter quantity is significant for cable sections and long transmission lines.

1.3 Composite Distribution Networks

In transmission systems cables are infrequently used due to the physical size of the conductor insulation needed at the high transmission voltages and a typical ten fold increase in cost over the equivalent overhead line construction.

In distribution systems (<132kV) cable is used more frequently. Insulation requirements are more practically achievable and jointing techniques are easier. Historically, there has been substantial use made of multi core underground cables to distribute power within urban areas. Recent environmental pressures have resulted in the use of more expensive underground cable networks, where previously an overhead line construction may have been selected (crossing national parks for example). Thus, there exists within distribution power networks, sections comprising of both underground cable and overhead line - composite feeders.

Cables vary in construction at the different voltage levels but all possess significant shunt capacitance. In the general case of a distribution cable oil impregnated paper is used as insulation between each phase conductor and a zero potential sheath. Consequently such cables exhibit significant operating capacitance per unit length. This capacitance varies with frequency. At fundamental frequency and at nominal operating voltage a cable will exhibit significant charging current per unit length. This charging current will increase as the operating voltage increases.

1.4 Distance Protection Applied to Composite Systems

Distance protection is being applied to composite networks for the economic reasons stated previously and especially as modern distribution switchgear increasingly includes system transducers such as measurement and protection transformers, thus making viable the application of distance protection relays. Such relays require the availability of both current and voltage transformers at the relaying point.

In 1976 Elkateb[12] investigated the performance of distance protection applied to underground cables and composite systems. The work focused on the application of a distance comparator type relay to both 275kV and 70kV cables either alone or mixed with overhead lines and subject to zero resistance earth faults. In conclusion the author found that in most cases a self polarised mho (s.p.m.) characteristic produced the best operating times and accuracy. A fully crosspolarised mho (f.c.p.m.) characteristic has limitations when applied to systems with lower short circuit levels – typical of distribution systems. When feeders are composite and comprise equal lengths of cable and line then an s.p.m should be applied from the cable end while a f.c.p.m characteristic should be used from the line end. Regardless of the characteristic chosen it should be provided with vectorial earth fault compensation factors. This latter observation is based on the fact that the zero sequence impedance angle of a cable is very different from that of an equivalent overhead line. Thus, previously used scalar compensation factors became subject to error when applied to cable circuits. For the most accurate setting and application of distance relays the zero sequence impedance should be measured during commissioning. Any doubts in accuracy should be eliminated by use of permissive blocking schemes, assuming a suitable communications channel is available.

1.6 New Distance Algorithm for Application to Composite Distribution Feeders

The work described in this thesis details the research and development of a novel distance protection algorithm for use in a microprocessor based relay that is suitable for application to composite distribution feeders.

The algorithm uses a distributed parameter long transmission line model to represent the protected composite system. It considers the shunt capacitance of cable sections and represents its non-homogenous nature; namely the series connection of cable and line sections of varying types and lengths. This is in contrast to previous works such as

Moore[32], which use a lumped parameter model suitable only for application to short overhead lines.

The distributed parameters of a transmission line vary with frequency. By considering the line to be ideally transposed and using quoted series and shunt parameters per unit length for specific cable and line sections, hyperbolic parameters applicable to the fundamental operating frequency and representing the distributed nature of the line can be calculated. This is the general solution described by Wedepohl [34].

At the sending end of a composite feeder, measured discrete time sampled voltage and current signals are transformed into the frequency domain by use of the discrete Fourier transform. The method creates voltage and current vectors rotating at the fundamental power system frequency reducing signal content at all other frequencies.

The complex values of voltage and current are combined mathematically with the hyperbolic line parameters to enable the calculation of voltage and current at a specific distance, X along the feeder length. By choosing X to be eighty percent of feeder length it becomes possible to calculate the voltage and current and thus impedance at the reach point of a classical distance zone one. No earth fault compensation is required for the measured or calculated voltage and current signals as Elkateb [12] found essential.

A novel quadrilateral characteristic is proposed which utilises the voltage and current measured at the relaying point and those voltage and current vectors calculated to be at the reach point. In this manner a zero Ohm fault can be determined as being in or out of zone one with great accuracy.

Single phase to earth faults on overhead line sections can contain significant fault path resistance. By estimating the remote end source impedance and through the use of a novel and simple pre fault load estimation technique the algorithm reduces substantially the inaccuracies in impedance calculation and thus fault discrimination caused by the presence of fault path resistance as first recognised by Lewis and Tippett[28].

Results of both steady state and transient simulations for 33kV composite networks subject to high resistance single phase to earth faults indicate algorithm operating times of between 30 and 40 msecs to be possible.

1.7 About the Structure of This Thesis

Chapter 2 describes power systems generally in terms of their construction and interconnection. Power systems are large interconnected networks, spread over wide areas that have to operate within stringent parameters. When designing protection relays, a good

appreciation of system design and operation combined with knowledge of likely system behavior occurring during power system faults is essential. Composite distribution networks in the context of this work are defined prior to a discourse on some of the principle physical and electrical features of power distribution cables. Consideration is given to a number of phenomena recognised as likely to influence protection relay performance. These include; system load flow considerations when supplied from two separate sources, harmonic distortion both at high and low frequencies, primary system fault types, their severity and typical clearance times.

Distance relays differ from other forms of protection relay with operation based on the ratio of applied voltage and current. When a fault occurs on a circuit the ratio of voltage to current at a fixed measurement point will depend on the impedance or distance between the relaying point and the point of fault. This ratio will be constant for any particular fault position. Chapter 3 explains the fundamental principles of power system protection, using distance schemes. Beginning with the early electromechanical relays, the basic plain impedance characteristic, reactance and self-polarised mho characteristics are investigated. Characteristics have evolved such that a number of different ones are available. Problems encountered when applying distance protection to certain types of distribution feeder are identified, through an analysis of existing U.K. distribution Company techniques and relaying principles. Previously identified inaccuracies of distance protection schemes, designed for overhead line homogeneous application but protecting composite or mixed feeder types, are detailed.

This work concerns the research and development of a new impedance measuring algorithm suitable for inclusion in a microprocessor based relaying platform. Chapter 4 describes the benefits of these relaying platforms and typical hardware layout. In order to test the performance of the algorithm developed in this work a software distance relay test harness must be built. The harness should reflect as near as possible the true nature of the distance relaying platform construction, simulating such things as primary system voltage and current through to the emission of a trip signal. The new protection algorithm developed in this thesis has been tested using two different power system software simulations. Chapter 4 describes these.

Chapter 5 describes the new algorithm suitable for measuring the impedance of a composite power distribution circuit and it's use within a software prototype distance protection relay. The method inherently accounts for feeder series and shunt parameters. Applying this circuit representation to zone one distance protection using an adaptive

quadrilateral tripping characteristic, an earth fault can be discriminated as in or out of zone. The effects of fault path resistance on discrimination accuracy are discussed.

Investigation in this work centres on the discrimination of a-e faults of varying fault path resistance occurring at various locations along a composite power distribution feeder. The new impedance relaying algorithm requires testing using simulated discrete time sampled three phase voltage and current signals. This approach to algorithm design and development is standard within relay development and precursors any real time simulation studies or practical field trials.

This work incorporates two different approaches to modelling composite 33kV power systems. One enables the assessment of reach boundary accuracy for in zone single phase to earth faults. This routine is described in Chapter 6. In addition transient simulation studies have been conducted. In this case the existing electromagnetic transient simulation package ATP has been utilised to investigate the operating time of the new algorithm for discriminating both phase and ground faults.

Chapter 7 presents and discusses the results obtained from the simulation studies and Chapter 8 seeks to conclude the work and outline scope for future work.

Chapter 2

Distribution Power Systems

2.1 Introduction

Power systems are large interconnected networks, spread over wide areas that have to operate within stringent parameters. When designing protection relays, a good appreciation of system design and operation combined with knowledge of likely system behaviour occurring during power system faults is essential.

This chapter describes in general the distribution power systems considered in this work, in terms of their construction, design and interconnection. The systems are based on the United Kingdom network and can be considered typical. Composite distribution networks in the context of this work are defined prior to a discourse on some of the principle physical and electrical features of power distribution cables.

Power systems are far from ideal and consideration is given to a number of phenomena recognised as likely to influence protection relay performance. These include; system load flow considerations when supplied from two separate sources, harmonic distortion both at high and low frequencies, primary system fault types, their severity and typical clearance times.

2.2 Power Distribution Networks

Power systems generally consist of two distinct networks, namely transmission and distribution. Generated power is transferred over long distances, to major areas of demand, by the transmission network. The distribution network is then utilised for localised power delivery. In the UK the typical operating voltage for transmission is either 275kV or 400kV. Distribution networks operate at voltages of typically 132kV, 66kV, 33kV and 11kV.

The transmission network is usually of overhead construction with conductors strung between steel pylons. In some circumstances underground cables may be used, though due to an average ten-fold increase in cost per meter, this is a relatively rare occurrence.

Distribution systems operate at lower voltage levels, where electrical stresses and insulation requirements are reduced and the use of cable becomes physically and economically viable. At 132kV, overhead construction is usually preferred, as cable costs

can still be high. However, at 33kV and 11kV, cables are common. This is because at these voltage levels the network has often penetrated urban or industrial areas, where aerial construction becomes difficult or unsightly.

It is common to find underground cables used for the first section of a distribution circuit, allowing it to exit a sub station easily or discretely. The circuit may then revert to aerial forms of construction when clear of densely populated areas. Historically, some cities' main bulk power supply points, have been interconnected via underground cable links through the city centre, to allow for predicted demand increases and to increase supply security.

Power distribution feeders can comprise only underground cable, as well as constituting overhead and underground construction i.e. the composite feeder. In the centre of U.K. urban areas, circuits are likely to be wholly underground.

This may not be the case in countries such as the USA, parts of Europe or developing nations. Here, usually for reasons of cost or less stringent legislation, overhead construction will be favoured at all voltage levels regardless of ergonomics or ease of operation. However, cable circuits may still be used for reasons of safety or overcoming engineering impracticalities.

2.3 Typical Network Constructions

This section describes the typical construction of power distribution feeders studied in this work and investigates some of the characteristics and types of cable commonly used.

2.3.1 Overhead Construction

There are many types of overhead construction, however, a typical one has been chosen. In this work 33kV systems have been studied and modelled and overhead circuits considered are of the wood pole flat construction type, shown in figure 2.1.

2.3.2 Underground Construction

The underground cable considered is the 'H' type 3-core variety depicted in figure 2.2. 'H' refers to the cable inventor Martin Hochstadter, a German scientist who first patented this type of cable in 1914. It can be considered a good general consideration for modelling a typical 33kV distribution system because of the reasons explained in sections 2.4 and 2.5.

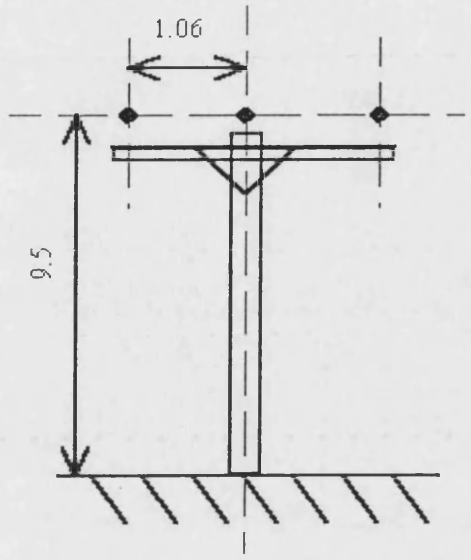

Conductor Data [@ 50Hz , nominal operating voltage]	
Conductor CSA & Type.	0.2 sq.in. hard drawn Cu
DC resistance Ω/km@20°C	0.1350
Reactance Ω/km@20°C	0.3478
Impedance Ω/km@20°C	0.3733
Note: all values PPS and 1 conductor per phase.	

Figure 2.1 : 33kV wood pole overhead line. Physical construction and electrical parameters. (all dimensions in meters).

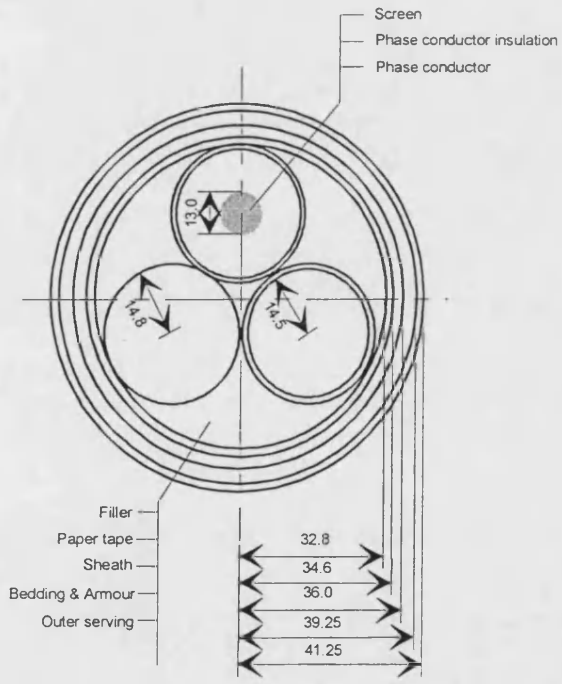

'H' type 3core cable data [@ 50Hz , nominal operating voltage]	
Conductor CSA & type	0.3 sq. in. Hard drawn Cu
DC resistance Ω/km@20°C	0.09195
AC resistance Ω/km@20°C	0.09278
Reactance Ω/km@20°C	0.09910
Impedance Ω/km@20°C	0.13575
Equivalent star capacitance micro Farads/km	0.405
Charging Current Amps/km	2.43

Figure 2.2 : 33kV 'H' 3c cable. Physical construction and parameters. (all dimensions in mm)

2.4 Power Distribution Cables

All power cables consist of three basic components, namely;

- Conducting Core, usually copper or aluminium

- Insulation, usually oil impregnated paper or Polymeric Materials
- External protective layer or sheath. This layer acts as mechanical protection, all or part of the earth return path and prevents the ingress of moisture.

Cables can be either 'solid' or pressurised in construction. Within 'solid' cables insulation pressure may rise above and below atmospheric pressure. Alternatively through the use of oil and gas pressurisation systems, pressures in excess of atmospheric can be maintained within the cable insulation. This has the advantage of preventing the formation of voids in insulation.

In the UK it is common to encounter pressurised cables at transmission voltage levels and the higher distribution voltage of 132kV, though some 33kV pressurised cables can be occasionally found. More commonly 'solid' type cables are found in use at 33kV and 11kV voltage levels where electrical stresses imposed insulation are less compared with those prevalent at higher voltages. The most common insulation material is Mass Impregnated Non Draining (M.I.N.D.), in which paper tapes are pre-impregnated with an oil or resin compound and form an inherently non-draining insulation post lapping.

There are two varieties of solid cable, namely 'Belted' and 'Screened'. Belted cables are used up to 11kV , but it is necessary to screen cores with paper foil or metallic tapes at higher voltages, to reduce the tangential stresses which inevitably arise in belted construction.

2.4.1 Belted Cable

A typical belted cable is 3 core, 95 mm2 copper or aluminium conductor, Corrugated Aluminium Sheathed (CAS).

2.4.2 Screened Cable

Typical screened cables are found at voltage levels of 33kV and above. A typical cable is the 3 core, 0.3 square inch copper conductor, 'H' type, screened variety, shown in figure 2.2.

In this cable the metallic-conducting layer of the screen may consist of perforated aluminium foil or may be made of thin copper tape applied with a narrow gap between turns. The screen is conducting and remains in intimate contact with the core insulation. The three cores are laid up with paper fillers in the usual way and overall is wrapped a copper woven fabric tape to ensure electrical contact between the metallic screen and the

outer sheath of the finished cable. The screens and each of the three outer core surfaces are therefore maintained at earth potential.

An additional variety of 33kV cable is 'HSL'. Similar to the 'H' type cable in that each of its cores are screened to reduce electrical stresses it differs in that each core is enclosed within it's own individual lead alloy sheath. These in turn are enclosed within a common sheath or encapsulating layer of steel wired armour.

Single core screened 33kV cables may also be found in service. To form a three phase system, three such cables are required. They may be laid in separate trenches, or in a single trench side by side or in a trefoil formation.

2.4.3 Cable Electrical Parameters

A typical 33kV cable will possess resistance, inductance, capacitance and conductance.

Resistance of each core is generally the same though sheath resistance is liable to be different (as it is made of alloy or lead). Due to the fact that voltages and currents are alternating quantities and vary over time, both a DC and AC value of resistance are relevant. DC resistance (R_{dc}) will vary with the temperature of the cable and the ambient. Losses caused by skin effects, eddy currents in both the metal sheath and in the armour coupled with magnetic reversal in the armour alone result in an AC resistance (Rac), which is greater than R_{dc}, where

$$R_{ac} = R_{dc} + \Delta R \qquad \Omega/km$$

Equation 2.1

The cable will further exhibit a value of inductance and capacitance per unit length. Conductance is normally considered negligible. Formulas for calculating these parameters from first principles are well known and are not repeated here.

Manufacturers publish series and shunt positive phase sequence per unit length values for R_{dc}, R_{ac}, reactance X_{l1}, equivalent star or operating capacitance C_{01} , and charging current I_{chg} . In this work reference to positive phase sequence (PPS) series resistance per unit length of a phase conductor, R_1, means the PPS AC value of resistance per unit length, R_{ac}. In considering overhead distribution lines of short to medium length shunt admittance is often considered negligible.

Cables possess significant shunt admittance per unit length when compared with overhead lines. This is due in part to the fact that in cables, distances between conductors

are very much less and the relative permitivity of insulation greater - 3 to 5 as opposed to 1 for air.

The operating capacitance of a particular cable depends on its structure and the relative permitivity (εr) of its insulation.

2.4.3.1 Belted Cable Operating Capacitance

For a 'belted' cable the PPS operating capacitance comprises capacitance between cores as well as from each core to earth.

2.4.3.2 Screened Multicore Cable Operating Capacitance

For the screened cable there exists only capacitance between each phase conductor and its earthed screen. All screens are at the same potential and so it is acceptable to use the manufacturers quoted value of PPS operating capacitance C_{01} or charging current I_{chg} to calculate PPS shunt capacitive reactance per unit length X_{c1}, and thus PPS shunt admittance per unit length Y_{c1}.

As an example consider the screened cable of figure 2.2. For this cable the manufacturer quotes C_{01} and I_{chg} as 0.405 μF and 2.43 Amperes per km per phase respectively.

The PPS shunt capacitive reactance X_{c1} can be calculated in two ways depending on the parameter used i.e.

$$X_{c1} = {}^{V_{ph-e}}\!/_{I_{chg}} \quad \Omega/\text{km/phase}$$

Equation 2.2

$$X_{c1} = {}^{1}\!/_{2 \cdot \Pi \cdot f \cdot \Omega/\text{km/phase}} \quad \Omega/\text{km/phase}$$

Equation 2.3

Selecting equation 2.3 and noting a fundamental power system frequency of 50Hz,

$$X_{c1} = 7859.50 \ \Omega/\text{km/phase}$$

Equation 2.4

and therefore....

$$Y_{c1} = 1/X_{c1} = 127.23 \ \mu\text{Mhos/km/phase}$$

Equation 2.5

This calculation is valid for the case of screened cables and overhead three phase lines.

2.5 Cables Selected for Simulation Studies

In the UK either the 'HSL' or the 'H' types have been the most commonly used. It is true that the 'HSL' cable avoids some of the magnetic losses, which would occur if each individual core were separately armoured with magnetic materials. This is true in the case of three individual single phase cables in trefoil, and has been considered in the past to be easier to terminate and joint than the 'H' type. However, with the advent of modern jointing and terminating techniques i.e. new plastic heat shrink termination's and cable joint kits this advantage has been negated. For use in hilly country where there may be a considerable head of oil in the cable, the 'HSL' type cable may be considered advantageous with it's smaller sheath diameters and absence of worming filled with oil located under the lead sheaths. In contrast 'H' type cable with its smaller overall diameter is often preferred due to its greater flexibility and smaller bending radius. However, there is little to chose between the technical performance of the two cables and choice has usually revolved around individual preference or historical electrical distribution company policy.

A recent survey of 33 kV distribution networks conducted in the South of England has shown that the 'H' type cable is the most popular. Results are summarised in table 2.1. The survey was conducted by South Western Electricity Plc (SWEB), and shows that in it's southern Region (County of Devonshire) 33.0 % of the distribution network is located underground, of which 58% is 'H' type cable. Communications with other electricity companies throughout the UK have confirmed 'H' type as a commonly used cable also.

Circuit Type	Length in metres
Overhead Line 3 phase	848,710
'H' Type Cable3 core	241,451
'HSL' Type Cable 3core	73,553
Single Core	4,281
XLPE Insulated 3core	264
Gas Cooled Cable 3 core	61,256
Oil Cooled Cable 3 core	34,995

Table 2.1 : Circuit Types in Use in SWEB Plc Devonshire, Operational Area.

In regard of these findings and in view of the technical considerations presented previously this work concentrates on modelling systems containing 'H' type cable with

round conductors as described in previous section 2.3.2.

2.6 Negative and Zero Sequence Parameters of 'H' Type Screened Cable

It has previously been shown that the positive sequence values of R_1, X_{l1} and X_{c1} can all be obtained from manufacturers data sheets. Mortlock & Davies[1], King & Halfter[2] and Lacky[3] show between them that, using a knowledge of these positive (PPS) , negative (NPS) and zero (ZPS) sequence series and shunt parameters can be estimated for the 'H' type screened 33kV cable in the following manner.

2.6.1 Sequence Series Parameters

For screened cables.

$$R_1 = R_2$$

Equation 2.6

$$X_{l1} = X_{l2}$$

Equation 2.7

ZPS impedance will be dependent on system earthing & the nature of the earth return path and may be accurately assessed through measurement once a system has been installed [4]. However, an approximation[2] would be that for screened three core cables,

$$X_{l0} / X_{l1} = 3.5$$

Equation 2.8

Zero sequence resistance R_0 ,assuming an earth return path through the sheath, can be approximated as,

$$R_0 = R_1 + 3 \cdot R_s \approx 3.5 \cdot R_1$$

Equation 2.9

where R_s is the PPS series resistance of the sheath per unit length.

2.6.2 Sequence Shunt Parameters

For a screened three core cable[2],

$$Y_1 = Y_2 = Y_o$$

Equation 2.10

Therefore,

$$X_{c0} = X_{c1}$$

Equation 2.11

2.7 Distribution Network Design and Interconnection

Power distribution systems in the UK are designed and constructed to meet specific standards as described in the Electricity Supply Industry Regulations and numerous national engineering recommendations, specifications and practices. These standards dictate not only the type of construction and materials to be used but also the parameters inside which the network should operate. Power supply frequency, voltage level, quality and security are all subject to strict specification or maximum and minimum. Of further consideration is the criteria of cost, power demand trends, efficiency and ease of system operation and maintenance. The network must also conform to relevant environmental policy.

Circuits are constructed, interconnected and operated in several ways. It is important to appreciate these different connections in order to understand the effects of differing network topologies on protection schemes.

There are three types of network design; radial, ring, and inter-connected systems.

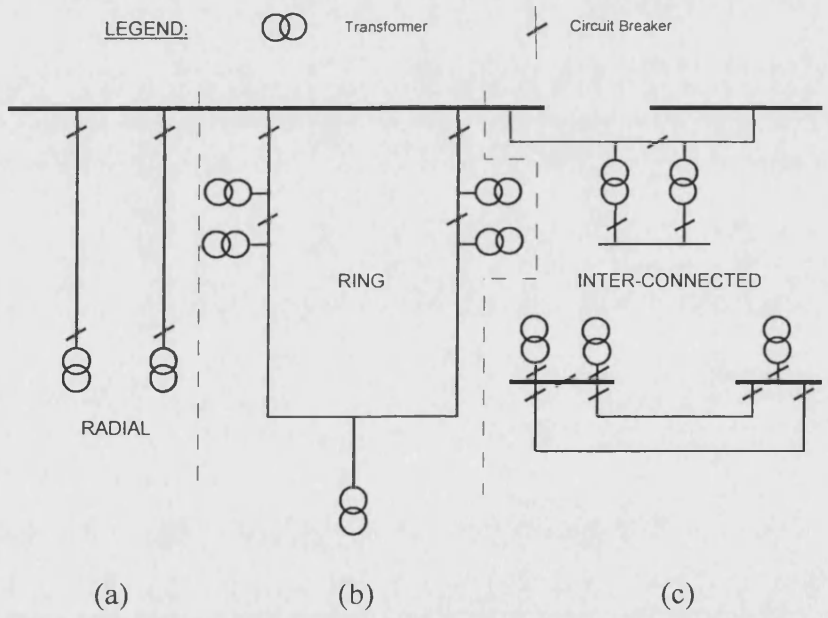

Figure 2.3 : (a)Radial , (b)Ring and (c) Inter-connected Power distribution networks.

2.7.1 Radial

Radial systems, figure 2.3a, are used at the higher voltage levels to supply large loads, often in urban or heavily populated areas, and consist of at least two circuits to provide security of supply. Also, this design is used in single feeder form, at lower voltages and load levels where security is not so important or justifiable - small 11kV customers or

the 400/230V low voltage network.

2.7.2 Ring

Ring systems, figure 2.3b, are generally used at higher voltages (33kV or 11kV), to provide a firm supply and cater for moderate loads. In the case of the UK 11kV system, it is run as a ring system but with a normally open point approximately half way around the circuit. This, increases supply security and affords a simple means of isolation and switching when locating faults.

2.7.3 Inter-connected

Inter-connected systems, figure 2.3c, offer the advantage of supplying a substation from two different bulk supply sources. At lower voltages there may be a normally open point at the substation allowing the load to be transferred from one source to the other. This is often used in rural locations and offers a higher level of security than a radial system. At higher voltage levels it is usual to find both sources supplying the substation in parallel, thus providing mutual support at times of transformer outages. Though sometimes not possible for reasons of excessive fault levels arising from the parallel connection of two bulk supply points, this practice has escalated in recent years as regional electricity distributors seek to reinforce systems at minimal engineering cost.

2.8 Connection of Composite Distribution Networks Simulated in This Work

Evidently, the considerations of circuit connection given above should have an influence on the type of circuit used for simulation studies. It would appear likely for a 33kV distribution feeder to be single end fed i.e. feeding from a source to remote end load. The load may well be a large industrial consumer or a 33kV to 11kV distribution substation feeding a populated or industrialised area. Feeders subject to supply from both ends could arise mainly as a result of parallel connection of bulk supply point and other principle 33kV substations. Therefore, this work tests the performance of the proposed protection algorithm's using both single and double end fed systems.

2.9 Pre-Fault Load Transfer Considerations

Whether a system is operating abnormally or is of an interconnected nature there is the possibility that a fault occurring on the network could be supplied by current flowing from both ends of the feeder.

Consider the simplified circuit shown in figure 2.4. A section of network is shown

for simplicity, the power system having been reduced to a two machine system [4]. The earth fault is one typical to an overhead line and constitutes a value of resistance, Rf. The source Eg is assumed to lead the source Eh due to pre fault load transfer. Under fault conditions the fault current, If , is the vector sum of the two line currents, Ig and Ih, in turn due to the applied potential of sources Eg and Eh. If is not in phase with either Ig or Ih and the fault resistance Rf appears as a complex

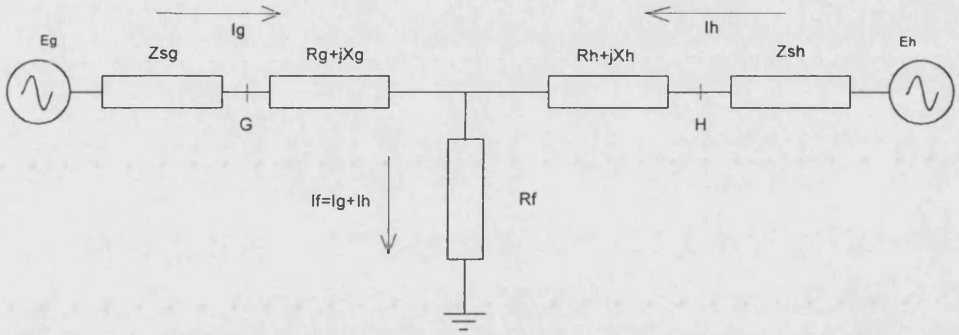

Figure 2.4 : Simplified Power System Showing Fault Current as the Resultant of Ig and Ih.[4]

component to both distance relays installed at G and H. As a consequence of this a reactance type relay (examined in chapter 3) installed at G, would see less than the actual line reactance to fault point and over reach. Alternatively, the same type of relay installed at H, where the source angle is lagging, will under-reach. This principle is shown clearly for a reactance relay at G, in figure 2.5.

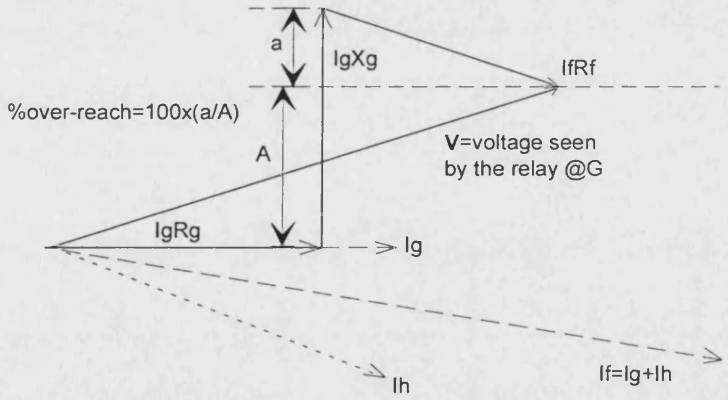

Figure 2.5 Vector Diagram Sketch Showing Effect of Fault Resistance on Reactance Relay at G.

The reactance relay has generally been superseded by relays utilising the quadrilateral type characteristic, which comprises a reactance line with directional and

resistive reach control characteristics. Quite often the reactance line is allowed to swing about its respective zonal reach point to cater for specific pre-fault load transfer conditions.

2.10 Embedded Generation

Section 2.9 highlighted the problems posed by pre fault load flows and possible causes of such loading conditions. Another potential source of dual current feed to a faulted section of the distribution network is when the system contains embedded generation.

Since the UK electricity industry privatisation in 1990 and under the provisions of the 1983 Energy Act and the 1989 Electricity act, there has been an increase in the amount of embedded generation connected to distribution systems. Often used by large power consumers for peak load lopping, emergency backup supply, or to utilise waste products excess capacity can be exported to the local distribution system. The increase in efficiency offered by combined cycle turbines and the savings afforded from the application of such secondary features as heat recovery units (combined heat and power), means the number of privately owned embedded generators is set to increase.

The connection of this type of plant to the distribution system presents many problems to the power distributor. However, in satisfying distribution company protection policies the star point of an embedded generator will not normally be connected to earth meaning there will be little contribution to any earth fault current for a fault occurring on the external distribution network. Should a phase fault or even an earth fault for the case of a generator with star point connected to earth occur, then suitable protection is applied to the generator such that disconnection can occur.

2.11 Distance Relays and Power Swings

Power swings are the oscillations of synchronous machines with respect to other synchronous machines else where on the system. They can be instigated by switching, load changes, or by the occurrence of faults. A swing does not necessarily mean the system is unstable.

The effect of a swing will manifest itself in a widening deviation in the system bus bar voltage angles, and an apparent impedance is presented to distance relays which according to the severity of the swing will encroach further and further into the distance relay operating characteristic. If the voltages at either end of the protected feeder were completely in anti-phase then it would appear to distance protection at either end to be a

three phase fault at the middle of the section[4].

A swing can encroach a distance protection relay characteristic operating area very rapidly or comparatively slowly. If the swing is slow a mal-operation is avoided by the use of timers to prevent tripping if the impedance fails to enter zone 2 tripping area having entered zone 3 tripping area, after a certain time has elapsed. In the case of severe system swings such as following a fault, blinder characteristics are used as the time delay theory is no longer valid because the characteristic zones will be penetrated by the impedance locus at approximately the same speed as for a fault. This sort of scheme is adequate to protect against feeder cascade tripping during severe disturbances on the system. However, it should be noted that the relay can not protect against faults on the feeder section while power swing blocking is in progress.

2.12 System Unbalance and Harmonics

2.12.1 Harmonics

Harmonic content of the power system waveforms was first recognised in the early 1900's. In the last ten to fifteen years particularly there has been an increase in the number of non-linear loads connected to the distribution system. These loads cause distortion in both the voltage and the current waveforms. Thyristors and power transistors, are common causes of harmonic distortion. Iron core devices such as solid-state converters, adjustable speed drive motors, input stages of power supplies and induction and arc furnaces - which are operating more towards their non-linear regions - are responsible for the harmonic distortion observed in current waveforms[5,6]. Consequently, the voltage and current waveforms present on today's power systems are quite often far from sinusoidal in nature.

It has been observed [6] that some solid state relays are prone to errors as a result of harmonics in the input waveforms. Typically delays in trip times are observed. Considering overcurrent relays of traditional design, but not those measuring true rms values, it is widely known that the waveshape can affect the pickup and time delay characteristics. Frequency relays and some metering devices such as watt-metric devices which respond to zero crossings can become inaccurate. Frequency relays and those relying on sampled data are most prone to the adverse affects of harmonics. As a consequence filtering is needed to ensure that the relay responds only to the fundamental frequency of the input signals. However, operating time will be increased as a result of this filtering . At transmission voltage levels where sub cycle or sub half cycle relay operating times are required, this can

be a problem. However, at distribution voltage levels the operating times are often between 1 and 2 cycles and use of specific filters or techniques which inherently filter the input signals are adequate.

2.12.2 System Unbalance

It is the intention of power system planners and designers to not only match supply with demand but to develop the system in such a way that balance between phases is made. However, there is always unbalance to some degree. Not only can a proliferation of single phase load connected to one phase of a system cause problems but the occurrence of unbalanced faults, system abnormal running conditions and long untransposed lines can all result in system load unbalance.

Engineers recognise this condition and approaches such as symmetrical components and modal analysis are but two techniques commonly used to de-couple an 'n' multi-phase system into 'n' single phase systems. This allows for accurate system studies, fault analysis with specifically symmetrical components having appeared in distance relay designs since their first inception[7].

2.13 Distribution System Faults.

As mentioned above power systems are far from ideal and one such cause is the occurrence of faults.

2.13.1 Fault Types

Faults can occur for a number of reasons and should be considered as either primary (system) or secondary (non-system) faults.

Primary system faults are those pertaining to short circuit conditions arising from degradation of interphase insulation or from a sudden open circuit, such as that caused by an overhead line or cable connection failure [8]. Primary system faults are typically the result of catastrophic equipment failure, third party damage, human error, extreme weather or environmental conditions, or a combination of some or all of the previous.

Secondary faults can be thought of as those arising from use of inaccurate setting data resulting in mal-operation of protection schemes or incorrect connections of secondary wiring. Secondary faults are sometimes termed non-system faults and are not a result of faults on the primary power system.

The work in this report is concerned with protecting against system faults and it is

necessary to understand the nature of such faults, in order for the effects on protection devices to be fully understood. Table 2.2 [9] below details the principle primary system faults and classifies them.

All of the above are fixed faults and are the most common. It is possible for a variable fault to be experienced however. This is one in which a single phase fault may develop into a phase to phase to ground fault then into a three phase fault due to the extension of a fault arc. This type of fault can generally be considered as a succession of fixed faults occurring one after the other.

Short Circuited Phases	Open-Circuited phases	Simultaneous Faults	Winding Faults
• Three phase fault clear of earth • Three phase to earth • Phase to phase • Single phase to earth • Two phase to earth • Phase to Phase plus single phase to earth	• Single phase open circuit • Two phase open circuit • Three phase open circuit	A combination of two or more faults at a time , the faults being similar or dissimilar type and occurring at the same time or different locations. Typical examples are cross country earth faults and open circuit with an earth fault condition.	• Winding to earth short circuit • Winding to winding short circuit • Short circuited turns • Open circuited winding.

Table 2.2 : Primary System Fault Types and Classifications [9].

2.13.2 Fault Severity

The severity of a power system fault depends on duration, the magnitude of fault current, the fault type and the amount of damage caused. The two former indicators are of most interest to the protection engineer.

There are a number of factors that affect fault severity.

1. Source Conditions. These conditions relate to the amount of connected generation and its disposition within the network. This will include any interconnections and embedded generation. The maximum and minimum conditions are of most interest with the limits often determined by the minimum and maximum connected load.
2. Neutral earthing. The number of system earthing electrodes, and the presence of earthing resistors or reactors will particularly affect those faults involving earth. Earth fault current on U.K. distribution systems is commonly restricted to below a regulatory

level by the use of such earthing impedance, thus minimising damage caused by otherwise high fault current levels. Taking this theory to it's limit, the fault current could be limited to a very small value, and this is the case when the system is earthed through such devices as the Peterson Coil, or a generator earthed through a voltage transformer.

3. Power system configuration. This particularly refers to whether the system is operating normally or abnormally, and also refers to changing system connections due to the reaction of protective schemes in isolating parts of the network as a result of the actual fault occurrence.
4. Nature and type of fault. The type of fault and its position in the power system affects the magnitude and distribution of the system fault current. Further, the effects of a given fault position may be considerably modified by the simultaneous presence of one or more other faults elsewhere on the system. Fault impedance derived from either fault arc resistance or the resistance of any metal structure in the fault path requires appreciation, particularly when applying distance protection as in this work.

The above considerations result in a range of fault severity. Commonly a standard fault type of the 'three phase fault' is referred to, and in turn the 'three phase fault level' - expressed as either a current in Ampere's or more commonly in MVA - depicts the level of severity. The fault level is the amount of electrical energy available at a point on the system if a fault of a particular type were to occur there. As the three phase fault is the most severe condition it is usually the case that the three phase fault level determines the maximum short circuit rating of the switchgear on the system.

For a solidly earthed system the single phase to earth fault current may exceed that experienced for a three phase fault. Commonly three phase fault levels range from 35MVA at 400/230V levels to 35,000 MVA at 400kV transmission levels. It is desirable to have fast fault clearance times where the fault levels are high to minimise the stress and damage imposed on the system.

2.14 Fault Induced Transient Effects

The occurrence of a fault on a distribution system will in turn cause transient effects which may be observed in both the voltage and the current measured at different points on the network. One such transient effect is that of the DC offset. This effect is often observed in measured current waveforms at the moment a fault occurs, and must be understood if it's

effect is not to cause mal operations in protection equipment reliant on measuring the voltage and current waveforms.

Consider a simple series circuit of resistance R and inductance L. The instantaneous value of voltage, V, applied to the circuit is,

$$V = |Vm| \sin(\varpi t + \alpha)$$

Equation 2.12

If the voltage of equation 2.12 is applied to this circuit at time t=0, then the magnitude of the voltage is governed by α at the moment of application.

If then the instantaneous voltage is zero and increasing in a positive direction then α equals zero also. If the voltage is at it's positive maximum instantaneous value α is equal to $\pi/2$.

The differential equation describing the circuit conditions is,

$$|Vm| \sin(\varpi t + \alpha) = Ri + L \, {di}/{dt}$$

Equation 2.13

and has the solution,

$$i = \frac{|Vm|}{|Z|} \left[\sin(\varpi t + \alpha - \theta) - e^{-R/L} \sin(\alpha - \theta) \right]$$

Equation 2.14

where,

$$|Z| = \sqrt{R^2 + (\varpi L)^2}$$

Equation 2.12

and

$$\theta = \tan^{-1}\left({\varpi L}/{R}\right)$$

Equation 2.13

The first term of equation 2.14 is sinusoidal in nature and can be considered as the steady state value of the current in the RL circuit for the given applied voltage. The second term is non-periodic and decays exponentially with time constant L/R. This term is called the DC component of the current.

If the value of the steady-state term is not zero when t=0, the DC component appears in the solution in order to satisfy the physical condition of zero current at the

instant of switch closure. The DC term does not exist if the switch were to be closed at $\alpha-\theta=0$ or $\alpha-\theta=\pi$.

If the circuit is closed at a point on the voltage wave such that $\alpha-\theta=\pm\pi/2$, then the DC component will have its maximum initial value, which will be equal to the maximum value of the sinusoidal component.

The DC component may have any value between zero and $|Vm|/|Z|$, depending on the instantaneous value of the voltage when the circuit is closed and on the power factor of the circuit. This latter point is best considered as the ratio between X and R of the circuit. At the instant of applying the voltage the DC and steady state components always have the same magnitude but opposite sign in order to satisfy the zero value of current at this time.

Overhead lines and cables have different typical X to R ratios and this in turn effects the amount of DC offset for a particular fault occurrence that may exist in the current waveform. For example a typical value of X/R ratio for a 400kV transmission line is approximately 10. For a 33kV overhead line the ratio falls to around 3 while for a 33kV cable it will likely be closer to 1[2]. Thus the rate at which the DC offset will decrease to zero will be faster in the case of a cable compared with that of the line. That is the cable network can be generally considered to damp out DC offsets in a shorter time than an overhead line.

This work is concerned with the distribution composite circuits and as such may contain both cable and line sections in the same protected feeder section. Thus the worst case X/R ratio of 3 is considered in experimental work.

2.15 Typical Maximum Fault Clearance Times

Because of the type of protection generally applied to the 132kV and 33kV distribution systems, the typical maximum fault clearance time is approximately 0.6 second.

Allowing for auxiliary equipment and circuit breaker operating time and any safety margin a modern day distance relay applied to a 33kV system should produce a trip signal after approximately 1 to 2.5 cycles of the power system fundamental frequency voltage and current waveforms (50Hz nominal).

2.16 Summary

In this chapter a typical power distribution system has been described. Power

distribution systems are not perfect and are subject to many types of electrical phenomena. The basic common construction of distribution systems are that of the wood pole 33kV overhead line or 132kV tower line, while the most commonly used cable is the three core screened 33kV 'H' type.

Feeders are typically designed and operated on a radial principle though in some cases may be paralleled between two different bulk supply substations (132kV/ 33kV) i.e. two different source infeeds.

The proliferation of embedded generation means that quite often an alternative source of system in feed to a fault may be in existence. Thus pre-fault load transfer considerations and a relays interpretation of fault resistance when a fault is subject to double end in feed can be a cause of error.

Some existing relays such as those utilising quadratic characteristics and the earlier electromechanical reactance relays are often considered as catering for the presence of fault resistance. However, in the presence of double end in feed, due to the resistance of a particular fault appearing as a complex quantity, the quadrilateral and the reactance relay may under or over-reach according to their location on the system. Often reactance lines of quadrilateral characteristics are allowed to rotate about the feeder reach point impedance setting in order to cater for this form of error.

Power system voltage and current waveforms are usually subject to some, if not significant, harmonic distortion. This harmonic disruption whether as a result of faults or due to non-linear loads connected to the system, can cause errors in certain types of relay and consideration should be given to the filtering of incoming voltage and current signals. Filtering introduces a time delay and due consideration should be given to ensure such increased trip times will not compromise system integrity or security.

Power systems in steady-state and faulted condition will contain some degree of unbalance and mutual coupling between phases of the network apparatus.

Power swings can occur for a number of reasons and it is essential that any relay is able to detect the difference between an encroachment of the measured impedance into it's characteristic operating region as being a result of either a fault or a power swing. When a power swing is rapid, the advancing impedance trajectory can penetrate the characteristic boundary at the same speed as experienced during faulted conditions. Thus, discrimination of fast power swings from faults is not feasible with timers between zone boundaries and blinders are utilised. However, in the case of blinder schemes, while operating for a power swing the relay is not available to detect faults.

Many types of fault can occur on modern day distribution power systems but the most commonly referred to is the three phase fault. The three phase fault level is a measure of the energy available at a point on the network and is often used as the criteria for switchgear short circuit ratings. System earthing and construction can determine severity of a fault in terms of differing earth return fault path impedance levels for earth faults and the effects of fault occurrence on other parts of the network due to construction or interconnection.

The occurrence of a fault on the primary system gives rise to transient effects, which can be observed, in the voltage and current waveforms. One such effect is that of the DC offset (where due to the point on voltage wave that the fault occurs and the reactance to resistance ratio of the protected feeder) which will vary between zero and voltage maximum and decay at varying time constants. Typically lines have an X/R ratio in the order of 2 to 3 while cables have a ratio of approximately 1. Thus, in the case of a cable network DC off sets decay to zero in a shorter time than the case of a line.

To maintain system security and integrity for all consumers there is a need to protect the system against the occurrence of faults. This protection should discriminate accurately the location of the fault and act as quickly as possible to remove the affected section of the network without disruption to other sections of the system.

Distance relays are a common form of protection utilised on distribution networks as they are independent requiring no form of communication channel, and possess inherent back up. Relay operating times of between 1 and 3 cycles of the power system fundamental waveforms are common.

Chapter 3

Distance Protection

3.1 Introduction

This chapter explains the fundamental principles of power system protection using distance schemes. Beginning with the early electromechanical relays, the basic plain impedance characteristic, reactance and self polarised mho (s.p.m.) characteristics are investigated. Characteristics have evolved such that a number of different ones are available through the use of static type relays and these are described briefly. Problems encountered when applying distance protection to certain types of distribution feeder are identified, through an analysis of existing distribution system practices and relaying principles.

In conclusion, previously identified inaccuracies of distance protection schemes, designed for overhead line homogeneous application but protecting composite or mixed feeder types, are detailed.

Distance relays differ from other forms of protection relay with operation based on the ratio of applied voltage and current. Electromechanical distance relays are constructed so that the operating torque produced by a current element is opposed by that produced by a voltage element, and the relay operates when the ratio of voltage to current is less than some predetermined value.

When a fault occurs on a circuit the ratio of voltage to current at a fixed measurement point will depend on the impedance or distance between the relaying point and the point of fault. This ratio will be constant for any particular fault position, irrespective of the magnitude of fault current and will only vary if the distance between the fault and the measuring point varies. The nearer the fault to the measuring point the lower the voltage to current ratio. Likewise, the further away the fault from the measuring point the larger the voltage to current ratio. By installing a distance relay at the supply end of a line, it's voltage to current ratio setting can be adjusted to represent only faults in a given section of the line and thus will remain inoperative for faults beyond it.

3.2 Definite Distance or Plain Impedance Relay

One particular type of definite distance relay is the balanced beam and might be constructed as shown in figure 3.1(a). Under normal conditions the pull of the voltage element is greater than that of the current element and the beam tilts in the non-operating

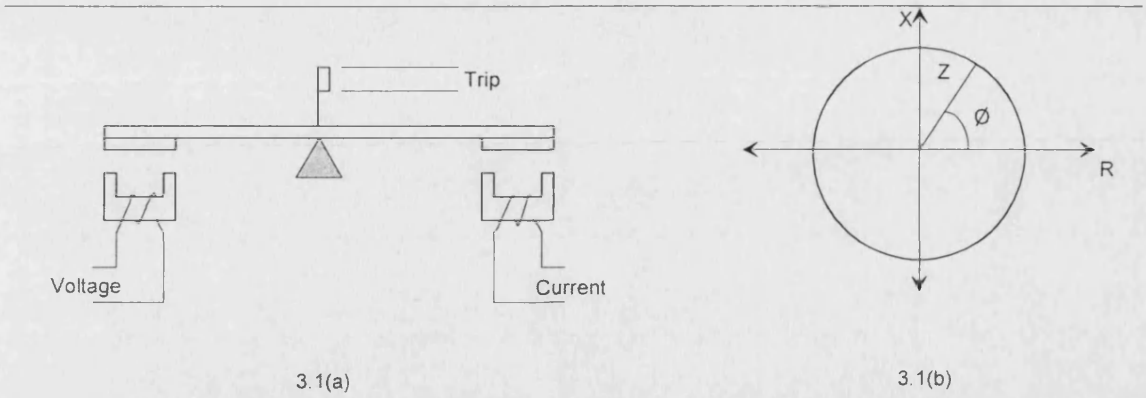

Figure 3.1 : Balanced Beam Electromechanical Relay (a), & the Plain Impedance Relay Characteristic (b).

position. When a fault occurs the pull of the voltage element is reduced and that of the current element increases and the beam tips to close the tripping contacts. The operating characteristic for such a relay is shown in figure 3.1(b), and is a circle of radius Z about the origin. The position of the impedance vector Z inside the circle is determined by the phase angle Ø between voltage and current. Clearly this impedance relay is non-directional. That is it will operate for faults both in front and behind the relaying point.

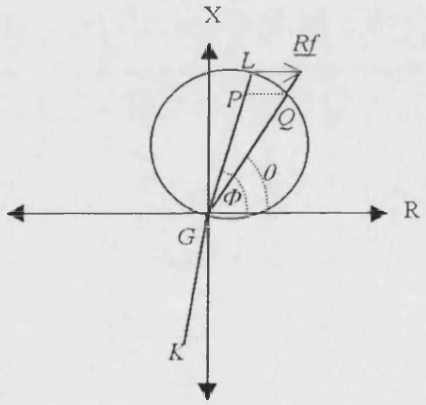

Figure 3.2 : Reduction of the relay characteristic Impedance angle setting, to allow for small amounts of Fault Resistance.

[Note: Ø = Characteristic Impedance angle of the protected line, θ = the compensated setting angle and knowing both these angles GQ = GL / [cos (θ - Ø)]]

The plain impedance relay will also be subject to errors in discrimination caused by the occurrence of high resistance faults, such as arcing faults or flash over to steel towers or steel supporting cross arms. Figure 3.2 demonstrates the effects of arc resistance upon the accuracy of a s.p.m. characteristic. With the relay set for a characteristic angle of Ø, the relay will under reach for a resistive earth fault at the reach point. If the setting angle is reduced to θ the impedance setting is then GL multiplied by cos(θ - Ø) and accuracy in the presence of fault resistance is maintained.

3.3 Reactance Relays

The electromechanical reactance relay, by design overcomes the problem of fault resistance. It measures the reactance of the line and theoretically is unaffected by the presence of fault resistance. An induction cup design is utilised.

In the reactance relay a third factor is introduced which is common to both voltage and current elements. As well as possessing the usual voltage and current windings as on the impedance relay of section 3.1, there are in addition two extra current windings which produce a polarising flux in two additional poles. The flux in the operating winding is out of phase with the polarising flux and the inter-action of these two fluxes produces a torque in the rotor proportional to the square of the current. Similarly, a flux is produced in the restrain winding which produces a torque proportional to V I sin Ø, where Ø is the angle by which the current lags the voltage.

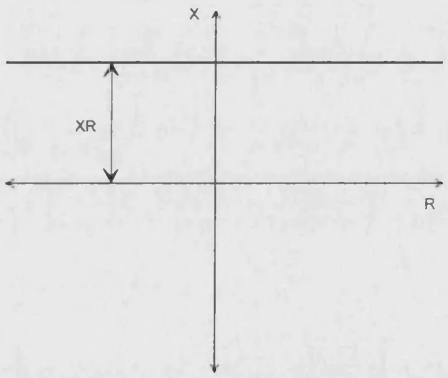

Figure 3.3 : Reactance Relay Characteristic.

The relay will now operate if the reactance seen by the relay, is less than some setting value X_R and the characteristic on the impedance plain will be a straight line parallel to the resistive axis, as shown in figure 3.3.

The reactance relay is generally considered subject to negligible error with respect to fault path resistance when applied to single in feed systems [8]. If however the line is fed from both ends by separate sources and the phase angle between the respective source voltages is large and fault path resistance is large, then the accuracy of the reactance relay may be affected [8]. In this case, the resultant fault current, which flows through the fault, will be out of phase with the relay current. This is shown in the phasor diagram of figure 2.5 (chapter 2). The reactance relay can be shown to overreach for a fault near the end of the protected zone, due to fault resistance appearing as a positive reactance.

3.4 Mho relay

The reactance relay reduces the errors in impedance measurement that arise from the presence of significant fault resistance, but it still suffers from the disadvantage that it is inherently non-directional.

By using a relay similar in construction to the reactance relay but supplying the polarising windings from the restraining winding;

$$Z = Z_R \cos(\varnothing - \theta)$$

Equation 3.1

Where, Z is the PPS impedance of the line, Z_R is the Ohmic setting of the relay, Ø is the angle by which the fault current lags the voltage and θ is the angle by which current lags voltage for maximum operating torque and maximum impedance reach.

This is the equation of a circle and on a polar diagram is as shown in figure 3.4, a circle of diameter Z_R which passes thorough the origin and whose centre is on a line at an angle θ from the real axis. This shows the mho relay to be inherently directional. The phase angle of the characteristic is the angle θ, between the diameter of the impedance circle and the real axis. By making θ approximate the phase angle of the line, the circle

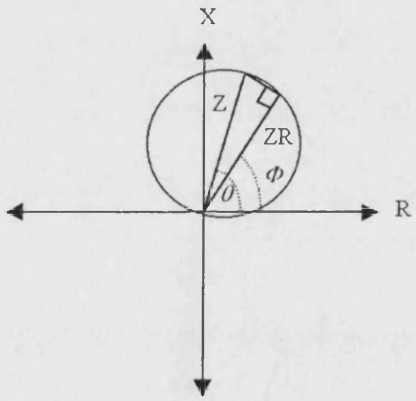

Figure 3.4 : The Mho Characteristic.

can be made to fit the fault area closely, thus reducing the effect of load swing on heavily loaded lines. The relay setting angle θ can be set less than the line angle to allow for a small amount of arc resistance which would otherwise cause under reach.

3.5 Arc Resistance

An approximate value of arc resistance can be assessed by using Van Warringtons equation[8];

$$R_a = \left(\frac{28710}{I_{arc}^{1.4}} \right) \cdot L_{arc}$$

Equation 3.2

where R_a is the arc resistance in Ohms, L_{arc} is the length of the arc in meters and I_{arc} is the current in the arc in Amperes.

The effect of arc resistance is most significant on short lines and with fault currents below 2000 Amperes [4], for example as might occur during periods of light loading. Where the line is carried on wooden poles without earth wires, the earth fault resistance can have serious consequences for the application of s.p.m relays used for earth fault measurement. To improve accuracy when detecting earth faults either reactance, quadrilateral or fully cross polarised mho (f.c.p.m) relays can be used.

3.6 Quadrilateral Relay

With the advent of static relay technology and more recently microprocessor based relaying platforms more complicated characteristics have been developed. One such characteristic is the quadrilateral.

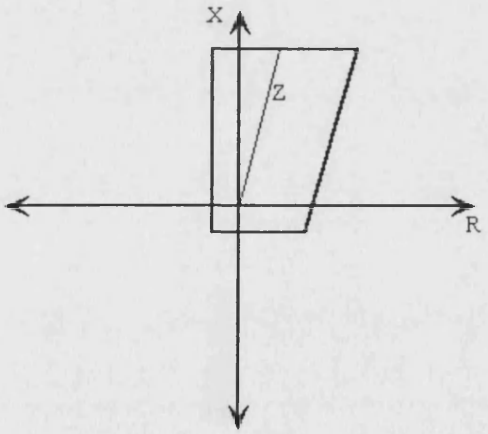

Figure 3.5 : Quadrilateral Characteristic.

The reactance relay has generally been superseded by the use of relays with quadrilateral characteristics. These relays combine the advantages of the reactance relay with directional and resistive reach control characteristics. Quadrilateral characteristics are generally applied for earth fault protection on short to medium length lines with 'strong'

sources of power in feed, where a high degree of tolerance towards fault resistance is required. A typical characteristic is shown in figure 3.5, where the quadrilateral tripping area is offset slightly to allow for close in fault detection.

3.7 Offset Characteristics

When a fault occurs close to the relaying point the voltage falls to zero or near zero, and a self polarised mho or directional relay may fail to operate. The offset characteristic can be used to cover this eventuality. As well as the off set quadrilateral an off set mho can be used.

If current bias is used a mho characteristic can be moved in the impedance plain to embrace the origin and thus the measuring element will now operate for close-up faults both in the forward and reverse directions. There are three main uses of the offset characteristic.

1. To provide carrier starting in distance schemes with carrier blocking.
2. Third zone and bus bar backup. Here, zone 3 protection is afforded and reverse reach can be arranged to extend backwards into the bus bar zone to provide backup. When large amounts of reverse reach are desired, a lenticular characteristic can be used. This avoids mal-operation caused by maximum load transfer when a mho is offset by a large amount.

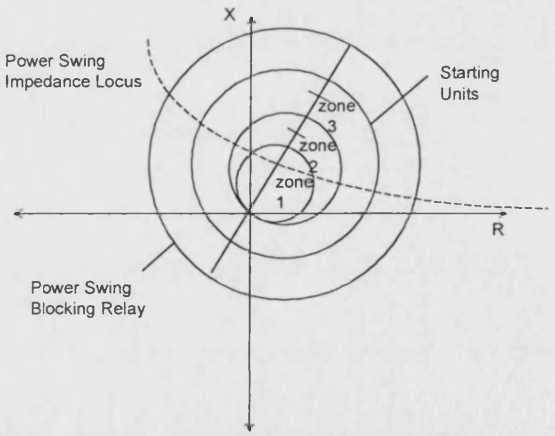

Figure 3.6 : Power Swing Blocking Relay Characteristic.

3. Power swing blocking. The relay is arranged to block operation of the distance scheme measuring units during a power swing. The typical arrangements of characteristics are shown in figure 3.6. A typical impedance locus as experienced during a power swing crosses both the blocking and distance characteristics. The distance elements are only allowed to emit a trip signal if

they operate within a preset time of the power swing blocking offset mho characteristic operating. Under fault conditions the measuring units and the blocking unit will operate almost simultaneously, while for a power swing when the measuring units do eventually operate a sufficient amount of time will have elapsed since operation of the offset mho that a trip will be prevented. Thus the danger of cascade tripping of transmission lines during power swings can be eliminated.

3.8 Relationship between Source Impedance, Line Impedance and Relay Voltage

Any fault on a three phase power system can be represented by a diagram shown in figure 3.7.

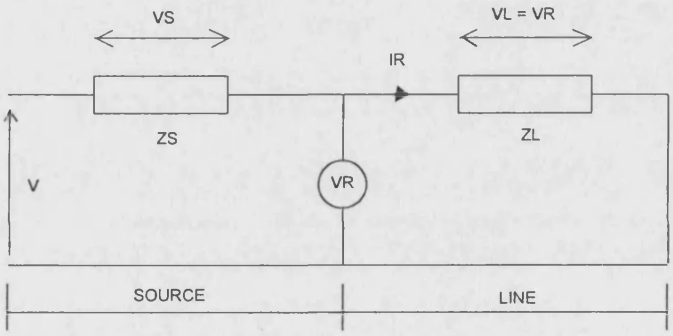

Figure 3.7 : Power System Simplified Arrangement

Z_S and Z_L are the source and line impedance respectively. Z_S indicates a measure of the fault level at the relaying point, and for faults involving earth will be dependent on the method of system earthing behind the relaying point[4]. Line impedance Z_L, represents the impedance of the protected feeder. For a fault at the reach point :

$$V_R = I_R \cdot Z_L$$

Equation 3.3

where V_R and I_R are respectively the voltage and current applied to the relay. V_R can be expressed in terms of Z_S/Z_L, and highlights an important relationship.

$$V_R = \frac{1}{\left(Z_S/Z_L\right)+1} \cdot V$$

Equation 3.4

where V is the open circuit voltage of the power system. This relationship between V_R and Z_S/ Z_L is valid for all short circuit faults provided:

1. For phase faults; V is the phase to phase voltage, Z_S/Z_L is the positive sequence source to line impedance ratio and V_R is the phase to phase relay voltage.
2. For earth faults ; V is phase to neutral voltage, V_R is the phase to neutral relay voltage and Z_S/Z_L is a composite ratio involving both the positive and zero sequence values of impedance and can be expressed as;

$$\frac{Z_S}{Z_L} = \frac{2Z_{S1} + Z_{S0}}{2Z_{L1} + Z_{L0}}$$

Equation 3.5

3.9 Fully and Partially Cross Polarised Mho Relay

The offset mho inherently covers close up faults. An alternative technique would be to use cross phase polarisation where a percentage of voltage from a healthy phase is added to the polarising voltage.

The f.c.p.m. characteristic offers the above advantage of cross polarisation as well as the ability to open out the mho circular characteristic along the resistive axis, as shown in figure 3.8, for all types of unbalanced faults. This is especially useful when protected lines are short and the zone 1 ohmic setting is low and the amount of the resistive axis covered is small compared with expected values of arc resistance.

The partially cross polarised Mho relay offers a compromise between excellent phase selection of self -polarised mho and the superior arc resistance coverage and directional response of the fully cross-polarised mho.

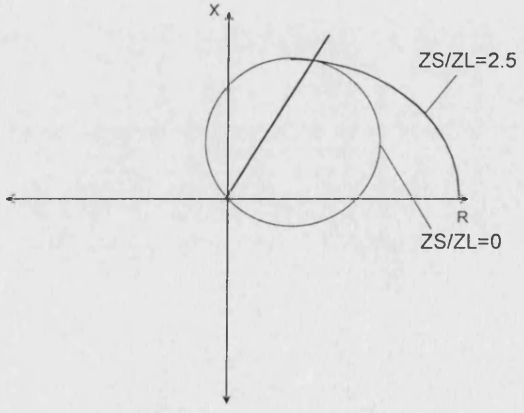

Figure 3.8 : Fully-Cross Polarised Mho Characteristic.[4]

3.10 Ohm Relay

During severe power swing conditions, the only solution to regain normal service is to separate the two swinging sources. Ideally this should be done so that plant capacity and connected load on either side of the split are matched. As mentioned previously ordinary distance schemes are not generally able to detect and isolate for this type of condition and the offset mho characteristic can be used to prevent operation of the relays and thus prevent cascade tripping. In order to ensure separation of the system at a preset point an out of step tripping scheme, employing ohm units can be used.

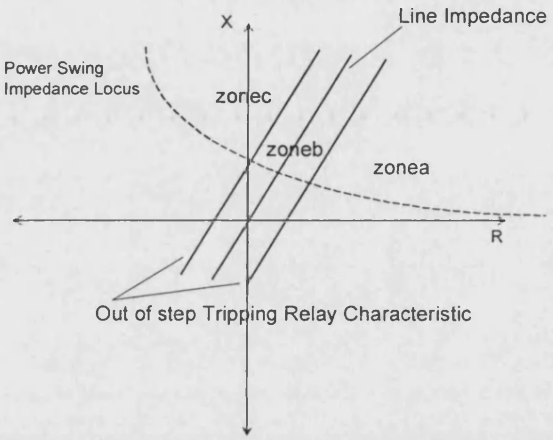

Figure 3.9: Application of Out of step Tripping Relay Characteristic.

The out of step scheme basically consists of two ohm units, arranged with their characteristics either side of the protected lines impedance vector, as shown in figure 3.9. The impedance diagram is now divided into three separate zones, namely a, b and c. The impedance locus during a power swing can be seen to enter firstly zone a then zone b then zone c, in turn causing each ohm unit and their associated auxiliary relays to operate. When the impedance enters zone c the trip sequence is considered complete and the circuit breaker trip coil is energised.

3.11 Distance Relays in Common Use

Historically, protection of distribution systems has been afforded by the use of electromechanical relays. During the 1950's and 60's static relays were developed making use of discrete components and logic circuits such as comparators and level detectors. The present generation protection relay takes advantage of the availability of powerful microprocessor DSP chip technology.

Microprocessor based relays are multifunctional and offer enhanced communication systems. The reliability of microprocessors, decreasing cost and lower maintenance requirement mean that relays produced today are usually numerical microprocessor based devices.

Typical characteristics in use are the mho, s.p.m. and quadrilateral (the latter two often being offset). The nature of this work is the protection of composite circuits as well as those comprising totally underground cable. Basically, the mho characteristic suits detection of faults clear of earth as well as those low impedance earth faults. The quadrilateral lends its self to the coverage of high impedance earth faults as well as phase faults.

3.12 Typical Settings and Scheme Type

In selecting a relay setting for a distance relay the following sources of error should be considered.

1. Accuracy and performance of the voltage and current transducers associated with the relays.
2. Accuracy of relay calibration.
3. Accuracy of transmission line impedance data.

Clearly it is not possible to set a distance relay to cover 100% of a feeders length, and maintain accurate discrimination. It is usual to allow for errors by setting the relay to cover 80 to 90% of the total length.

Settings normally applied to an accurate three step distance relay would be :

- Zone1

$$\text{Setting} = 0.9 \cdot Z_L \cdot \left(\frac{\text{C.T.Ratio}}{\text{V.T.Ratio}} \right)$$

Equation 3.8

This setting would be reduced for a less accurate relay. In the case of a reactance relay, ZL is substituted with the PPS reactance of the line section.

Where a Mho relay is used with a characteristic angle, θ, which is not equal to that of the protected feeder, the Ohmic setting must be increased by dividing it by $\cos(\theta - \varnothing)$.

- Zone2

The zone is typically set to reach greater than 75% of the next feeder section. If there is a source feed at the next bus, the zone 2 reach is reduced as the relay will not see all the fault current. The effect can be seen in figure 3.10, where the additional feed at B decreases the zone 2 reach at A from AD to AE, where;

$$\frac{BE}{BD} = \frac{IA}{IA + IB}$$

Equation 3.7

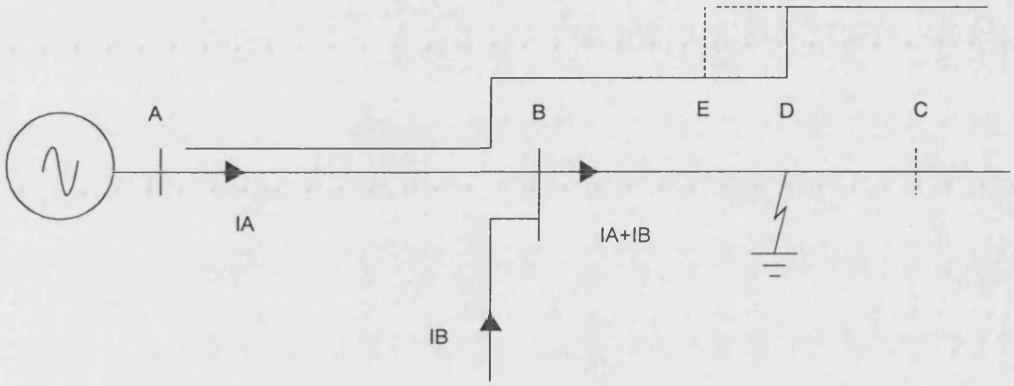

Figure 3.10 Zone 2 Setting With Infeed at Bus Bar B

- Zone 3

The zone is generally for backup, and whereas zones 1 and 2 are for preserving continuity of supply, zone 3 is for minimising damage to equipment and danger to personnel in the case of a protection or operation failure.

Zone 3 is set to cover the whole of the neighboring section, and while zones 1 and 2 can not over reach with out upsetting discrimination, zone 3 can not under reach without giving adequate back-up protection. Zones 1 and 2 are commonly set for the actual line impedance ignoring in feeds, but zone 3 is set for the maximum in feed. In figure 3.11, it must be set for P + QR Ohms, where P is the impedance of the protected line, Q is the impedance of the next line, and R is the maximum ratio of the total current entering the next section to the amount flowing through the protected line.

Sometimes, this setting could be high enough to cause zone 3 operation on load. This problem can be overcome either by using a relay with an elliptical characteristic, or by reversing the direction of the zone 3 units.

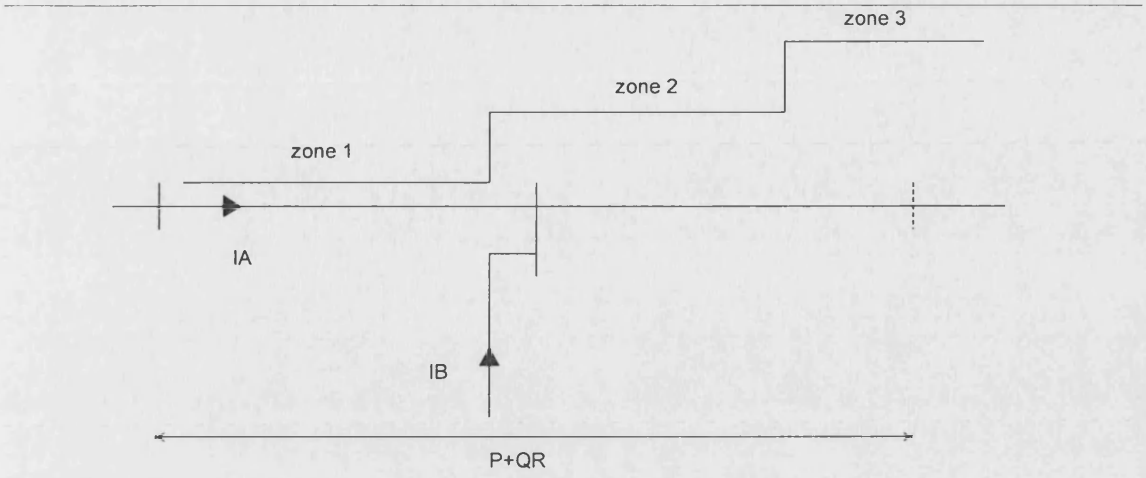

Figure 3.11 : Zone 3 Setting. The P+QR Criteria.

In figure 3.12, the relay at A normally provides zone 3 back-up for the section BC, but there is no reason why this should not be provided by the relay at B. By reversing the zone 3 relay units they will cover the next section behind them. The same protection will be provided, but the setting of the zone 3 unit will be reduced by the impedance of the protected section (the relay at A has to reach a distance AC, whereas the relay at B only has to reach a distance BC). This is less by AB, and may therefore eliminate the risk of operating on overload.

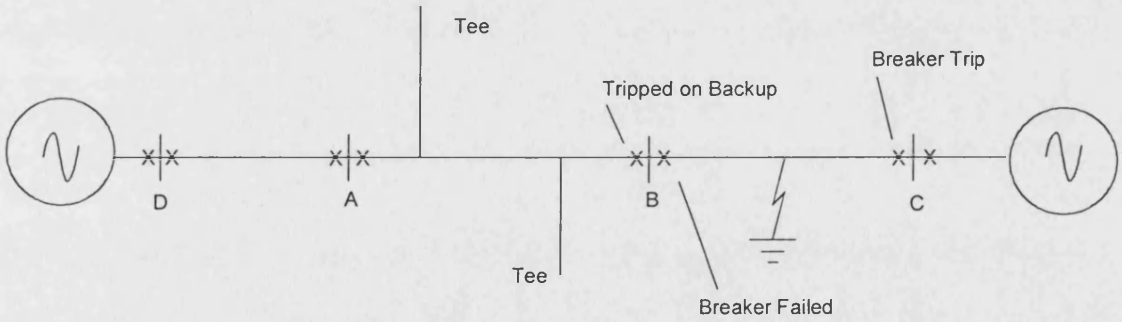

Figure 3.12 : Reversal of Zone 3 Units to Cover Section Behind Relay.

With this type of arrangement giving backup with relays nearest to the fault, the teed lines on the healthy sections will remain in service. The major disadvantage is that the relays giving backup have the same AC or DC supplies as the equipment they are backing up, and could also fail from a common power supply failure.

3.13 Plain and Switched Schemes

Distance protection can comprise six elements, three for phase faults and three for earth faults. If these are plain impedance or reactance relays, a separate directional relay will be required. Starter relays are used and may be multi-element directional relays, or long reach mho relays. These will also start timing relays to extend the reach of the main relays to give zones 2 and 3 operation.

On switched schemes only one distance element may be employed, usually a mho variety, and instantaneous current operated starting relays are necessary. According to the nature of the fault, the appropriate starting units will operate and apply the correct voltage and current to the measuring element.

3.14 Practical Considerations When Applying Distance Protection

There are a number of practical considerations to be made when applying distance protection relays to power distribution networks. Already highlighted are; considerations of teed circuits and their effects on reach point settings, feeds from both ends causing fault resistance to appear as a complex component, the option of characteristic angle adjustment to cater for fault resistance at the reach point setting when using a s.p.m. characteristic and the relationship between the relay voltage and the source to line impedance ratio.

There are a number of other technical considerations to consider, particularly related to the application of distance protection to composite distribution feeders.

Cable circuit earth return paths can depend on many factors such as cable sheath bonding, sheath earth points and any conducting parallel paths laid along side the cable i.e. water pipes. Cables can often be found laid in steel pipes or ducts causing changes in the ZPS impedance Z_0. The accurate way of determining Z_0, is to measure it after cable installation. Past studies [12] have shown that correction factors of ±20% need sometimes to be applied to zero sequence calculations due to the unpredictable nature of the zero sequence impedance value.

One result of this is that $\angle Z_0 \neq \angle Z_1$ for cables. In the case of overhead lines $\angle Z_0 = \angle Z_1$. This has particular importance when considering the case of a single phase to earth fault. The exact nature of the earth path resistance is unknown and it is common to compensate the measured impedance according to the following equation:

$$Z_R = \frac{V_R}{I_R + kI_N}$$

Equation 3.8

where Z_R , V_R and I_R are the impedance, voltage and current respectively measured by the relay. I_N is the neutral current, and k is a compensation factor given by:

$$k = \frac{1}{3} \cdot \left(\frac{Z_0}{Z_1} - 1 \right)$$

Equation 3.9

where Z_0 and Z_1, are the zero and positive sequence impedance values of the protected line.

Relays protecting overhead lines can utilise scalar earth fault compensation. It is clear however that when protecting composite or entirely underground cable networks earth fault compensation factors such as k in equation 3.9, should be complex in order to avoid inaccuracies.

It has been shown that for high resistance faults at the reach point, problems of over and under reach can occur. For a cable circuit values of fault resistance are sometimes considered negligibly low [12]. However, for a composite circuit there may exist a high resistance earth fault on an overhead line section. This would have to be accurately detected by a relay protecting such a mixed construction feeder.

Returning to the question of accurate earth fault compensation, for a composite type feeder the earth fault compensation factor k should be generally expressed as

$$k = \frac{1}{3} \cdot \left(\frac{\sum_{k=0}^{n} Z_{0k}}{\sum_{k=0}^{n} Z_{1k}} - 1 \right)$$

Equation 3.10

where n is the number of line and cable section.

Cable sheaths may be connected to earth at both ends or at one end only. In the case of only one earth connection there is probably a need to reduce circulating charging current in order to reduce thermal loading on the cable section. Elkateb [12] shows that zero sequence impedance seen by distance relays at different ends of such a cable feeder will be subject to different earth fault paths. A relay at one end of a feeder may be subject to return current through the cable sheath, while at the other the return fault current path is through the earth only. Different zero sequence impedance values are experienced. Elkateb[12], concludes that when applying comparator type relay technology to composite circuits the use of complex compensation factors and a s.p.m. characteristic provides the most accurate solution to protecting composite distribution circuits, particularly cable sections between 1 and 25km in length. The s.p.m. characteristic is often applied to distance protection cable

circuits. They are suited to the lower characteristic angles of cable circuits caused by the fact that series resistance and shunt capacitance elements are significant as compared with lines. Reach point difficulties have been further recognised in the presence of arc resistance at the reach point when protecting composite circuits[12].

3.15 Digital Impedance Distance Algorithms

Research and development of digital impedance based relaying algorithms, has been an area of significant investigation for the past thirty years. Several fundamental approaches have been taken in the pursuit of suitable accuracy and operating times. Many such approaches have been developed primarily for use in protecting short to medium length overhead lines (where short is ≤100km and medium is ≤250km). Consequently, few authors have concentrated on the distributed shunt capacitance of the line and it's affect on impedance measurement. As the scope of this work is to develop an algorithm suitable for distance protection of composite circuits, which contain significant shunt capacitance, it would suggest a long line model to be an ideal representation of a composite system of similar lengths. This is because distributed parameter long line transmission line models account for all the parameters of the circuit.

3.16 Investigation of Distance Algorithm Approaches and Development

The algorithm described in this thesis uses a distributed parameter model of the composite system and is explained in detail in chapter 5. An assessment of existing research in the field to date is essential to be able to benchmark the development work described.

One of the main approaches is that based on the solution of the simple first order line equation:

$$V_{ph-e} = IR \times L \cdot \frac{dI}{dt}$$

Equation 3.11

where V_{ph-e} and I are the relay voltage and current respectively. R and L are the series PPS resistance and PPS inductance between the relay and the point of fault. This equation represents the simplified transmission line model and neglects any shunt capacitance of the protected network. It is a lumped model, neglecting the distributed nature of the transmission line parameters. This makes it suitable for application to short lines

(≤100km). Different techniques for solving equation 3.11 give rise to a range of algorithm principles.

An early work by McInnes & Morrisson [15] recognised that equation 3.11 could be solved numerically for R and L if V_{ph-e}, I, and dI/dt were known at two separate time intervals. However, 'noise' present in current and voltage signals would likely give rise to inaccuracies in the resistance and reactance calculations. The authors suggest integrating equation 3.11 over two consecutive time intervals to obtain higher accuracy and avoid the use of smoothing filters and associated time delays. Later Ranjbar & Cory[16], extend the investigation of this consecutive time integral integration theory, and highlight a further mean square error minimisation principle designed to reduce errors caused by neglecting the distributed capacitive element of the overhead transmission line. Requiring a fast operating time (less than 1 cycle of the power system fundamental waveform) it was discovered that these approaches were susceptible to low order harmonics in the voltage and current signals. The authors suggest a further improved digital harmonic filtering method based approach. Rockefeller & Udren [17], undertook an investigation of the practical nature of the approach as defined by McInnes & Morrison [15], while Brenigan *et al* [18], developed a similar relay based on the simplest difference equation solution to equation 3.11 and incorporating fault location, based on calculated reactance readings.

All the above mentioned techniques however can be found to exhibit poor high frequency characteristics as well as being susceptible to low frequency distortion, such as the DC offset problem. Further numerical burden on early processor technology was found to be excessive and would lead to the construction of special relaying equipment.

Suda *et al* [19], recognised the above methods as essentially relying on alternating current theory derived from the Fourier Transform of the input signals. Thus, there existed inherent time delay, while a single fundamental frequency was extracted for use by either filters or integrators. The authors propose an approach based on treating the transmission line as distributed in nature deriving a suitable line equation from the distributed line model partial differential equations (PDE), and consequently considering resistance, inductance, conductance and capacitance. Highlighting how conductance and capacitance can be neglected for short overhead lines they also derive algorithms suitable for long overhead line and cable networks. Using the operator method to integrate the PDE for the distributed constant parameter transmission line, the instantaneous values of voltage and current are given by higher order polynomials in Y (where Y is the distance between relay and fault point). A first order solution was found to be adequate for the short line condition, while a second order solution coped with the inclusion of a capacitance element. The most

important observation is that as the algorithm takes on the consideration of distributed capacitance the implementation of such a routine became more arithmetically demanding on microprocessors.

Ohura *et al*[20], highlights the susceptible nature of numerical differential equation solution approach to low frequency distortion. Both authors work [19,20] exhibit better than previous high frequency distortion immunity, however, the problems of DC offset still remain. Ohura, explains, that there are two approaches to the solution of this low frequency distortion susceptibility. Firstly, a digital filter can be implemented to remove the unwanted distortion at the cost of a time delay. A second approach is however promoted, in which the differential approximation accuracy of the distorted wave is improved. This is achieved by the use of a modified differential approximation algorithm.

Further publications present techniques employing recursive computation, to address the problems of overcoming both high and low frequency distortion. They are all seeking ultra-high speed operating times. Johns & Martin [21,22] and D'Amore & Ferrero [23], suggest algorithms based on differential equations combined with Fourier Transform solutions, and these present better results in terms of both DC rejection and high frequency immunity. The computational burden, however, was found to be high. In the work of Johns & Martin [21], an analogue filter is suggested to reduce the digital processing time and maintain accuracy. In their later work [22] the same authors offer a variable sampling rate as a solution.

When applying Fourier Transform techniques Wiszniewski [24] notes that to obtain a solution to the equation 3.11, a fixed sample data window will also cause problems. A short window does not satisfy the first zone reach criteria while long data windows add to the operating time. This led the author to suggest a variable window technique be applied. However, the problem caused by decaying DC offset components still remained.

Xia & Li [25], develop the variable window ideology applying the Fourier Transform to equation 3.11, reporting improved DC component rejection and high frequency distortion immunity. Of principle importance is the relationship between sample rate and accuracy. For a fixed window length an increase in sample rate leads to a more accurate calculation of R and L, assuming the microprocessor used is capable of completing the necessary calculations in the inter sample time. Further, if the window length is allowed to start from the point of fault inception only and vary up to a maximum value, at which point the Fourier Transform solution based equations are utilised, then improved DC rejection could be afforded. There is a maximum window length restriction to enable recovery time to be kept to within realistic limits.

A further approach in the development of impedance algorithms is to utilise the theory of symmetrical components. Here formulation of the distance relay equations are in terms of symmetrical components as opposed to phase voltage and currents. Phadke et al[26,27], basing their fundamental theory on the work of Lewis & Tippet[28], were among the first to utilise this approach. Although previous papers have been published, Phadke's approach attempts to address the transient nature of the relay input signals. By pursuing the derivation of a single performance equation suitable for the detection of all fault types, the author's state advantages in increased operating time based primarily on the notion of decreased computational burden. The fundamental equations used in the development of the algorithm are mathematically manipulated into a common trip equation. The effects of distortion in the input signals is said to be reduced while errors due to fault resistance and pre fault loading are highlighted. This error is stated as no worse than other methods or techniques. Inherent in this technique is pre multiplication of the incoming zero sequence current with the zero sequence impedance of the protected circuit. This is not a reliable factor when considering the cable network where as previously highlighted the zero sequence impedance can not often be accurately calculated. This symmetrical component approach has also been adopted by Waiker *et al* [29,30,31]. The authors in this case claiming further reductions in operating time due to decreased computational burden.

3.17 Summary

This chapter has shown that by measuring the impedance between a relay and a point of fault an indication of the distance to that fault can be made by comparing the measured value with known circuit parameters.

The early distance relays were of the electromechanical design and used characteristics such as the plain impedance (circle about the origin) or the reactance relay. Both these characteristics had to be used with a separate directional relay element to enable discrimination between forward and reverse faults. The reactance relay is often considered to be more suited to applications where fault resistance may be encountered. However there are some problems with fault resistance appearing complex to reactance relays at each end of a faulted line that is fed from both ends.

The introduction of static relay technology and the early microprocessor based relays has resulted in the creation of many different characteristics. Examples are the quadrilateral, which is thought of as one of the best suited for earth fault protection of short over head lines, where high values of fault resistance may be encountered. The

characteristic is made up of a reactance line, a resistive line and a directional line. The s.p.m. is utilised for protection of phase to phase as well as earth faults along with the f.c.p.m.. In this work it is the quadrilateral and the self polarised Mho which have been used. This is thought to provide a good general basis on which to judge performance.

A fault on a distribution feeder may posses fault resistance and it has been shown that careful selection of characteristics can reduce inaccuracies manifested in relay under or over reaching. Other considerations are the effect of source to line impedance ratios. It has been shown that the higher the source impedance the smaller the voltage which a certain distance relay will measure for a particular fault.

Power swinging has to be considered. Ohm relay elements have been traditionally used to create out of step schemes, which are designed to prevent cascade or unpredictable tripping during a severe power swing condition.

Modern distance relays are microprocessor based. They offer advantages such as selectable multifunction protection features, communication systems, decreasing costs, decreased maintenance and good reliability. Further, they are being integrated into established installations as traditional equipment becomes due for renewal or fails maintenance tests.

A typical scheme employed by the distribution companies in the U.K. might be a three zone scheme with zone one protecting 80% of section one. Zone two protects all of zone one and no greater than 75% of zone two, while zone three is employed as a backup for minimising damage, or ensuring safety for the utility personnel. Zone three may in some cases be 'reversed' to provide backup behind the relaying position. Schemes may be plain or switched. In the plain scheme, three earth fault relays and three phase to phase fault relays are used. In the switched scheme one distance relay is utilised with several starter elements used to selected the faulted phases to apply inputs to the relaying element.

Most early distance relays were developed for use on homogeneous overhead line feeders. However, when applied to mixed type or composite feeders, i.e. those consisting of underground and overhead lines, consideration must be given to the inaccuracies caused by design constraints.

Cable networks generally have differing zero and positive sequence impedance angles. Thus scalar earth fault compensation factors are not suitable, a more suitable variety being complex. Cable circuit earth return paths are often unpredictable and it is not uncommon to measure the zero sequence impedance of cable sections after installation to accurately determine the value. Earth fault compensation factors should reflect in positive and zero sequence impedance parameters, the true nature of the feeder sections, their series

connection and their lengths. It is also clear that a distance relay at one end of a composite feeder of different section lengths will require a different earth fault compensation factor than a relay installed at the other end. The practice of earthing a section of cable at one end only could mean that earth return paths are through the sheath for the relay at the earthed end and through the earth at the other. Thus, the earth path impedance values will be different.

Previous research into distance protection techniques has taken many directions. From the literature searched, Fourier based techniques, where the fundamental power system quantities of voltage and current are derived as vectors at fundamental power system frequency, offer a simple solution which should remove significantly the effects of DC off set in the current waveform. The Discrete Fourier Transform (DFT) is the technique used to derive these voltage and current vectors. This frequency domain technique offers simplicity and is proven in the relaying industry.

Before the new algorithm can be described in detail chapter 4 describes microprocessor based relaying in detail and explains the DFT.

Chapter 4

Digital Microprocessor Based Distance Protection & Distance Relay Test Harness Development

4.1 Introduction

This work concerns the research and development of a new impedance measuring algorithm suitable for inclusion in a microprocessor based relaying platform. This chapter starts by describing briefly the benefits of these relay platforms and a typical hardware layout.

It follows that most of the research and development work in this thesis should comprise creating software protection algorithms. However, in order to test the prototype algorithms performance a software distance relay test harness must be built. The harness should reflect as near as possible the true nature of the distance relaying platforms construction, simulating such things as primary system voltage and current through to the emission of a trip signal. Additionally, facilities unique to the testing and development of prototype software algorithms should be incorporated such as back end data processing, results preparation and production of any other performance assessment data that may be required. Into this harness the prototype impedance measuring algorithm described in chapter 5 can be inserted.

The new protection algorithm developed in this thesis has been tested using two different power system software simulations. Thus, two separate and quite distinctly different test harnesses have been developed. The two harnesses are described and in so doing some of the peripheral distance relay simulation requirements, such as power system transducers, anti alias filtering, and time decimation of input signals are discussed.

4.2 Micro Processor Based Relaying

Electromechanical relays, such as the induction cup or moving coil types, have a well proven track record for reliability and durability. However, a relay of this type is usually only capable of one protection function, requires expert commissioning and routine maintenance, possess many delicate moving parts and affords no means of communicating

activity sensed on the primary system, other than visually to personnel in the immediate location.

There are distinct advantages to be gained by the use of microprocessor based relays. The units are generally multipurpose, requiring minimum time or capability to affect changes in functionality. Units are generally compact and can easily be integrated with others of similar design to form more comprehensive protection solutions. They require less maintenance than traditional designs and are more resilient to shock induced damage. They offer the chance to utilise high performance and more sophisticated characteristics, which are needed to meet the requirements and complexity of a modern power system. These relays are commonly faster and more sensitive, than their electromechanical predecessors. A relay can not only detect faults on the primary system and react to instigate circuit disconnection, but also offer fault finding features, event recording and self diagnostic routines. By use of a fully integrated supervisory system control and data acquisition network (SCADA), relay functionality, setting, and interrogation can all take place from a remote location. Today, it is rare to find electromechanical relays supersede the use of micro processor based protection in newly commissioned sections of power system networks.

There are advantages unique to designers and produces of such multi-functional relaying platforms. By creating a common basic hardware platform different variations of hosts and protection software routines may be added to create completely different relay functionality. This promotes lower costs in design & development, production and support and maintenance. Purchase prices as a consequence are decreasing.

Of principle importance to any microprocessor relay is the protection algorithm. It is the software routine through which mathematical manipulation of the incoming discretised system quantities, detects an abnormal condition, discriminates the fault position and acts to instigate disconnection of the relevant sections of the network.

4.3 Typical Components of a Microprocessor Based Relaying Platform

A typical outline of a digital distance relay is shown in figure 4.1, where the primary inputs of voltage and currents are shown as the input signals to the relay hardware. Analogue anti-alias filters are required, as this is a digital device, which samples input signals at regular intervals, to form a discrete time signal. The Nyquist criteria must be satisfied [34] and frequencies greater than half the sampling frequency are removed.

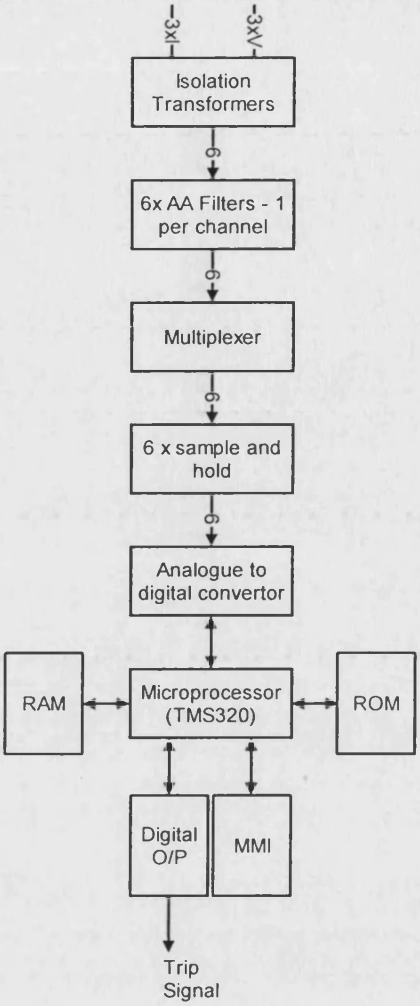

Figure 4.1: Basic Hardware of a Digital Distance Relay.

Input signals are multiplexed then digitised by an analogue to digital converter (ADC). Since this device requires a finite period of time to operate a sample and hold device is usually placed before the ADC to ensure the signal does not change during the conversion process. Having obtained the required discrete time input signals they are mathematically manipulated within the protection processor, by the protection algorithm stored in the relays memory devices (ROM). This is the heart of the relay and is likely to be a 16 bit device. Commonly used are digital signal processing chips (DSP), for example the TMS320 processor from Texas Instruments. Only one processor is shown in figure 4.1, but it might be the case that multiple processors are connected in parallel or 'pipelined', in order to meet the processing requirements of some complex protection schemes.

Other features of the relay hardware may be a man machine interface for interrogation and commissioning, a serial communications port, diagnostics and SCADA connection, and a digital output board or scheme logic, from which one output might be a trip signal. It is worthwhile to note that the above can be considered as one half of the relay,

the other being the 'host' processor. This device is responsible for powering up and relay 'house keeping', and is as important as the aforementioned protection features and processor(s).

The protection algorithm resides in the memory devices of the relaying platform and may be executed continuously at time steps equal to the inter- sample time, by the microprocessor.

4. 4 Distance Relay Specification

A basic specification for relay operation was outlined at the commencement of the project by the sponsoring company ALSTOM T&D P&C.

4.4.1 Requirement

An impedance measuring algorithm suitable for inclusion in a medium voltage multi- function microprocessor based relaying platform, suitable for application to composite circuits. 'Composite circuit' implies one comprising both overhead lines and underground cable.

4.4.2 Basic specifications

Several parameters and operating limits are defined in table 4.1.

Relay Parameter	Specification
Basic Unit Cost	£1200.00
System Voltage Level	11,33, and 66 kV
Sampling Frequency	600 Hz
Power System Frequency	50 Hz nominal
ADC	16 bit
Relay Operating Time	40-60 msecs (2-3 cycles at nominal fundamental power system frequency)
Typical System X:R ratio	2 or 3
Tripping Characteristic	Quadrilateral for all Elements

[Note: X:R ratios 1:1 for cable sections but 2:3 for overhead line sections.]

Table 4.1 : Distance Relay and Protection Algorithm Operating Parameters

4.4.3 Simulation Requirements & Specifications

The work required simulations of typical 33kV single and double end fed composite power distribution networks. Specific simulation specifications are summarised in table 4.2.

Simulation parameter	Specification
System Voltage	33kV
Overhead line	0.2 Sq.' inch C.S.A. Hard Drawn Copper (HDC), 3 wire, flat wood pole construction on steel cross arms and pin insulators
Cable	0.3 sq.' inch C.S.A. 3 core Copper stranded circular conductors, 'H' type, screened 33kV, M.I.N.D insulated.
Max. Composite feeder length. (comprises varying length of cable and line connected in series)	100.0 km
Min. source SCL	10 MVA
Max. source SCL	1000 MVA
For single end fed system remote end load	No load - 50.0 MVA @ 30Degrees lagging.
Faults applied	'a'-'e' : 'b'-'c'
Earth fault resistance values	0.0 - 50.0 Ohms

Table 4.2 : Simulation Specifications

4.5 Distance Relay Test Harness Development

Figures 4.2 and 4.3 show the test harnesses built for this research development project. The need for two separate harnesses arises because of the fact that the prototype impedance based protection algorithm required testing in the steady state and transient environments.

4.5.1 Steady state Harness

In the steady state case, figure 4.2, the harness comprises three distinct sections. Section one consists of a bespoke software based power system simulator, created to allow for trip boundary accuracy comparison's between the prototype algorithm and other existing distance relaying algorithms and techniques.

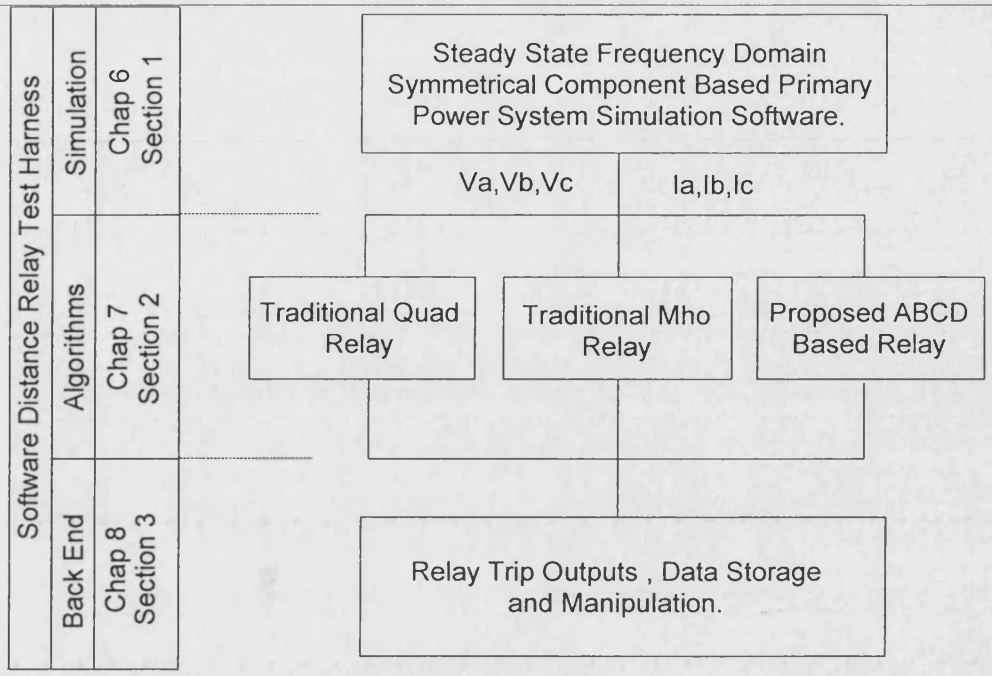

Figure 4.2 : Integrated Software Based Power System Steady State Simulation and Distance Relaying Test Harness

Section two comprises three separate impedance based protection algorithms, namely the new prototype algorithm described in chapter 5, and two other traditional algorithms utilising a s.p.m. and quadrilateral tripping characteristic respectively. Chapter 6 explains the principles upon which this simulation software is based and details the alternative algorithms and test methods adopted.

Section three can best be described as the data output logic and manipulation stage. Here the data and trip outputs from the three relaying algorithms are processed to allow presentation of results and analysis. This forms Chapter 7.

4.5.2 Transient Harness

The necessity for a transient based test harness, figure 4.3, arises from the requirement to test the new prototype algorithm in 'as near real life' conditions as possible prior to assembling and testing any physical relay prototype hardware.

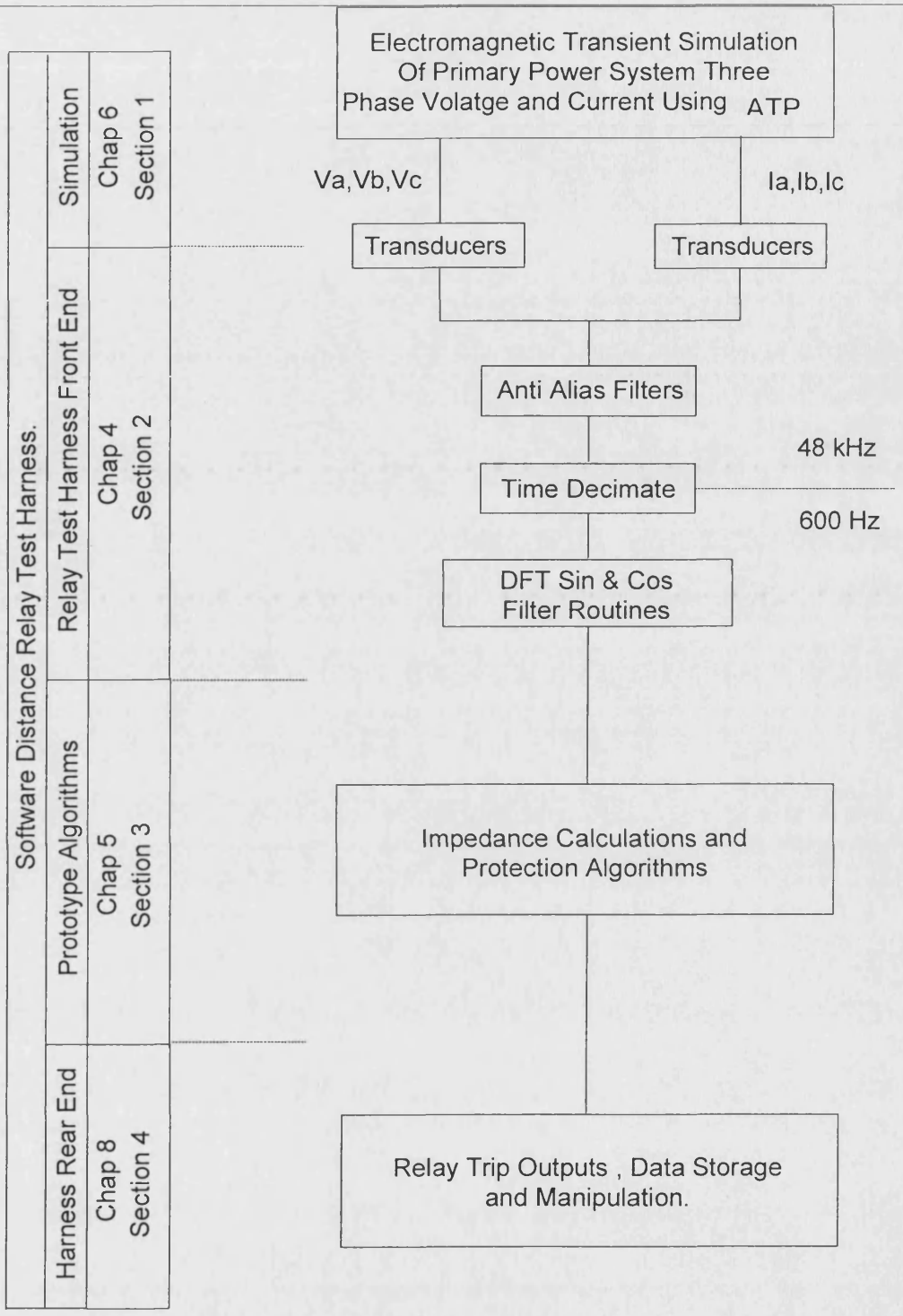

Figure 4.3 : Integrated Software Based Transient Power System Simulation and Prototype Distance Relay Test Harness.

This commonly adopted technique in relay algorithm development allows significant assessment of performance to be made prior to the more involved prototype hardware real time testing. The harness must represent as accurately as possible the

transient nature of primary power system measurands and the common input stages of a relaying platform, such as anti alias filtering and pre-filtering stages. It also incorporates a more comprehensive discriminatory and tripping regime as would be required in practice.

Figure 4.3 shows the transient test harness to comprise four main sections each of which are detailed in the respective chapters indicated on the left hand side. The first section is the primary power system simulation stage. For the studies in this thesis the electromagnetic transient simulation program (ATP) has been selected for provision of the three phase voltage and current signals. Chapter 6 describes this.

The second section can be considered as the distance relay test harness front end. It includes all the necessary software routines to simulate the creation of discrete time sample input signals as would be seen by the relay's protection function microprocessor. The components here are dealt with in detail in this chapter as section 4.6.

Impedance measurement and protection algorithms form the third section. The fundamental basis, development and creation of the prototype impedance based protection algorithms and routines are described in detail in Chapter 5.

The relay and data manipulation stages and trip output form the fourth section and rear end of the test harness. Detail of this stage can be found in Chapter 7.

4.6 Transient Relay Test Harness Front End

The rest of this chapter now explores section 2 of the test harness of figure 4.3.

4.6.1 Primary Power System Voltage and Current Algorithm Inputs

The discrete time voltage and current inputs to the relay are taken from the ATP at time step (ΔT). In this work ΔT has been selected to represent a simulation frequency of 48 kHz. The selection criteria being a balance between simulated circuit length and travel time, type of line model used (frequency dependent etc.), desired resolution of system quantities, and simulation run time and data storage restrictions. In line with general approaches to simulation work of this nature, ΔT has been set far higher than the sampling rate of the prototype relaying algorithm which will utilise the simulated data. In this manner any 'erroneous conditions' or hidden affects in the modeling procedure will be catered for while allowing the anti alias filter simulation and time decimation simulation stages to affect the 12 samples per cycle sampling rate of the relay.

All simulations are run to steady state prior to the capture of a system parameters snapshot file, which allows future simulations to commence from this steady state condition.

4.6.2 Transducers

Transducers are assumed ideal in this work. Simulations are of a typical composite 33kV system and therefore CT and VT ratios are assumed to be 400:1 and 300:1 respectively. The 1 Amp secondary of the CT caters for the burden of longer secondary circuit runs.

4.6.3 Anti Alias Filters

The Nyquist criteria states that the sampling frequency must be greater than twice the highest frequency to be sampled. If this should be disobeyed then aliasing effects may distort the sampled waveform, as higher frequencies are ' folded down' to impersonate lower frequencies.

Table 4.1 indicates that the impedance based algorithm will work at a sample rate of 600Hz or 12 samples per cycle at power system fundamental frequency. To satisfy the Nyquist sampling theorem and thus prevent aliasing analogue 1^{st} order low pass filters are placed in the input stage of digital relays.

These anti alias filters (AA) have been simulated in the relay test harness using a digital FIR low pass filter exhibiting the magnitude against frequency plot of figure 4.4. Possessing a cut off frequency of 130 Hz the filter ensures that frequencies above half the maximum sampling frequency of 600 Hz are filtered out before they reach the analogue to digital converters.

It can be seen from figure 4.4 , that the digital AA filter simulation has been designed to exhibit approximately the same characteristic as a discrete filter design already in use by the sponsoring company. The filter has a 'gentle' cut off so as to achieve the desired filtering function but not to increase group delay and thus the relay operating time.

As mentioned in section 4.6.1, the simulated power system data files of voltage and current possess a sample rate of 48kHz to ensure simulation data integrity. The fact that the simulation time step has been set at this level enables the AA filters and the time decimation stage (section 4.6.4) to simulate the sampling function of the relay hardware.

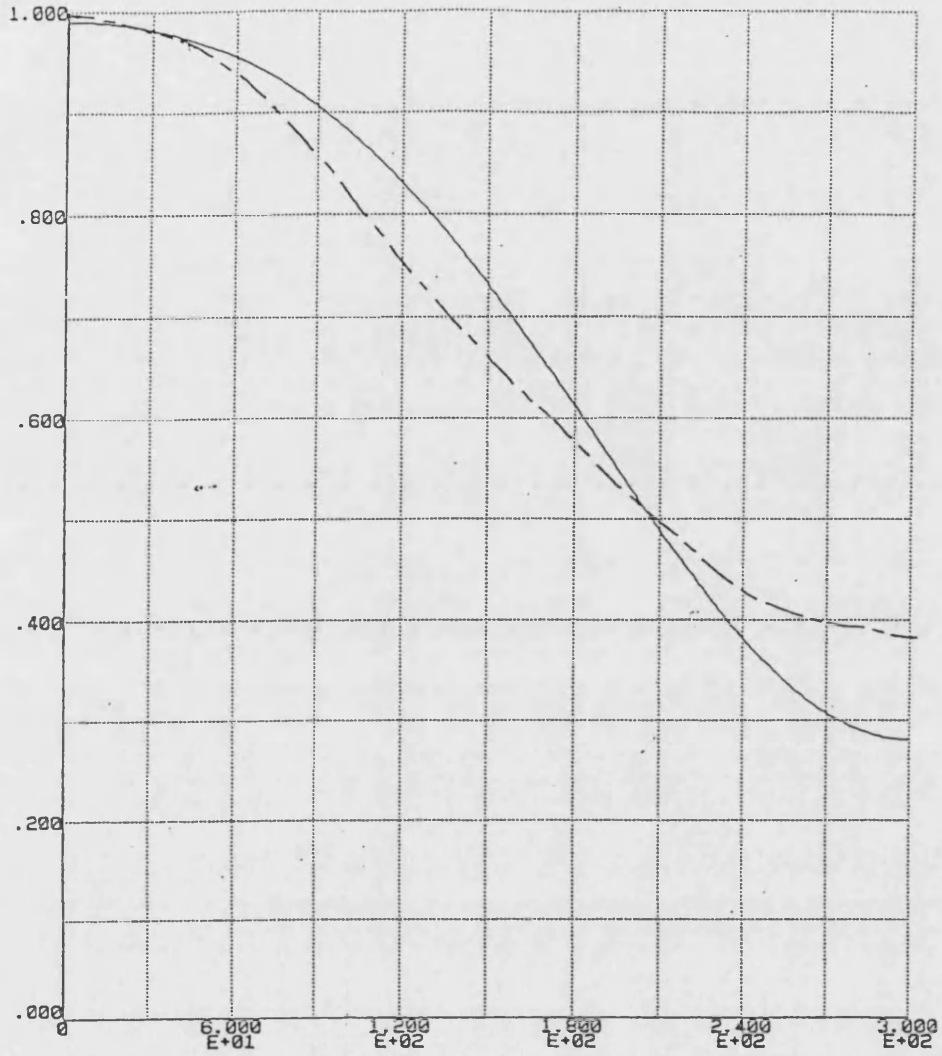

Figure 4.4 : Simulated and Actual AA Filter Magnitude against Frequency Plot.

---------- Actual _____ Simulated

4.6.4 Time decimation

This stage accounts for the change in sampling frequency that is necessary to accurately simulate the AA filters described in section 4.6.3. Thus to change the sampling frequency from 48kHz to 600Hz - a process known as time decimation - every 80th sample of the discreet time input series is taken. Hence the discrete time sampled series,

$$x(0), x(1), x(2), \ldots\ldots x(79), x(80), x(81), \ldots\ldots x(159), x(160), x(161), \ldots\ldots\ldots x(240), \ldots\ldots\ldots x(320), \ldots\ldots$$

would become,

$$x(0), x(80), x(160), x(240), x(320), \ldots\ldots\ldots$$

4.6.5 Discrete Fourier Transform (DFT)

It is common to utilise the Fourier Transform to transfer a continuous time domain signal into the frequency domain and hence obtain information detailing spectral content. The Fourier Transform may be adapted for use with discrete time signals and is referred to as the Discrete Fourier Transform (DFT).

It is necessary to estimated the 50Hz component of the discrete time input signals of voltage and current. In practice the DFT is implemented by equations 4.1 and 4.2.

$$\mathrm{Real(Xm)} = \sum_{k=0}^{N-1} x(n-k) \cdot \cos\left(\frac{2\pi mk}{N}\right)$$

Equation 4.1

$$\mathrm{Imaginary(Xm)} = \sum_{k=0}^{N-1} x(n-k) \cdot \sin\left(\frac{2\pi mk}{N}\right)$$

Equation 4.2

where N is the number of samples in the discrete time sequence x(n), m is termed the harmonic index and x(m) is the frequency component. The DFT is applied to a discrete time signal and as such produces discrete frequencies. Equations 4.1 and 4.2, evaluate the frequency information in terms of real and imaginary components. These are simply related to magnitude and phase description. Thus for a phasor I, having magnitude A and phase angle ∅,

$$\text{real(I)}=A\cos\varnothing \qquad \& \qquad \text{imaginary(I)}=A\sin\varnothing$$

The range of discrete frequencies which can be evaluated by the DFT is determined by N, the number of samples in the input sequence and the sampling frequency f_s. All frequencies evaluated are related to the lowest non-dc frequency or fundamental frequency component. The fundamental frequency is given by f_s / N. The second harmonic frequency is given by twice the fundamental frequency, and so on.

The relay developed in this work has a sample rate of 600Hz or 12 samples per cycle at fundamental frequency. Therefore the DFT equations for a current signal are,

$$I_{(real)} = \frac{1}{6}\left[\frac{1}{2}(i_1 + i_5 - i_7 - i_{11}) + \frac{\sqrt{3}}{2}(i_2 + i_4 - i_8 - i_{10}) + i_3 - i_9\right]$$

Equation 4.3

$$I_{(imaginary)} = \frac{1}{6}\left[\frac{1}{2}(i_2 - i_4 - i_8 + i_{10}) + \frac{\sqrt{3}}{2}(i_1 - i_5 - i_7 + i_{11}) - i_6 + \frac{1}{2}(i_0 + i_{12})\right]$$

Equation 4.4

and

$$I\angle\Phi = I_{(real)} + jI_{(imaginary)}$$

Equation 4.5

The AA filter described in section 4.6.3 acts with the DFT to attenuate the 11th harmonic thus allowing only the fundamental frequency components (50Hz) through and removing other unwanted harmonic components. DC components are also rejected.

From the Fourier sine and cosine derived components, the magnitude and the phase quantities of a signal, at 50 Hz, can be calculated. Chapter 5 describes how such quantities are utilised by the new protection algorithm.

4.7 Summary

Microprocessor based relays offer increased versatility, at reduced purchase and operating cost, faster and more accurate responses and offer the capability of remote communication and self diagnostics. Units require little maintenance, and are the popular choice for protecting modern day power systems.

A typical microprocessor based relaying platform comprises; input stage isolation, anti alias filtering, sample and hold, multiplexers and typically a 16 bit analogue to digital converter. Once a discrete time signal has been obtained it is processed within a DSP chip, by one or more protection algorithms stored in the relay memory (ROM). There may be a number of such DSP chips connected in parallel, to allow for the complex protection functions required by modern day power systems.

In order to test prototype protection relay algorithms software test harnesses are assembled to accurately represent a real protection relay platform within which a protection algorithm will be required to operate. Both a 'steady state' and a 'transient based' harness are used in this work. Both have been introduce in this chapter. The fundamental construction of each has been described briefly, while the second input stage of the transient test harness has been described in detail. Here anti alias filters, time decimation, and pre-filtering of input signals using a pair of full cycle discrete Fourier Transform (DFT) filter routines have been described. The DFT derives both real and quadrature fundamental

frequency components of a discrete time sampled input signal. It is these quantities that are delivered to the protection microprocessor for use by the protection algorithm described in chapter 5.

Chapter 5

New Impedance Measurement Algorithm

5.1 Introduction

This chapter details a novel distance protection algorithm for use in a microprocessor based relay that is suitable for application to composite distribution feeders.

The algorithm uses a distributed parameter long transmission line model to represent the protected composite system. It considers the shunt capacitance of cable sections and represents its non-homogenous nature; namely the series connection of cable and line sections of varying types and lengths. This is in contrast to previous works such as Moore[32], which use a lumped parameter model suitable only for application to short overhead lines.

The distributed parameters of a transmission line vary with frequency. By considering the line to be ideally transposed and using quoted series and shunt parameters per unit length for specific cable and line sections, hyperbolic parameters applicable to the fundamental operating frequency and representing the distributed nature of the line can be calculated. This is the general solution described by Wedepohl [34].

At the sending end of a composite feeder, measured discrete time sampled voltage and current signals are transformed into the frequency domain by use of the discrete Fourier Transform (as described in Chapter 4). The method creates voltage and current vectors rotating at the fundamental power system frequency reducing signal content at all other frequencies.

The complex values of voltage and current are combined mathematically with the hyperbolic line parameters to enable the calculation of voltage and current at a specific distance, X along the feeder length. By choosing X to be eighty percent of feeder length it becomes possible to calculate the voltage and current and thus impedance at the reach point of a classical distance zone one. No earth fault compensation is required for the measured or calculated voltage and current signals as Elkateb [12] found essential.

A novel quadrilateral characteristic is proposed which utilises the voltage and current measured at the relaying point and those voltage and current vectors calculated to

be at the reach point. In this manner a zero Ohm fault can be determined as being in or out of zone one with great accuracy.

Single phase to earth faults on overhead line sections can contain significant fault path resistance. By estimating the remote end source impedance and through the use of a novel and simple pre fault load estimation technique the algorithm reduces substantially the inaccuracies in impedance calculation and thus fault discrimination caused by the presence of fault path resistance as first recognised by Lewis and Tippett[28].

5.2 Single Phase Two Port Network Representation

Long overhead transmission lines (>250km) and distribution cables possess significant shunt admittance between phase conductors and earth. Lumped circuit modeling techniques (single or cascaded PI sections) become inefficient when modeling such circuits. In reality the electrical parameters of the line are distributed uniformly along its length and in ac systems will be frequency dependent. Previous work has sort to represent long lines accurately [35,36,37].

The well known equations for voltage and current at a length X along a transmission line are found by Grainger & Stevenson [37].

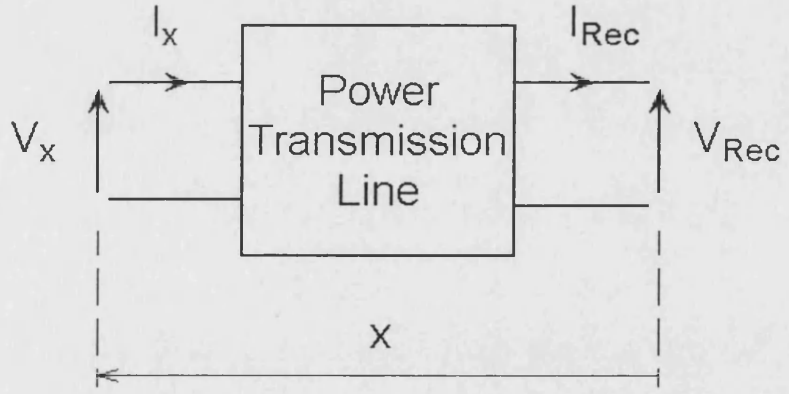

Figure 5.1 : Simplified Distributed Parameter Transmission Line Length X (Single Phase)

Referring to the simplified single phase power transmission line diagram of figure 5.1 the equations are written as 5.1 and 5.2.

$$V_x = V_{Rec} \cdot \cosh \gamma x + Z_c \cdot I_{Rec} \cdot \sinh \gamma x$$

Equation 5.1

$$I_x = V_{Rec}/Z_c \cdot \sinh \gamma x + I_{Rec} \cdot \cosh \gamma x$$

Equation 5.2

Where V_x and I_x are the voltage and current calculated at distance x along the transmission line from V_{Rec} and I_{Rec} the receiving end measured values of voltage and current. Z_c and γ are the line characteristic or surge impedance and propagation coefficient respectively. If z and y are the series impedance and shunt admittance per unit length, then

$$Z_c = \sqrt{z/y}$$

Equation 5.3

$$\gamma = \sqrt{z \cdot y}$$

Equation 5.4

Equations 5.1 and 5.2 represent a two port network . The network represents the transmission line of figure 5.1 by hyperbolic parameters A,B,C, and D.

Where,

$$A = \cosh \gamma x \qquad \textbf{Equation 5.5}$$

$$B = Z_c \cdot \sinh \gamma x \qquad \textbf{Equation 5.6}$$

$$C = 1/Z_c \cdot \sinh \gamma x \qquad \textbf{Equation 5.7}$$

$$D = A \qquad \textbf{Equation 5.8}$$

The complex quantity γx and can be written,

$$\gamma x = (\alpha.x + j\beta.x)$$

Equation 5.9

Solution of the complex hyperbolic trigonometric values can be found using equations 5.10 and 5.11.

$$\cosh(\alpha x \pm j\beta x) = \cosh \alpha x \cdot \cos \beta x \pm j \sinh \alpha x \cdot \sin \beta x$$

Equation 5.10

$$\sinh(\alpha x \pm j\beta x) = \sinh \alpha x \cdot \cos \beta x \pm j \sinh \alpha x \cdot \sin \beta x$$

Equation 5.11

Figure 5.2 shows the two port network representation where V_x, I_x, V_{rec} and I_{rec} have been substituted for convenience by V_{rel}, I_{rel}, V_{rp} and I_{rp} respectively.

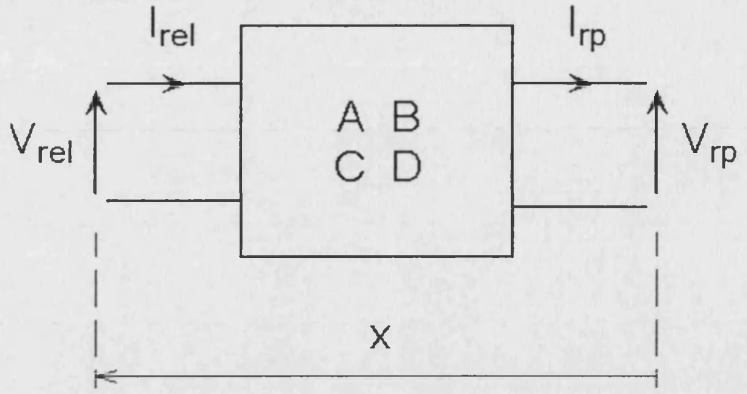

Figure 5.2 Single Phase Two Port Network Representation Described by Equation 5.3

Writing equations 5.1 and 5.2 in matrix form, substituting equations 5.5 to 5.8 and making the same variable substitutions as in figure 5.2 gives,

$$\begin{bmatrix} V_{rel} \\ I_{rel} \end{bmatrix} = \begin{bmatrix} A & B \\ C & D \end{bmatrix} \cdot \begin{bmatrix} V_{rp} \\ I_{rp} \end{bmatrix}$$

Equation 5.12

Equation 5.12 should be interpreted accordingly. V_{rel} and I_{rel} are the voltage and current measured at a relaying point. V_{rp} and I_{rp} are the voltage and current some distance x from relaying point along the line. By choosing x equal to 80% of line section length, V_{rp} and I_{rp} are the voltage and current at the reach boundary of zone 1 – the reach point.

The network of figure 5.2 can be considered passive, linear and bilateral. Equation 5.12 may thus be transposed to yield equation 5.11.

$$\begin{bmatrix} V_{rp} \\ I_{rp} \end{bmatrix} = 1/\text{Det} \cdot \begin{bmatrix} D & -B \\ -C & A \end{bmatrix} \cdot \begin{bmatrix} V_{rel} \\ I_{rel} \end{bmatrix}$$

Equation 5.13

where the determinant is given by,

$$\text{Det} = [AD - BC] = 1$$

Equation 5.14

Equation 5.14 always equals 1 for a symmetrical, passive, linear, bilateral two port network[37]. Assuming ideal transposition of the composite circuit equation 5.13 becomes,

$$\begin{bmatrix} V_{rp} \\ I_{rp} \end{bmatrix} = \begin{bmatrix} D & -B \\ -C & A \end{bmatrix} \cdot \begin{bmatrix} V_{rel} \\ I_{rel} \end{bmatrix}$$

Equation 5.15

Equation 5.15 enables voltage and current at the zone 1 reach point to be calculated. The assumptions made here are that V_{rel} and I_{rel} are available as vectors at fundamental power system frequency (50Hz), and the relationship between line and cable PPS and ZPS series and shunt parameters per unit length are as described in section 2.6.1 and 2.6.2.

5.3 Three Phase Network Representation

The power systems considered in this work are three phase and thus possess some degree of mutual coupling. The extent of which will depend upon circuit construction type and electrical conditions. In order for the theory of section 5.2 to be useful to the development of an impedance based relay algorithm it must be extended to the three phase case.

There exists a procedure for this, originally conceived by Wedepohl [34]. The method relies upon the assumption of ideal transposition of circuit phases. In distribution systems lines are short in length and cable cores a laid together in a helical construction within an outer sheath making this latter assumption reasonable.

For a distance x along a transmission line the ABCD parameters are now evaluated from equations 5.16 to 5.19.

$$[A_x] = [S] \cdot [\cosh(\gamma x)] \cdot [S]^{-1}$$ **Equation 5.16**

$$[B_x] = [Z_0] \cdot [S] \cdot [\sinh(\gamma x)] \cdot [S]^{-1}$$ **Equation 5.17**

$$[C_x] = [Y_0] \cdot [S] \cdot [\sinh(\gamma x)] \cdot [S]^{-1}$$ **Equation 5.18**

$$[D_x] = [A_x]$$ **Equation 5.19**

where,

$$[Z_0] = [S] \cdot [Z_c] \cdot [S]^{-1}$$ **Equation 5.20**

$$[Y_0] = [S] \cdot [Y_c] \cdot [S]^{-1}$$ **Equation 5.21**

$$[\cosh(\gamma x)] = \begin{bmatrix} \cosh(\gamma_1 x) & 0 & 0 \\ 0 & \cosh(\gamma_2 x) & 0 \\ 0 & 0 & \cosh(\gamma_3 x) \end{bmatrix}$$ **Equation 5.22**

$$[\sinh(\gamma x)] = \begin{bmatrix} \sinh(\gamma_1 x) & 0 & 0 \\ 0 & \sinh(\gamma_2 x) & 0 \\ 0 & 0 & \sinh(\gamma_3 x) \end{bmatrix}$$ **Equation 5.23**

$$[Z_c] = \begin{bmatrix} Z_{c1} & 0 & 0 \\ 0 & Z_{c2} & 0 \\ 0 & 0 & Z_{c3} \end{bmatrix} = [Y_c]^{-1}$$ **Equation 5.24**

$$\gamma_1 = (z_{10} y_{10})^{1/2}$$ **Equation 5.25**

$$\gamma_2 = \gamma_3 = (z_{11} y_{11})^{1/2}$$ **Equation 5.26**

$$Z_{c1} = \left(\frac{z_{10}}{y_{10}}\right)^{1/2}$$ **Equation 5.27**

$$Z_{c2} = Z_{c3} = \left(\frac{z_{11}}{y_{11}}\right)^{1/2}$$ **Equation 5.28**

the subscripts 0 and 1 denote ZPS and PPS component quantities respectively. For convenience , Karrenbauer's modal transformation is used:

$$[S] = \frac{1}{3}\begin{bmatrix} 1 & 1 & 1 \\ 1 & 0 & -1 \\ 1 & -1 & 0 \end{bmatrix}$$ **Equation 5.29**

Each of the ABCD parameters of equations 3.5 to 3.8 is replaced with a 3 x 3 matrix of self and mutually coupled parameters. System voltage and current matrices are now 1 x 6 column matrices. Equation 5.12 becomes,

$$\begin{bmatrix} V_{arel} \\ V_{brel} \\ V_{crel} \\ I_{arel} \\ I_{brel} \\ I_{crel} \end{bmatrix} = \begin{bmatrix} \begin{bmatrix} A_{x11} & A_{x12} & A_{x13} \\ A_{x21} & A_{x22} & A_{x23} \\ A_{x31} & A_{x32} & A_{x33} \end{bmatrix} & \begin{bmatrix} B_{x11} & B_{x12} & B_{x13} \\ B_{x21} & B_{x22} & B_{x23} \\ B_{x31} & B_{x32} & B_{x33} \end{bmatrix} \\ \begin{bmatrix} C_{x11} & C_{x12} & C_{x13} \\ C_{x21} & C_{x22} & C_{x23} \\ C_{x31} & C_{x32} & C_{x33} \end{bmatrix} & \begin{bmatrix} D_{x11} & D_{x12} & D_{x13} \\ D_{x21} & D_{x22} & D_{x23} \\ D_{x31} & D_{x32} & D_{x33} \end{bmatrix} \end{bmatrix} \cdot \begin{bmatrix} V_{arp} \\ V_{brp} \\ V_{crp} \\ I_{arp} \\ I_{brp} \\ I_{crp} \end{bmatrix}$$

Equation 5.30

Equation 5.15 becomes,

$$\begin{bmatrix} V_{arp} \\ V_{brp} \\ V_{crp} \\ I_{arp} \\ I_{brp} \\ I_{crp} \end{bmatrix} = \begin{bmatrix} \begin{bmatrix} D_{x11} & D_{x12} & D_{x13} \\ D_{x21} & D_{x22} & D_{x23} \\ D_{x31} & D_{x32} & D_{x33} \end{bmatrix} & \begin{bmatrix} -B_{11} & -B_{12} & -B_{13} \\ -B_{21} & -B_{22} & -B_{23} \\ -B_{31} & -B_{32} & -B_{33} \end{bmatrix} \\ \begin{bmatrix} -C_{x11} & -C_{x12} & -C_{x13} \\ -C_{x21} & -C_{x22} & -C_{x23} \\ -C_{x31} & -C_{x32} & -C_{x33} \end{bmatrix} & \begin{bmatrix} A_{11} & A_{12} & A_{13} \\ A_{21} & A_{22} & A_{23} \\ A_{31} & A_{32} & A_{33} \end{bmatrix} \end{bmatrix} \cdot \begin{bmatrix} V_{arel} \\ V_{brel} \\ V_{crel} \\ I_{arel} \\ I_{brel} \\ I_{crel} \end{bmatrix}$$

Equation 5.31

5.4 Representation of Non-homogenous Network Sections

This work seeks to investigate the composite or non-homogenous network where two or more sections of line or cable may be connected in series to form the continuos feeder.

Consider the two three phase sections of differing lengths and electrical parameters connected in series as in figure 5.3.

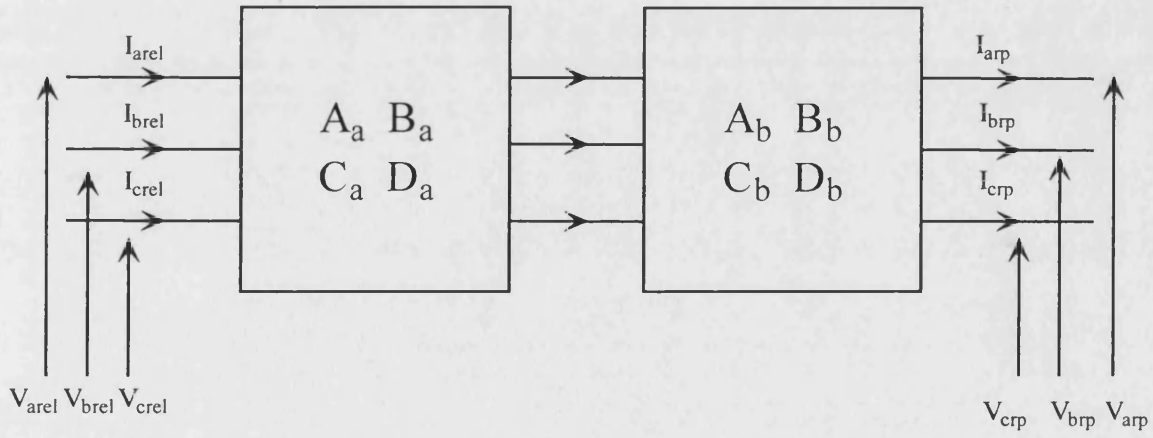

Figure 5.3 Two Non-Homogenous Network Sections in Series

In order to arrive at an equation similar to 5.30 the two matrices of hyperbolic parameters for each section (in this case denoted by subscripts a and b) are first multiplied together i.e.

$$\begin{bmatrix} \begin{bmatrix} A_a \end{bmatrix} & \begin{bmatrix} B_a \end{bmatrix} \\ \begin{bmatrix} C_a \end{bmatrix} & \begin{bmatrix} D_a \end{bmatrix} \end{bmatrix} \cdot \begin{bmatrix} \begin{bmatrix} A_b \end{bmatrix} & \begin{bmatrix} B_b \end{bmatrix} \\ \begin{bmatrix} C_b \end{bmatrix} & \begin{bmatrix} D_b \end{bmatrix} \end{bmatrix} = \begin{bmatrix} \begin{bmatrix} A_x \end{bmatrix} & \begin{bmatrix} B_x \end{bmatrix} \\ \begin{bmatrix} C_x \end{bmatrix} & \begin{bmatrix} D_x \end{bmatrix} \end{bmatrix}$$

Equation 5.32

Substituting the result of equation 5.32 into equation 5.30 and transposing gives,

$$\begin{bmatrix} V_{arp} \\ V_{brp} \\ V_{crp} \\ I_{arp} \\ I_{brp} \\ I_{crp} \end{bmatrix} = \begin{bmatrix} \begin{bmatrix} D_x \end{bmatrix} & \begin{bmatrix} -B_x \end{bmatrix} \\ \begin{bmatrix} -C_x \end{bmatrix} & \begin{bmatrix} A_x \end{bmatrix} \end{bmatrix} \cdot \begin{bmatrix} V_{arel} \\ V_{brel} \\ V_{crel} \\ I_{arel} \\ I_{brel} \\ I_{crel} \end{bmatrix}$$

Equation 5.33

The method extends to the general case of 'n' number of series connected three phase sections. For simplicity the composite feeders in this work are restricted to two sections.

5.5 Scope for Use in Zonal Distance Protection Fault Discrimination

Setting x equal to 80% of the total length (L_{en}) of a composite circuit comprising two sections and calculating the 6x6 ABCD hyperbolic parameters matrix in equation 5.32, equation 5.33 yields the complex values of voltage and current at the reach point.

Figure 5.4 depicts a simplified composite network comprising section 1 and 2. The rest of the system has been reduced to two electrical sources. A relay installed at S measuring three phase voltage and current and using equation 5.33 can thus calculate the voltage and current signals at the 80% reach point.

To explain the operation of the impedance based algorithm consider an a-earth fault of zero Ohms at the reach point (flt_a). The sketch graph of figure 5.4 shows an approximation of the voltage profile over the composite circuits total length. V_{arp} at the fault point will theoretically equal zero thus making Z_{arp} equal to zero also. It can be shown [38] that the impedance at the reach point can be calculated using equation 5.34.

$$Z_{arp} = {}^{V_{arp}}\!/_{I_{arp}} = R_{arp} + jX_{arp}$$

Equation 5.34

If however the same fault were to occur either behind or beyond the reach point (flt_b or flt_c respectively) then V_{arp} has some value and equation 5.34 will now yield some value of impedance Z_{arp}. The sign of the imaginary component jX_{arp} can be used to indicate if an earth fault is in front or beyond the reach point. Table 5.1 summarises the discrimination criteria.

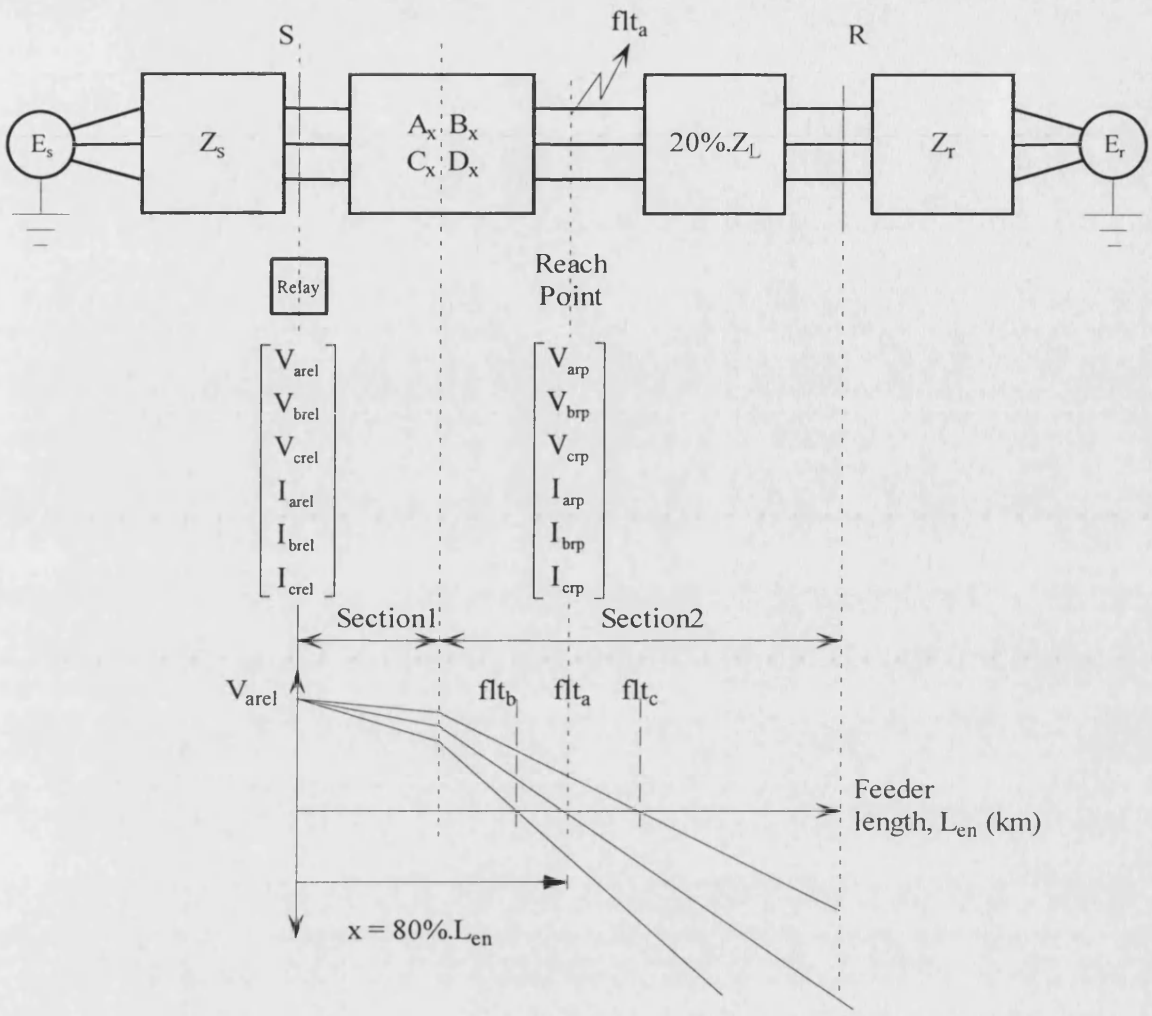

Figure 5.4 : Application of Equation 5.33 to Representation of Composite Circuit Zone One.

Reach Point Impedance Quadrature Component	Discrimination Meaning
$-jX_{arp}$	In Zone
$jX_{arp} = 0$	On Reach Point
$+jX_{arp}$	Out of Zone

Table 5.1 : Discrimination Criteria Utilising the Sign of Reach Point Impedance Quadrature Quantity jX_{arp}

The accuracy of the criteria summarised in table 5.1 has been demonstrated for a typical 33kV composite power distribution feeder. Consider a single end fed feeder comprising 20km 0.3 sq. in., 3 Core, Cu, 'H' type 33kV MIND insulated cable and 20km of 0.2 sq. in., 3 wire, Cu, flat wood pole construction line connected in series. The source bars have a three phase short circuit level of 500 MVA and a three phase inductive load of 0.8 power factor lagging is connected at the remote end. The circuit was modeled using the

steady state test harness described in chapter 6. A zero Ohm a - earth fault was applied between 50% and 100% of the circuits total length in 1% incremental steps. A plot of jX_{arp} for varying remote end load levels (0.0 to 50.0 MVA) is shown in figure 5.5. jX_{arp} can be seen as equaling zero for an earth fault at the reach point (80%). For the faults beyond the reach point (80 to 100%) jX_{arp} becomes a positive value. For those a-earth faults occurring behind the reach point jX_{arp} is negative. Thus, a simple test for the sign of jX_{arp} as described in table 5.1 can be used for fault discrimination. Exhaustive testing proved this discrimination technique for zero Ohm a -earth faults on all realistic combinations of composite circuit operating parameters and lengths.

Figure 5.5 : jX_{arp} v's Fault Position. Src Bars SCL = 500MVA, Composite Circuit (20km Cable+20km Line), Varying Remote End Load @ 0.8 pf lag. Fault = 'a' - 'earth' of 0.0 Ohms Resistance.

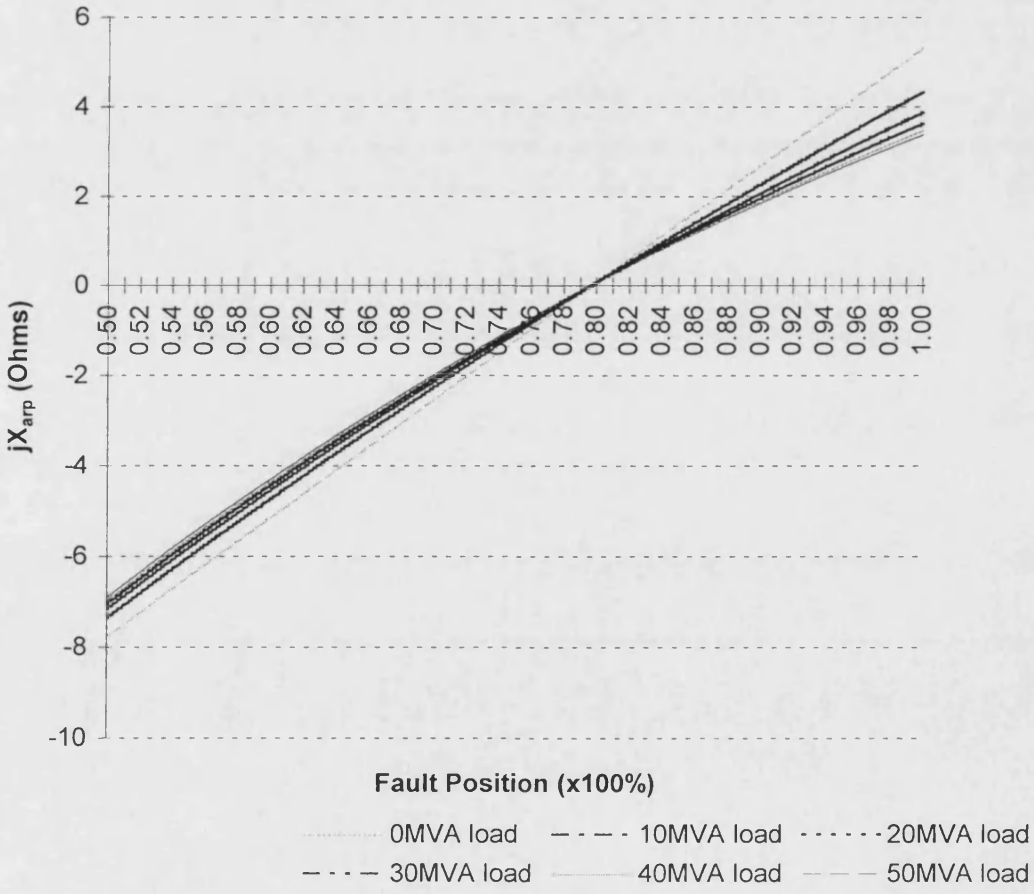

5.6 Implementation of Earth Fault Discrimination Using a Quadrilateral Tripping Characteristic

A novel quadrilateral tripping characteristic is used for the discrimination of earth faults. Figure 5.6 shows this for the case of an a-earth fault. Calculated impedance at both the relaying point and the reach point in addition to a user defined resistive blinder setting R_b are required to describe a suitable quadrilateral characteristic.

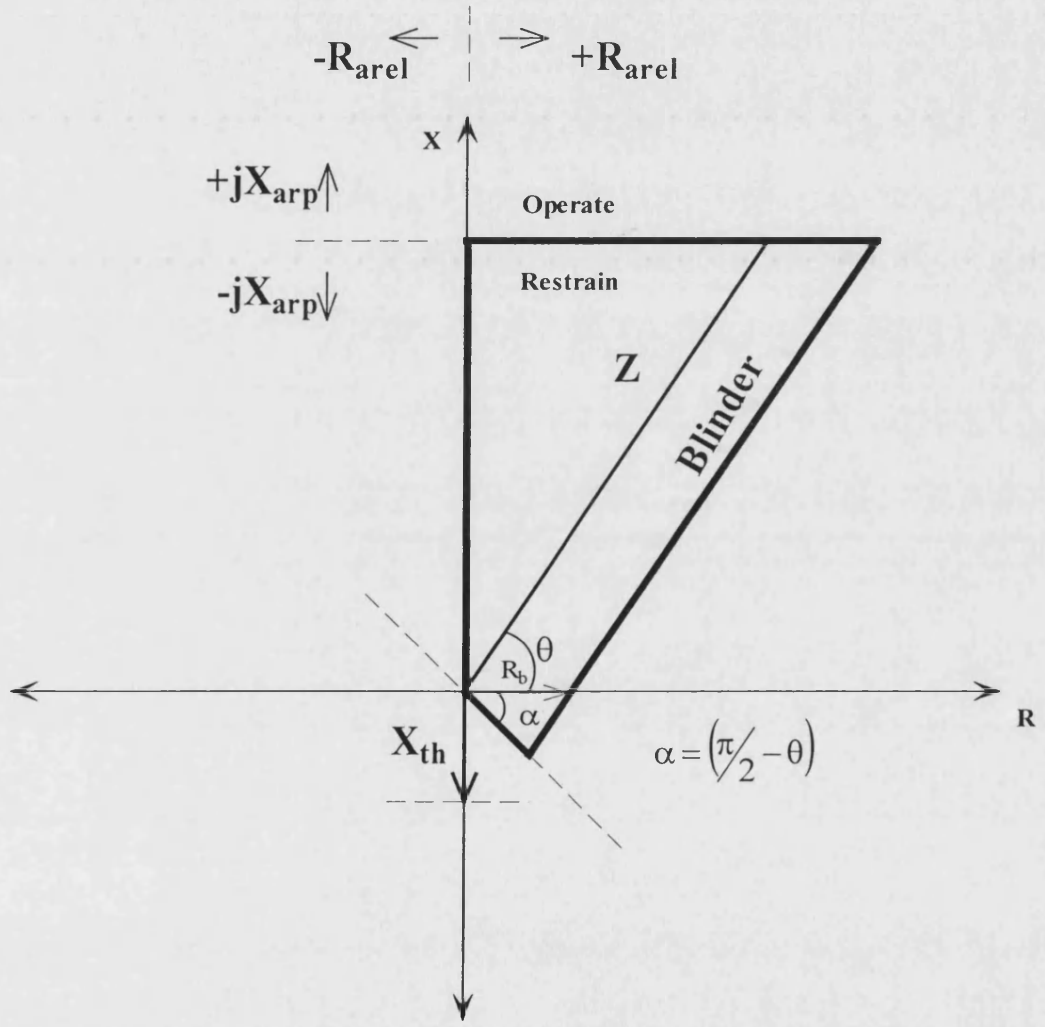

Figure 5.6: Earth Fault Element Quadrilateral Tripping Criteria.

The top reactance line is defined using the sign of jXarp obtained from equation 5.34.

To define the bottom and left hand boundaries the impedance at the relaying point must be found using equation 5.35.

$$Z_{arel} = \frac{V_{arel}}{I_{arel}} = R_{arel} + jX_{arel}$$

Equation 5.35

The left boundary is defined by the sign of R_{arel}. Zero or positive values of R_{arel} define a possible in zone event.

To implement the bottom of the characteristic and provide directionality to the discriminatory procedure a reactance threshold value, X_{th} must be defined. Such a value may be found from equation 5.36.

$$X_{th} = R_b \tan \alpha$$

Equation 5.36

R_b represents a resistive blinder value that must be defined in commissioning and

$$\alpha = \left(\pi/2\right) - \theta$$

Equation 5.37

where θ represents the characteristic impedance angle of the protected feeder.

X_{arel} must be obtained by using equation 5.35, such that a comparison with X_{th} and may be made to define the bottom boundary. A possible in zone event would be indicated by the condition $X_{arel} \geq X_{th}$. Such a definition allows those earth faults occurring close in to the relay to be detected.

Earth fault compensation of the measured or calculated phase currents is not required. The characteristic of the network in terms of zero and positive phase sequence parameters are inherent in the hyperbolic parameters.

The right side of the characteristic is a resistive blinder. Such a blinder allows the coverage of earth fault resistance as estimated likely to occur, and would be derived with consideration to construction and likely loading of a particular circuit.

5.7 Effect of Fault Resistance on Discrimination Accuracy

In practice faults on overhead line sections often result in arcs which possess resistance of some value. Further more, steel work , cast iron cable termination boxes and line supports represent significant resistance to the flow of fault current to earth. Composite networks contain overhead line sections thus the effect of high resistance earth faults must be considered.

Using the same circuit as in section 5.5, additional experiments involving the application of a-earth faults of resistance values 1.0 through 50.0 Ohms were conducted. Figures 5.7 and 5.8 show the resulting plots of jX_{arp} against fault position for varying load levels at fault path resistance values of 10.0 and 30.0 Ohms respectively. The remaining results exhibit the same general trend.

In figure 5.7 for the circuit on no load accurate discrimination can be seen to be maintained. However, significant amounts of overreach can be observed for increasing terminating load. For example, when supplying a load of 30.0 MVA the algorithm would be subject to overreach of 7% of the total zone length.

Figure 5.7 : jX_{arp} v's Fault Position. Src Bars SCL = 500 MVA, Composite Circuit (20km Cable+20km Line), Varying Remote End Load @ 0.8 PF Lag. Fault = 'a' to 'earth' of 10.0 Ohms Resistance.

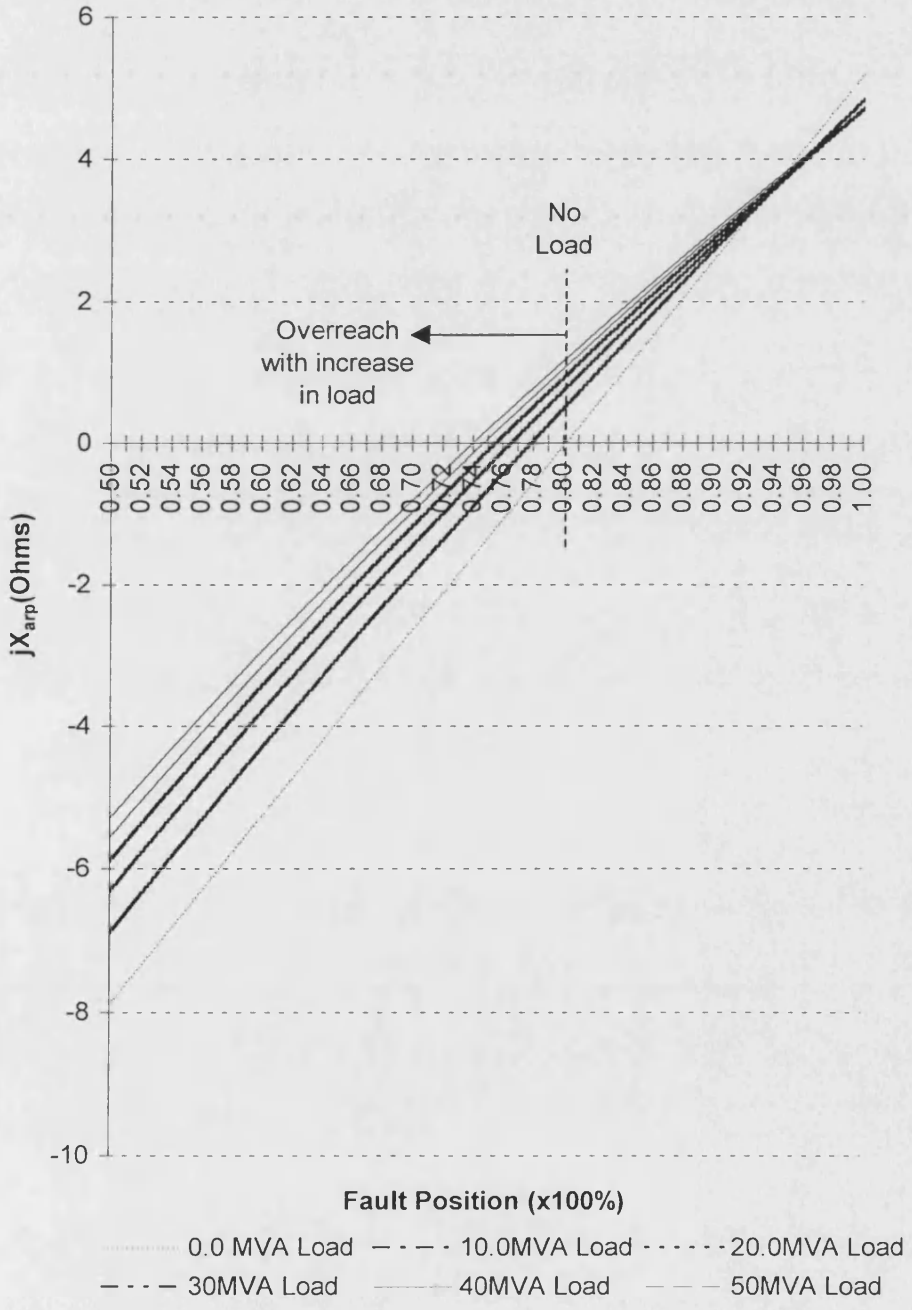

Figure 5.8 : jX_{arp} v's Fault Position. Src Bars SCL = 500MVA, Composite Circuit (20km Cable+20km Line), Varying Remote End Load @ 0.8 PF Lag. Fault = 'a' to 'earth' of 30.0 Ohms Resistance.

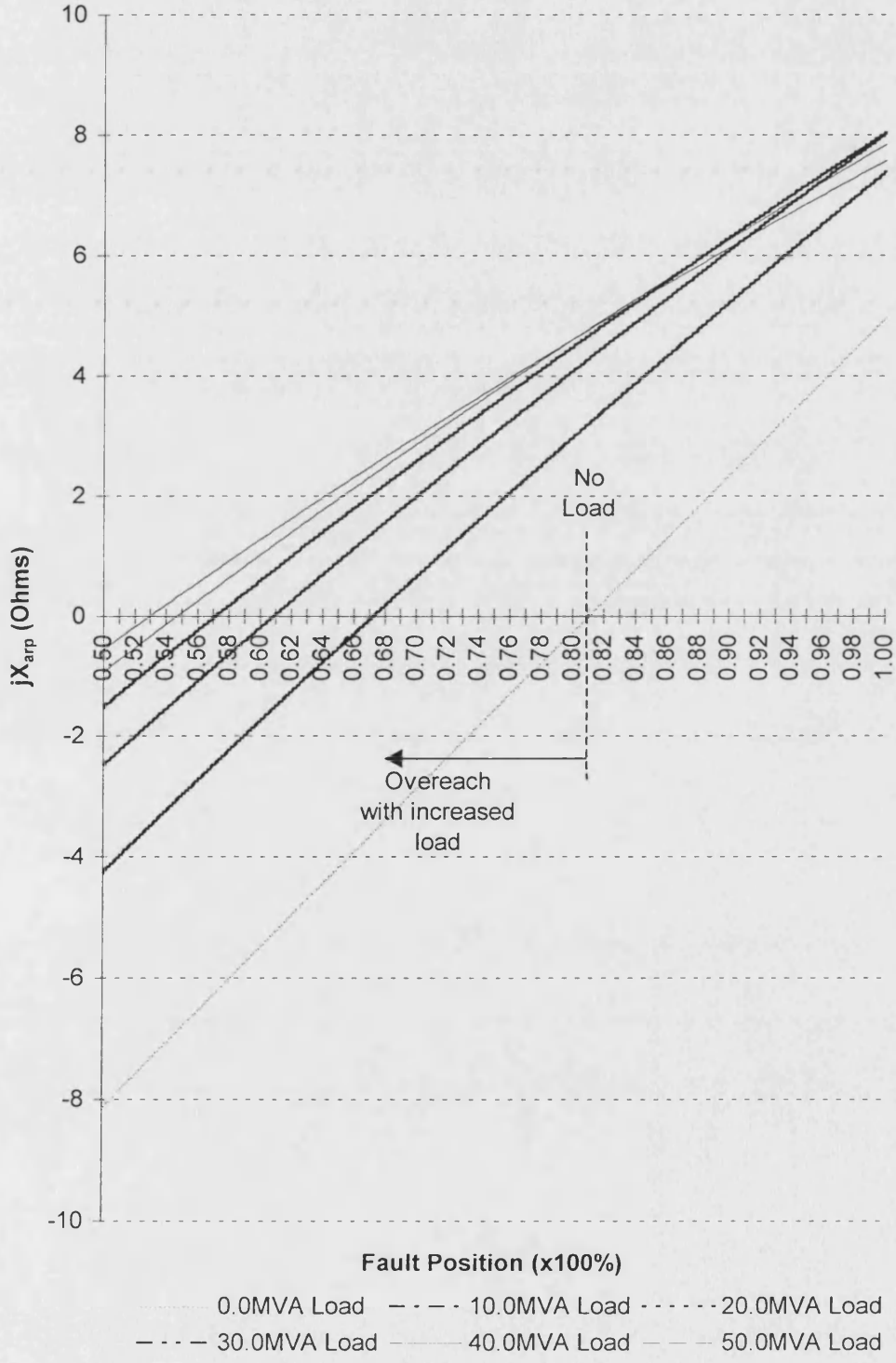

For the circuit subject to the same load conditions but now having an a-earth fault of 30.0 Ohms applied overreach becomes significant. For a remote end load value of 30.0 MVA overreach of 40.0 % of total zone length is experienced.

Most circuits are electrically loaded to some extent. Earth faults are likely to comprise some value of resistance whether attributable to arc formation or support structures. The affect of circuit loading and earth fault path resistance on the polarity of the reach point measured impedance quadrature component, jX_{arp} , must be reduced.

5.8 Improved Reach Point Earth Fault Discrimination Using Pre - Fault Load Estimation

When earth fault path resistance becomes significant under certain remote end load conditions a parallel circuit will be formed and can be seen in figure 5.9. The 20% of feeder total length between the load and fault resistance values is included in Y_l . The argument for determining a reach point imaginary impedance value jX_{arp} and using its polarity to determine an in or out of zone fault - as summarised in table 5.1 - now becomes subject to error. Impedance Z_{arp} calculated at the reach point terminals for these conditions is that of the parallel single phase circuit of figure 5.9(b). Fault path resistance and remote end load are expressed as admittance values to simplify computation. An estimation of Y_{al} the phase 'a' pre- fault load must be made in order for the parallel circuit of figure 5.9(b) to be resolved and the effect of remote end load reduced. In this manner the polarity of jX_{arp} becomes more accurate under high resistance earth fault conditions.

With reference to figure 5.9 during pre-fault,

$$Y_{al} = I'_{arp} / V'_{arp}$$

Equation 5.38

and post fault .....

$$Y_{af} = (I_{arp} / V_{arp}) - Y_{al}$$

Equation 5.39

Y_{af} is then the fault path admittance which can be expressed as an impedance using,

$$Z_{af} = 1/Y_{af} = R_{af} + jX_{af}$$

Equation 5.40

and for a high resistance earth fault at the reach point should have a negligible imaginary component. i.e.

$$Z_{af} \approx R_{af}$$

Equation 5.41

The polarity of the jX_{af} should now be used in place of jX_{arp} to approximate the top line of the tripping characteristic of figure 5.6, and as summarised in table 5.1.

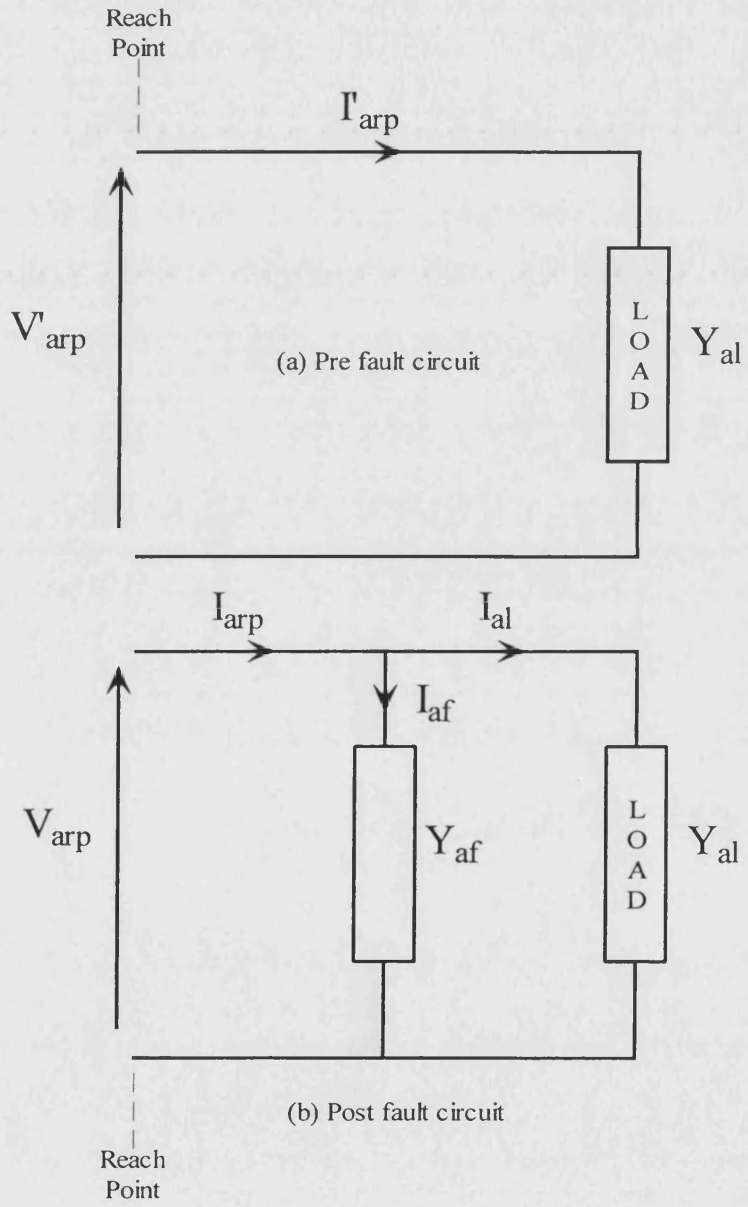

Figure 5.9 : Single Phase Circuit representation (a) Pre Fault Circuit at Reach Point (b) Post Fault Parallel Circuit Formed By Earth Fault Path Resistance and Remote End Load (expressed as admittance).

Repeating the experimentation of section 5.7, figures 5.10 and 5.11 are obtained. For the earth faults of 10.0 Ohms, significant improvement in discrimination is achieved. A small under reach of approximately 1.25 % can be observed for a remote end load of 30.0 MVA. For the case of a 30.0 Ohms fault at the reach point of the circuit subject to the same remote end load an under reach of 3.7% is now observed.

The method represents an approximation of remote end load. The assumption of no mutual coupling within the load is made. However, significant improvement in accuracy is observed. When considering the likely error represented by inaccuracies of the data records defining circuit length or the approximation in data sheet parameters and their use, this approximation becomes tenable.

5.9 Phase Fault Discrimination

The approach for a-earth faults applies equally to the 'b' and the 'c' phase thus there exists in the prototype three separate earth fault elements. These elements also operate for the occurrence of three phase faults (a-b-c and a-b-c-e).

Applying the theory of symmetrical components[37] it can be shown that for a b-c fault equation 5.39 becomes,

$$Y_{bcf} = \frac{(I_{brp} - I_{crp})}{(V_{brp} - V_{crp})} - Y_{bcl}$$

Equation 5.42

where,

$$Y_{bcl} = \frac{(I'_{brp} - I'_{crp})}{(V'_{brp} - V'_{crp})}$$

Equation 5.43

and

$$Z_{bcf} = 1/Y_{bcf} = R_{bcf} + jX_{bcf}$$

Equation 5.44

The sign of jX_{bcf} is now used to determine the top line of a quadrilateral characteristic similar to that of figure 5.6. To complete the determination of the characteristic equation 5.35 becomes,

$$Z_{bcrel} = \frac{(V_{brel} - V_{crel})}{(I_{brel} - I_{crel})} = R_{bcrel} + jX_{bcrel}$$

Equation 5.45

The resistance in a b-c fault will differ from that for single phase faults to earth. Therefore a phase fault resistive blinder setting R_{bp} is used to determine the right side of the tripping characteristic. As a consequence an additional reactance threshold value X_{thp} must also be calculated using equation 5.46.

$$X_{thp} = R_{bp} \tan \alpha$$

Equation 5.46

Where α is defined by equation 5.37.

A possible in zone event would be indicated by the condition $X_{bcrel} \geq X_{thp}$ .The method extends in a similar manner for a-b and a-c faults.

5.10 Algorithm Status

The prototype impedance algorithm has been coded in the high level computing language FORTRAN77. This algorithm is embedded within the transient test harness described in section 4.6. Complex values of the fundamental voltage and current derived using the DFT filters described in section 4.6.5 are input. A full cycle of discrete time sampled input fundamental voltage and current is required prior to the first output of complex quantities.

Three earth fault elements and three phase fault elements are provided. A phase selection technique would be required to determine which elements should be allowed to operate for certain fault conditions. Currently, for an a-earth fault the necessary voltage and current inputs are manually pre-selected for application to the a-earth fault element. Presently, only zone 1 protection is afforded. Both phase and earth faults are discriminated using the quadrilateral characteristic of section 5.6.

The algorithm models a two section composite circuit. Four system configurations are allowed; line-line, line-cable, cable-line and cable-cable. At start up the 6x6 matrix of hyperbolic parameters to the zone 1 reach point is calculated. The complex hyperbolic trigonometric functions of equation 5.10 and 5.11 are solved using high level programming language library functions. It would be proposed to find these solutions using the relevant series expansion. In this way the solution would progress using a sequence of multiplication, division, addition and subtraction operations more suited to implementation on a DSP chip. The algorithm requires one cycle of power system fundamental voltage and current waveforms such that pre fault load compensation can be made. During start up back up protection could be afforded by instantaneous overcurrent functionality.

Figure 5.10 : jX_{af} v's Fault Position. Src Bars SCL = 500MVA, Composite System(20km Cable+20km Line), Varying Remote End Load@0.8 PF Lag. Fault = 'a' to 'earth' of 10.0 Ohms Resistance. Prefault Load Estimation Initialised.

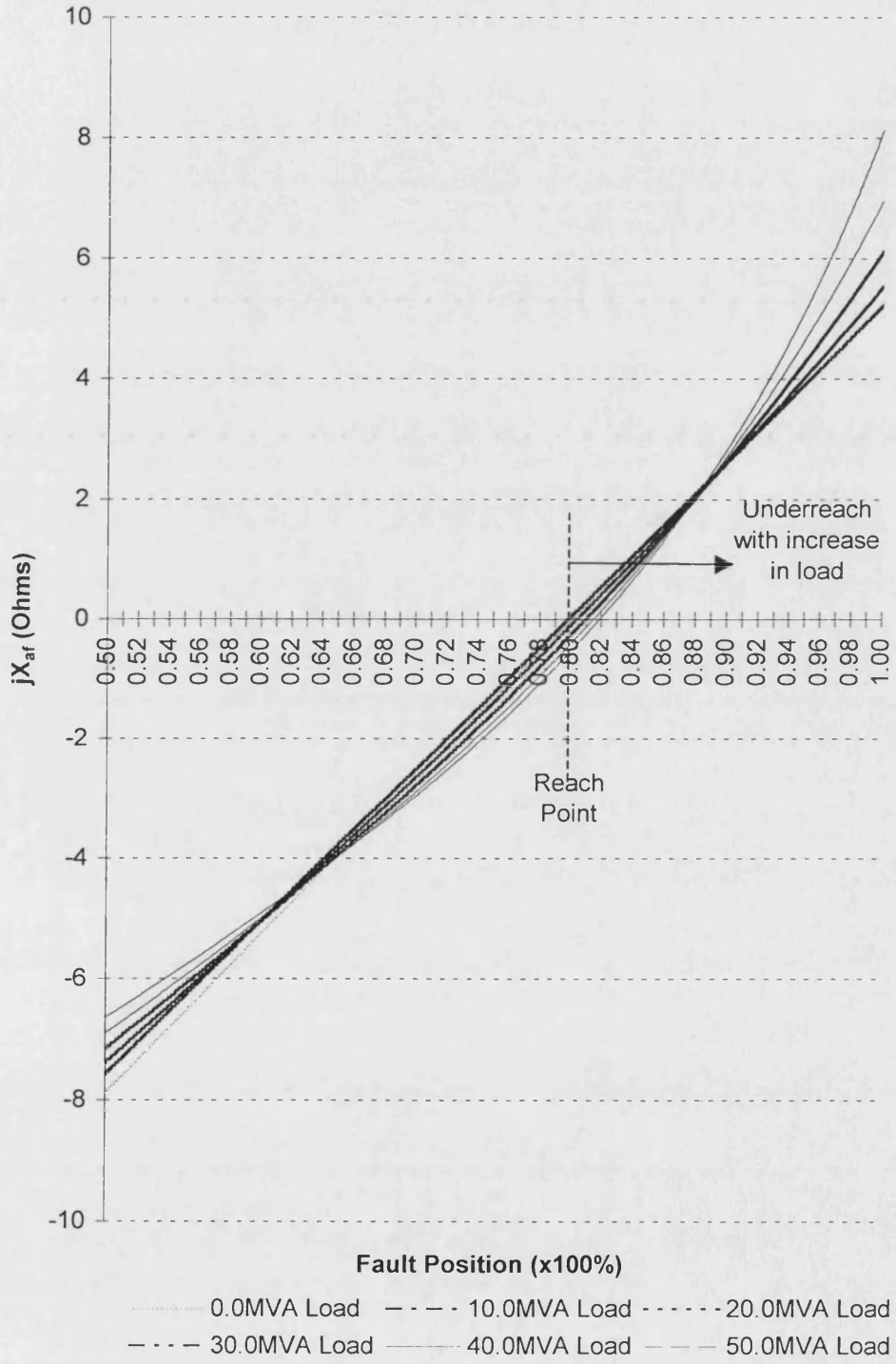

Figure 5.11 : jX_{af} v's Fault Position. Src Bars SCL = 500MVA, Composite System(20km Cable+20km Line), Varying Remote End Load@0.8 PF Lag. Fault = 'a' to 'earth' of 30.0 Ohms Resistance. Prefault Load Estimation Initialised.

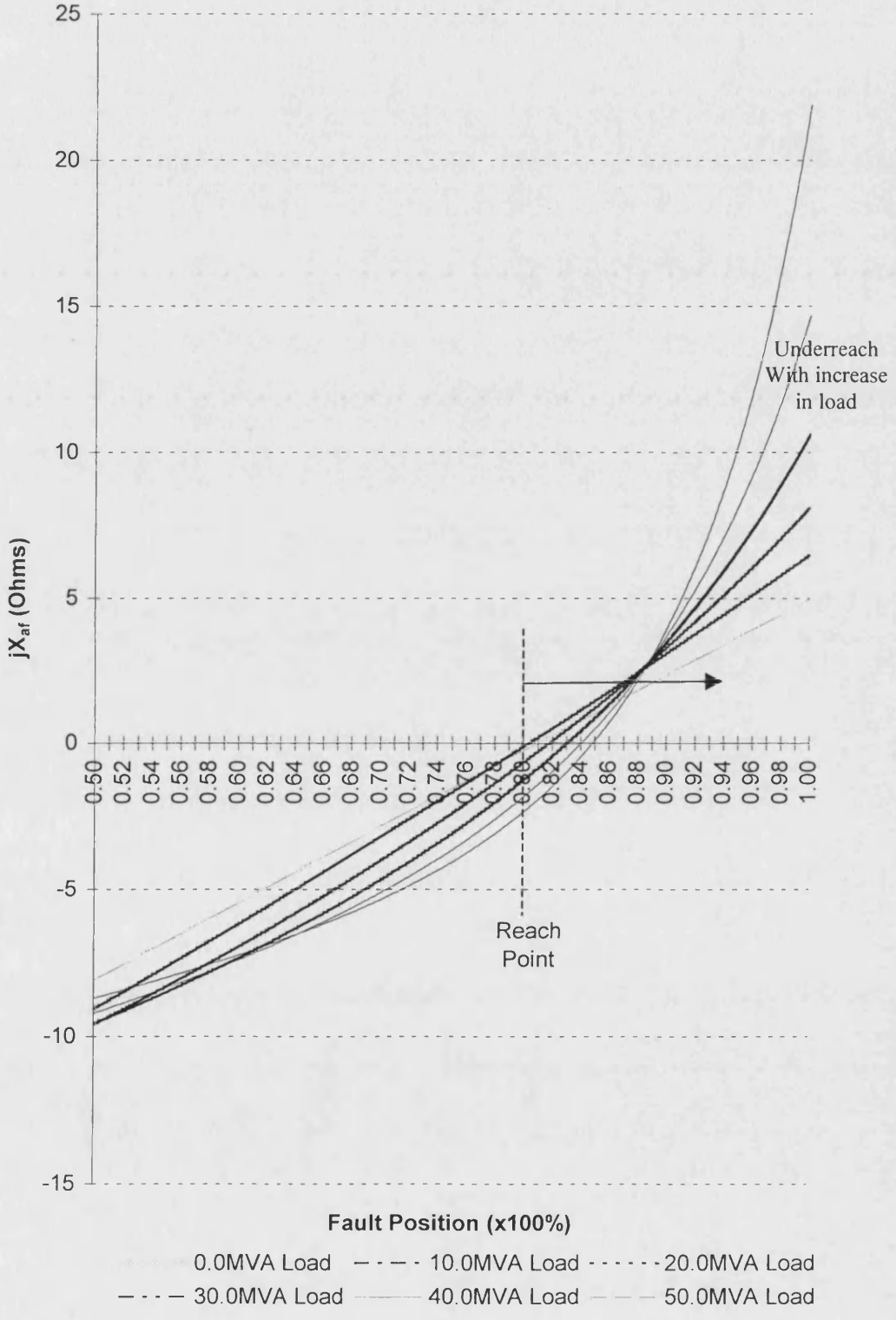

Table 5.2 lists the parameters required for input to the prototype impedance algorithm. They can be obtained from manufacturers data sheets.

Parameter	Section 1	Section 2	Unit
Length	D_1	D_2	km
PPS Resistance	R_{11}	R_{21}	Ω/km
ZPS Resistance	R_{10}	R_{20}	Ω/km
PPS Self Inductance	X_{11}	X_{21}	Ω/km
ZPS Self Inductance	X_{10}	X_{20}	Ω/km
PPS Admittance	$1/Xc_{11}$	$1/Xc_{21}$	μmhos/km
ZPS Admittance	$1/Xc_{10}$	$1/Xc_{20}$	μmhos/km
Conductance	Neglected	Neglected	-
Resistive Blinder Earth Fault	R_b		Ω
Resistive Blinder Earth Fault	R_{bp}		Ω
Reach Point	$x = 0.8 * L_{en}$ where $L_{en}=(D_1+D_2)$		% of L_{en}

Table 5.2 Input Parameters Required by Impedance Algorithm

5.11 Summary

In this chapter through the use of existing transmission line theory, a new impedance measuring algorithm has been developed. Being based on the derivation of the hyperbolic line equations it inherently accounts for both the series and shunt parameters of the protected circuit.

By setting x equal to 80% of total composite feeder length the zone one area of a protected network can be represented. Measurement and extraction of the fundamental three phase voltage and current at the relaying point allows complex quantities of fundamental voltage and current at the reach point to be calculated.

In the case of an a-e fault it is possible to calculate both the impedance at the relaying point and at the zone 1 reach point. It is the knowledge and use of the latter impedance value which is new and aids discrimination of an in or out of zone earth fault by

analysing the sign of the quadrature component of such an impedance. The new quadrilateral characteristic was described.

Account has been taken of the remote end characteristics of the network, and pre-fault load estimation technique is used to improve accuracy in the presence of high resistance a-earth faults.

The prototype algorithm has been created with three earth fault elements and three phase elements. It is a requirement that the data entered to the algorithm should be simple and readily available. Only PPS and ZPS parameters detailed in manufacturers data sheets are required, together with a setting for section lengths and zone 1 reach point.

As described previously both steady state and transient simulation studies have been conducted in this work. Chapter 6 discusses the techniques used for both simulation studies.

Chapter 6

Power System Simulation

6.1 Introduction

Investigation in this work centres on the discrimination of a-e faults of varying fault path resistance occurring at various locations along a composite power distribution feeder.

The prototype impedance relaying algorithm described in chapter 5 requires testing using simulated discrete time sampled three phase voltage and current signals. This approach to algorithm design and development is standard within relay development and precursors any real time simulation studies or practical field trials.

This work uses two different approaches to modelling nominal composite 33kV power systems. One is steady state and relies on the derivation of steady state phasor based derivations of voltage and current vectors using a frequency domain modelling technique. The model forms the front end (section 1) of the steady state software test harness referred to in chapter 4 section 4.5.1. These studies concentrate on discriminating earth faults occurring on a multitude of system configurations. It investigates reach point accuracy of the prototype algorithm in comparison with other common impedance relaying methods.

In addition transient simulation studies have been conducted. In this case the existing electromagnetic transient simulation package ATP has been utilised. Having generated voltage and current waveforms for composite networks subject to differing fault conditions the data is input to the new prototype impedance protection relay. This investigation is limited to a few system configurations and operating parameters but measures the relay operating time for both zone 1 a-earth and b-c phase faults.

Results obtained are presented and discussed in Chapter 7. This chapter outlines the modelling techniques.

6.2 Steady State Phasor Based Simulation Software

This modelling is based on the theory of superimposed networks. A faulted network is represented as the sum of the pre fault and superimposed networks.

The method allows for modelling of a two section composite network, and is based on a three phase distributed line model of hyperbolic parameters. The method is most easily described by reference to figure 6.1.

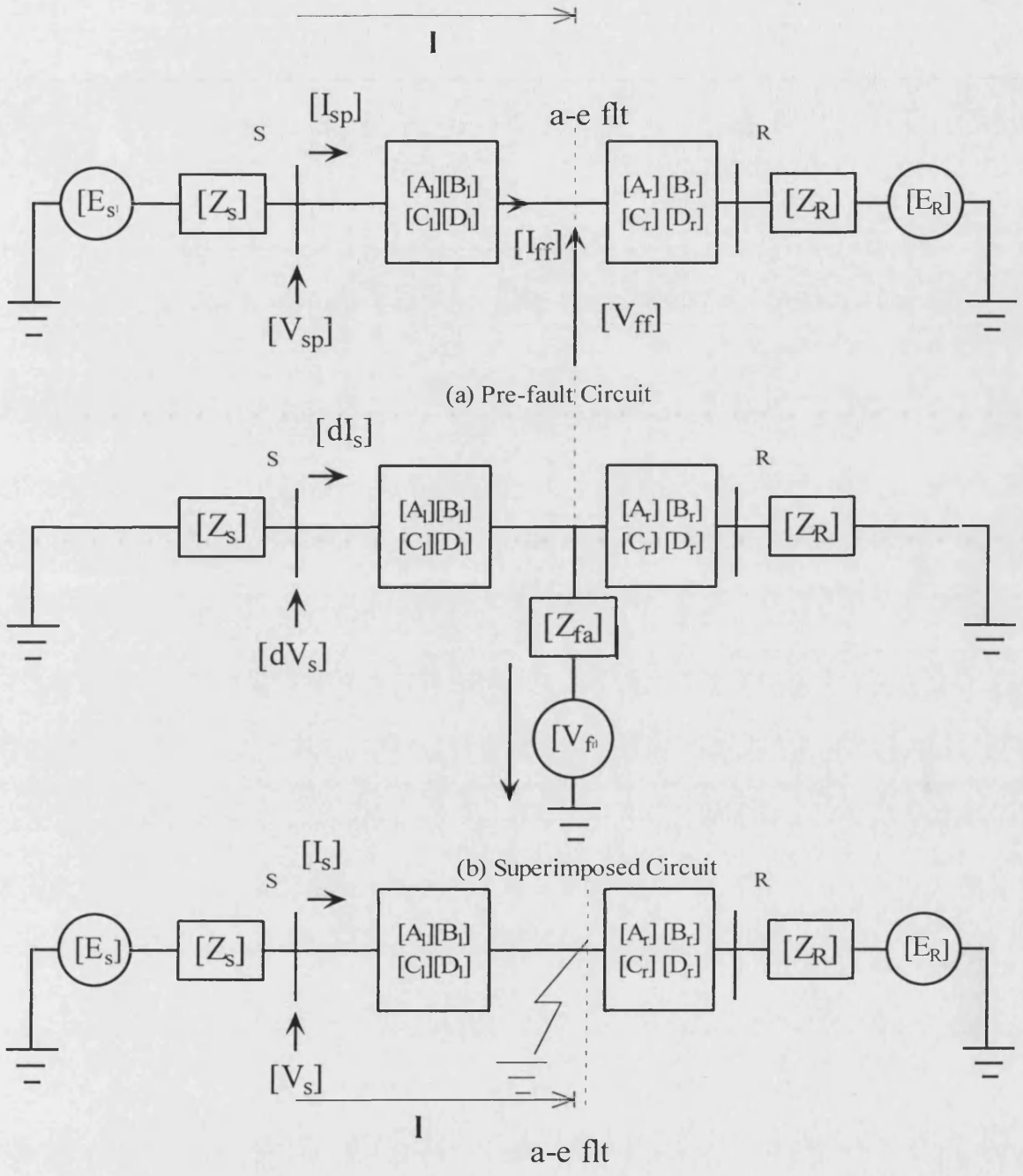

Figure 6.1 Steady State Faulted Simulation System Model (a) Pre-fault Circuit (b) Superimposed Circuit (c) Resolved Circuit.

Figure 6.1 shows a three phase representation of a pre-fault circuit (a), a superimposed circuit (b), and a final resolved circuit (c). In all three circuits power flow is assumed from S to R. In circuit (c) [Vs] and [Is] are 1x3 matrices of three phase voltage and current respectively, at the sending end bus bar of the earth faulted circuit. These are the quantities required for input to the prototype algorithm.

The 3x3 matrices of hyperbolic parameters $[A_l][B_l][C_l]$ and $[D_l]$ are found for the

system fundamental frequency and represent the system between the sending end bars and the a-earth fault location. Similarly, $[A_r]$ $[B_r]$ $[C_r]$ and $[D_r]$ are found for the system beyond the fault point. Source voltages $[E_S]$ and $[E_R]$ and user defined inputs. The source impedance matrices $[Z_S]$ and $[Z_R]$ are derived at fundamental frequency using PPS and ZPS impedance values as shown in Appendix 6.2.

The pre-fault circuit (a) is solved in the frequency domain at fundamental power system frequency (50.0Hz). The pre-fault voltage and current $[V_{ff}]$ and $[I_{ff}]$ at the fault point are calculated from a knowledge of the hyperbolic parameters of the total circuit length and the source voltages. The sending end voltage and currents [Vsp] and [Isp] can then be calculated using equation 6.1.

$$\begin{bmatrix}[V_{sp}]\\ [I_{sp}]\end{bmatrix} = \begin{bmatrix}[D_l] & [-B_l]\\ [-C_l] & [A_l]\end{bmatrix} \cdot \begin{bmatrix}[V_{ff}]\\ [I_{ff}]\end{bmatrix}$$

Equation 6.1

The superimposed circuit (b) removes the source voltages and determines a single matrix representation of the parallel circuit seen from the fault point. For an a-earth fault the 'a' phase of the circuit is injected at the fault point with a voltage equal and opposite to $[V_{ff}]$. Note , the inclusion of fault resistance in matrix $[Z_{fa}]$ where,

$$[Z_{fa}] = \begin{bmatrix} R_{fa} & 0 & 0\\ 0 & 0 & 0\\ 0 & 0 & 0\end{bmatrix}$$

Equation 6.2

The sending end voltage and current $[dV_s]$ and $[dI_s]$ are found using the method outlined in Appendix 6.2.

Figure 6.1(c) shows the final resolved circuit. Sending end voltage and current matrices $[V_s]$ and $[I_s]$ are found simply using equations 6.3 and 6.4.

$$[V_s] = [V_{sp}] + [dV_s]$$

Equation 6.3

$$[I_s] = [I_{sp}] + [dI_s]$$

Equation 6.4

These voltage and current matrices supply three software distance relay a-earth fault element simulations described in section 6.3. Appendix 6.1 presents the steady state simulation software in flowchart form. Appendix 6.2 details the matrix mathematics and underlying principles of this modelling technique.

6.3 Distance Relaying Principles Tested using the Frequency Domain Modelling Software

Three relay simulations are included. In each case the necessary parameters for operation are passed from the main simulation routines described in section 6.2 and outlined in the flowcharts of Appendix 6.1. An indication in the form of an individual trip flag setting is returned to the main simulation code according to the specific relay module response where 1 indicates a trip and 0 indicates restrain.

6.3.1 Mho Relay (s.p.m.)

This was described in detail in section 3.4 and the characteristic is shown in figure 3.4. The method of implementing such a relay is simple and described in flowchart Mho()in Appendix 6.1.

6.3.2 Quadrilateral Relay

As described in section 3.6 the method uses the tripping characteristic shown in figure 3.5. A certain value of fault resistance is accounted for by setting a resistive blinder. Flowchart Quad() in Appendix 6.1 details the technique.

6.3.3 New Impedance Algorithm ABCD

The prototype impedance measuring and fault discrimination algorithm was described in detail in chapter 5 and in flowchart form in Appendix 6.1 – Newrel(). No AA or DFT Filters are required as the three phase matrices $[V_S]$ and $[I_S]$ comprise complex vectors of fundamental voltage and current.

6.4 Simulation Automation

To facilitate the simulation studies several controlling loops are incorporated into the simulation routine to allow for multiple runs with varying system parameters. Table 6.1 details these parameters and their limits of variation.

For each composite circuit and associated operating parameters, a value of fault path resistance is first chosen and faults of the selected type applied at incremental positions along the feeder's length. For each fault location the trip signal received from each relay simulation routine is recorded. The next incremental value of fault resistance is then selected and the fault applied again along the length of the network. In this fashion, and

using a controlling loop to detect a change from trip to restrain the reach point boundary is determined for each iterative step in the fault resistance value at each location.

Parameter	Max and Min Values and incremental Values	Units
Cable Section Length (Sec1)	0.0 – 50.0 in inc of 10.0	Km
Line Section Length (Sec2)	0.0 – 30.0 – 50.0	Km
Source Fault Level (P)	10.0 – 1000.0	MVA
For Double end fed Circuit Remote Fault Level (Q)	10.0 – 1000.0	MVA
For Double end fed system Phase shift of remote end Voltage phasors	14.0	Degrees
Fault Type	a-e and a-b-c	N.A.
Fault Resistance	0.0 – 40.0 inc of 2.0	Ohms
Fault Position	0.0 – 100.0 in inc of 1.0	% of total circuit length
For single end fed system Remote end connected load	0.0 – 50.0 in inc of 10.0 (Power Factor = 0.8 lagging)	MVA

Table 6.1 : Steady State Phasor Simulation Parameters

For each adjustment in a circuit parameter or operating condition a separate output file is written to memory. A typical file is shown in figure 6.2, where it can be seen that location of the reach point for each value of fault path resistance is recorded under the respective relaying module title. Data from these files can be easily plotted to show a representation of the reach boundary for each relaying module by plotting fault path resistance against fault position. The results are presented and discussed in detail in Chapter 7.

FAULT RESISTANCE OHMS	MHO BOUNDARY	QUAD BOUNDARY	ABCD BOUNDARY
0.00	0.76	0.77	0.77
4.00	0.67	1.00	0.80
8.00	0.55	0.94	0.82
12.00	0.28	0.88	0.82
16.00	0.20	0.82	0.81
20.00	0.00	0.74	0.79
24.00	0.00	0.60	0.77
28.00	0.00	0.00	0.74
32.00	0.00	0.00	0.72
36.00	0.00	0.00	0.70
40.00	0.00	0.00	0.68

Figure 6.2 : Typical Output file format from Steady State Simulation Software.

6.5 Electromagnetic Transient Simulation

The EMTP in its many forms – such as the ATP used in this work - is a commonly used time domain based tool for the modelling of electromagnetic transients in power systems. As such a long discourse on the workings of EMTP is not necessary here. Instead the reader is referred to references [39].

Of interest here however, is the methods employed within the ATP to model cable and line sections. In the case of overhead line modelling, theories and models are well founded and again the reader is invited to inspect references.

In describing the approach to cable modelling the reader finds the in built cable parameter calculation routines are based on well understood formulae. However, when considering simulation there is a number of options that should be considered.

The work of Marti [40], highlights the main two model types, namely Lumped Parameter models and distributed parameter models. Marti recommends the use of Lumped parameter nominal Pi Circuits for use in modelling cable sections.

In this model the series branch of the nominal Pi circuit is the series impedance of the cable, and the shunt branches consist of half the shunt capacitance of the cable. Shunt conductance is assumed negligible.

The main advantage of this model is it is quick to execute. However, the main draw back is the poor frequency response beyond the frequency at which the cable parameters are calculated. In this work we are interested in modelling the system at the fundamental power frequency (i.e. 50Hz), and hence this is not a concern. Cascading a number of Pi sections approximates the distributed nature of the cable parameters[40].

By the use of measuring components within the programme it is a simple matter to extract discrete time sampled data representing sending end voltage and current to ASCII text output files at each time step of the simulation run. Care should be taken choosing this time step as mentioned in section 4.6.1.

It is this output which is used as input data for the prototype relay when it is inserted into the transient based software test harness described in section 4.5.2.

6.6 Circuits Tested Using The Alternative Transients Program

The steady state simulation described in previous sections is used to assess prototype algorithm performance on a widely varying basis for a–earth faults. The transient simulation studies are limited to a few carefully chosen circuits (as a result of performance based on steady state testing see chapter 7) though b–c phase faults are also studied.

6.7 Output of Results and Formatting of Transient Tests

Having studied the reach boundary performance under varying fault path resistance and fault location parameters, the transient studies provide an indication of typical operating times for the prototype impedance measuring and fault discriminating algorithm. For a given set of circuit parameters a plot of operating time against fault position can be produced.

6.8 Summary

In this chapter two power system modelling techniques have been described.

Firstly, a steady state distributed parameter model solved in the frequency domain and based on superimposed components is used. For a composite circuit subject to an a-earth fault of varying fault path resistance and at various locations along its length, it derives $[V_S]$ and $[I_S]$ at power system fundamental frequency. These are the three phase matrices of complex voltages and current at the sending end busbar. The modelling software routine is automated having a number of loops to allow multiple simulation runs, offering the possibility of simulating many circuit types and operating conditions.

The results of this work take the form of reach boundary plots for a-earth faults and are discussed in Chapter 7. From this discussion the most relevant composite circuit configurations are selected for transient simulation studies.

Transient studies have been completed using the Alternative Transient Simulation Package (ATP) and in particular use is made of the nominal Pi lumped parameter model. Several sections cascaded together provide an estimation of the composite network distributed electrical parameters. The model is valid only at fundamental frequency.

Both a-earth and b-c phase faults are studied with results obtained presented in the form of algorithm operating time against fault location plots. These are discussed in Chapter 7.

Chapter 7

Results

7.1 Introduction

Chapter 6 described the simulation techniques used in this work to test the performance of the prototype impedance protection algorithm proposed.

This chapter presents the results from the studies and discusses the performance of the algorithm in terms of zone 1 reach boundary accuracy and operating time.

Firstly reach boundary performance of the algorithm is investigated for both single and double end fed systems. The single phase to earth fault discrimination performance is compared with that of the s.p.m and quadrilateral impedance based protection techniques. As a result of this investigation, transient studies have been conducted in which typical operating times for the algorithm are presented when applied to double end fed systems.

Steady State testing has been conducted exhaustively for the case of single phase to earth faults while the transient simulation study gives indication of operating time for the discrimination of both a-earth and b-c phase faults.

7.2 Steady State Results

Presentation of results is restricted to only those circuits of a practical nature, which are likely to generalise the real world operating parameters of power systems. It can be reported that in all cases the new prototype relay out performed the existing distance relaying approaches and analysis of the results presented reinforces this. Both double and single end fed systems as described in table 6.1 have been studied.

7.2.1 Double end fed system

The results take the form of a comparison between reach boundary accuracy of the new prototype impedance relay (ABCD), self polarised mho (MHO) and quadrilateral (QUAD) based algorithms for circuits subjected to a-e faults of varying fault path resistance and position. Many composite circuits have been simulated and it is not practical to show all results here. To aid analysis circuits subject to particular SCL at sending and remote end busbars can be selected according to the criteria summarised in table 7.1

Study No	Sending End Fault Level MVA	Receiving End Fault Level MVA
Study 1	250	250
Study 2	250	500
Study 3	500	250

Table 7.1 Categorisation of studies based on fault level

Further classification of studies can be made according to the individual circuit section lengths. Table 7.2 summarises this selection, which also shows the cross-referencing of studies to the figure numbers of the results.

Study No	Cable length	Line Length	Figure Number
1a	0,10,20,40,50,80	10	7.1 (a) to (f)
1b	0,10,20,40,50,80	30	7.2 (a) to (f)
1c	0,10,20,40,50,80	50	7.3 (a) to (f)
2a	0,10,20,40,50,80	10	7.4 (a) to (f)
2b	0,10,20,40,50,80	30	7.5 (a) to (f)
2c	0,10,20,40,50,80	50	7.6 (a) to (f)
3a	0,10,20,40,50,80	10	7.7 (a) to (f)
3b	0,10,20,40,50,80	30	7.8 (a) to (f)
3c	0,10,20,40,50,80	50	7.9 (a) to (f)

Table 7.2 Classification of Studies Associated with Figure Numbers

The intention of selecting these circuits is to study not only composite circuits but also short and long circuits at practical sending and receiving end fault levels.
For all tests conducted the setting of the resistive blinder, R_b , of the QUAD and ABCD tripping characteristics is set to 40.0 Ohms.

To assess performance some assessment criteria is required. In terms of the first zone earth fault coverage it is normal practice to specify the boundary discrimination accuracy as a percentage of the PPS characteristic impedance setting of the distance relay. At the characteristic angle ±5% would be a typical tolerance at common source to line impedance ratios. Such criteria are utilised in the following analysis and are defined in table 7.3.

Criteria	% Error band (at PPS characteristic angle of the zone circuit)
Zone 1 earth fault reach accuracy	$Z_{set} \pm 5\%$
Resistive Reach Coverage	Fault path resistance value at which cut off commences in Ohms.

Table 7.3 Performance Assessment Criteria.

7.2.2 Discussion of Results from Studies 1,2,3

The definition for over reach means that for a fault occurring at 80% feeder length the relay would measure a greater line impedance and thus assess the same fault as further along the length of the feeder, i.e. a true zone two event may be discriminated as a zone 1 event.

The definition for under reach is for a fault at 80% of the feeder length the relay would see less impedance and thus assess the same fault as a zone 1 event, but would therefore become reliant on zone2 to clear some zone1 faults. Zone 2 is of course generally subject to a greater time delay than zone 1. Consequently, under reach may be considered the most undesirable in terms of efficiently protecting the network from damage and stress and also from the point of view of accurately discriminating the correct faulted section of the network to be disconnected.

These facts and the criteria of table 7.3 allow the following general observations and discussion points can be made.

Maximum over reach exhibited by the QUAD routine is approximately 10 – 20%. It should be noted that no compensation of the reactance line to cater for double end in feed and prefault load transfer conditions (section 2.9) is made. This might be implemented using negative sequence current polarisation [4].

Both the QUAD and ABCD algorithms result in under reach at higher values of fault path resistance as uncertainty around the resistive cut off occurs. Assessment of this is left to the reader's observation of the figures 7.1 to 7.9.

It is immediately apparent that some of the ABCD characteristics are promisingly close to the ideal boundary characteristic. i.e. No under or over reaching right up to the resistive cut off which occurs at 40 Ohms - the actual resistive blinder setting value. This is discussed in detail later.

Following is a detailed analysis of the results shown in figures 7.1 – 7.9.

7.2.2.3 Consider the reach boundary accuracy of the ABCD algorithm. For all circuits in the tests that were short feeders (i.e. 10km line alone or 10km of cable and 10km of line), very good performance close to the ideal is observed, while the performance of the ABCD and Mho characteristics are poor or unpredictable. Lines are difficult to protect against high resistive earth faults using distance protection techniques (as section 3.5 explained) when lines are short, unearthed and light load conditions exist.

7.2.2.4 For line lengths of 10km and cable lengths in excess of 30km, the ABCD characteristic resistive cut off begins to take effect at a lower resistive value than set by the resistive blinder setting. The worse case is for the circuit with fault levels at sending and receiving ends of 250 and 500 MVA respectively (study 2b), where resistive cut off at 8 Ohms is measured for cable lengths in excess of 50km. The worst case over reach for the ABCD under these circuit conditions is a maximum of 10% of total feeder length. Compared with the QUAD, which exhibits resistive cut off at 8 Ohms and 15 to 20 % over reach.

7.2.2.5 For studies 1b 2b and 3b when line lengths are 30km, for any length of cable section or source parameter conditions the ABCD reach boundary performance is very good and close to the expected ideal characteristic. For the same tests and operating conditions, the QUAD exhibits premature cut off for cable lengths above 20km. For equal lengths of line and cable (say 30km for each section), the ABCD exhibits 10% over reach, but only when sending end source impedance is higher than that at the receiving end. Other wise there is generally only a 4% maximum over reach exhibited by the ABCD algorithm. The ABCD does exhibit some under reaching when cable lengths exceed 30km and source fault levels are 250MVA sending and 500 MVA receiving. In this case the greatest amount of under reach is measured as 10% for the circuit containing 50km cable and 30 km line.

7.2.2.6 For studies 1c, 2c and 3c with line lengths of 50km, the reach boundary for ABCD algorithm is generally close to that expected. However, measurements made for the circuits in study 2 category are different from those exhibited during study 1 and 3. In study 2 source impedance values at the sending and receiving ends are 250 and 500 MVA respectively. Now the QUAD always over reaches by typically 15 %, while the ABCD exhibits very small under reach in the order of 1 to 3 %. It should be noted that at longer cable lengths (i.e. > 50km and with higher fault path resistance values) the under reach can become excessive (i.e. 12 to 18 %). In the

case of equal sending and receiving end source impedance values (study 1) the ABCD exhibits under reach in the order of 1 to 4 % regardless of cable lengths. The quad over reaches for all study 1 and 3 test circuits by 18 to 20 %.

7.2.3 Summary of Double end Fed results

With respect to single phase to earth fault coverage. Generally the ABCD algorithm offers improved performance over existing relaying techniques.

When sending end fault levels are lower than receiving end, all relays performed at their worst. However, generally the ABCD is still within acceptable tolerance limits (+-5% of reach boundary setting impedance value) for practical real world circuits. When cable lengths increase to significant lengths (>50km) the ABCD resistive reach boundary is degraded by at worse 12 to 18 % for high resistance faults. Distribution cable lengths in the real world are unlikely to be this long due to economics.

The ABCD algorithm offers improvement in terms of high resistance earth fault discrimination on short lines and composite feeders.

The ABCD offers more predictable resistive cut off features than the QUAD.

7.3 Single End Fed System Results

The single end fed systems modelled in this work have produced results in the same format as for the double end fed results of section 7.2 above. However, results from only two typical example circuits are presented here. Still the indication of performance has been found to be typical over the range of tests completed.

Higher single phase to earth fault path resistance values (0 to 200 Ohms) have been used for this range of studies and as such the resistive blinders have been set to higher values of 80 Ohms.

The two circuits and associated parameters are detailed below with results presented in figures 7.10 and 7.11.

Circuit 1

Load	0MVA, 10MVA, 20MVA, 30MVA, 40MVA
Load angle	30 Degrees Lagging
Cable length	60km
Line length	30km
Source Flt Level	250 MVA

Circuit 2

Load	0MVA, 10MVA, 20MVA, 30MVA, 40MVA
Load angle	30 Degrees Lagging
Cable length	10km
Line length	20km
Source Flt Level	250 MVA

The same modelling software was used for the tests but the remote end source impedance matrix and driving voltages were removed and replaced by a matrix representation of typical loads. Remote end bus bar voltage is now not determined as an input but rather is calculated by the software according to known sending end bars voltage parameters.

7.3.1 Discussion of Results Circuits 1 and 2

Some observations can be made. The criteria for assessing performance are the same as that for double end fed systems described earlier.

7.3.1.1 For the short circuit (circuit 2), the ABCD reach boundary is close to ideal performance irrespective of circuit loading.

7.3.1.2 The QUAD reach boundary appears unpredictable in the cases of application to both circuits 1 and 2 (long and short feeders). It exhibits either substantial over reaching or under reaching.

7.3.1.3 For the short circuit (circuit 2), the ABCD algorithm exhibits no more than 3% inaccuracy in terms of reach boundary for al loading conditions.

7.3.1.4 For the short circuit (circuit 2), the QUAD exhibits up to 40% inaccuracy under low fault path resistance values for a loaded circuit.

7.3.1.5 For the long circuit (circuit 1), The ABCD exhibits no more than 6% inaccuracy for circuits loaded up to 20MVA at 0.8 pf lag. When loads exceed this magnitude inaccuracy reaches 10%. However, 20MVA and below can be considered a typical maximum magnitude for a single breaker remote end substation for example.

7.3.1.6 For the long circuit (circuit 1), the QUAD exhibits very inaccurate reach boundary at all loading conditions. Thus, extensive over reaching is observed of the order of 40 to 90 % of total feeder length.

7.3.2 Summary

Reach boundary performance always better for ABCD algorithm.

Good resistive earth fault coverage for short feeders.

QUAD unpredictable in reach boundary accuracy.

A visual inspection of figures 7.10 and 7.11 indicates preferential performance.

7.4 Transient Studies Results

In order to assess operating time for the prototype impedance measuring algorithm transient based studies are necessary.

It would be impractical to study all possible circuits and operating conditions so testing can not be exhaustive. Only a few representative studies are given here. An indication of expected operating times for two practical circuit connections is given.

These are circuits 1 and 2 as described in section 7.2. This is judged to give a good representation of both long and short length circuits. Simulations are for double end fed systems with sending and receiving end fault levels of 250 and 500 MVA respectively. These fault levels have been chosen because the steady state studies completed indicated some degradation in reach boundary accuracy for certain systems subject to these prevailing operating conditions. Both 'a' phase to earth faults and 'b' – 'c' phase faults are simulated.

Results are presented which show operating time with respect to fault position. Tables 7.4 and 7.5 summarise the circuits modelled and figures 7.12 to 7.19 present graphically the results. Circuit connectivity is sending end bar, cable, line, and receiving end bar.

Parameter	Value	Units
Sending End Fault Level	250	MVA
Receiving End Fault Level	500	MVA
Cable length	60	Km
Line Length	30	Km
Fault Path Resistance	0.0 and 20.0	Ohms
Fault Inception Angle	0.0 and 90.0 degrees on voltage wave	Degrees
Fault types	A – E and B-C	-
Loading	Full Load Forward	-

Table 7.4 Circuit 1 – For Transient Testing

Parameter	Value	Units
Sending End Fault Level	250	MVA
Receiving End Fault Level	500	MVA
Cable length	10	Km
Line Length	20	Km
Fault Path Resistance	0.0 and 10.0	Ohms
Fault Inception Angle	0.0 and 90.0 degrees on voltage wave	Degrees
Fault types	A – E and B-C	-
Loading	Full Load Forward	-

Table 7.5 Circuit 2 – For Transient Testing

7.4.1 Discussion of Transient Results

The performance criteria for assessing algorithm operating time was defined in table 4.1 as between 20 –60 msecs (or 2 –3 cycles at fundamental power system frequency). Assessment of the results in figures 7.12 to 7.19 shows that all operating times are within this criteria.

In all transient testing no anomalies were found. Given the experience of the steady state simulation studies, this would imply that no significant anomalies exist, but, of course, it is difficult to be certain of this. Transient testing of two composite power systems has indicated the algorithm to operate within specification and requirements.

Further observations can be made.

7.4.1.1 The results indicate that the algorithm will successfully discriminate an in zone b-c phase fault. Even under conditions of high fault path resistance (20 Ohms, see figure 7.18 and 7.19) the fault is discriminated.

7.4.1.2 Consider circuit 1. A bolted earth fault at 0 degrees inception angle in zone 1 is discriminated by the algorithm in 28 msecs. This time rises to 43 msecs close to the reach boundary due to the delay of the trip decision counter. Reach point accuracy is achieved as was indicated during the steady state results investigations and analysis.

7.4.1.3 For the same fault occurrence and circuit as described in 7.3.1.2 but at 90 degrees fault inception angle, operating times are seen to increase so that now the fastest operating time is 36 msecs rising to 48 msecs close to the reach point. This is likely due to the residual effects of dc offset in the current waveforms, which is prevalent at this inception angle. Some reduction of the effects of dc

offset may be attributable to the full cycle DFT filters used to extract real and imaginary fundamental vectorial values of voltage and current. However, some time delay is still evident as the algorithm seeks a reduced dc offset content to allow reliable operation. For circuit 2 where circuit length is shorter (less cable) the X:R ratio of the total circuit is not as close to 1:1 as for the case of the longer circuit 2. It is possible that the slightly longer delay time in waiting for the dc offset to decay results in best case operating times of 38 msecs.

7.4.1.4 Addressing the results plot of figure 7.13, it is evident that operating times are within specification though a 3% under reach is observed. This is confirmed by the steady state results of figure 7.5 (e).

7.4.1.5 A worse case under reach is noted in figure 7.19, where for a phase to phase fault 5% inaccuracy is noted at the extremities of the zone reach setting. However, over the length of the feeder the general operating times are the quickest recorded for the algorithm when applied to this long circuit example with high resistance in the fault path at 30 msecs up to 50% feeder length.

7.4.1.6 Reach problems are not encountered during any of the tests on circuit2 (the short network). These results are again confirmed by addressing the steady state results for reach boundary performance of similar circuits for a-e faults. The performance for phase to phase fault is of course encouraging.

7.5 Summary

Both steady state frequency domain and transient based time domain modelling techniques have revealed two discrete sets of test results. These have been presented in this chapter.

The steady state results show clearly the proposed algorithms a –e fault reach boundary plots for varying fault position and fault path resistance. Many circuit conditions have been modelled and representative selections of results obtained have been presented. Generally, in terms of reach boundary accuracy under high resistance earth faults, the performance of the algorithm has been shown to be significantly better than either the Self Polarised Mho or Quadrilateral relaying approach to earth fault protection in zone 1 of a composite feeder.

The transient based results give an indication of the operating time that can be expected. It appears apparent from the transient results that operating times are well within the criteria of 2 – 3 cycles at power system fundamental frequency (i.e. 50Hz) required.

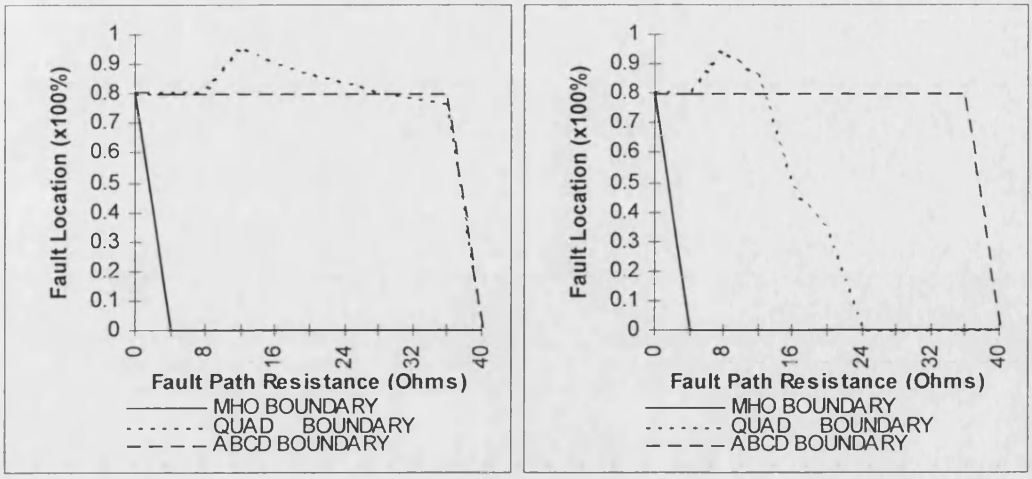

(a) Cable = 0km

(b) Cable = 10km

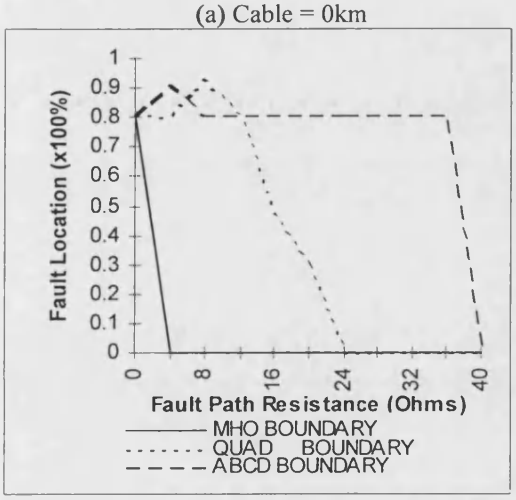

(c) Cable = 20km

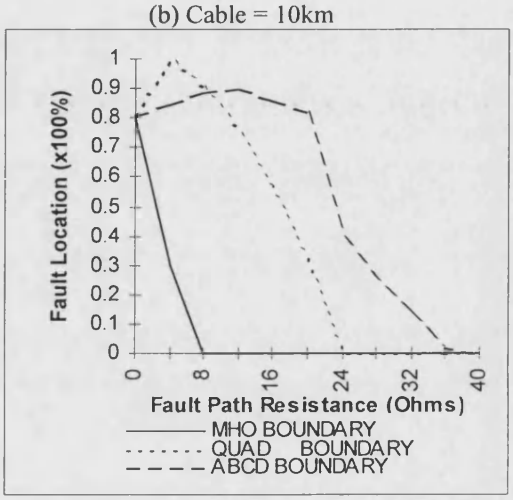

(d) Cable = 40km

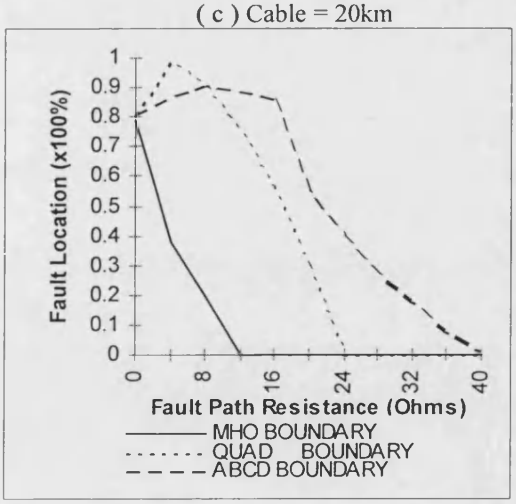

(d) Cable=50km

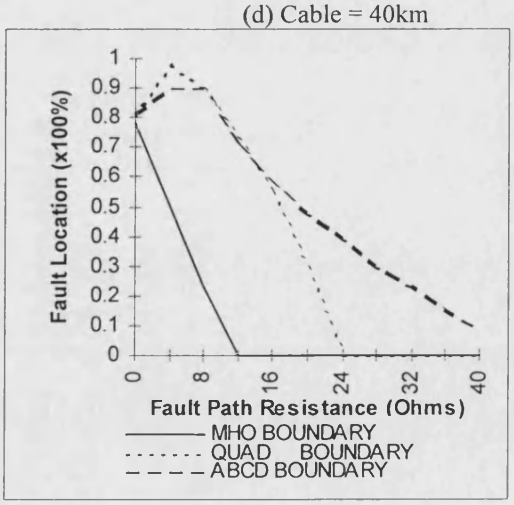

(e) Cable=80km

Figure 7.1 Reach Boundary Plots for Varying a-e fault path Resistance. Sending end Fault Level = 250MVA, Receiving end Fault Level = 250MVA, Cable length varies as indicated below figure. Line length = 10km.
Alpha = 14 degrees.
(where alpha is angle between receiving and sending end voltage vectors)

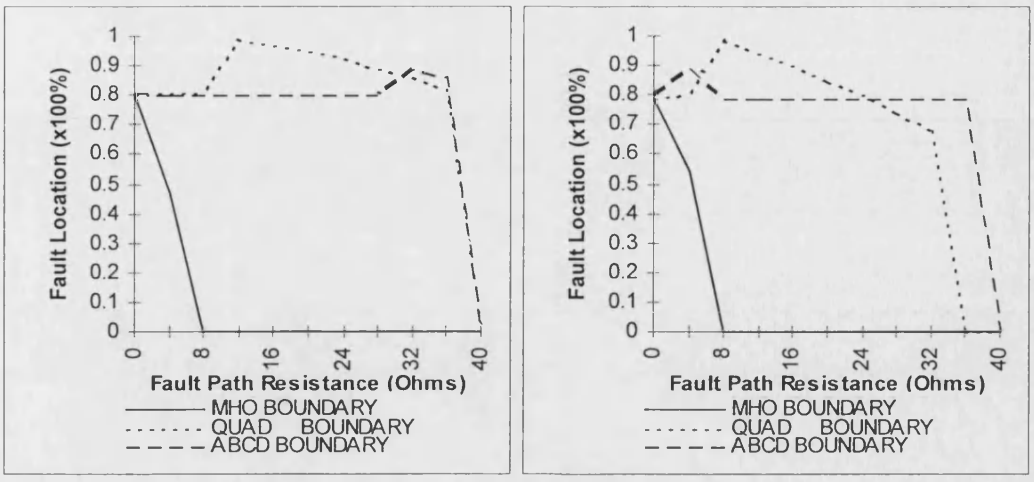

(a) Cable = 0km

(b) Cable = 10km

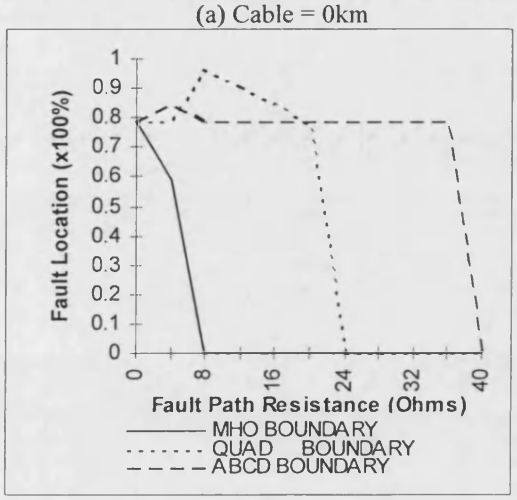

(c) Cable = 20km

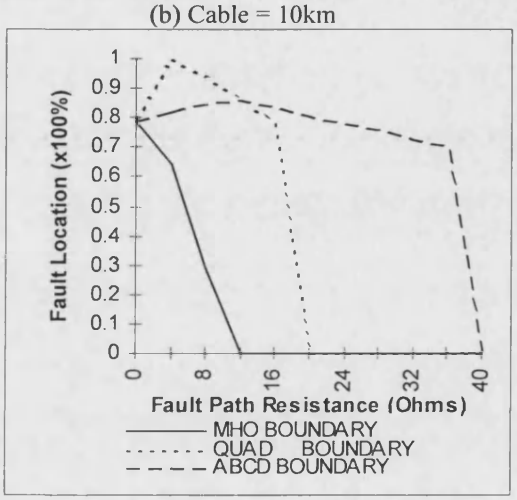

(d) Cable = 40km

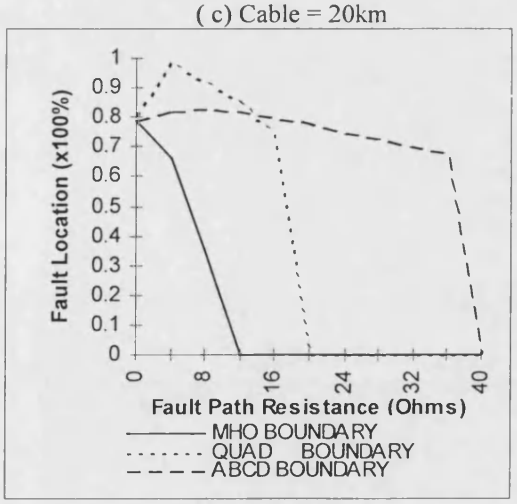

(e) Cable = 50km

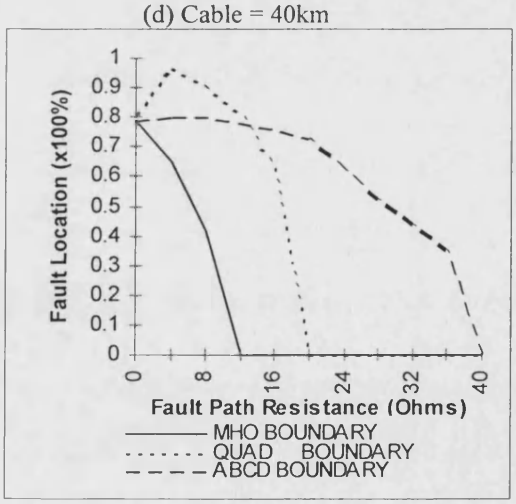

(f) Cable = 80km

Figure 7.2 Reach Boundary Plots for Varying a-e fault path Resistance. Sending end Fault Level = 250MVA, Receiving end Fault Level = 250MVA, Cable length varies as indicated below figure. Line length = 30km.
Alpha = 14 degrees.
(where alpha is angle between receiving and sending end voltage vectors)

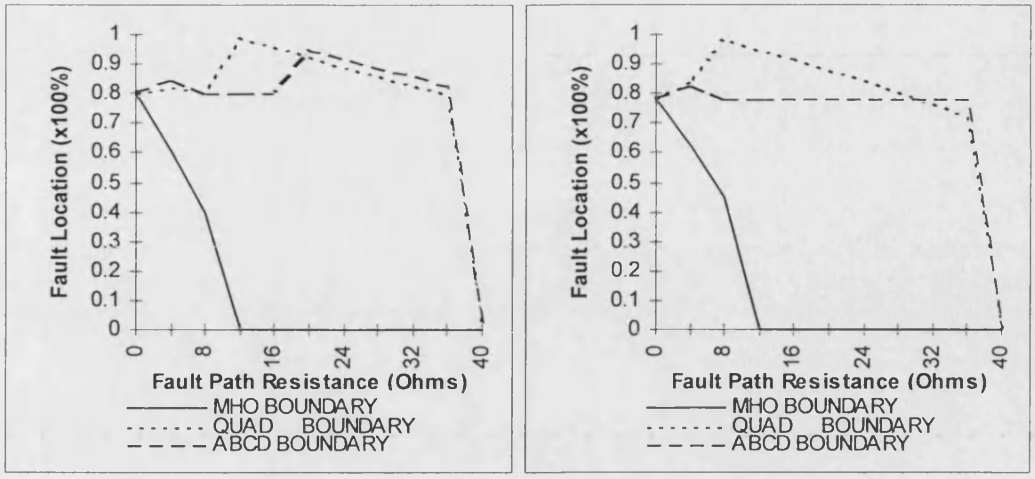

(a) Cable = 0km

(b) Cable = 10km

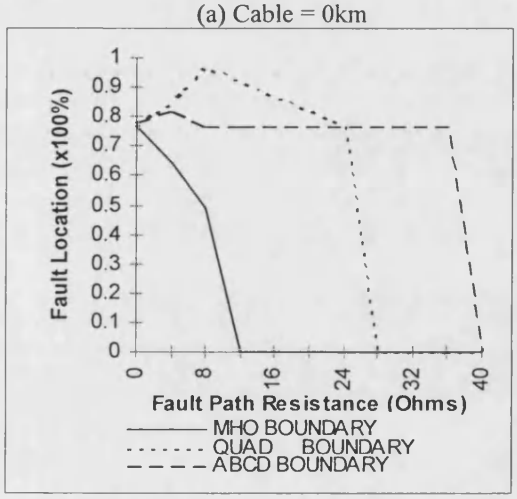

(c) Cable = 20km

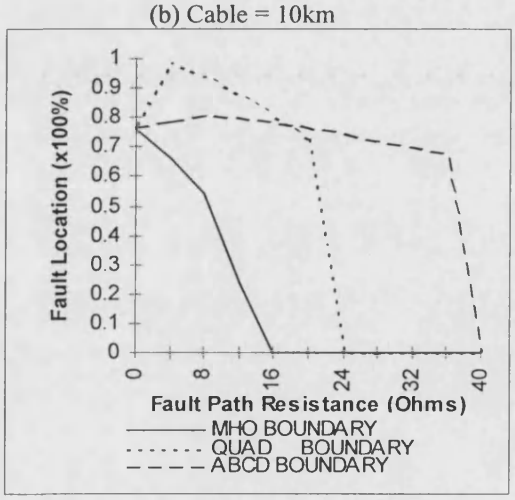

(d) Cable = 40km

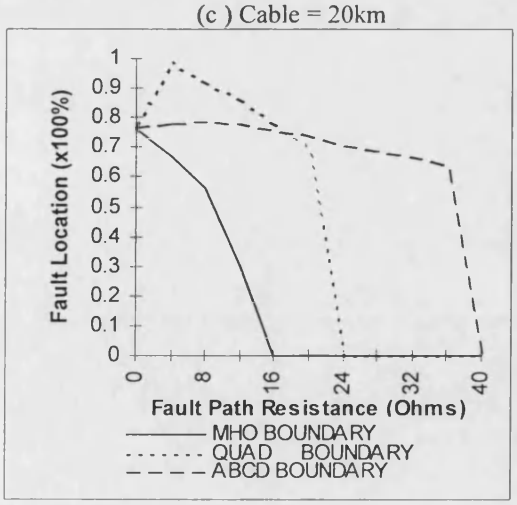

(e) Cable = 50km

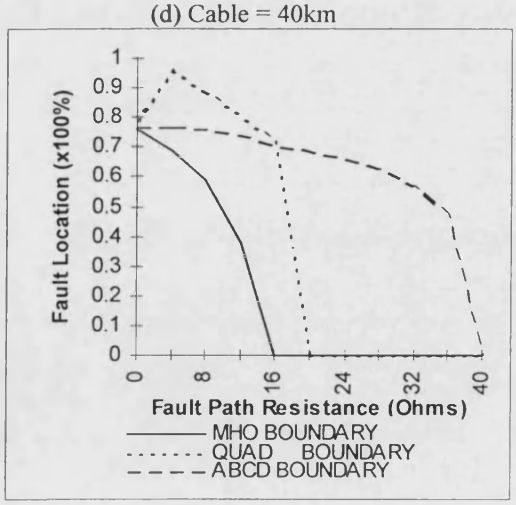

(f) Cable = 80km

Figure 7.3 Reach Boundary Plots for Varying a-e fault path Resistance. Sending end Fault Level = 250MVA, Receiving end Fault Level = 250MVA, Cable length varies as indicated below figure. Line length = 50km.
Alpha = 14 degrees.
(where alpha is angle between receiving and sending end voltage vectors)

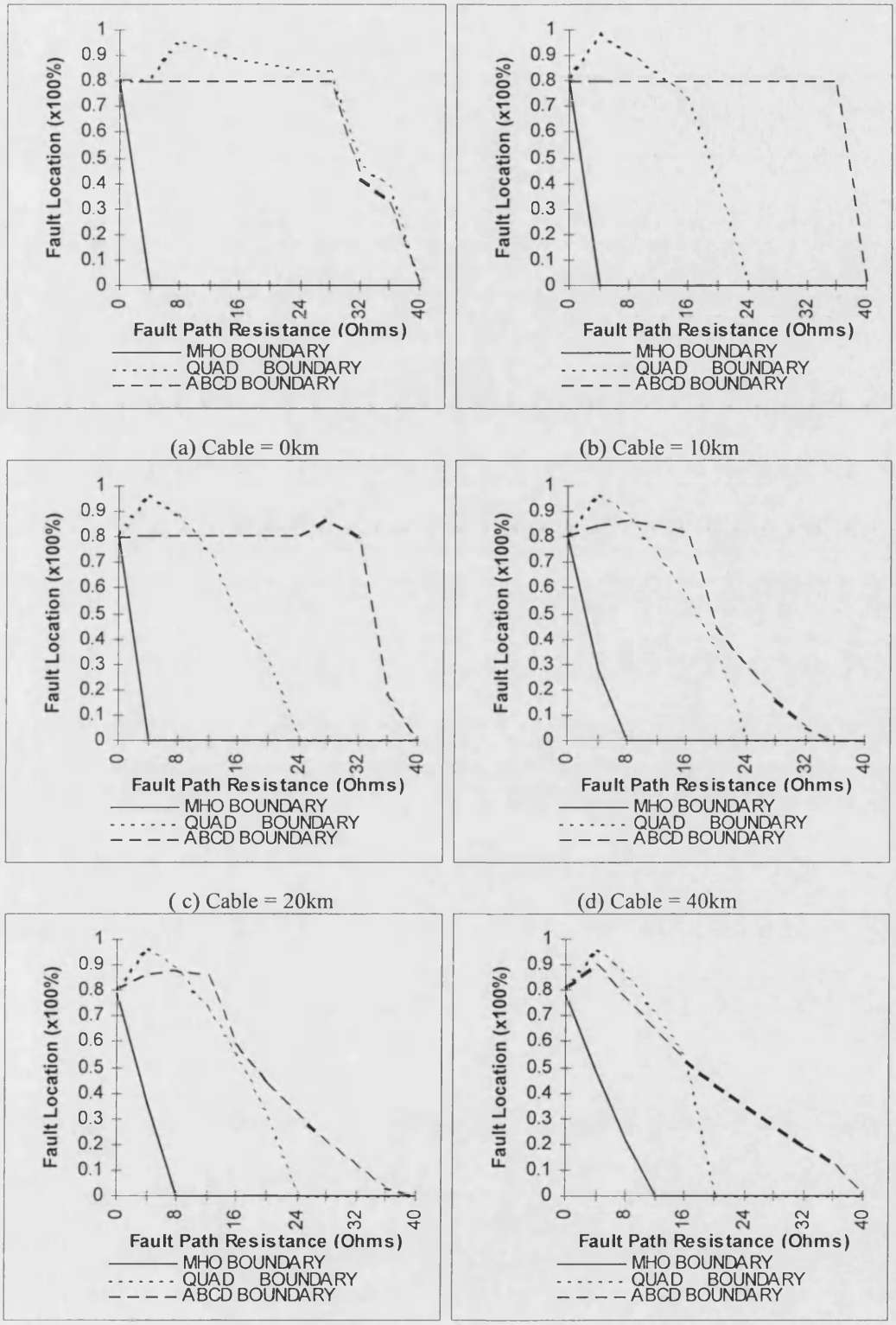

(a) Cable = 0km (b) Cable = 10km

(c) Cable = 20km (d) Cable = 40km

(e) Cable = 50km (f) Cable = 80km

Figure 7.4 Reach Boundary Plots for Varying a-e fault path Resistance. Sending end Fault Level = 250MVA, Receiving end Fault Level = 500MVA, Cable length varies as indicated below figure. Line length = 10km.
Alpha = 14 degrees.
(where alpha is angle between receiving and sending end voltage vectors)

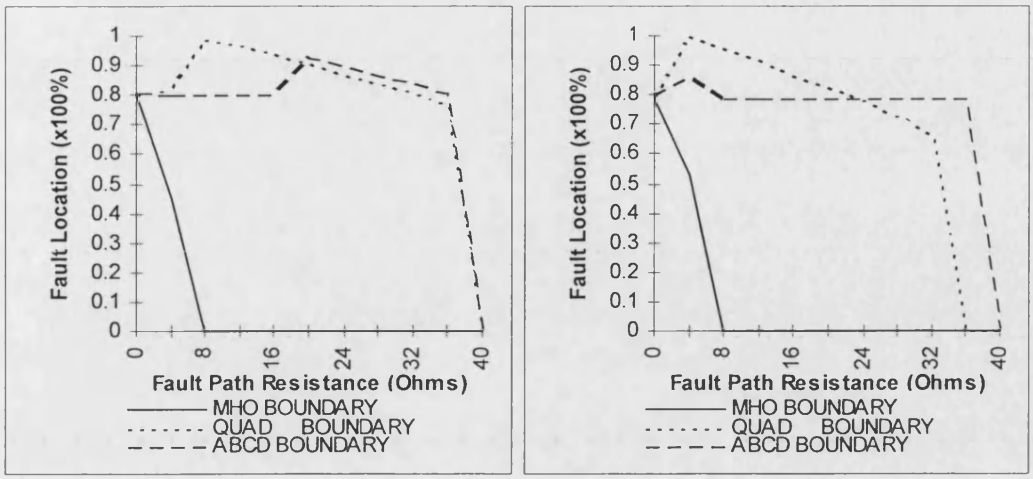

(a) Cable = 0km

(b) Cable = 10km

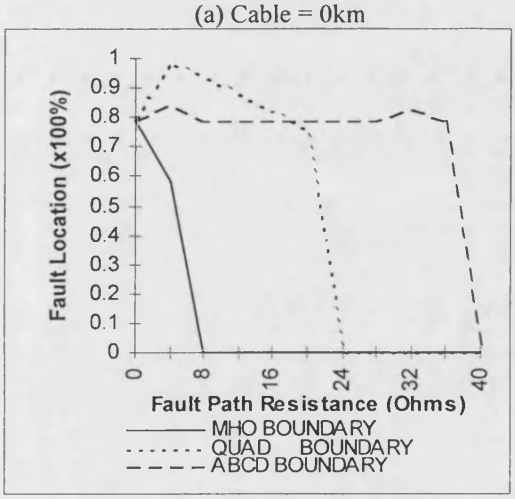

(c) Cable = 20km

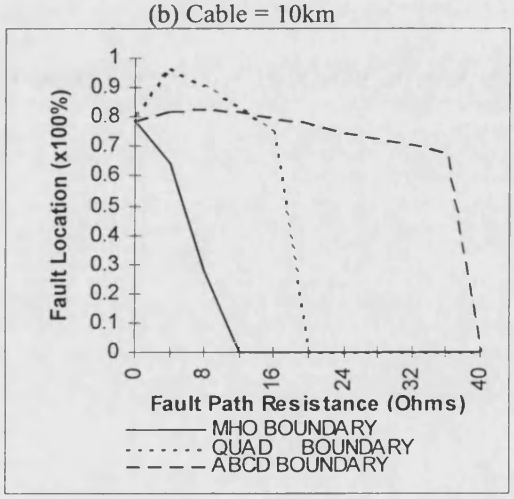

(d) Cable = 40km

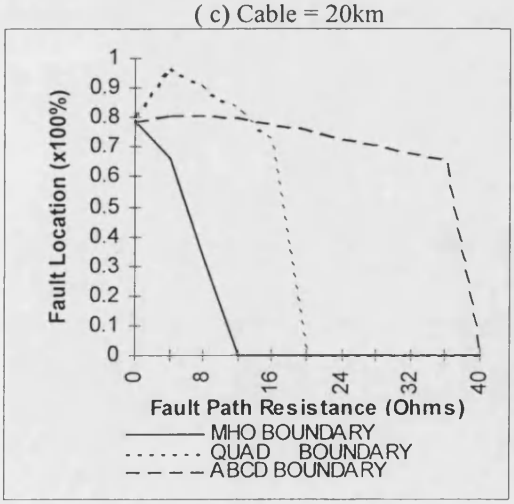

(e) Cable = 50km

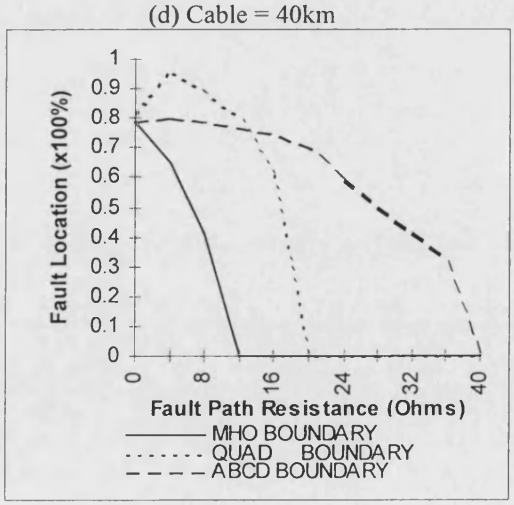

(f) Cable = 80km

Figure 7.5 Reach Boundary Plots for Varying a-e fault path Resistance. Sending end Fault Level = 250MVA, Receiving end Fault Level = 500MVA, Cable length varies as indicated below figure. Line length = 30km.
Alpha = 14 degrees.
(where alpha is angle between receiving and sending end voltage vectors)

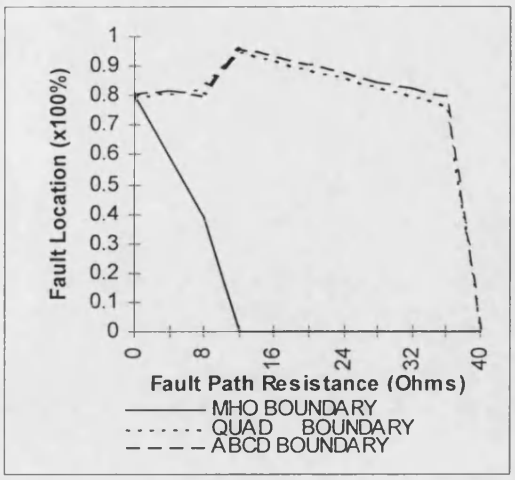

(a) Cable = 0km

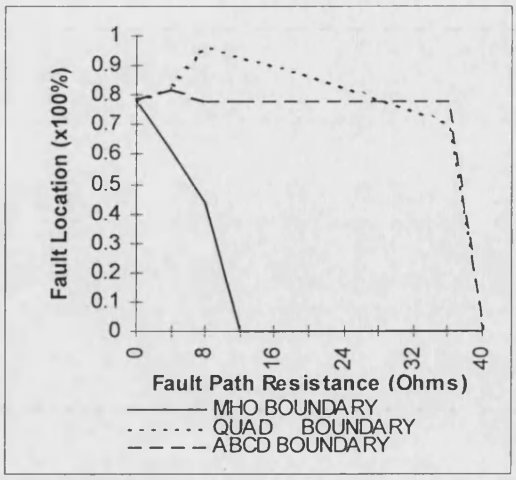

(b) Cable = 10km

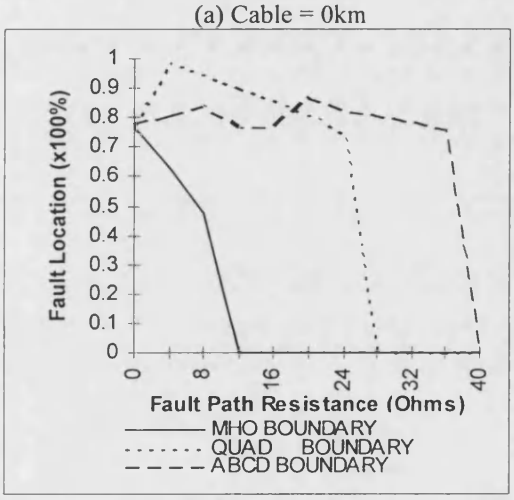

(c) Cable = 20km

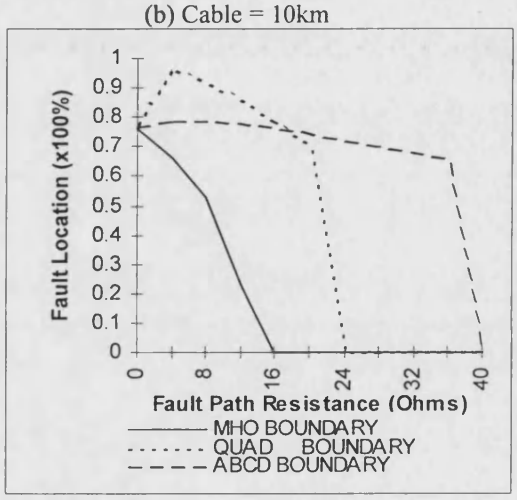

(d) Cable = 40km

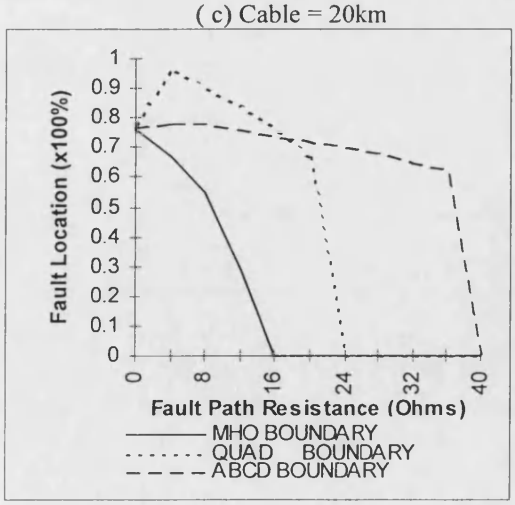

(e) Cable = 50km

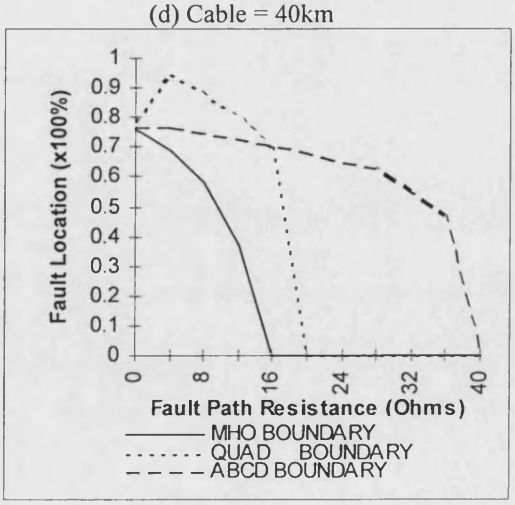

(f) Cable = 80km

Figure 7.6 Reach Boundary Plots for Varying a-e fault path Resistance. Sending end Fault Level = 250MVA, Receiving end Fault Level = 500MVA, Cable length varies as indicated below figure. Line length = 50km.
Alpha = 14 degrees.
(where alpha is angle between receiving and sending end voltage vectors)

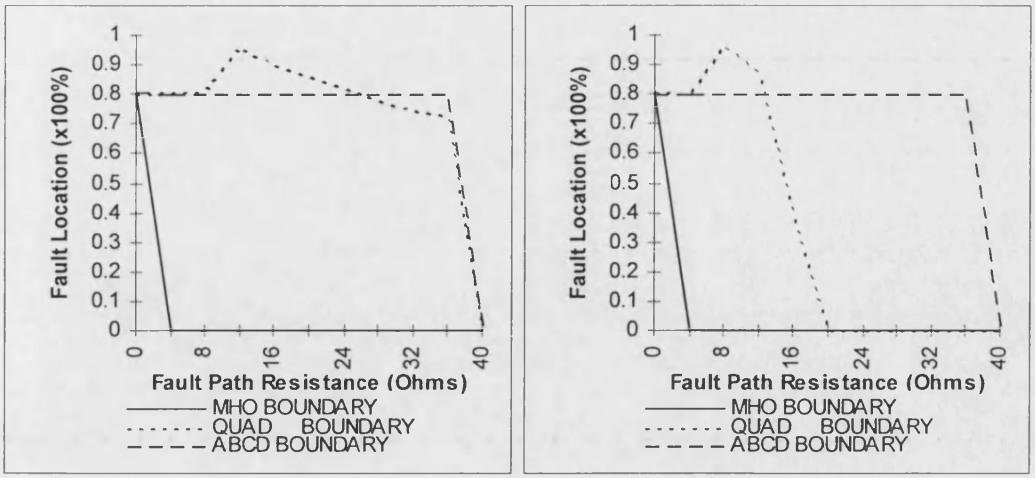

(a) Cable = 0km

(b) Cable = 10km

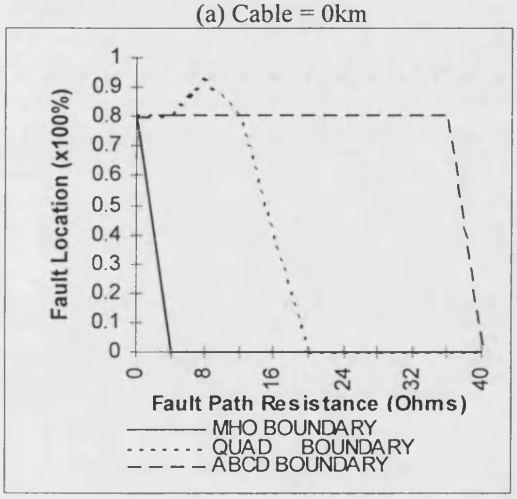

(c) Cable = 20km

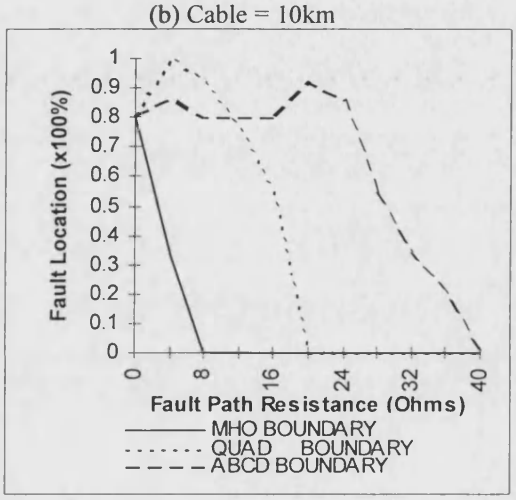

(d) Cable = 40 km

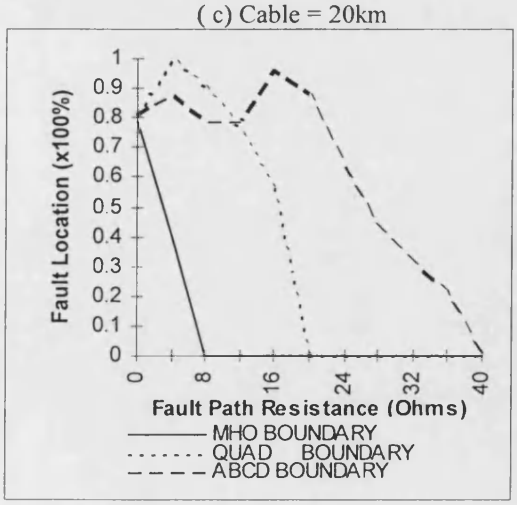

(e) Cable = 50km

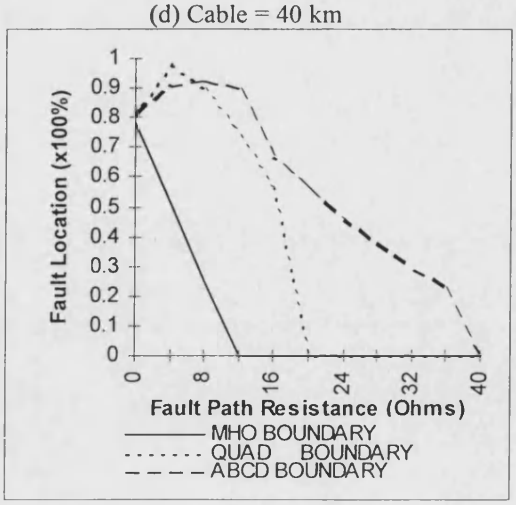

(f) Cable = 80km

Figure 7.7 Reach Boundary Plots for Varying a-e fault path Resistance. Sending end Fault Level = 500MVA, Receiving end Fault Level = 250MVA, Cable length varies as indicated below figure. Line length = 10km.
Alpha = 14 degrees.
(where alpha is angle between receiving and sending end voltage vectors)

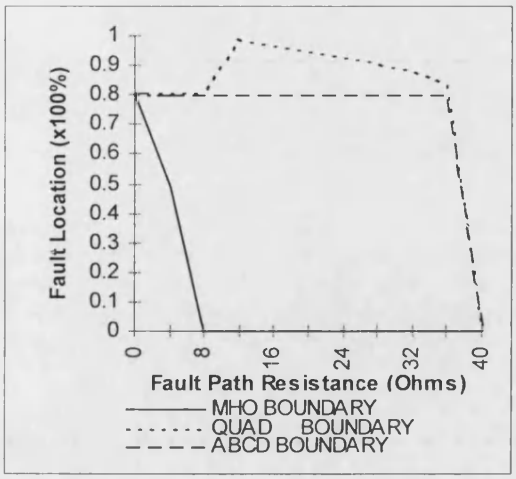

(a) Cable = 0km

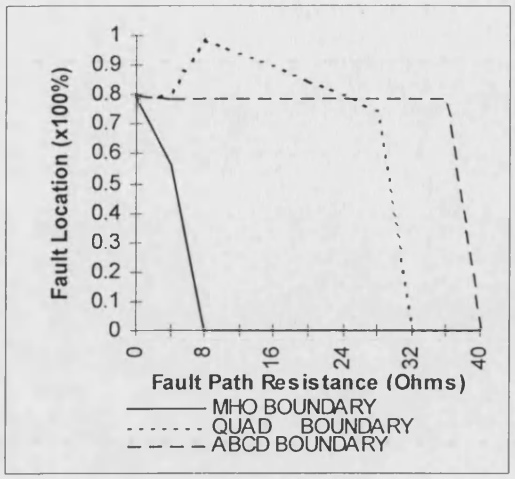

(b) Cable = 10km

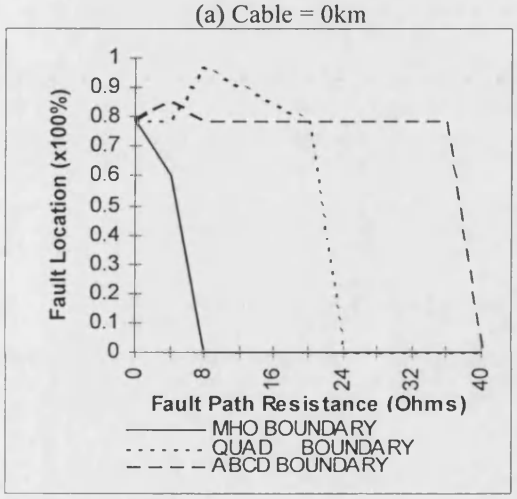

(c) Cable = 20km

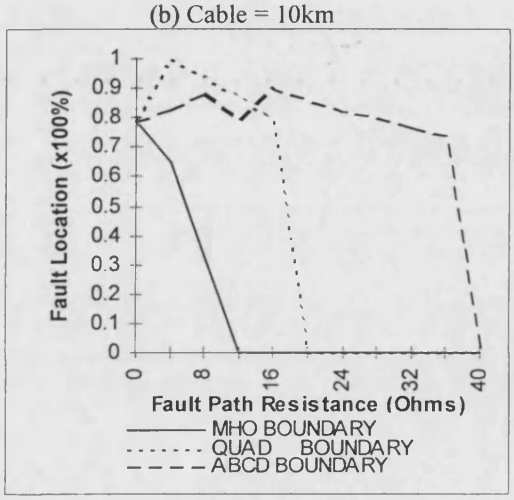

(d) Cable = 40km

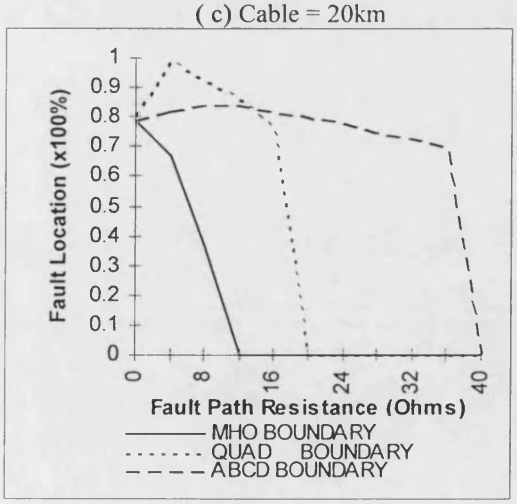

(e) Cable = 50km

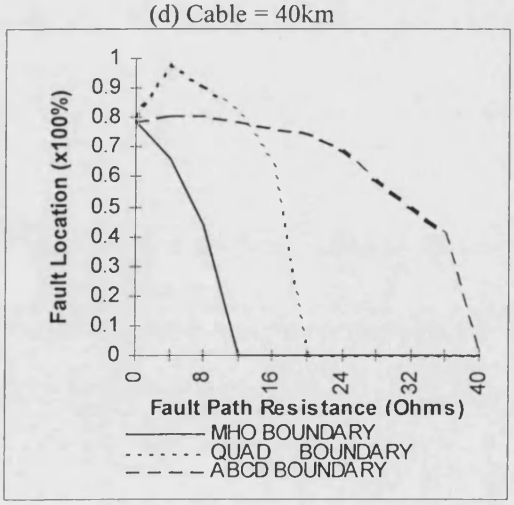

(f) Cable = 80km

Figure 7.8 Reach Boundary Plots for Varying a-e fault path Resistance. Sending end Fault Level = 500MVA, Receiving end Fault Level = 250MVA, Cable length varies as indicated below figure. Line length = 30km.
Alpha = 14 degrees.
(where alpha is angle between receiving and sending end voltage vectors)

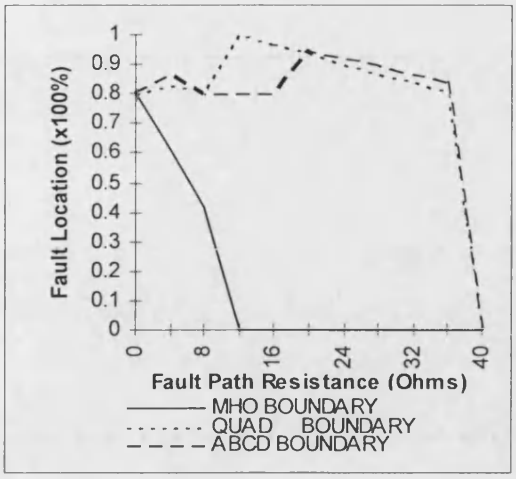

(a) Cable = 0km

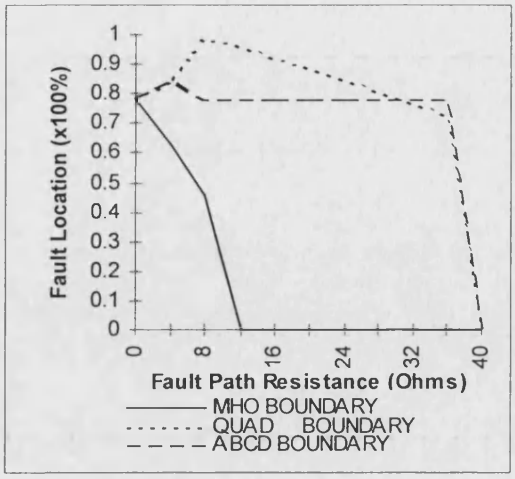

(b) Cable = 10km

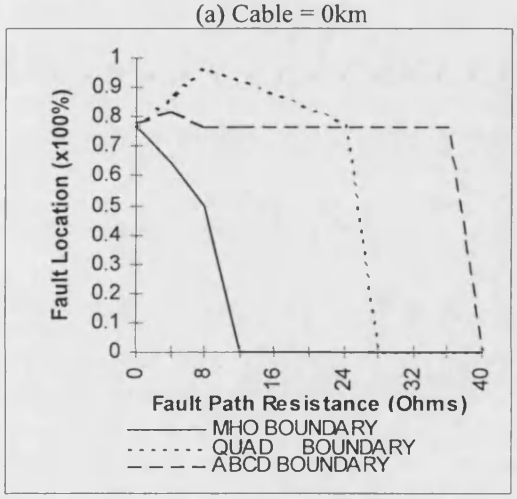

(c) Cable = 20km

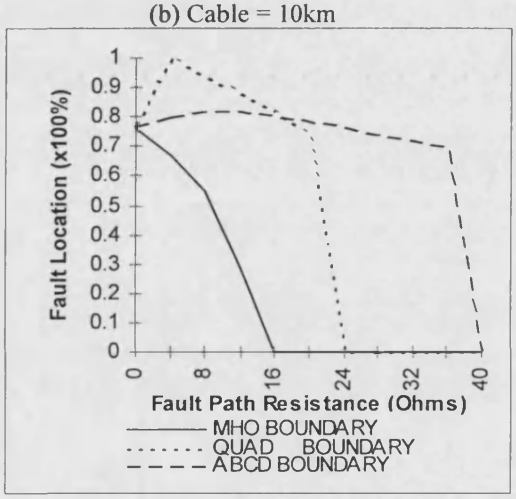

(d) Cable = 40km

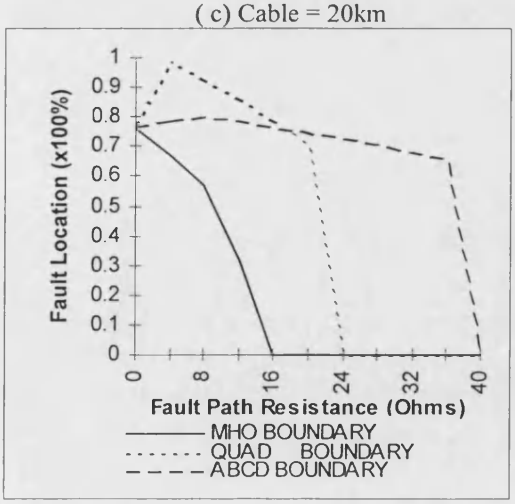

(d) Cable = 50km

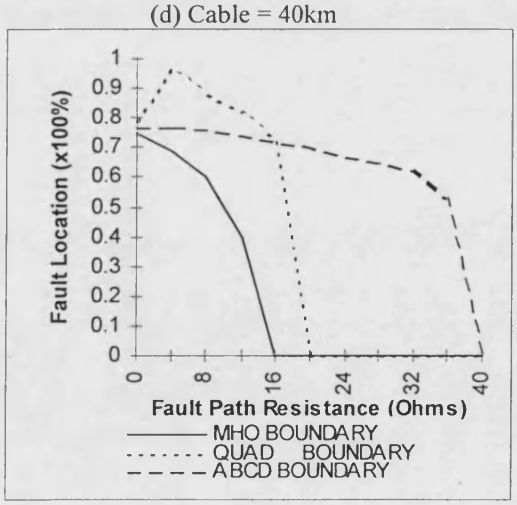

(e) Cable = 80km

Figure 7.9 Reach Boundary Plots for Varying a-e fault path Resistance. Sending end Fault Level = 500MVA, Receiving end Fault Level = 250MVA, Cable length varies as indicated below figure. Line length = 50km.
Alpha = 14 degrees.
(where alpha is angle between receiving and sending end voltage vectors)

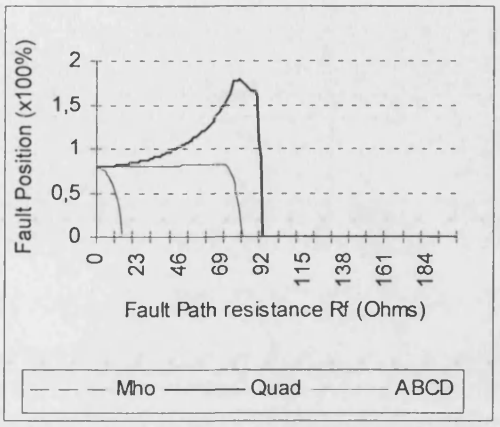

Figure 7.10 (a) Resistive Trip Boundary for Mho, Quad and ABCD Relays. Resistive Blinders = 80.0 Ohms. Fault = 'a' - 'erth'. Src Bars SCL : 250MVA, Load : 0 MVA, Sec 1 : 60 km Cable, Sec 2 : 30 km Line.

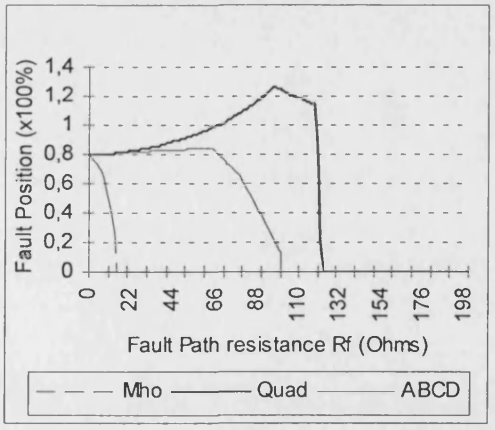

Figure 7.10(b) Resistive Trip Boundary for Mho, Quad and ABCD Relays. Resistive Blinders = 80.0 Ohms. Fault = 'a' - 'erth'. Src Bars SCL : 250MVA, Load Angle : 30 Deg's, Load : 10 MVA, Sec 1 : 60 km Cable , Sec 2 : 30 km Line

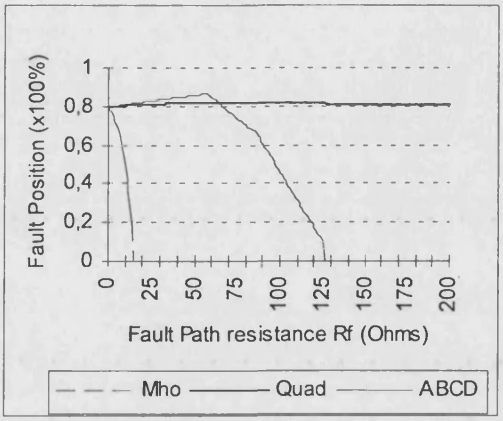

Figure 7.10(c) Resistive Trip Boundary for Mho, Quad and ABCD Relays. Resistive Blinders = 80.0 Ohms. Fault = 'a' - 'erth'. Src Bars SCL : 250MVA, Load Angle : 30 Deg's, Load : 20 MVA, Sec 1 : 60 km, Sec 2 : 30 km.

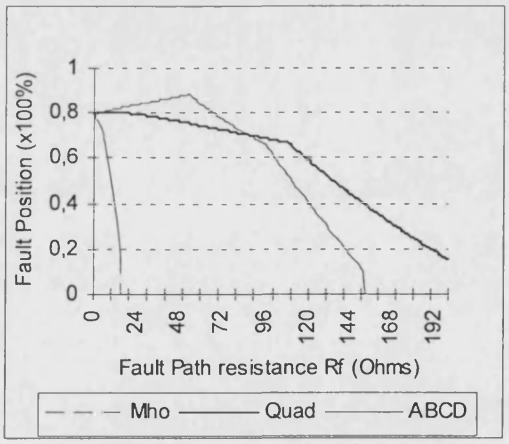

Figure 7.10(d) Resistive Trip Boundary for Mho, Quad and ABCD Relays. Resistive Blinders = 80.0 Ohms. Fault = 'a' - 'erth'. Src Bars SCL : 250MVA, Load Angle : 30 Deg's, Load : 30 MVA, Sec 1 : 60 km Cable, Sec 2 : 30 km Line.

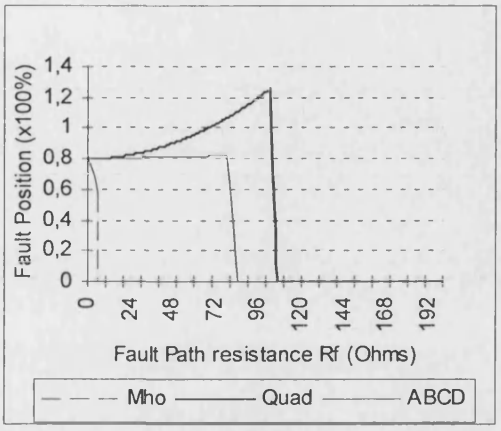

Figure 7.11 (a) Resistive Trip Boundary for Mho, Quad and ABCD Relays. Resistive Blinders = 80.0 Ohms. Fault = 'a' - 'erth'. Src Bars SCL : 250MVA, Load Angle : 30 Deg's, Load : 0 MVA, Sec 1 : 10 km Cable, Sec 2 : 20 km Line.

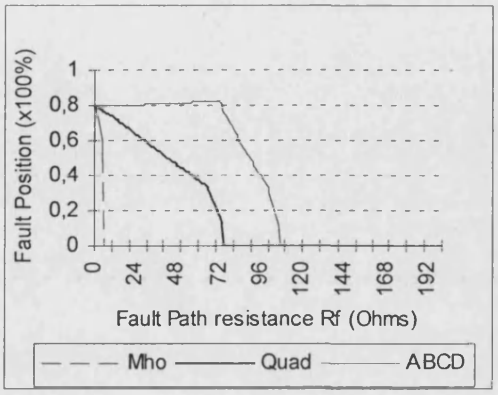

Figure 7.11 (c) Resistive Trip Boundary for Mho, Quad and ABCD Relays. Resistive Blinders = 80.0 Ohms. Fault = 'a' - 'erth'. Src Bars SCL : 250MVA, Load Angle : 30 Deg's, Load : 20 MVA, Sec 1 : 10 km Cable, Sec 2 : 20 kmLine.

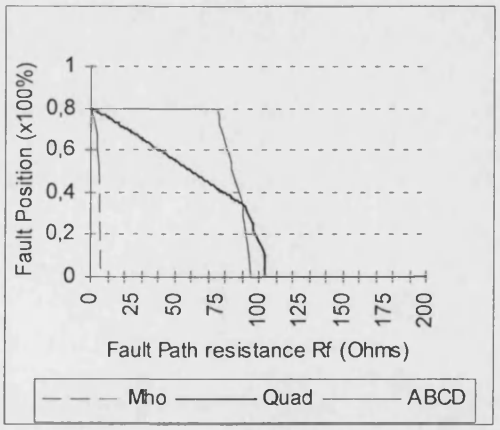

Figure 7.11 (b) Resistive Trip Boundary for Mho, Quad and ABCD Relays. Resistive Blinders = 80.0 Ohms. Fault = 'a' - 'erth'. Src Bars SCL : 250MVA, Load Angle : 30 Deg's, Load : 10 MVA, Sec 1 : 10 km Cable, Sec 2 : 20 km Line.

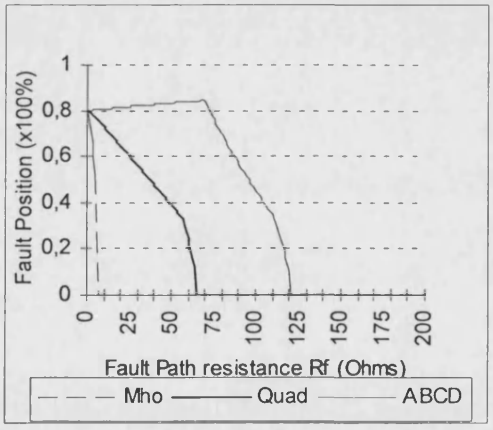

Figure 7.11 (d) Resistive Trip Boundary for Mho, Quad and ABCD Relays. Resistive Blinders = 80.0 Ohms. Fault = 'a' - 'erth'. Src Bars SCL : 250MVA, Load Angle : 30 Deg's, Load : 30 MVA, Sec 1 : 10 km, Sec 2 : 20 km.

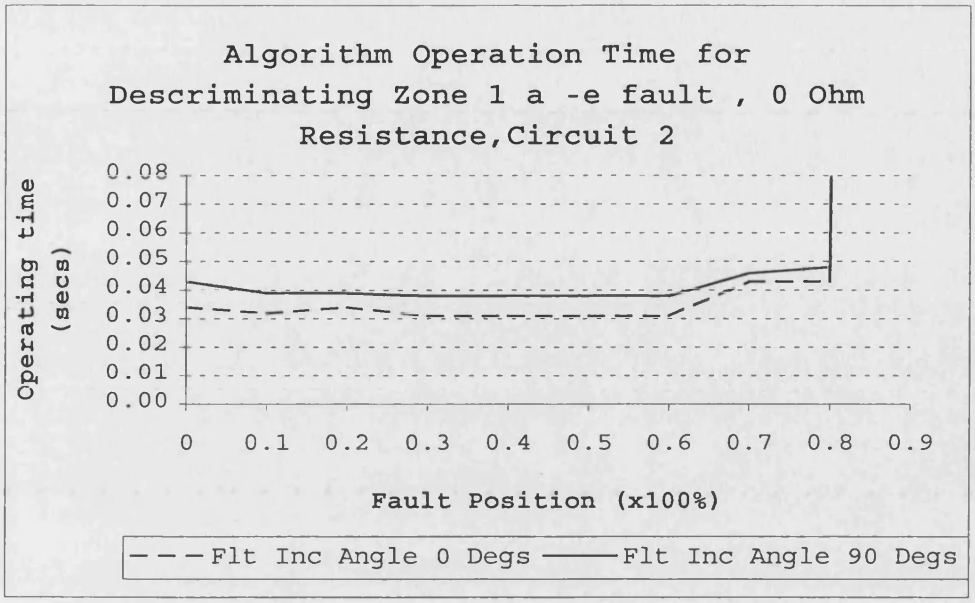

Figure 7.12 Algorithm Operating Time. Cable = 10km, line =20km.
Sending End Fault Level = 250MVA
Receiving End Fault Level = 500MVA

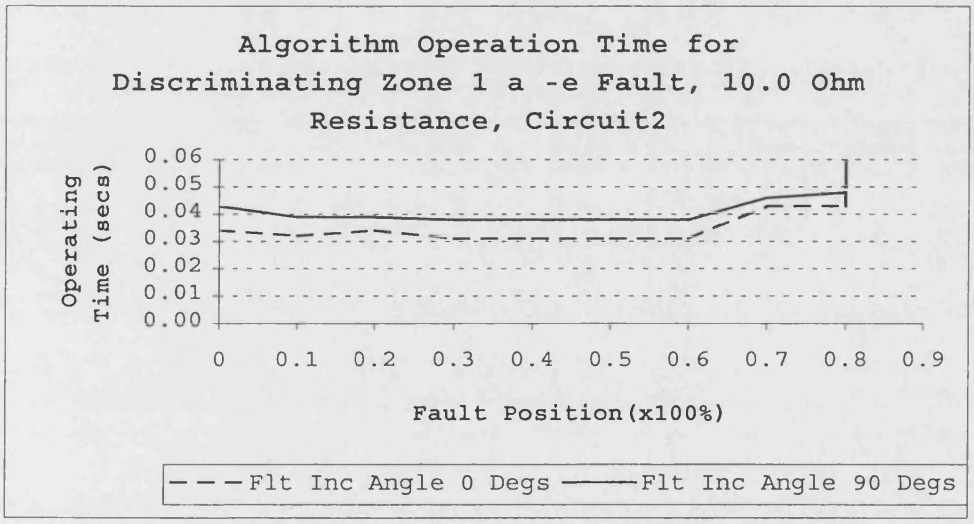

Figure 7.13 Algorithm Operating Time. Cable = 10km, line =20km.
Sending End Fault Level = 250MVA
Receiving End Fault Level = 500MVA

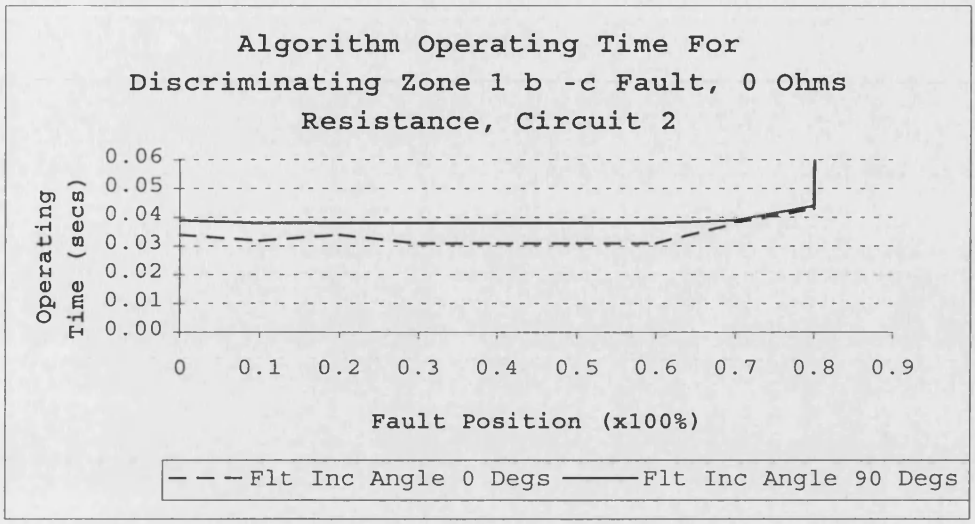

Figure 7.14 Algorithm Operating Time. Cable = 10km, line =20km.
Sending End Fault Level = 250MVA
Receiving End Fault Level = 500MVA

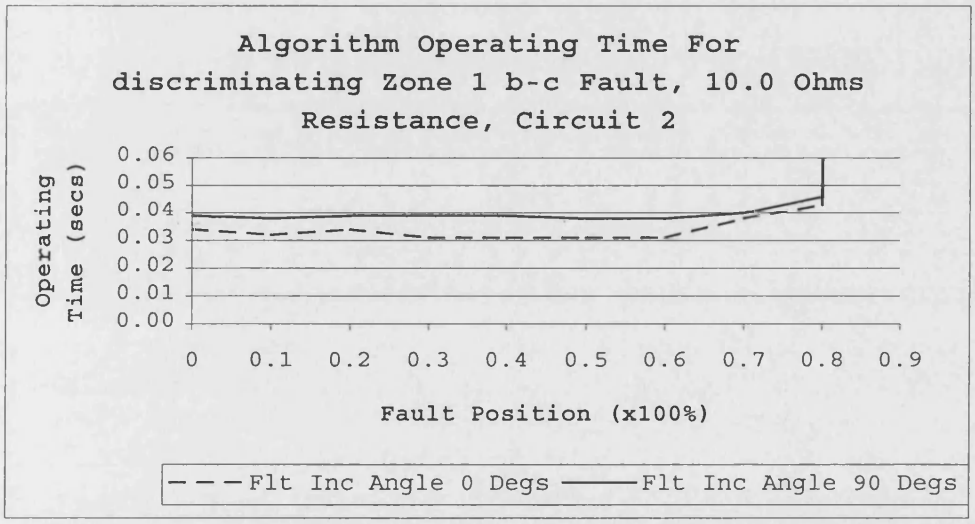

Figure 7.15 Algorithm Operating Time. Cable = 10km, line =20km.
Sending End Fault Level = 250MVA
Receiving End Fault Level = 500MVA

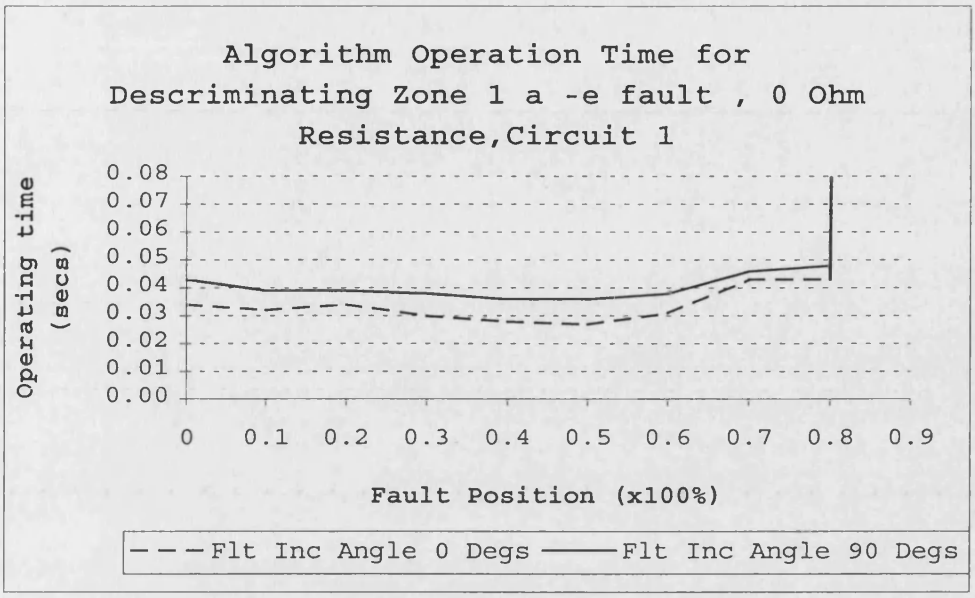

Figure 7.16 Algorithm Operating Time. Cable = 60km, line =30km.
Sending End Fault Level = 250MVA
Receiving End Fault Level = 500MVA

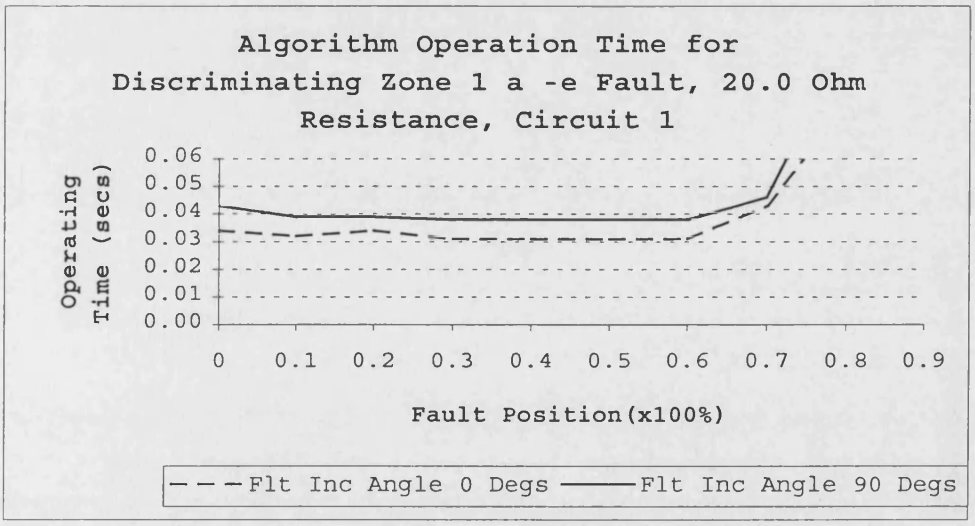

Figure 7.17 Algorithm Operating Time. Cable = 60km, line =30km.
Sending End Fault Level = 250MVA
Receiving End Fault Level = 500MVA

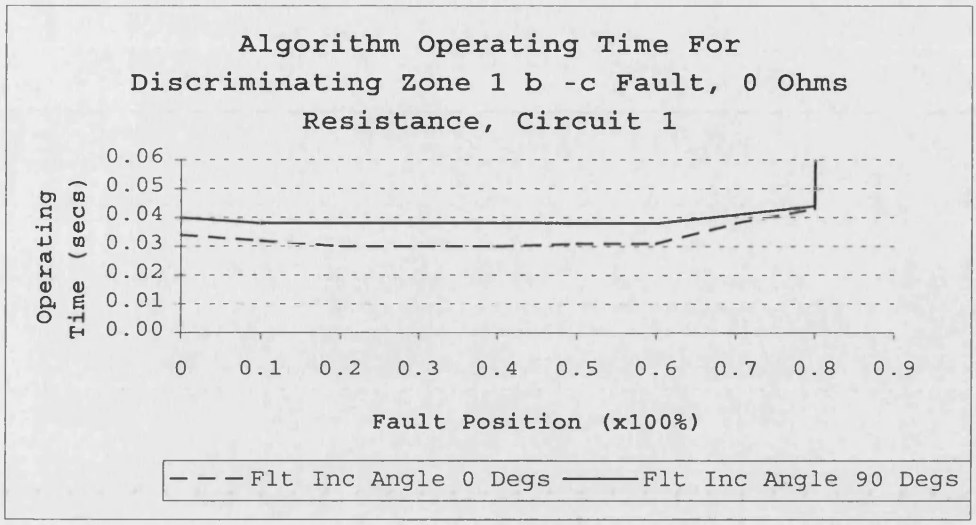

**Figure 7.18 Algorithm Operating Time. Cable = 60km, line =30km.
Sending End Fault Level = 250MVA
Receiving End Fault Level = 500MVA**

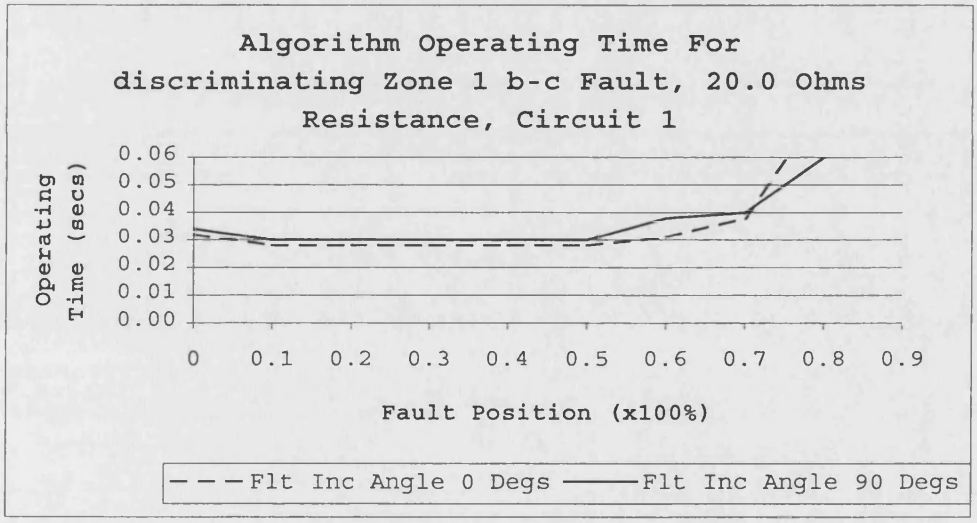

**Figure 7.19 Algorithm Operating Time. Cable = 60km, line =30km.
Sending End Fault Level = 250MVA
Receiving End Fault Level = 500MVA**

Chapter 8

Conclusion and Future Work

8.1 Conclusion

Distribution power systems are those operating at nominal line voltage of 132kV and below. In this work 33kV composite distribution systems are studied. Typical overhead lines and cables have been selected. A 3 wire Copper flat wood pole construction line and a 3 core Hochstadter type mass impregnated non draining insulated cable have been chosen.

Power system waveforms are far from ideal being subject to harmonics and unbalance due to amongst other things the occurrence of faults. Many types of fault occur on distribution power systems but by far the most common are single phase to earth faults. Single phase faults often possess the highest values of fault path resistance due to arcing and also to the high resistance of steel work and support structures. Accurate discrimination of high resistance earth faults on short, especially lightly loaded circuits, is difficult using present approaches to distance protection.

Distance protection is commonly applied to transmission systems as both main and backup protection schemes. At distribution voltage levels main and backup protection schemes are uncommon at the same relaying point, back up being afforded by some other protective function within the same relay or by down stream devices. Distance relays provide back up to protection relays installed further downstream.

Many authors [11-32] have written on the application of distance protection to transmission systems. Moore [32] is one such author modelling the protected transmission system with a lumped parameter model. Such an approach is only suitable for application to short overhead transmission lines as it neglects both the distributed nature of electrical parameters and the shunt admittance of cables and long lines.

At distribution voltages where fault levels are lower and electrical stresses on insulation are less, cables are used quite often. As such, distance protection is being applied to such systems.

Elkateb [11,12] when applying comparator distance relay technology to composite transmission and distribution systems finds that several considerations should be made to maintain accuracy.

These are:

1. As earth return paths and earthing connection practices are difficult to determine often the only way to be sure of the zero sequence characteristics of a cable installation is to measure it. Distance relays installed at different parts of a composite system which is subject to earthing at one end only may see different earth return paths and hence different zero sequence impedance parameters. The zero sequence characteristics of all existing cable installations may be considered onerous to determine.
2. For cable networks $\angle Z_0 \neq \angle Z_1$, therefore complex earth fault compensation factors must be applied to measured current quantities.
3. When studying composite 75kV systems where single core cables of between 1 and 25km are present, complex earth fault compensation factors and a self polarised mho (s.p.m.) tripping characteristic are recommended. Research in this work has found that most distribution cables are of the 33kV 3 core variety. No account is made for this fact.
4. Reach point inaccuracy is generally observed for the case of the composite systems being subjected to a high resistance earth fault. This is not addressed directly, rather, a permissive scheme of operation is recommended by the author to ensure reliability.
5. The comparator relays studied are in common use in power systems, protecting composite systems.

There is a need for investigation of the accuracy of the current approaches to distance relaying when applied to composite distribution circuits.

A novel distance protection algorithm for use in a microprocessor based relay that is suitable for application to composite distribution feeders has been developed.

The algorithm uses a distributed parameter long transmission line model to represent the protected composite system. It considers the shunt capacitance of cable sections and represents its non-homogenous nature; namely the series connection of cable and line sections of varying types and lengths. This is in contrast to previous works such as Moore[32], which use a lumped parameter model suitable only for application to short overhead lines.

The distributed parameters of a transmission line vary with frequency. By considering the line to be ideally transposed and using quoted series and shunt parameters per unit length for specific cable and line sections, hyperbolic parameters applicable to the fundamental operating frequency and representing the distributed nature of the line can be calculated.

Measured discrete time sampled voltage and current signals are transformed into the frequency domain by use of the discrete Fourier transform. The method creates voltage and current vectors rotating at the fundamental power system frequency reducing signal content at all other frequencies.

The complex values of voltage and current are combined mathematically with the hyperbolic line parameters to enable the calculation of voltage and current at a specific distance, X along the feeder length. By choosing X to be eighty percent of feeder length it becomes possible to calculate the voltage and current and thus impedance at the reach point of a classical distance zone one. This is in effect a 'virtual differential' protection scheme using impedance values at both ends of the protected zone. No earth fault compensation is required for the measured or calculated voltage and current signals as Elkateb [12] found essential.

A novel quadrilateral characteristic is proposed which utilises the voltage and current measured at the relaying point and those voltage and current vectors calculated to be at the reach point. In this manner a zero Ohm fault can be determined as being in or out of zone one accurately.

Single phase to earth faults on overhead line sections can contain significant fault path resistance. By estimating the remote end source impedance and through the use of a novel and simple pre-fault load estimation technique the algorithm reduces substantially the

inaccuracies in impedance calculation and thus fault discrimination caused by the presence of fault path resistance as first recognised by Lewis and Tippett[28]. Immunity to high resistance earth faults on short composite circuits (<15km) has been significantly improved.

Results of both steady state and transient simulations for typical 33kV composite networks subject to high resistance single phase to earth faults indicate algorithm operating times of between 30 and 40 msecs to be possible. Similar performance is observed for b-c phase faults.

A typical composite circuit studied consists of 10km of cable and 20 km of line. The circuit can be considered to be operating at a nominal line voltage of 33kV and with short circuit levels of 250MVA and 500MVA at the sending and receiving end respectively. When the new algorithm is applied to such a circuit when subject to a zero ohm a-earth fault occurring at various locations along its length, operating times of the order of 28msecs are possible at zero degrees fault inception. Zone one reach boundary accuracy is of the order of ±1% of zone 1 impedance setting.

For the same circuit but subject to an a-earth fault of 10 Ohms fault path resistance the operating time is maintained in the order of 28msecs rising to 40msecs approaching the reach boundary. Reach boundary accuracy is exhibited by the new algorithm is maintained at ±1% of zone 1 impedance setting.

For the same circuit subject to phase faults of zero and 20 Ohms the algorithm exhibits an operating time of the order of 30 msecs. Reach boundary accuracy as for the case of earth faults is maintained.

Again for the same circuit operating conditions but when circuit lengths increase, as for the case of 60km cable and 30km of line, operation under high resistance earth fault conditions becomes subject to a maximum over reach of 7% total zone 1 impedance setting, and operating times of between 30 and 40 msecs are typical for zero fault inception angles.

There follows a list of assumptions made during the development of the new algorithm.

1. Distributed parameter model is valid at fundamental frequency only.

2. Series and shunt PPS parameters per unit length at fundamental power system frequency (50Hz) are used with some commonly agreed conversion factors[1,2,3] to estimate the ZPS per unit length values.
3. PPS and ZPS shunt admittance per unit length are valid only at nominal operating voltage; the affect of tap changers and other voltage regulating equipment not having been considered.
4. Voltage and current transducers are ideal.
5. The algorithm requires one cycle of power system voltage and current such that the pre-fault load estimation can function.
6. Selection of relevant fault element relies on phase selection methods currently developed and in application on existing micro processor based relaying platforms.

8.2 Future Work

8.2.1 There is a need to study the algorithms response to phase to phase to ground faults.

8.2.2 The algorithm is currently written in a high level computer language. Optimisation is required prior to conversion to a low level language suitable for implementation on a relay processor. This has been described in the text.

8.2.3 In calculating the distributed parameters of the protected circuit a nominal operating line voltage of 33kV is assumed. Consideration should be given to the errors in the algorithm's model of the system caused by tap changers and other components of a distribution power system which influence the operating voltage.

8.2.4 The algorithm derived in this work is designed for application to composite circuits comprising screened three core cables, where the screen is at the same potential as the earthed sheath. A study of the validity of the technique when applied to other cable constructions such as 'HSL' or separate single core cables is required.

8.2.5 The method should be extended to cover multiple zones for a typical distance relaying scheme application. This is best achieved at the optimisation stage mentioned in 8.2.2.

8.2.6 Field trials following real time simulated data studies should progress for assessment of earth fault performance on real but typical 33kV power distribution feeder.

References

[1] 'Power System Analysis', Mortlock and Davies, (1952), Chapman and Hall, London.

[2] 'Underground Power Cables', King and Halfter, 1982, Chapman and Hall, London.

[3] 'Fault Calculations', Lackey C H W, (1951) Oliver and Boyd Ltd., London.

[4] 'Protective Relays Application Guide', GEC ALSTHOM, Third Edition, 1987.GEC ALSTHOM Measurements Ltd.

[5] 'A Digital Recursive Measurement scheme for online Tracking of Power System Harmonics.' Girgis A.A et al, IEEE PES Winter Meeting, New York, February 3, 1991,pp 1-8.

[6] 'Harmonics and their Effect on Power System Protection', Lai L.L. & Johns A.T., Universities Power Engineering Conference, 1990, pp147-150.

[7] 'Power System Protection Principles and Components', Vol 1, Edited by the Electricity Council, 1981,Peter Peregrinus Ltd.

[8] 'Protective Relays Theory and Practice.' Warrington, A.R. Van C. (1962). London: Chapman and Hall, Vol 1.

[9] 'Analysis and Protection of Electric Power Systems.' Jones, D. (1971). Pitman Publishing.

[10] 'Power System stability.' Kimbark E.W. (1956) Chapman and Hall, London .

[11] 'Improving Distance Protection for Underground Cables.' Elkateb, M.M. (1978). Electrical Review, Vol 202, No. 19(19 May), 43-44.

[12] 'Performance of Distance Protection Applied to Underground Cables Alone or Mixed with Overhead Lines.' Elkateb, M.M. (1979). Proc. IEE, Vol 126, No. 9 (September), 805-814.

[13] 'Protection of MHV Overhead Lines and Cables by Digital Distance Relays-Results of Laboratory Tests and Field Experience in a Belgian MHV Network.' Lienart, P. *et al.* (1989). Proceedings of 10th Annual IEE Conference, CIRED, Vol 2, 137-144.

[14] 'Digital Simulation of the Effects of Shunt Capacitance on the Operation of a Digital Distance Protection Algorithm.' Moore, P.J. *et al.* (1995). 3rd International Conference on Advances in Power System Control, Operation and Management, APSCOM-95, Hong Kong (November 1995), 266-270.

[15] 'Real Time Calculation of Resistance and Reactance for Transmission Line Protection by Digital computer', McIness A D & Morrison I F, Institute of Australia, Electrical Engineering Transactions, March 1971.pp 16- 23.

[16] 'An Improved Method for the Digital Protection of High Voltage Transmission Lines', Ranjbar AM & Cory B J, IEEE Trans. PAS, Vol PAS – 94, No, 2, March/April 1975. Pp 544 – 550.

[17] 'High Speed Distance Relaying Using a Digital Computer II- Test Results', Rockefeller G D & Udren E A, IEEE Summer Meeting and International Symposium on High Power Testing, Portland, Ore., July 18 – 23, 1971. Pp 1244 – 1258.

[18] 'The Laboratory Investigation of a Digital System for the Protection of Transmission Lines', Breingan et al, IEEE Trans. PAS, Vol. PAS-98, No. 2 March/April 1979. Pp 350 – 368.

[19] 'High Speed Protection for a Transmission Line in Time Domain', Suda et al, IEEE PES Winter Meeting, New York, NY, February 3-8, 1979. A 80 065-3.

[20] 'Digital Distance Relay with Improved Characteristics Against Distorted Transient Waveforms', Ohura et al, IEEE Trans. Pow. Del., Vol. 4, No. 4, October 1989. Pp 2025 – 2031.

[21] 'New Ultra High Speed Distance Protection Using Finite-Transform techniques', Johns A T & Martin M A, IEE Proc., Vol. 130, Pt. C, No. 3, May 1983.pp 127 – 137.

[22] 'Fundamental Digital Approach to the Distance Protection of EHV Transmission Lines', Johns AT & Martin M A, Proc. IEE, Vol. 125, No. 5, May 1978. Pp 377 – 384.

[23] 'A Simplified Algorithm for Digital Distance Protection Based on Fourier Techniques', D'Amore D & Ferrero A, IEEE Trans. Power Delivery, Vol. 4, No 1, January 1989.pp 157 – 164.

[24] 'Digital High Speed Calculation of the Distorted Signal Fundemental Component', Wiszniewski A, IEE Proc., Vol. 137, Pt. C, No. 1, January 1990.pp 19 – 24.

[25] 'Development and Implementation of a Variable Window Algorithm for High Speed and Accurate Digital Distance Protection', Xia Y Q & Li K K, IEE Proc. Gen. Trans. And Distribution, Vol. 141, No 4, July 1994.pp 383 – 389.

[26] 'Fundamental Basis for Distance Relaying with Symmetrical Components', Phadke et al, IEEE Trans PAS, Vol. PAS-96, No.2, March/April 1977.pp 635 – 646.

[27] ' A Microcomputer Based Symmetrical Component Distance Relay', Phadke et al, IEEE Power Industry Computer Applications Conference, Cleveland, May 1979.pp 47 – 55.

[28] 'Fundamental Basis for Distance Relaying on 3-Phase Systems', Lewis W A & Tippet L S, AIEE Trans., Paper 47-66 Winter Meeting, New York, NY,January 27-31, 1947.pp 694 – 709.

[29] 'Symmetrical Component Based Improved fault Impedance Estimation Method for Digital Distance Protection Part II. Computational Aspects and Validation', Waiker et al , Electric Power Systems Research, 26 (1993) 149 – 154.

[30] 'Fault Impedance Estimation Algorithm for Digital Distance Relaying', Waiker et al, IEEE Trans. On Power Delivery, Vol. 9, No.3, July 1994.pp 1375 – 1382.

[31] 'Performance Comparison of Symmetrical Component Based Fault Impedance Estimation Methods for Digital Distance Relay Applications', Waiker et al, IEE 2nd Conf. On Advances in Power System Control, Operation and Managemement, Dec. 1993, Hong Kong. Pp 83 – 90.

[32] 'Distance Protection of Power Systems Using Digital Techniques', Moore, P.J. and Johns, A.T., IEEIE Electrotechnology, October November 1990, pp 194 - 198

[33] 'Digital Signal Processing – A Practical Approach', Ifeachor E C & Jervis B W, (1993), Addison Wesley Publishers Ltd, Harlow England.

[34] 'Application of Matrix Methods to the Solution of travelling-wave Phenomena in Polyphase Systems', Wedepohl L M, Proc IEE, Vol 10,No. 12, December 1963.pp. 2200-2212.

[35] 'Calculation of Electrical Parameters for Short and Long Polyphase Transmission Lines', Galloway R H et al, Proc. IEE, Vol. 111, No. 12, December 1964.pp. 2051-2059.

[36] 'Multiconductor Transmission Lines', Wedepohl et al, Proc IEE, Vol. 116, No.9, September 1969.

[37] 'Power system Analysis', Grainger J J & Stevenson W D, (1994),McGraw Hill, New York.

[38] 'New Technique for the Accurate Location of Earth Faults on Transmission Systems', Johns A T et al, IEE Proc Gen, Trans, Dist, Vol. 142, No. 2, March 1995.pp 119 – 127.

[39] 'Electromagnetic Transients Program Reference Manual(EMTP Theory Book)', Dommel H W, The University of British Columbia, Vancouver B.C., Canada, August 1986.

[40] 'Simulation of Electromagnetic Transients in Underground Cables Using the EMTP', Marti L, IEE 2nd International Conference on Advances in Power System Control, Operation and Management, December 1993, Hong Kong, pp 147 – 152.

Appendix 6.1

Flowcharts

Flowchart - Main

Subject:	Steady State Simulation	Author:	R Hewett
Date:	08.02.98	email:	-

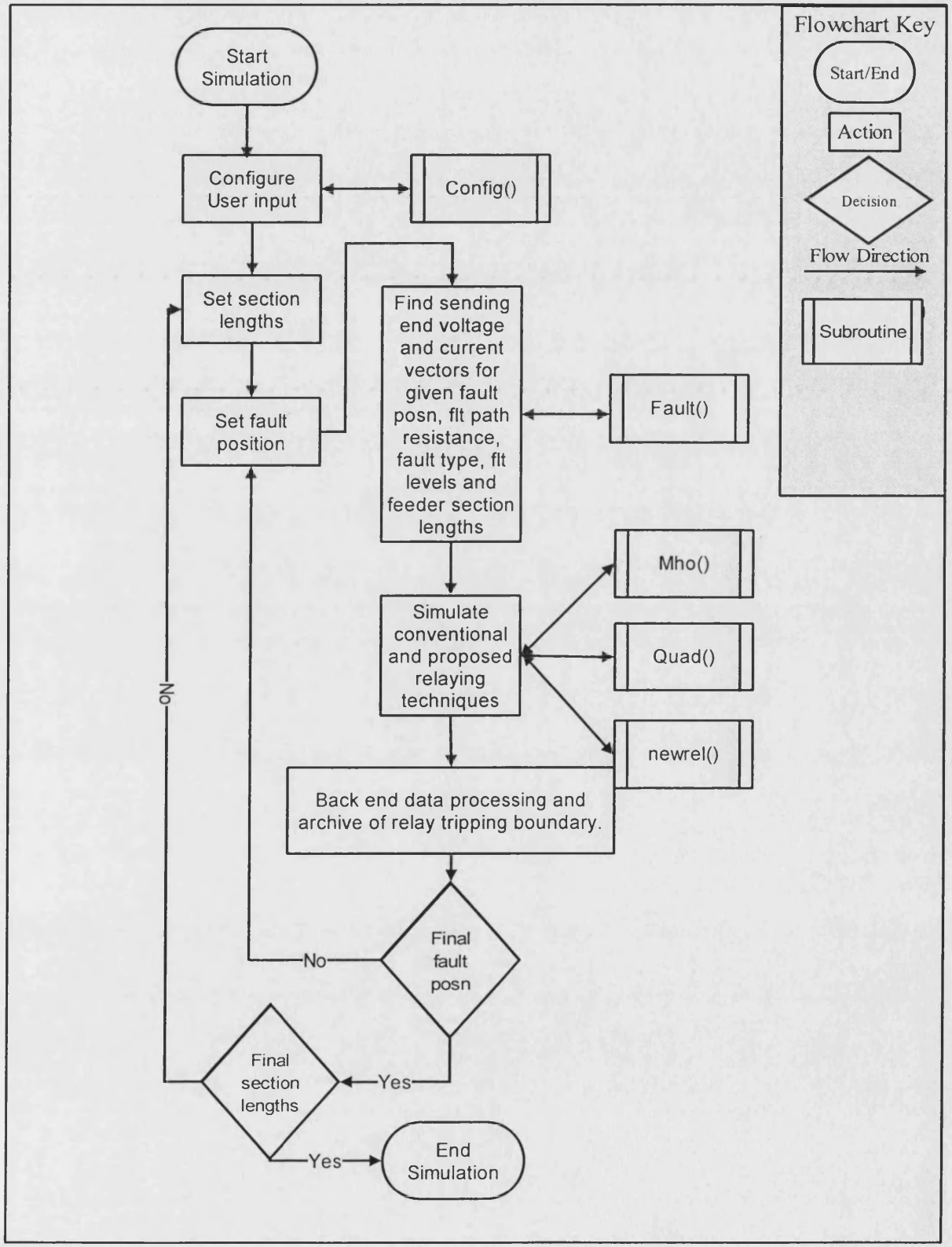

Flowchart - Config()

Subject:	Steady State Simulation	Author:	R Hewett
Date:	08.02.98	email:	-

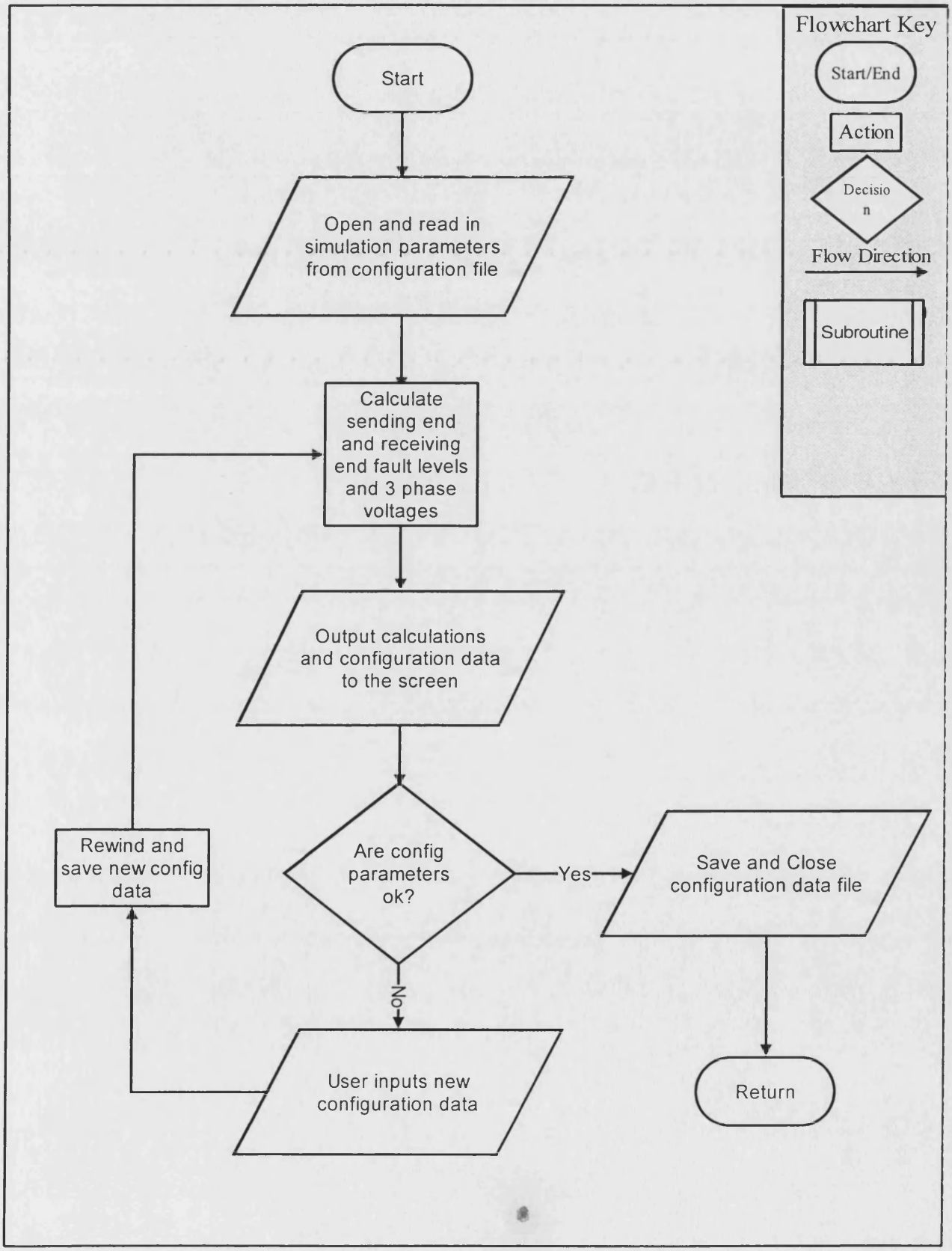

Flowchart - Fault()

Subject:	Steady State Simulation	Author:	R Hewett
Date:	08.02.98	email:	-

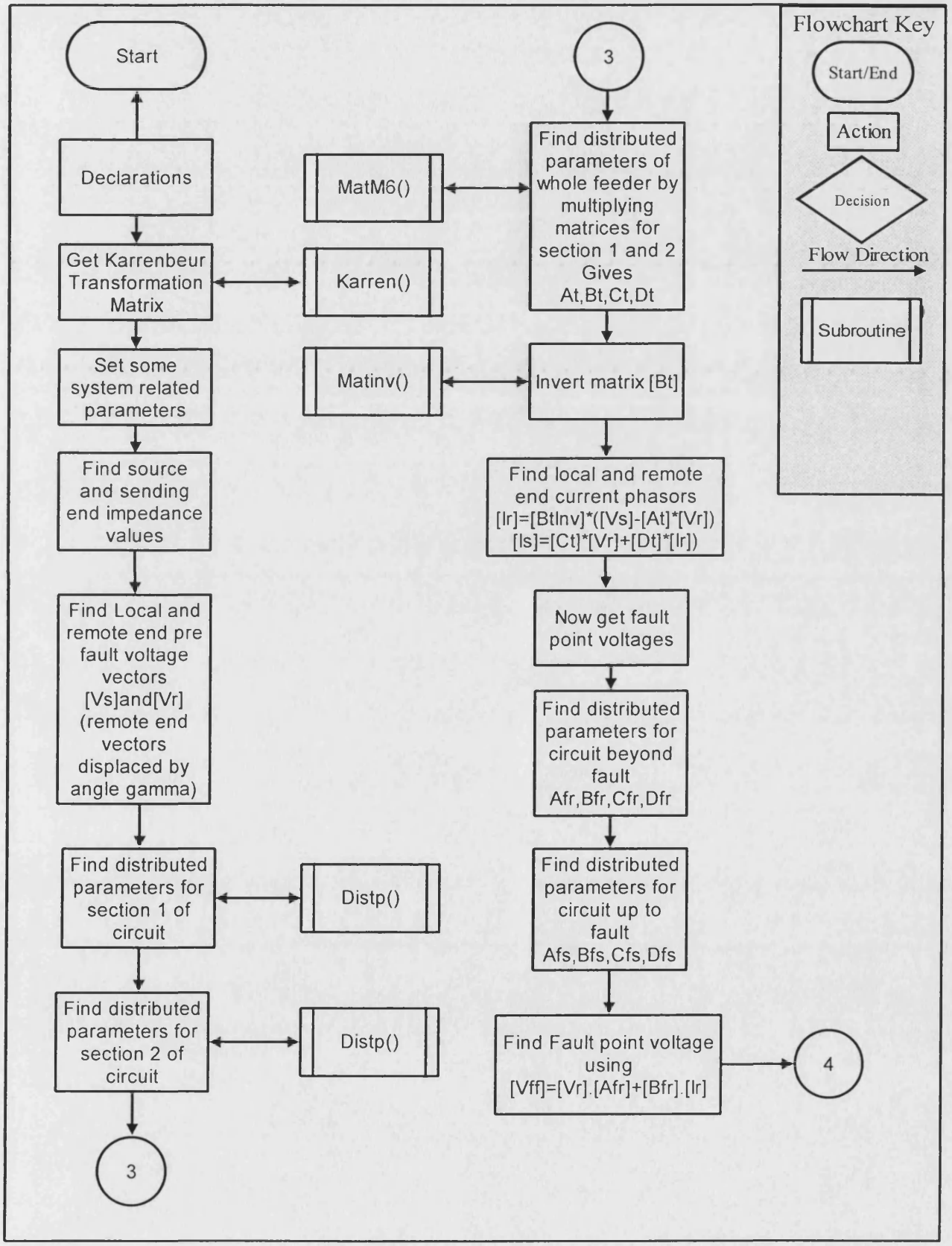

Flowchart - Fault()

Subject:	Steady State Simulation	Author:	R Hewett
Date:	08.02.98	email:	-

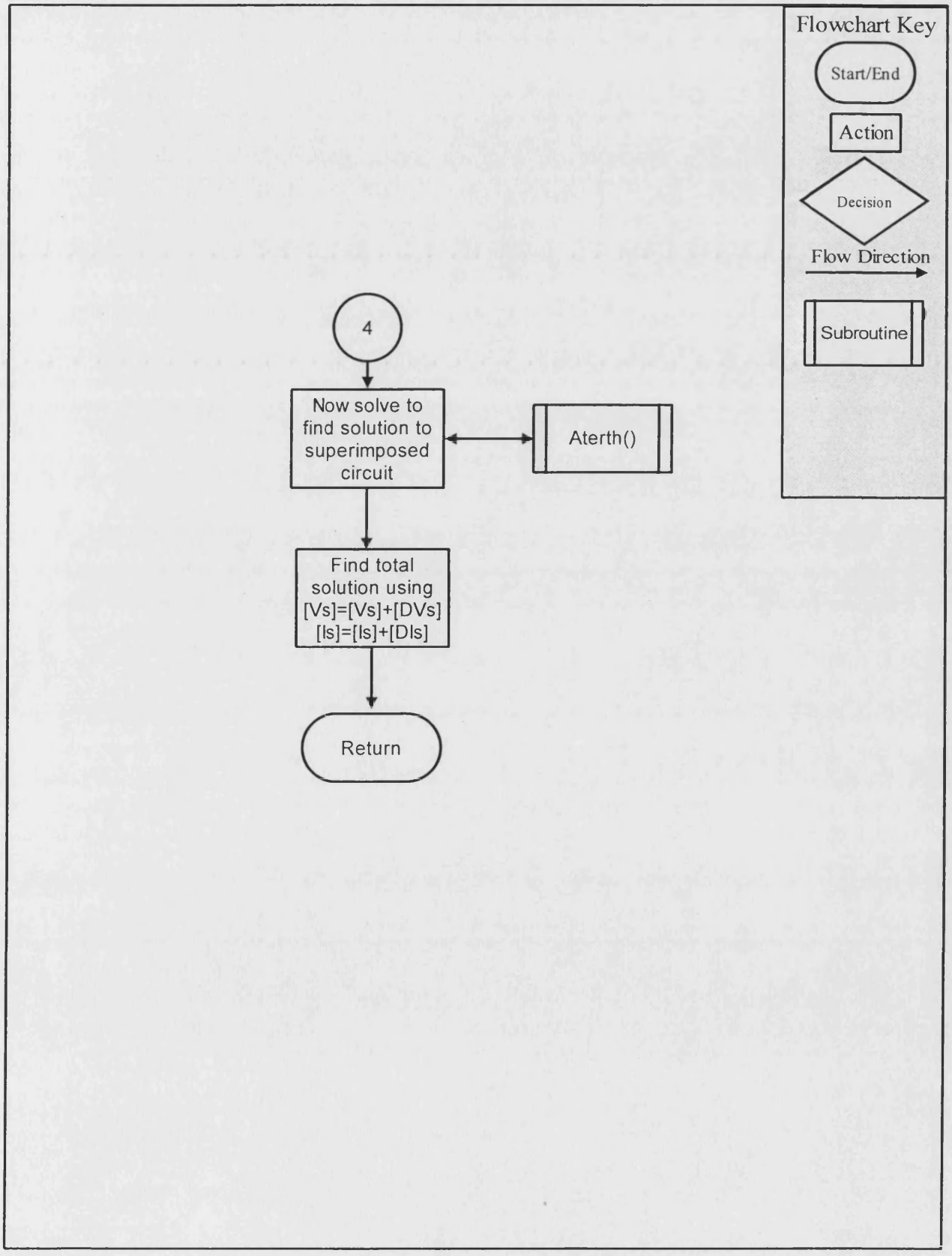

Flowchart - MatM6()

Subject:	Steady State Simulation	Author:	R Hewett
Date:	08.02.98	email:	-

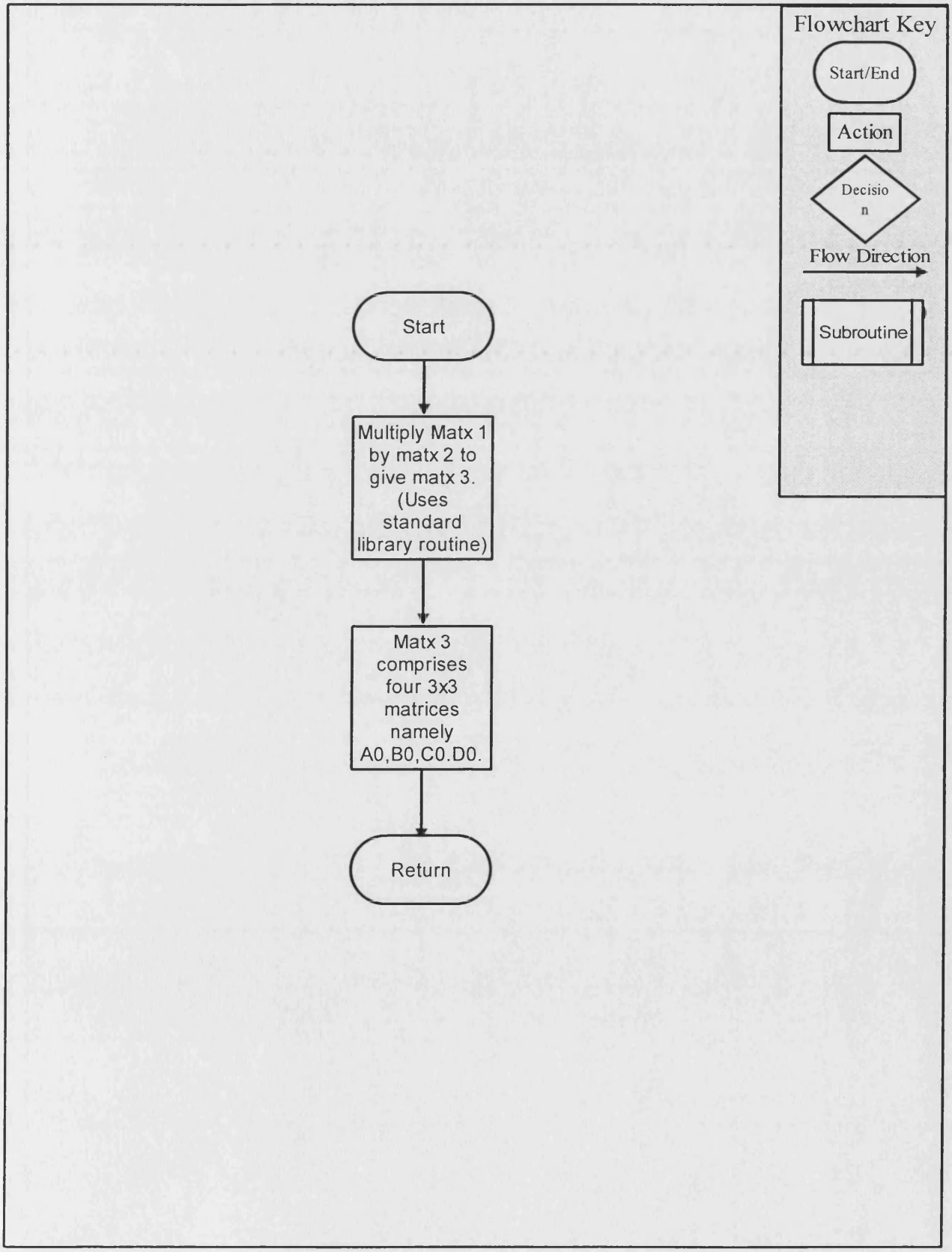

Flowchart - Karren()

Subject:	Steady State Simulation	Author:	R Hewett
Date:	08.02.98	email:	-

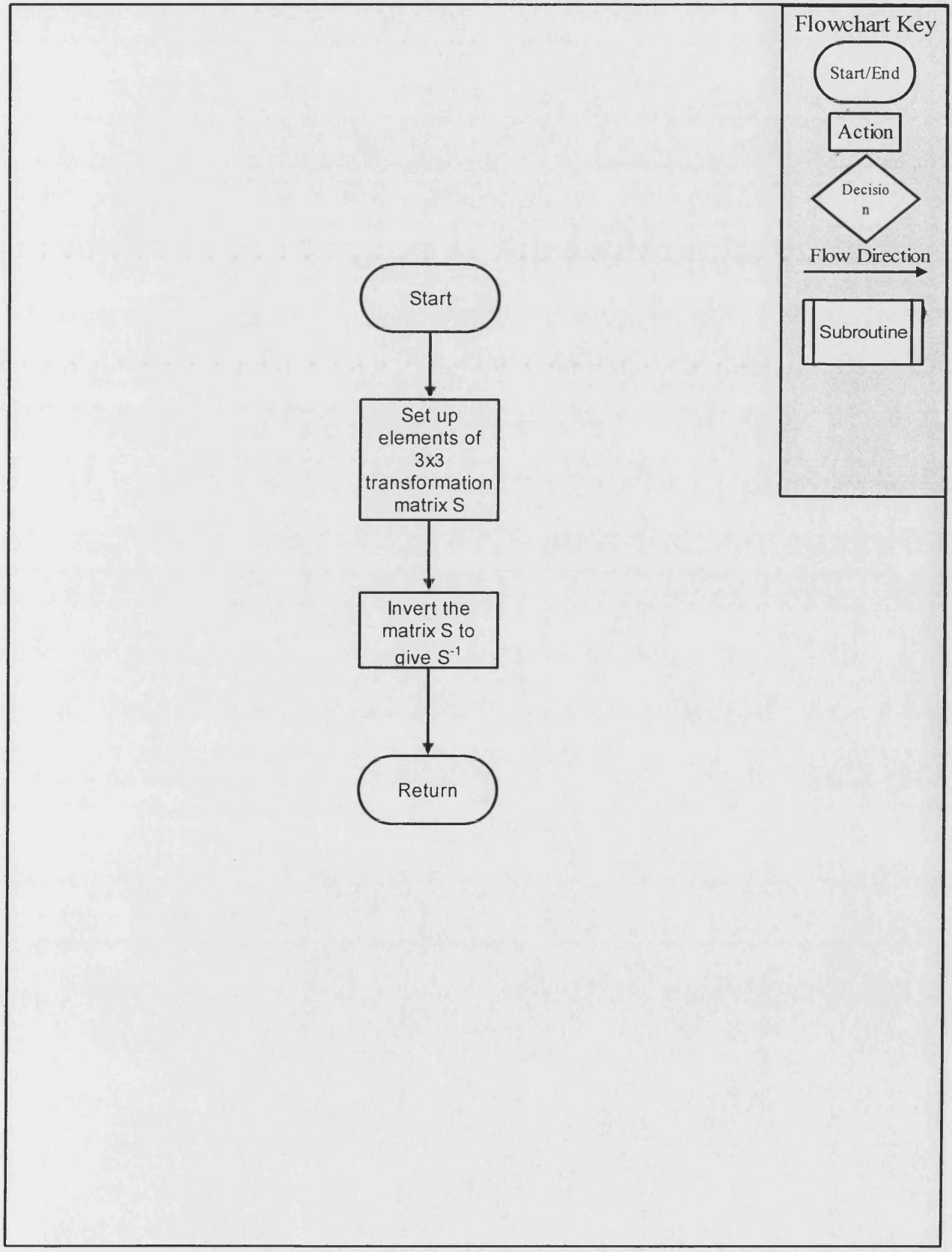

Flowchart - Matinv()

Subject:	Steady State Simulation	Author:	R Hewett
Date:	08.02.98	email:	-

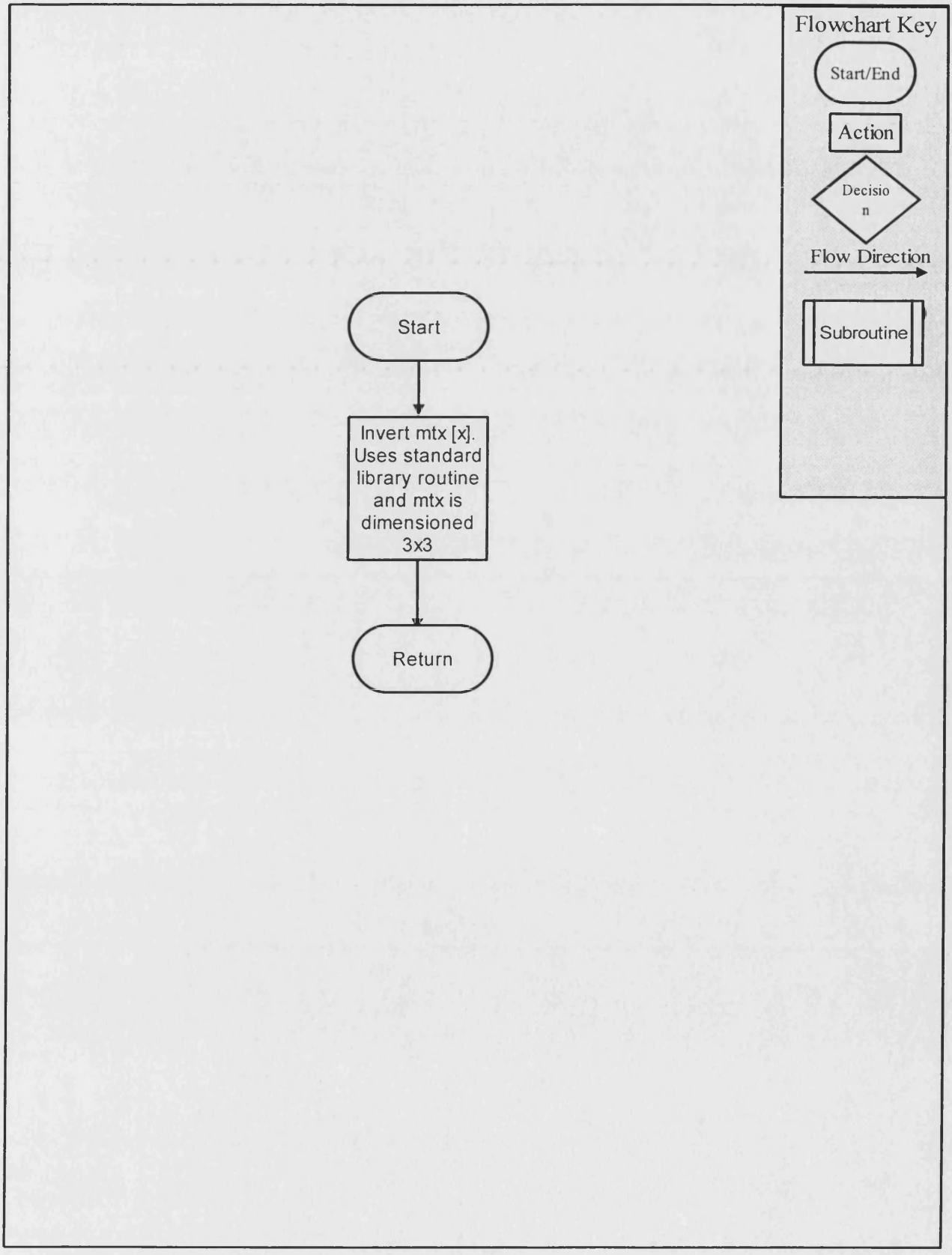

Flowchart - Distp()

Subject:	Steady State Simulation	Author:	R Hewett
Date:	08.02.98	email:	-

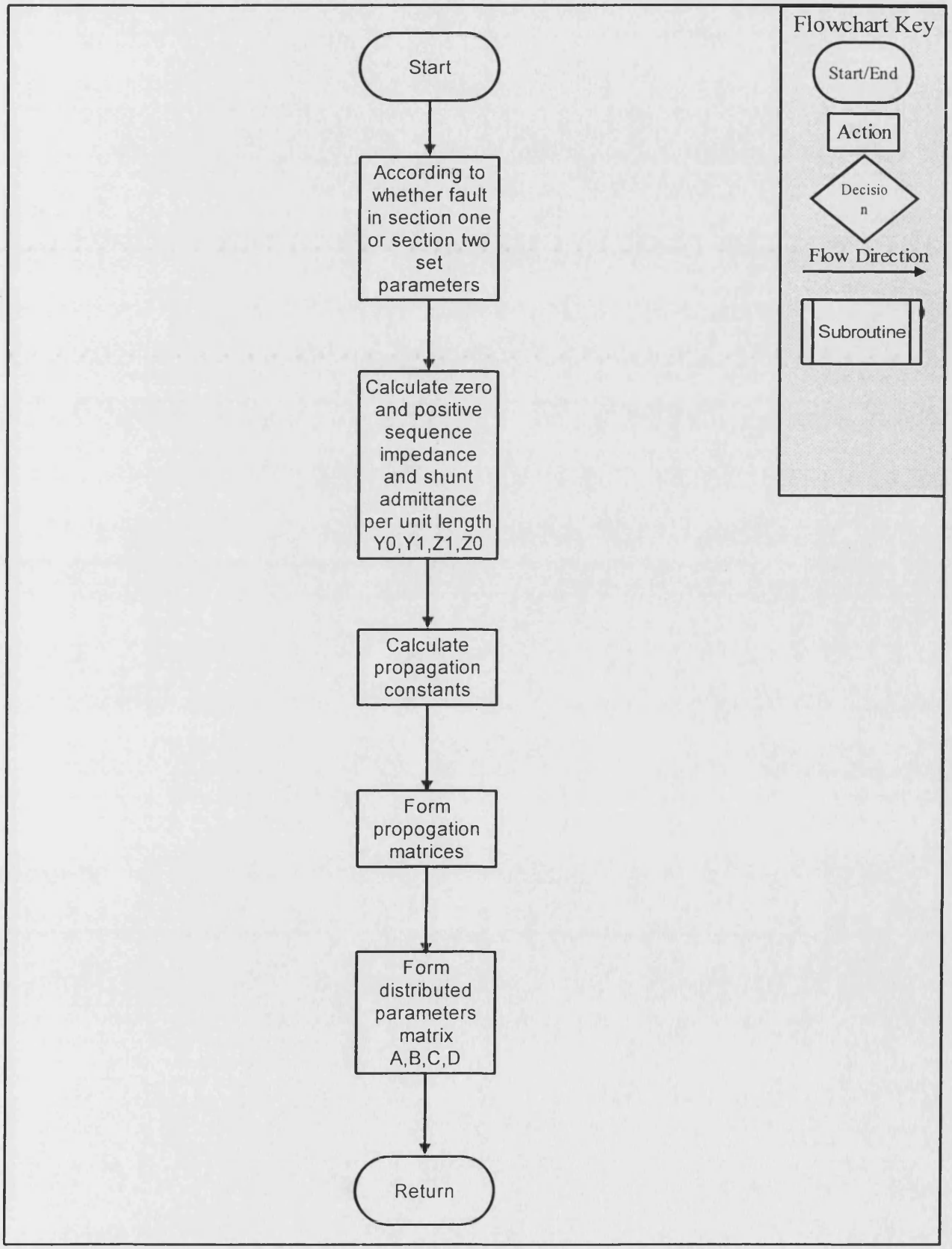

Flowchart - Aterth()

Subject:	Steady State Simulation	Author:	R Hewett
Date:	08.02.98	email:	-

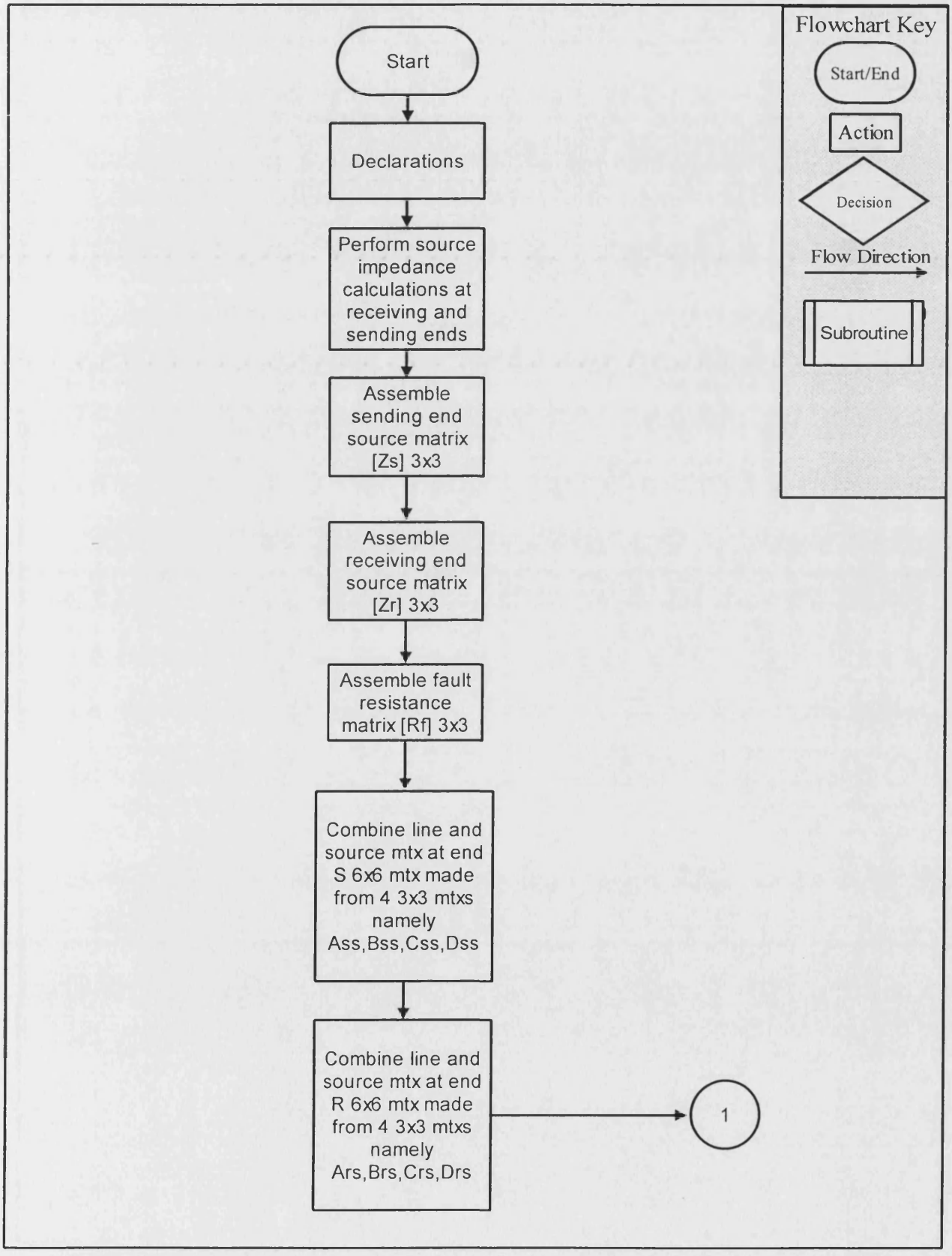

Flowchart - Aterth()

Subject:	Steady State Simulation	Author:	R Hewett
Date:	08.02.98	email:	-

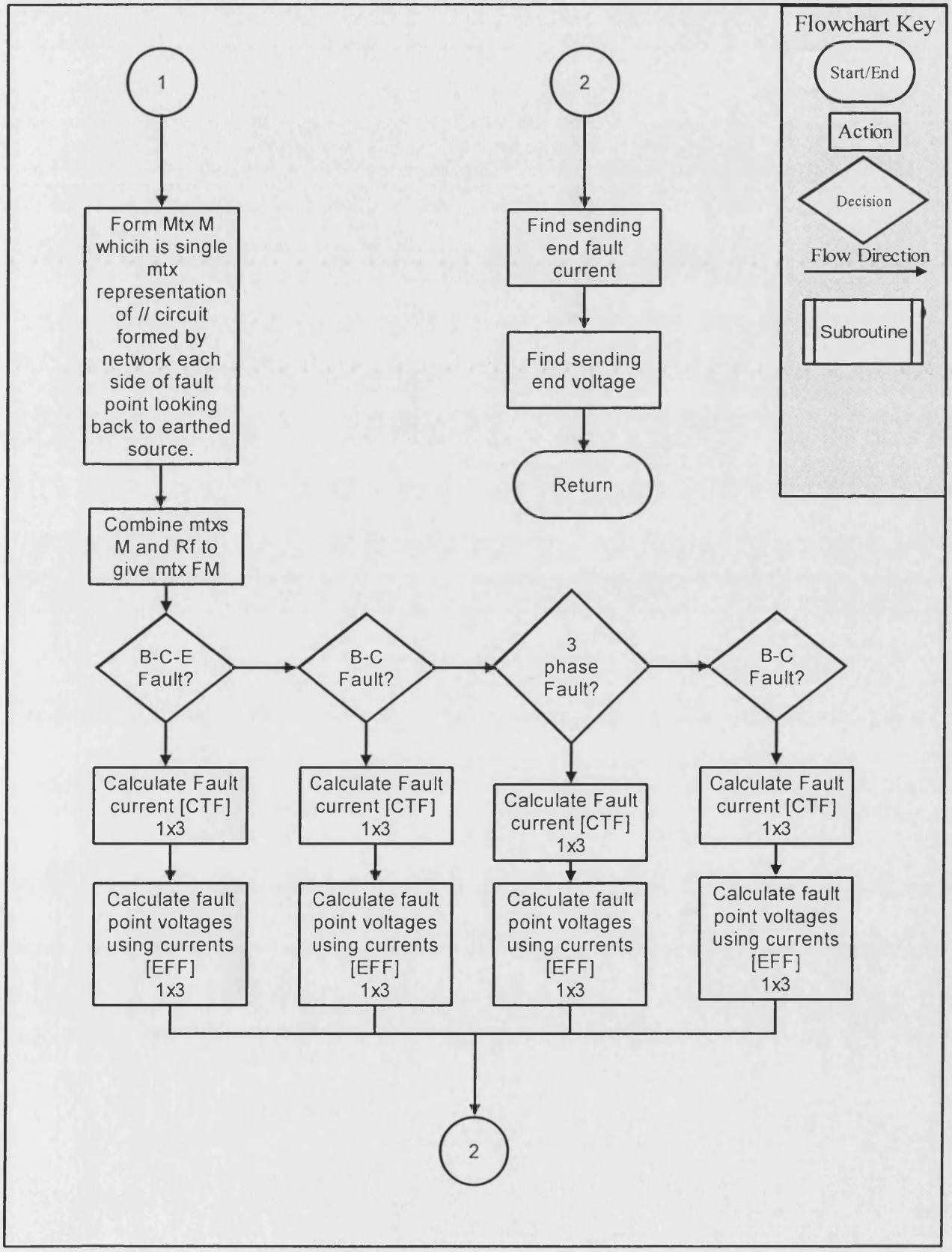

Flowchart - Mho()

Subject:	Steady State Simulation	Author:	R Hewett
Date:	08.02.98	email:	-

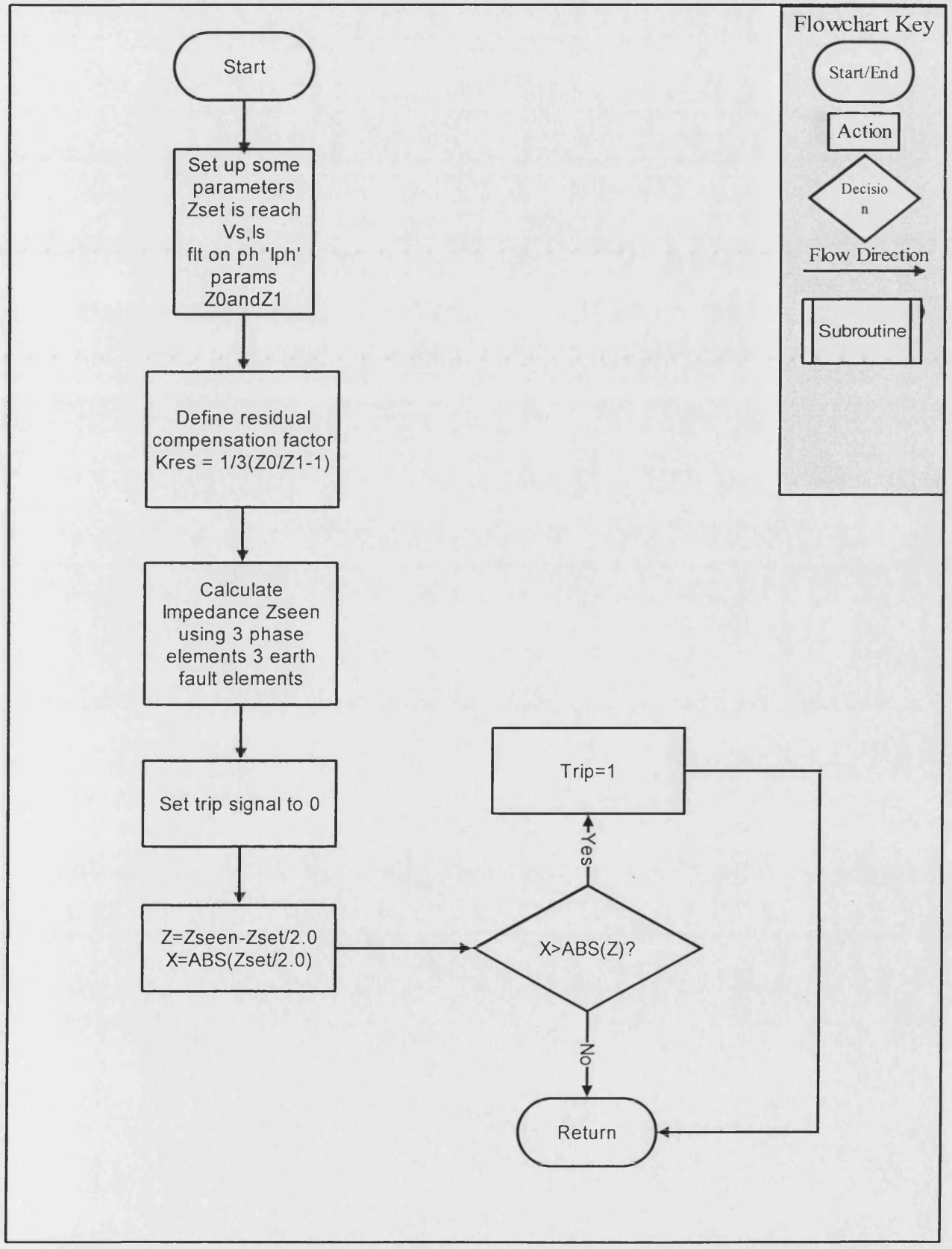

Flowchart - Quad()

Subject:	Steady State Simulation	Author:	R Hewett
Date:	08.02.98	email:	-

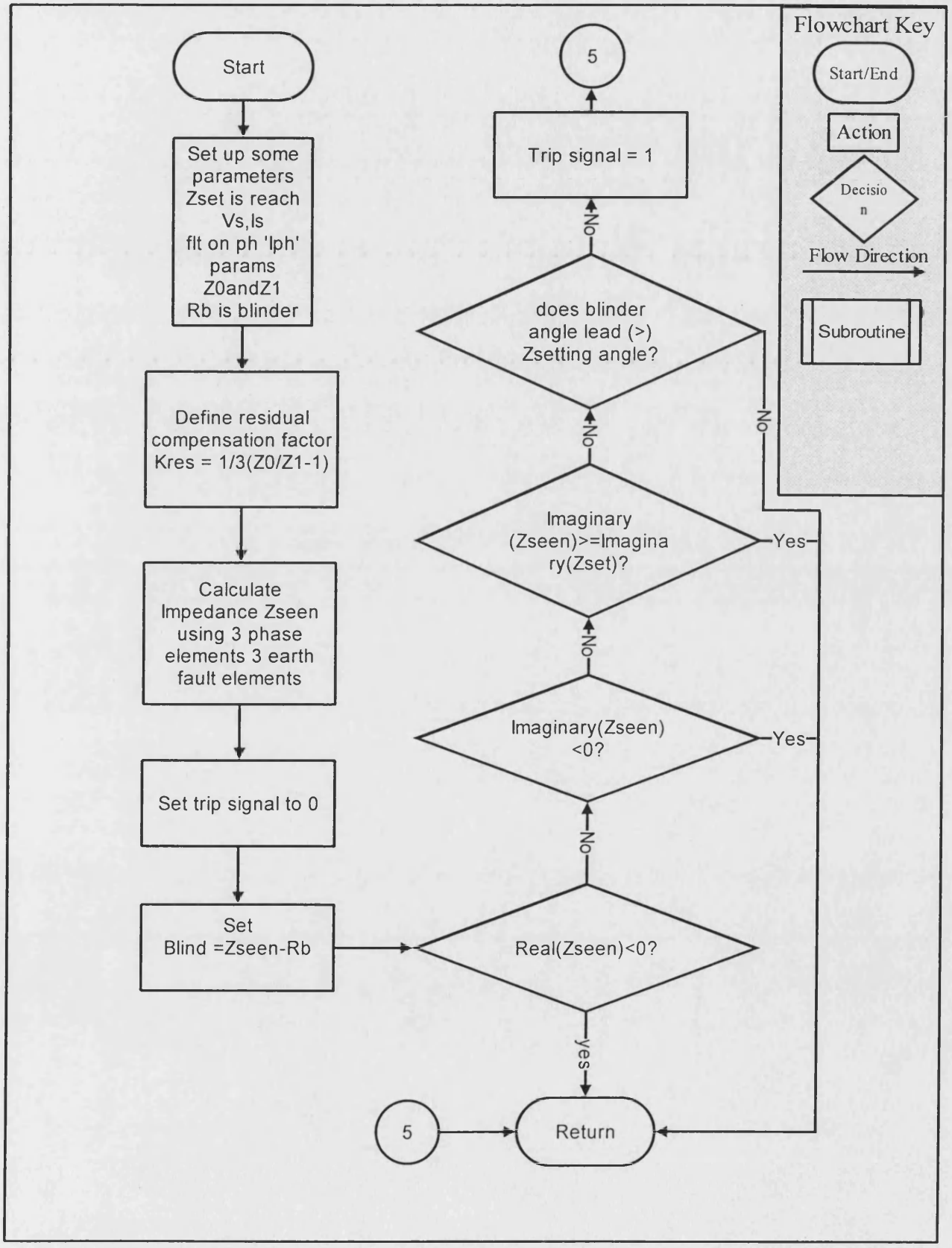

Flowchart - Newrel()

Subject:	Simulation	Author:	R Hewett
Date:	08.02.98	email:	-

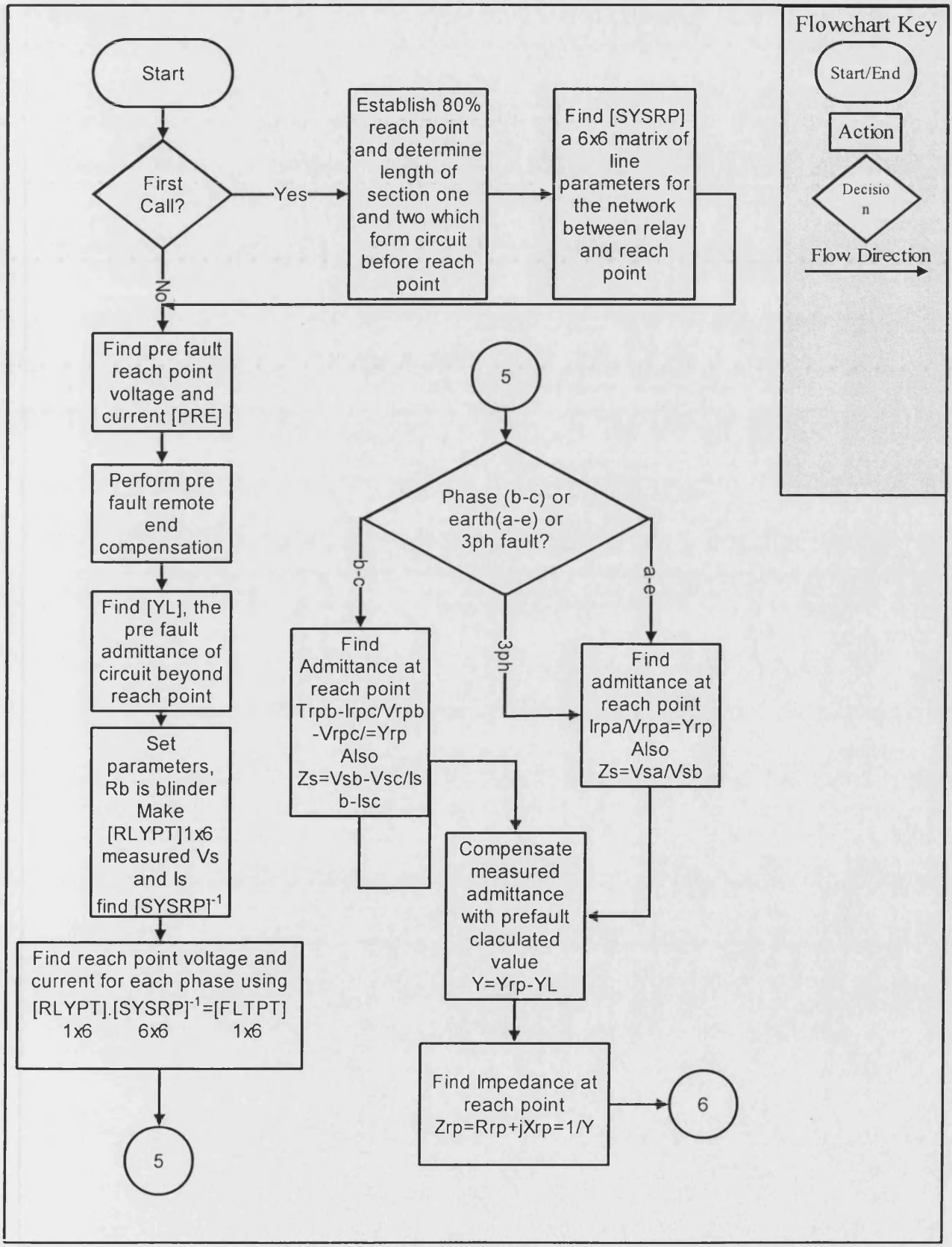

Flowchart - Newrel()

Subject:	Simulation	Author:	R Hewett
Date:	08.02.98	email:	-

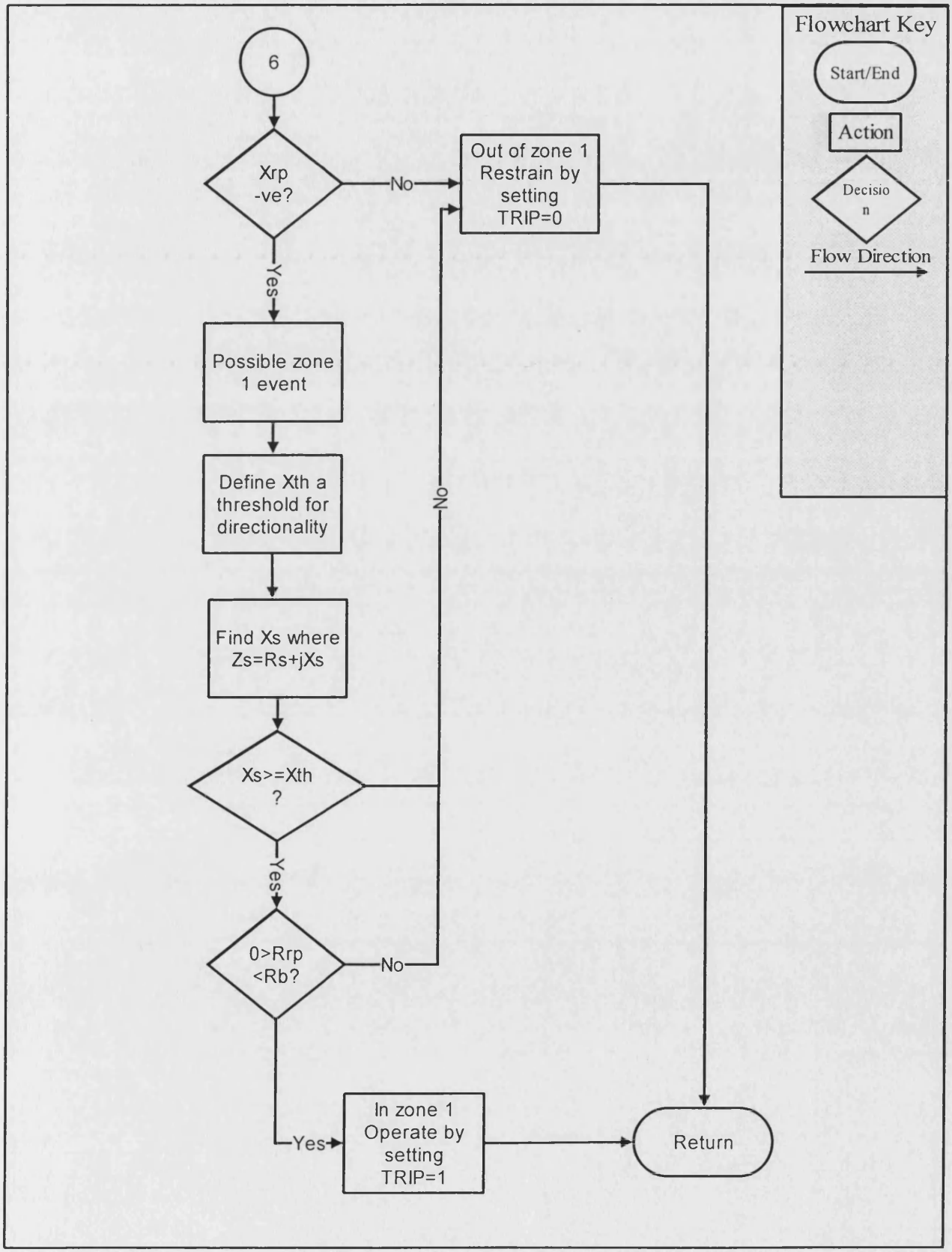

Flowchart - Matmul()

Subject:	Steady State Simulation	Author:	R Hewett
Date:	08.02.98	email:	-

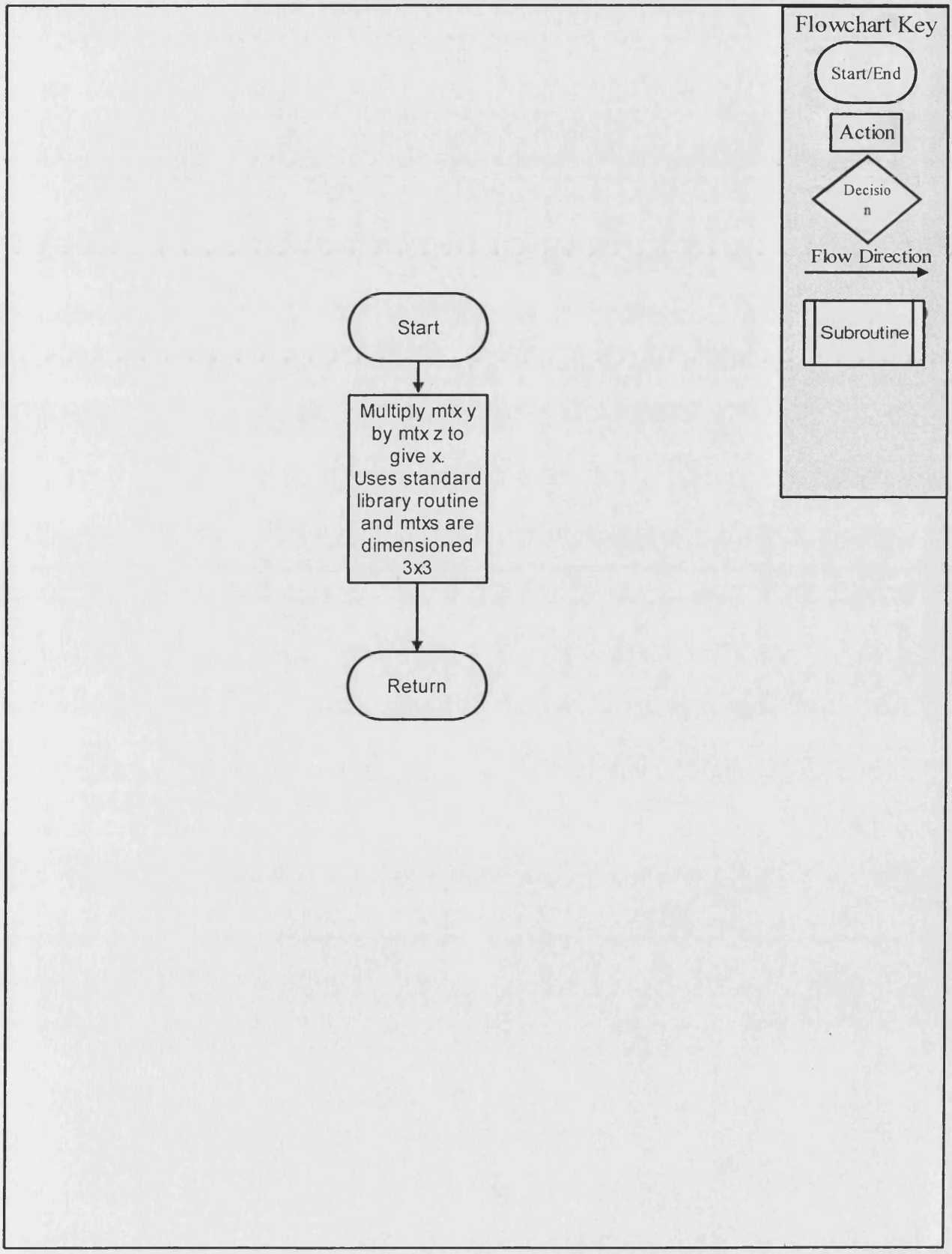

Appendix 6.2

Superimposed Circuit Method

Appendix 6.2 Superimposed Circuit Modeling Theory

Derivation of Source Impedance Matrix [Z_S] and [Z_R]

Let $Z_{s0}(\omega)$ and $Z_{s1}(\omega)$ be the zero and positive phase sequence values of the same impedance at busbar S of figure 6.1, at frequency ω.

$$Z_{ss}(\omega) = \tfrac{1}{3}(Z_{s1}(\omega) + 2Z_{s0}(\omega))$$

Equation 1

$$Z_{sm}(\omega) = \tfrac{1}{3}(Z_{s0}(\omega) - Z_{s1}(\omega))$$

Equation 2

Therefore,

$$[Z_s] = \begin{bmatrix} Z_{ss}(\omega) & Z_{sm}(\omega) & Z_{sm}(\omega) \\ Z_{sm}(\omega) & Z_{ss}(\omega) & Z_{sm}(\omega) \\ Z_{sm}(\omega) & Z_{sm}(\omega) & Z_{ss}(\omega) \end{bmatrix}$$

Equation 3

[Z_R] may be found in a similar manner.

Determination of Hyperbolic Transmission Line Parameters

These are found using equations 5.16 to 5.19 with variable substitution.

Substituting x with l gives,

$$[A_x]=[A_l]$$

$$[B_x]=[B_l]$$

$$[C_x]=[C_l]$$

$$[D_x]=[D_l]$$

Similarly, substituting x with r gives,

$$[A_x]=[A_r]$$

$$[B_x]=[B_r]$$

$$[C_x]=[C_r]$$

$$[D_x]=[D_r]$$

Combining Circuit from S to Fault Point and [Z_S]

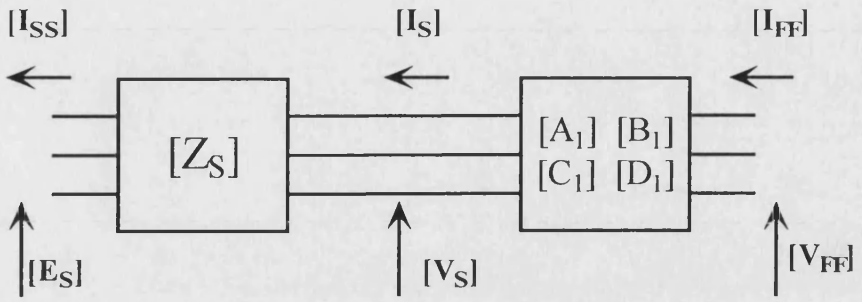

Figure A6.1 Circuit from Fault Point to Source Impedance Matrix [Z_S]

With reference to figure A6.1,

$$\begin{bmatrix}[V_{FF}]\\[I_{FF}]\end{bmatrix}=\begin{bmatrix}[A_1]&[B_1]\\[C_1]&[D_1]\end{bmatrix}\cdot\begin{bmatrix}[V_S]\\[I_S]\end{bmatrix}$$

Equation 4

$$\begin{bmatrix}[V_S]\\[I_S]\end{bmatrix}=\begin{bmatrix}[I]&[Z_S]\\0&[I]\end{bmatrix}\cdot\begin{bmatrix}[E_S]\\[I_{SS}]\end{bmatrix}$$

Equation 5

Where,

$$[I]=\begin{bmatrix}1&0&0\\0&1&0\\0&0&1\end{bmatrix}$$

Equation 6

Eliminating $\begin{bmatrix}[V_S]\\[I_S]\end{bmatrix}$ gives,

$$\begin{bmatrix}[V_{FF}]\\[I_{FF}]\end{bmatrix}=\begin{bmatrix}[A_1]&[B_1]\\[C_1]&[D_1]\end{bmatrix}\cdot\begin{bmatrix}[I]&[Z_S]\\0&[I]\end{bmatrix}\cdot\begin{bmatrix}[E_S]\\[I_{SS}]\end{bmatrix}=\begin{bmatrix}[A_1]&[A_1][Z_S]+[B_1]\\[C_1]&[C_1][Z_S]+[D_1]\end{bmatrix}\cdot\begin{bmatrix}[E_S]\\[I_{SS}]\end{bmatrix}=\begin{bmatrix}[A_1]&[B_1]\\[C_1]&[D_1]\end{bmatrix}\cdot\begin{bmatrix}[E_S]\\[I_{SS}]\end{bmatrix}$$

Equation 7

Similarly, circuit from R to fault point in Figure 6.1 Chapter 6, can be combined with source impedance matrix [Z_R] to give,

$$\begin{bmatrix}[V_{FF}]\\[I_{FF}]\end{bmatrix}=\begin{bmatrix}[A_2]&[B_2]\\[C_2]&[D_2]\end{bmatrix}\cdot\begin{bmatrix}[E_R]\\[I_{RR}]\end{bmatrix}$$

Equation 8

Solving the Superimposed Circuit

The circuit from the fault point can be represented as figure A6.2.

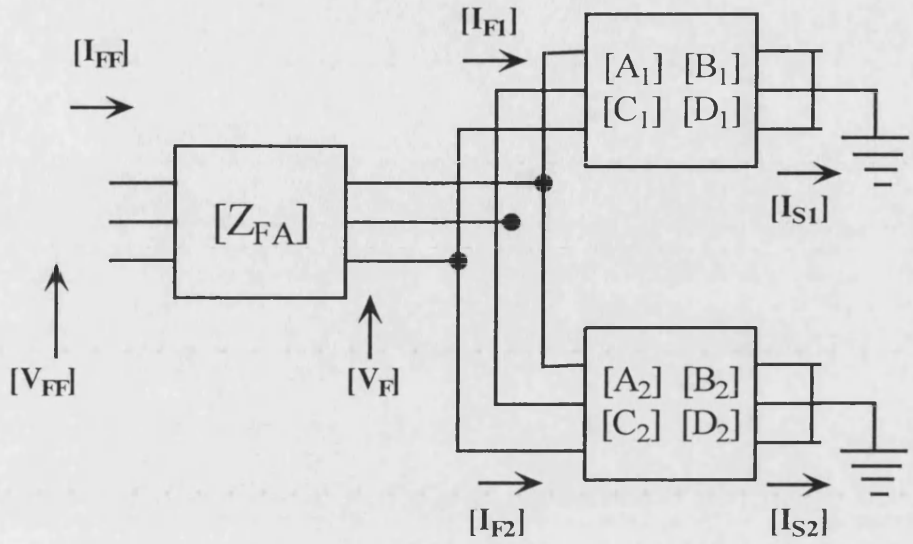

Figure A6.2 Superimposed Circuit as Viewed from the Fault Point

From inspection of figure A6.2,

$$\begin{bmatrix}[V_F]\\[I_{F1}]\end{bmatrix}=\begin{bmatrix}[A_1]\ [B_1]\\[C_1]\ [D_1]\end{bmatrix}\cdot\begin{bmatrix}0\\[I_{S1}]\end{bmatrix}$$

Equation 9

Therefore,

$$[I_{S1}]=[B_1]^{-1}\cdot[V_F]$$

Equation 10

and

$$[I_{F1}]=[D_1][B_1]^{-1}\cdot[V_F]$$

Equation 11

Similarly,

$$\begin{bmatrix}[V_F]\\[I_{F2}]\end{bmatrix}=\begin{bmatrix}[A_2]\ [B_2]\\[C_2]\ [D_2]\end{bmatrix}\cdot\begin{bmatrix}0\\[I_{S2}]\end{bmatrix}$$

Equation 12

Therefore,

$$[I_{S2}]=[B_2]^{-1}\cdot[V_F]$$

Equation 13

and

$$[I_{F2}] = [D_2][B_2]^{-1} \cdot [V_F]$$

Equation 14

Thus,

$$[I_{F1}] + [I_{F2}] = [D_1][B_1]^{-1}[V_F] + [D_2][B_2]^{-1}[V_F]$$

Equation 15

Now,

$$[I_{FF}] = [I_{F1}] + [I_{F2}]$$

Equation 16

Using equation 16 in 15, and rearranging gives,

$$[I_{FF}] = \left([D_1][B_1]^{-1} + [D_2][B_2]^{-1}\right) \cdot [V_F]$$

Equation 17

Hence,

$$[V_F] = \left([D_1][B_1]^{-1} + [D_2][B_2]^{-1}\right)^{-1} \cdot [I_{FF}] = [M_{12}] \cdot [I_{FF}]$$

Equation 18

Therefore,

$$[V_{FF}] = [Z_{FA}][I_{FF}] + [V_F] = [Z_{FA}][I_{FF}] + [M_{12}][I_{FF}] = ([Z_{FA}] + [M_{12}])[I_{FF}] = [M][I_{FF}]$$

Equation 19

where,

$$[M] = \begin{bmatrix} M_S & M_M & M_M \\ M_M & M_S & M_M \\ M_M & M_M & M_S \end{bmatrix}$$

Equation 20

From equation 19,

$$[I_{FF}] = ([Z_{FA}] + [M_{12}])^{-1} \cdot [V_{FF}]$$

Equation 21

For the case of an a-earth fault,

$$[I_{FF}] = \begin{bmatrix} I_{FFA} \\ 0 \\ 0 \end{bmatrix}$$

Equation 22

And,

$$[Z_{FA}] = \begin{bmatrix} R_{FA} & 0 & 0 \\ 0 & 0 & 0 \\ 0 & 0 & 0 \end{bmatrix}$$

Equation 23

Thus,

$$V_{FA} = M_S I_{FFA}$$

Equation 24

Therefore,

$$I_{FFA} = V_{FA} / M_S$$

Equation 25

Note that equation 24 and 25 are not matrix equations.

Hence,

$$V_{FFA} = V_{FA} - R_{FA} I_{FFA}$$

$$V_{FFB} = M_M I_{FFA}$$

$$V_{FFC} = M_M I_{FFA}$$

Equations 26

The current flowing into the source S are given by the matrix equation,

$$[I_{SI}] = [B_1]^{-1}[V_F]$$

Equation 27

And the superimposed voltages at the busbar S are given by,

$$[V_{SP}] = [Z_S][I_{SI}]$$

Equation 28

Published Material

The following conference papers have been published and presented as detailed on each cover sheet.

Paper 1

The following Paper was presented and published in the proceedings of the 32nd Universities Power Engineering Confernece, UPEC97, UMIST, Manchester, UK, 10th – 12th September 1997 , Vol. 2.pp 279 – 282.

INVESTIGATION INTO DISTANCE PROTECTION OF A 33kV COMPOSITE FEEDER USING THE EMTDC/PSCAD.

R.J.Hewett and P.J.Moore.

University of Bath, UK.

ABSTRACT

The paper initially introduces the typical arrangements of a composite distribution network and highlights it's unique characteristics. Recently, development of a new impedance algorithm, involved an investigation of the performance of an existing impedance algorithm based on the simple series resistance and inductance line equation, applied to a composite distribution feeder. Using the EMTDC/PSCAD electromagnetic simulation package, results are presented which show inaccuracies in impedance measurement. The paper highlights a suitably accurate three core distribution cable model and explains how the physical construction of a commonly used cable enables such a model to be valid.

INTRODUCTION

Power distribution composite circuits comprise both overhead line and underground cable sections, and may have an operating voltage of between 33kV and 132kV. They present a unique set of problems which must be considered when applying distance protection algorithms, if errors are to be avoided.

Impedance algorithms previously developed, such as Moore & John's [1], have been based on the simple resistance (R) and inductance (L) series line model. Shunt admittance of a circuit has been neglected.

Recently, a composite power distribution network has been modeled using the EMTDC electromagnetic simulation package.

It is shown that as cable lengths within composite circuits increase, so the error in impedance measurement increases, due to the cable's shunt admittance. Further, a single phase to earth fault in a particular composite feeders first zone, is discriminated as a second zone fault due to these measurement errors.

THE COMPOSITE DISTRIBUTION NETWORK

For a variety of reasons a power distribution feeder, may consist of both underground and overhead sections. Distribution substations in urban locations may only be accessible via underground routes. In the UK particularly environmental considerations have resulted in cables being used to cross areas of outstanding beauty, sites of scientific interest, and urban or heavily industrialised areas.

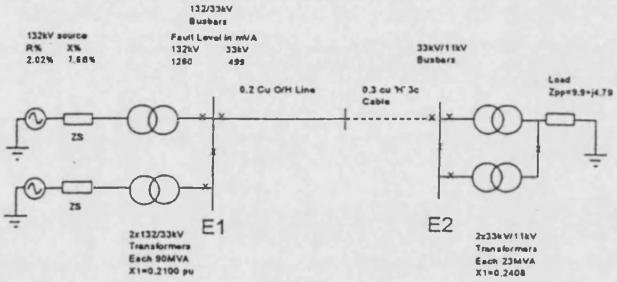

Figure 1 Section of Composite 33kV distribution Network (SWEB Plc).

TYPICAL COMPOSITE NETWORK

The composite network of figure 1, has been used for the simulation work described in this paper and is one section of a more comprehensive South Western Electricity Plc (SWEB Plc) power distribution network.

A recent survey, conducted in the southern region of SWEB's operational area ascertained that 'H' type 33kV three core cable constitutes over 65 percent of total cable length installed.

'H' type cable is often preferred over other cable types, due to it's increased flexibility and bending radius, and ease of jointing. It is a screened, solid type cable having either round or shaped copper stranded conductors of typically 0.2 or 0.3 square inch cross sectional area. Each conductor is covered with a layer oil impregnated paper tape insulation and enclosed within a perforated aluminum tape screen. A further layer of oil impregnated tapes are wrapped around the outside of the three screened cores to form a 3 core cable in turn

enclosed within a lead-alloy sheath to provide an earth and mechanical protection. A further layer of protection is provided by steel wire or tape armour and an outer plastic serving. The core screens are maintained at the same potential as the sheath due to strands of conductive material woven into the outer layer of paper tapes used between the screens and the sheath. The screen reduces electrical stresses set up in the core insulation.

A typical power distribution overhead line in use in the U.K. would be the three phase, copper stranded conductor, in flat formation on wooden pole construction. Technical data for both the underground cable and overhead line are given in Appendix I.

The 'H' type 3 core Copper cable described previously, has been modeled in the EMTDC using a 'PI' model approximation, which is valid for this type of cable only. Because the 'H' type cable is screened, the equivalent star capacitance of the cable is that between each phase conductor and its respective screen, the screen being assumed at earth potential (zero voltage). The Steel wire armour is also assumed to be at earth potential as it is bonded to the cable sheath and sub station earth at source. The substation earth bar resistance in this case is assumed to be negligible and thus the assumption that the screen of each core is at zero voltage can be made. Conductors are circular in cross section.

COMPOSITE CIRCUIT CHARACTERISTICS AND DISTANCE PROTECTION

Composite distribution circuits possess a number of unique characteristics which must be addressed if distance protection is to operate correctly.

Consider the simplified power system of figure 1. The overhead line and underground cable are those detailed in appendix I and are 20 km and 30 km in length respectively. It is clear that the impedance to an 80% reach point when looking from each end will be different. A distance relay should accurately represent the feeder section types and their sequence of connectivity.

The zero sequence impedance angle of a cable is different to that of the positive or negative sequence impedance. Therefore, earth fault compensation should be vectorial in nature [2,3]. For a cable earthed at one end only, zero sequence impedance will be different at each end[3].
Considering the composite circuit, significant amounts of arc resistance could be contained in faults occurring on the overhead line sections. Though arc resistance can be thought of as negligible in cables, for the composite circuit it must be accounted for.

Long lines (greater than 200 km) and cables (greater than 20 km) exhibit significant shunt admittance to earth[4]. This shunt admittance should be considered by an impedance measuring algorithm, to maintain accuracy.

NETWORK SIMULATION AND RELAY TESTING

In developing a new distance protection algorithm suitable for the protection of composite circuits, the errors of a series line model algorithm [1], when applied to a composite distribution feeder have been investigated.

The circuit shown in figure 1 was modeled using the EMTDC electromagnetic transient simulation package. The algorithm has been coded in FORTRAN and can be called from a user written relay component. It is possible to connect this relay component anywhere in the simulation circuit, and can be set to operate circuit breakers within the simulation run time, according to the detection of faults [5]. Faults are applied via a fault logic module at predetermined times and can be set to included predefined values of fault resistance.

The overhead line and cable sections are modeled by cascading the 'PI' sections previously described. In this manner simulations are valid at the fundamental frequency only and for short to medium lengths. In all tests the overhead line section is 20 km long and the cable section length is increased from 0 km to 100 km in varying increments. The relay component linking the impedance algorithm to the simulation data file was installed at E1. A reach point setting of 80% of the total feeder length has been used in all simulations.

For every increment in the cable length, an 'a' phase to earth fault at the reach point is simulated and the impedance seen by the algorithm[1], is recorded in table 1. Through the application and solution of the well known two port theory equations [4], the actual impedance has been calculated and included in table 1 for comparison purposes. The impedance plain sketch of Figure 2 represents these results graphically.

Results are presented in impedance plot segment of figure 3, for an 'a' phase to earth fault at the reach point of a circuit comprising 20 km of overhead line and 42.5 km of cable. Consequently there is 30 km of cable included in the first zone of protection when looking from E1. A trip output from the user defined relay component can be linked to a circuit breaker at bus bar E1 to simulate feeder isolation if required. Fault resistance is negligible.

Table 1 Comparison of Impedance Measurements between R&L Algorithm and True Impedance

Actual Impedance		R and L Impedance		Circuit Length
Zmag	Z Arg	Z Mag	Z Arg	km
9.91	63.12	10.16	63.28	line +20 km cable
11.22	61.12	11.52	61.5	line +30 km cable
12.5	59.51	12.89	60.13	line +40 km cable
13.9	58.0	14.3	59.03	line +50 km cable
16.02	54.19	17.03	57.3	line + 70 km cable
19.7	53.75	21.21	55.6	line + 100 km cable

Table 2 Summary of Errors in Table 1

Error in Measured impedance magnitude and angle		
Z Mag	Z Arg	Circuit Length (km)
0.25	0.16	20 km line +20 km cable
0.30	0.38	20 km line + 30 km cable
0.39	0.62	20 km line +40 km cable
0.40	1.03	20 km line +50 km cable
1.01	1.5	20 km line +70 km cable
1.51	1.85	20 km line +100 km cable

RESULTS

From Table 1 it is evident that errors due to shunt admittance of the cable section do not become significant until cable section length reaches 20 km. Both the magnitude and phase angle error in the impedance measurement returned by the series model algorithm, for increasing cable section length are given in table 2. Appreciable error occurs when the cable length exceeds 20 km with a magnitude and phase angle error of 0.2 Arg. 0.16 degrees, respectively. This represents an overreach of some 102.5% for a measurement to the end of the feeder - 1 km in terms of physical distance.

For an 'a'phase to earth fault at the reach point of a composite circuit, where zone 1 contains a 30 km section of cable, the locus of impedance measurement returned by the series R and L algorithm is shown in figure 3.

The self polarised Mho characteristic is set using accurate calculation of the impedance to an 80% reach point. It is clear that the fault is seen as a second zone fault rather than a first zone activity. Thus, a time delay in fault detection would result, before second zone protection becomes active

A degree of instability is evident in the impedance locus indicating a further time delay incurred while waiting for a stable solution to the line equations [1].

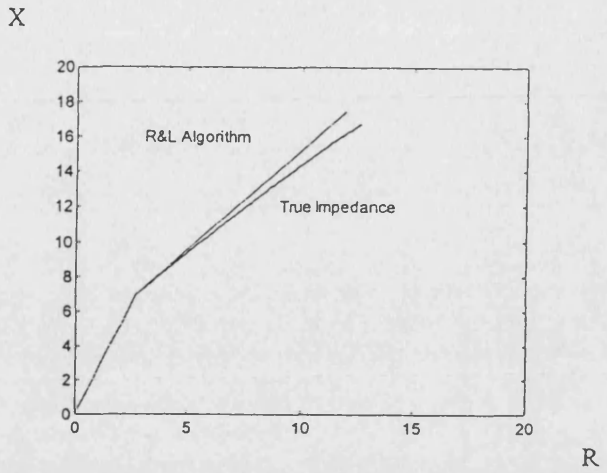

Figure 2 Impedance Plain Sketch of R&L Algorithm Measurements Compared with True Impedance. (Curves are representative of the movement of the end of the Characteristic Impedance Line as Cable Length Increases.)

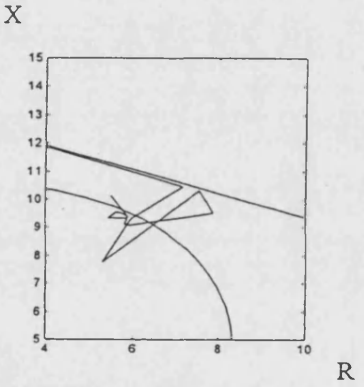

Figure 3 Sketch showing Impedance Locus settling in Zone Two Operating Region.

CONCLUSION

Arc resistance, earthing practices, the need for vectorial earth fault compensation, and the presence of arc resistance should be considered when developing an impedance algorithm suitable for application to composite power distribution circuits. Most importantly, shunt admittance of cables must be considered.

It has been shown that for a typical composite circuit containing 20 km or more of cable errors arise when using a series resistance and inductance model based algorithm, to measure impedance and discriminate accurately the occurrence of single phase to earth faults.

There is a need for a new accurate impedance measuring algorithm for inclusion in a digital distance relay, suitable for application to composite feeders.

ACKNOWLEDGMENTS

The authors would like to thank the University of Bath, GEC ALSTHOM T&D P&C, and EPSRC for the provision of facilities and support for this project. Further, thanks are extended to Mr. A Wallis, Mr. J Heath, and Mr. R Richards, South Western Electricity Plc.

REFERENCES

1. Moore, P.J & Johns, A.T., Distance Protection of Power Systems Using Digital Techniques, IEEIE Electrotechnology, pp194-198, Oct/Nov 1990.
2. ElKateb, M.M., Performance of Distance Protection Applied to Underground Cables Alone and or Mixed with Overhead Lines, Proc. IEE, Vol. 126, No. 9, pp805-814, Sept 1979.
3. ElKateb, M.M., Improving Distance Protection for Underground Cables, Electrical Review, Vol. 202 no. 19, pp-43-44, May 1978.
4. Shepherd, J. Morton, A.H. & Spence, L.F., Higher Electrical Engineering, Longman Scientific and Technical, pp 242-258, 2nd ed, 1986.
5. Gole A.M. *et al* , A Graphical Electromagnetic Simulation Laboratory for Power Systems Engineering Programs, IEEE Trans PS, Vol 11, No. 2, pp599-606, May 1996.

AUTHORS ADDRESS

The first author may be contacted at

Department of Electronic and Electrical Engineering,
University of Bath,
Claverton Down,
Bath, England. BA1 7AY.

email eeprjh@bath.ac.uk

APPENDIX I

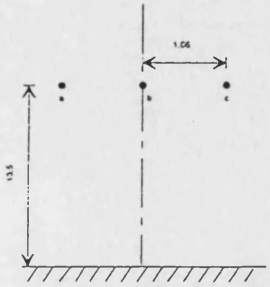

Figure AI.1 33kV, 0.2 sq. in. Cu, Wood Pole Flat Construction, Overhead Line.[All Dimensions in m]

Table AI.1 Electrical Parameters for overhead Line (SWEB Plc)

33kV Wood Pole Construction. 3'6'' conductor centre	
Conductor	0.2 square Inch
DC Resistance pps Ohms/km	0.1350
AC Resistance pps Ohms/km	0.1356
Inductive Reactance pps Ohms/km	03478
Charging Current Amperes/km/phase	0.063
Impedance pps Ohms/km	0.3733

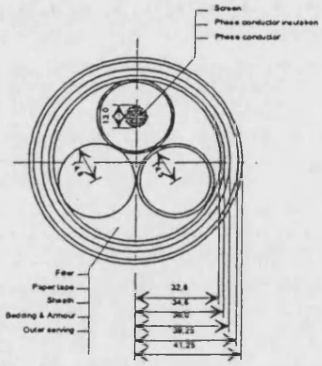

Figure AI.2 : 'H' Type 0.3 sq in, 3 core Cu, Solid, Cable Cross Section.[all dimensions in mm]

Table AI.2 Cable Electrical Parameters (SWEB Plc)

33kV 3 core copper circular conductor underground cable 'H' type	
Conductor	0.3 square Inch
DC Resistance pps Ohms/km	0.09195
AC Resistance pps Ohms/km	0.09278
Inductive Reactance pps Ohms/km	0.09910
Charging Current Amperes/km/phase	0.2.43
Equivalent Star Capacitance Co uF/km	0.405

Paper 2

The following Paper was presented and published in the proceedings of the EMPD International Conference on Energy management and Power delivery 1998, Singapore, 3 –5 March 1998.

Investigation into Impedance Measurement of Composite Power Distribution Feeders, Using the EMTDC.

R J Hewett
University of Bath, UK.

PJ Moore
University of Bath, UK.

G Weller
GEC ALSTHOM T&D P&C,
Stafford,UK

Abstract - **The paper defines a composite power distribution circuit and identifies a commonly used 33 kV, 3 core power distribution cable. A typical single end fed distribution network has been modeled using the EMTDC/PSCAD electromagnetic transient simulation package. User defined code such as prototype algorithms can be interfaced with the EMTDC executable to form integrated simulation studies. This process is outlined. Results show comparison between impedance measurements obtained by two separate algorithms. One accounts for the protected circuit shunt admittance, the other does not. Results show a non linear relationship between earth fault resistance and the component of network impedance attributable to the shunt element.**

I. COMPOSITE POWER DISTRIBUTION SYSTEMS

In this work a composite power distribution system refers to a 33 kV network comprising both overhead line and underground cable.

Composite circuits exist for a number of reasons. Distribution sub stations in urban areas may be accessible only via underground routes. Further, safety considerations from the view point of proximity infringements of existing objects (tree's buildings etc.) may promote the use of cable installations. Increasingly there are environmental pressures prevailing upon the distribution network planning engineer to underground feeders across sites of outstanding natural beauty or scientific interest.

Networks may be connected to form radial, ringed or interconnected systems. Interconnected systems and radial networks with embedded generation connected at the remote end are two instances which may result in a double end infeed to an earth fault.

This work deals with the simple case of a single end fed composite feeder. Such a network may comprise sections of overhead line of a flat wooden pole construction and multicore screened cable. The overhead line combines good current carrying capacity with strength in construction and is commonly found in UK distribution systems. One of the most commonly used cables is the 'H' type cable, which due to it's screened cores can be modeled to a suitable degree of accuracy in electromagnetic transient (EMT) simulation software [1].

II.'H' TYPE CABLE

Figure 1. Three core, 'H' Type Power Distribution Cable [2]

Named after its inventor M. Hocthstadter, 'H' type cable is often preferred over other cable types, due to it's flexibility, increased bending radius, and ease of jointing. It is a screened, solid type cable having either round or shaped copper stranded conductors of typically 0.2 or 0.3 square inch cross sectional area. Each conductor is covered with a layer of oil impregnated paper tape insulation and enclosed within a perforated aluminum tape screen, figure 1. A further layer of oil impregnated tapes are wrapped around the outside of the three screened cores to form a 3 core cable in turn enclosed within a lead-alloy sheath to provide an earth and mechanical protection. Finally, a layer of protective steel wire or tape armour and an outer plastic serving encapsulate the finished cable. The core screens are maintained at the same potential as the sheath due to strands of conductive material woven into the outer layer of paper tapes used between the screens and the sheath. The screens reduce electrical stresses set up in the core insulation by non uniform flux patterns.

III. OPERATING CAPACITANCE & SHUNT ADMITTANCE

The operating capacitance, Co, of this type of screened cable may be determined relatively accurately from knowledge of charging current or equivalent star capacitance per unit length. Figure 2 shows how capacitance only exists between conductors and the earthed screens, as opposed to the more complex capacitive coupling in the belted cable. From the operating capacitance the shunt reactance can be determined. By neglecting shunt conductance the shunt admittance, Y, is composed only of the shunt susceptance, B, which is the inverse of shunt reactance, Xc.

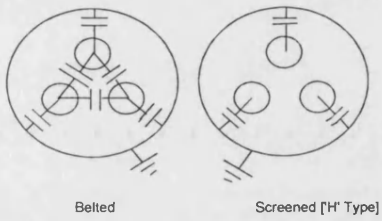

Figure 2. Capacitive Coupling in Belted & Screened Cables

Consider a 'H' type, 0.3 square inch, copper conductor, screened, 33 kV MIND insulated distribution cable, possessing a charging current of 2.43 Amperes per km per phase and equivalent star capacitance of 0.405 μF per unit length, operating at 50 Hz fundamental power system frequency, then

$$Xc = {}^{V_{ph-e}}\!/_{I_{chg}} \qquad (1)$$

or,

$$Co = {}^{1}\!/_{2 \cdot \Pi \cdot f \cdot Xc} \qquad (2)$$

further shunt admittance can be found from,

$$Y = -\,{}^{1}\!/_{jXc} \qquad (3)$$

This cable has a shunt reactance value of 7,859 Ω, very much less than a typical line shunt reactance of 302,421 Ω. Series impedance can be determined using resistance, R, and inductance, L, electrical parameters per unit length.

Cascaded nominal PI sections may now be used to model the 'H' type cable in the EMTDC. Such a model is quick though it evaluates system voltage and current at one frequency only [3].

IV. DISTRIBUTION CIRCUIT MODELED

Figure 3 shows the circuit used for simulation studies. The source is represented by a Thevenin equivalent model the positive and zero phase sequence resistance and inductance derived from knowledge of the three phase fault level at the supply bars (E1). This has been chosen as 500 MVA considering fault levels may typically vary between 50 and 1000 MVA, according to fault position, generating variables, season, abnormal running conditions or transformer outages.

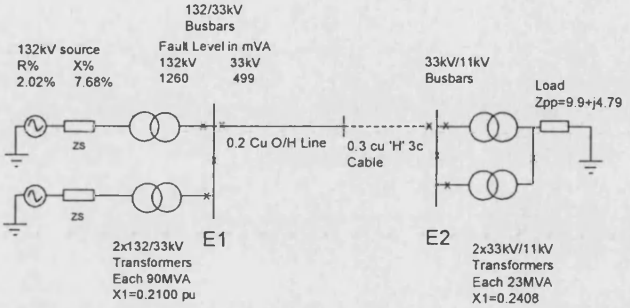

Figure 3. Composite Distribution Networked Modeled

The overhead line is 20 km long and is modeled adequately by a nominal PI section. The cable is represented in lengths varying from 10 to 100 km. In the later case the model comprises 10 cascaded nominal PI sections. For this to be a reasonably valid representation of the cable, additional assumptions are made. Cable conductors are assumed round in cross section, and sheath and armour are at earth potential. Further, due to negligible earth bar resistance earth potential is true earth potential. The voltage profile along the earth plain of the cable is assumed zero as a result of adequate intermediate earthing of cable sections.

Remote end load has been arbitrarily chosen as 11 MW for all simulation studies.

V. ELECTROMAGNETIC TRANSIENT SIMULATION SOFTWARE

Researchers have in the past largely utilised the well known EMTP software for electromagnetic transient simulation studies. However, the EMTP is not intuitive in its usage (primarily due to the need to drive it from the command line) and the user requires additional software to process and present results.

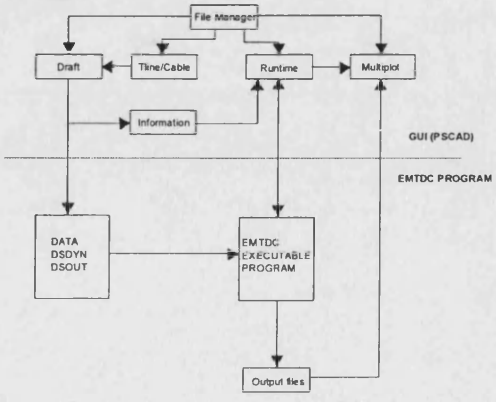

Figure 4. Block Diagram Showing Structure of EMTDC/PSCAD[4].

The EMTDC/PSCAD incorporates all the facilities required to conduct electromagnetic transient studies, it's constituent parts shown in figure 4.
The user assembles circuits in a CAD type drawing pallet (DRAFT) solving cable and line constants via the LINE and CABLE constants routines. The drafted circuit once compiled and linked forms a data file which is analogous to the EMTP input data file. Also formed at this stage are dynamic input DSDYN and user defined output DSDOUT files. It is from the DSDYN file that prototype relaying algorithms can be called via user defined components [5]. This process is shown in figure 5.

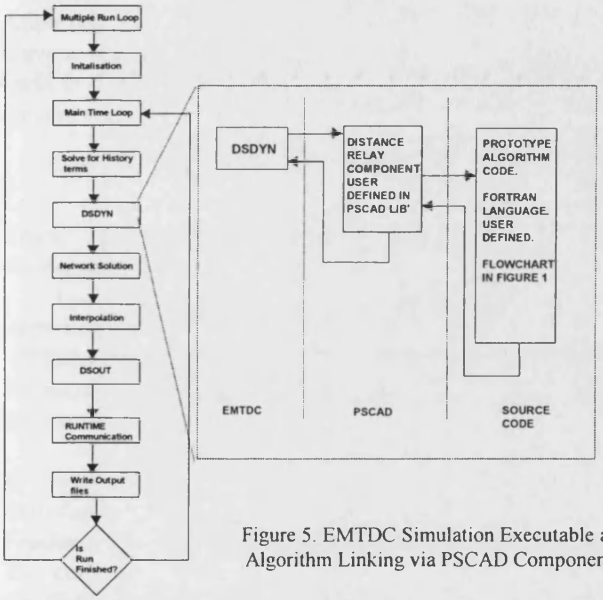

Figure 5. EMTDC Simulation Executable and Algorithm Linking via PSCAD Components.

The impedance measuring algorithms under test have been coded in the FORTRAN programming language. The PSCAD relaying components which link the algorithms to the EMTDC main executable are written using the EMTDC/PSCAD proprietary language and methodology [4]. Through inclusion of the PSCAD user defined relaying component within DRAFT simulation circuits, the impedance measuring algorithm is compiled and linked to the EMTDC executable ready for running simulation cases. In this manner parameters are passed from the circuit to the algorithm and algorithm outputs can be passed back to the circuit ready for the next simulation time step. In this way a breaker may be tripped as a result of a prototype algorithm detecting a fault. Also variables and parameters from within the algorithm can be monitored during and after simulation runs. Results can be presented for display using the MULTIPLOT component.

VI. IMPEDANCE MEASURING ALGORITHMS

In general impedance algorithms must model the system they protect such that measured impedance can be correlated to physical distance. Currently, most impedance algorithms developed have relied on the simple series resistance and inductance representation. Such a model is suitable for over head line applications but would likely give rise to errors in impedance measurement when applied to a composite circuit, principally due to shunt admittance (section III) being neglected.
Two impedance measuring algorithms have been applied at bus bar E1, in figure 3. One utilises the RL approach to modeling the system while the other through use of generalised line constants (ABCD) and two port network theory, inherently accounts for shunt components of circuit impedance.

A. RL Impedance Measuring Algorithm

The algorithm models the protected network as an R and L series circuit. Described fully in [6,7] it estimates the system resistance and inductance through the solution of the equation

$$v = iR + L\,di/dt \qquad (4)$$

the positive phase sequence impedance can be assessed by calculating

$$Z = R + j\omega L \qquad (5)$$

B. ABCD Two Port Network Impedance Measuring Module

The ABCD MODULE, inherently accounts for shunt admittance in it's measurement of a networks impedance. It uses generalised circuit constants and the well known two port theory network representation [8]. Utilising knowledge of voltage and current (Vf and If) at the fault point and distance to fault X it calculates ABCD parameters for the protected composite network. Calculation of sending end voltage and current (Vs and Is) is then made using (6).

$$\begin{bmatrix} Vrel \\ Irel \end{bmatrix} = \begin{bmatrix} A & B \\ C & D \end{bmatrix} \cdot \begin{bmatrix} Vf \\ If \end{bmatrix} \qquad (6)$$

Parameters A,B,C, and D are hyperbolic trigonometric functions calculated from the known electrical parameters per unit length for the protected circuit, and a knowledge of the distance x between the measuring point and an earth fault.
The 50 Hz component of Vf and If is extracted via the use of the discrete Fourier transform (DFT) in the form of sine and cosine filters. Real and imaginary fundamental frequency components of voltage and current form a vector on the impedance plain. Positive phase sequence impedance can be derived by calculating,

$$Z_{ABCD} = Vs/Is \quad . \qquad (7)$$

Vectorial earth fault compensation is achieved by adding a proportion *Kn* of the residual current *In*, to the 'a' phase current.

$$Ia = Ia + KnIn \qquad (8)$$

where, Ia is the phase current, *In=Ia+Ib+Ic*, and *Kn=((Z0/Z1)-1)/3*.

Both the above mentioned algorithms have been coded in the FORTRAN high level computing language and incorporated into EMTDC simulations via the method described in section V above.

Apparent positive phase sequence values of voltage and current are used as inputs to the algorithm, which are also ideal in that no distortions or effects attributable to voltage or current transducer error are represented.

VII. EXPERIMENTAL METHOD.

There are two objectives of the experimental work conducted. These are:

1) Investigation of differences in impedance measurement when neglecting shunt admittance.

2) Effects of fault resistance on impedance measurement.

To satisfy these objectives the following simulation studies have been completed.

A. Investigation into the Effect of Shunt Admittance on Impedance Measurement of a Composite Distribution Feeder.

The composite system previously described was modeled in the EMTDC, figure 6. Both the ABCD MODULE and RL MODEL impedance measuring algorithms were installed at the sending end bus bar E1.

Cable section length was set to 10 km. An 'a' phase to earth fault of negligible resistance (Rf=0.01Ω), at the far end of the feeder was simulated. The impedance measured by both the RL and the ABCD algorithms (Z_{RL} & Z_{ABCD}) installed at E1 was recorded.

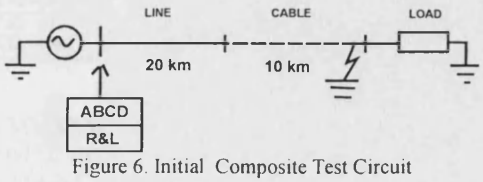

Figure 6. Initial Composite Test Circuit

The cable length was incremented through the addition of another 10 km PI section, figure 7. The above process was repeated with impedance measured by both algorithms recorded in table 1. This method was repeated up to a maximum cable length of 100 km.

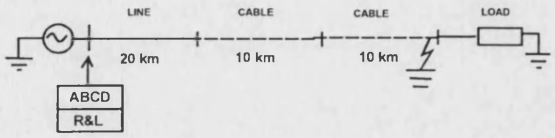

Figure 7. Test Circuit With Cable Length Incremented by 10 km.

B. Effects of fault resistance on impedance measurement.

The same experimental method as described in VII.*A*. above was followed. However, in each case earth fault resistance was set to values of 5.0 Ω and 10.0 Ω. This process can be clarified by reference to figure 8 below. Again cable length was increased to a maximum length of 100 km in 10 km increments. Impedance values are recorded in tables 2 and 3.

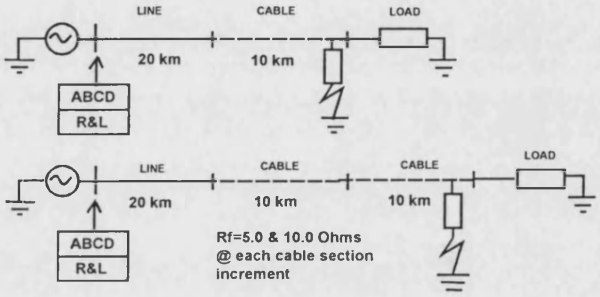

Figure 8. Circuit Diagram Showing Arrangement for Fault Resistance Investigation.

VIII RESULTS & DISCUSSION

The tables 1,2,&3 present the results to the previously described two simulation studies in tabular format. Figure 9 presents the above tabular results graphically.

For the composite systems described in this paper subject to an 'a' phase to earth fault of negligible resistance, cable lengths must exceed 50 km before shunt admittance gives rise to significant effect on impedance measurement.

However, figure 9 indicates a non linear relationship between earth fault resistance and the actual impedance (Z_{ABCD}) of the circuit. This can be explained by consideration of the voltage profile sketch in figure 10. For a fixed length of cable, as fault resistance increases, so the voltage profile over the cable length is increased and the voltage impressed across the distributed shunt capacitive elements of the cable increase. In this manner *Ish* increases and the component of impedance attributable to the shunt losses of the cable becomes more significant.

Reference to figure 9 shows that this relationship is reflected in the more significant difference between impedance measurement locus plots for the case of 5.0 and 10.0 Ω fault resistance. When Rf is negligible, cable lengths of up to 50 km caused negligible difference in impedance measurement locus Z_{ABCD} and Z_{RL}. Now, with reference to table 3,

significant difference in impedance locus is noticeable when fault resistance equals 10.0Ω and cable lengths exceed 20 km.

TABLE 1
IMPEDANCE MEASUREMENTS FOR EXPERIMENT VII.*A*
RF=0.01Ω

ABCD Module				R and L Algorithm				Line Length	Cable Length	Rf
real	Imag	Mag Ω	Arg Degs	real	Imag	Mag Ω	Arg Degs	km	km	Ω
2.71	6.95	7.455	68.69	2.74	6.97	7.489	68.531	20	0	0.01
3.64	7.94	8.738	65.37	3.67	7.96	8.7651	65.244	20	10	0.01
4.56	8.93	10.02	62.94	4.61	8.96	10.079	62.773	20	20	0.01
5.47	9.92	11.32	61.12	5.56	9.96	11.406	60.828	20	30	0.01
6.37	10.91	12.63	59.72	6.52	10.96	12.753	59.254	20	40	0.01
7.25	11.9	13.98	58.645	7.51	11.96	14.128	57.875	20	50	0.01
8.11	12.88	15.29	57.803	8.53	12.97	15.523	56.668	20	60	0.01
8.94	13.86	16.49	57.177	9.58	13.98	16.947	55.578	20	70	0.01
9.74	14.84	17.75	56.721	10.67	14.99	18.399	54.556	20	80	0.01
10.5	15.81	18.97	56.410	11.82	16	19.892	53.544	20	90	0.01
11.23	16.7	20.12	56.080	13	17.01	21.408	52.610	20	100	0.01

TABLE 2
IMPEDANCE MEASUREMENTS FOR EXPERIMENT VII.*B*,
Rf=5.0Ω

ABCD Module				R and L Algorithm				Line Length	Cable Length	Rf
Real	Imag	Mag Ω	Arg Deg's	Real	Imag	Mag Ω	Arg Deg's	km	Km	Ω
7.7	6.95	10.37	42.069	7.6	6.72	10.144	41.483	20	0	5.0
8.62	7.99	11.75	42.827	8.63	7.71	11.572	41.777	20	10	5.0
9.52	9.02	13.11	43.455	9.59	8.68	12.934	42.148	20	20	5.0
10.4	10.07	14.47	44.076	10.58	9.63	14.306	42.308	20	30	5.0
11.25	11.13	15.82	44.692	11.59	10.58	15.697	42.410	20	40	5.0
12.07	12.2	17.16	45.306	12.6	11.48	17.045	42.337	20	50	5.0
12.85	13.27	18.47	45.921	13.73	12.4	18.500	42.086	20	60	5.0
13.59	14.34	19.75	46.538	14.86	13.31	19.949	41.850	20	70	5.0
14.29	15.41	21.01	47.159	16.04	14.2	21.422	41.518	20	80	5.0
14.94	16.48	22.24	47.806	17.28	15.06	22.921	41.073	20	90	5.0
15.55	17.55	23.44	48.457	18.6	15.9	24.469	40.525	20	100	5.0

TABLE 3
IMPEDANCE MEASUREMENTS FOR EXPERIMENT VII.*B*,
Rf=10.0Ω

ABCD Module				R and L Algorithm				Line Length	Cable Length	Rf
real	Imag	Mag Ω	Arg Deg's	real	Imag	Mag Ω	Arg Deg's	km	km	Ω
12.7	6.96	14.48	28.724	12.25	7.07	14.143	29.991	20	0	10
13.61	8.09	15.83	30.727	13.3	8.01	15.525	31.058	20	10	10
14.49	9.24	17.18	32.524	14.28	8.84	16.794	31.759	20	20	10
15.32	10.41	18.52	34.196	15.31	9.65	18.097	32.223	20	30	10
16.11	11.6	19.85	35.755	16.37	10.43	19.410	32.502	20	40	10
16.85	12.8	21.16	37.221	17.48	10.78	20.536	31.662	20	50	10
17.54	14	22.44	38.596	18.62	11.61	21.943	31.944	20	60	10
18.17	15.21	23.69	39.932	19.81	12.42	23.381	32.085	20	70	10
18.74	16.42	24.91	41.224	21.06	13.19	24.849	32.059	20	80	10
19.2	17.62	26.05	42.542	22.36	13.76	26.254	31.607	20	90	10
19.68	18.81	27.22	43.705	23.73	14.28	27.695	31.038	20	100	10

TABLE 4
SUMMARY OF IMPEDANCE MEASUREMENT FOR COMPOSITE CIRCUIT COMPRISING 20 KM OF LINE AND 50 KM OF CABLE, SUBJECT TO EARTH FAULT OF RESISTANCE 0.01, 5.0 & 10.0 Ω.

Fault Resistance Ohms	Impedance Measured Ohms		
	RL Algorithm Z_{RL}	ABCD Module Z_{ABCD}	Traditional spm Setting
0.01	14.12∠57.87°	13.93∠58.64°	13.99∠58.31°
5.0	17.04∠42.33°	17.16∠45.3°	17.1∠44.0°
10.0	20.53∠31.66°	21.16∠37.22°	21.1∠34.5°

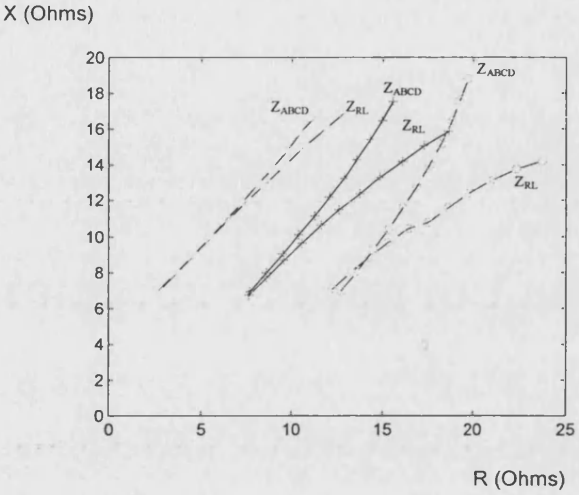

Figure 9. Impedance Locus Returned by RL and ABCD Algorithms for Increasing Cable Length and Fault Resistance Variation.
x---x---x *Rf=0.01Ω* +---+---+ *Rf=5.0Ω* o---o---o *Rf=10.0Ω*

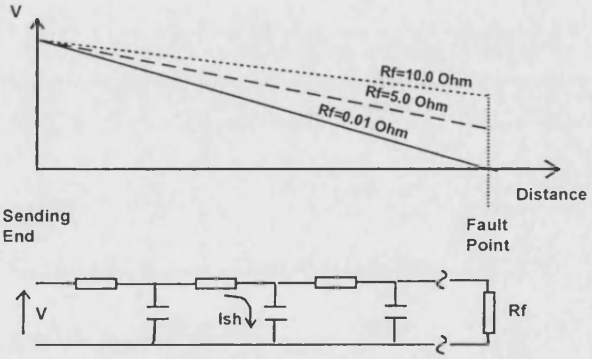

Figure 10 . Sketch Showing Voltage Profile Over the Cable Section Length as Earth Fault Resistance Increases.

Table 4 summarises the case for a composite circuit with a 50 km cable section. This example can be placed in context by noting there is in the real world a similar 57 km submarine 33 kV AC cable link between the Isle of Scilly the UK main land.

The table shows three impedance measurements attributable to the ABCD and RL algorithm's and a traditional calculation of protected circuit characteristic impedance magnitude and angle suitable for setting a self polarised mho (spm) characteristic (Zspm). This latter method can be regarded as a common way of setting an existing distance relay tripping characteristic and relies on knowledge of the series resistance and inductance of the protected circuit and an approximation of the maximum or likely value of any fault resistance. The setting impedance is initially set according to the series resistance and inductance of the circuit line and cable components. The characteristic impedance setting angle is

then reduced by a suitable amount, to allow for coverage of a predefined fault resistance, [9].

Table 4 reveals several important observations.

1) It can be seen that when fault resistance is negligible(RF=0.01Ω) the Z_{RL} magnitude under reaches in comparison with the Z_{ABCD} by 1.36%. Arg Z_{RL} is -0.77° less than Arg Z_{ABCD}. Traditional s.p.m. calculations give a characteristic impedance setting of 13.99∠58.31°. Comparing the magnitude of Z_{RL} with this setting data an under reach of 0.92% and angular difference of -0.44°, can be observed. These errors are attributable directly to small errors in the RL algorithm's estimation of resistance and inductance and the influence of the shunt admittance of the cable section. In reality these errors are likely insignificant when contrasted with errors in data such as measurement of feeder length or cable and line parameters.

2) When Rf equals 10.0 Ω noticeable difference between Z_{RL} and Z_{ABCD} is apparent. The RL impedance algorithm now over reaches in terms of impedance magnitude by 2.97 % and measures an angular difference of -5.56°. Comparing Z_{RL} with the traditionally calculated s.p.m. characteristic impedance setting (adjusted for 10.0 Ohms fault resistance), shows a 2.7 % over reach and an angular difference of 2.84°. Comparison of Z_{ABCD} with Zs.p.m. magnitudes are the same at 21.16Ω and 21.1Ω respectively. Angular difference can be observed, however, as $\angle$Zs.p.m. is 2.72° less than the $\angle_{ZABCD}$.

3) Similarity between the two later impedance magnitudes should be placed in context by realisation that occurrence of a 10.0Ω resistive earth fault needs to be anticipated when setting the s.p.m. characteristic. This method relies on the determination of likely earth fault resistance and only discriminates earth faults possessing less than or equal to this predefined value. Faults of resistance greater than the preset estimation, will likely be discriminated as outside the trip boundary of the s.p.m. characteristic.

4) The s.p.m. characteristic setting not only has the disadvantage of accounting only for the occurrence of specific predefined fault resistance, but it does not account for the nonlinear effect of fault resistance on the shunt component of impedance. This later effect being most evident in the impedance angular difference of 2.72°.

X. CONCLUSIONS

Most impedance measuring algorithms have been developed for application to overhead line systems. As a consequence they model the system they protect as a simple resistance and inductance series circuit (RL). For many reasons distribution systems may be composite in nature possessing both cable and overhead line sections. Cables possess significantly larger shunt admittance than overhead lines. As a consequence application of these RL algorithms to protect such circuits can prove inaccurate in terms of fault discrimination.

Results presented show that when earth fault resistance is negligible the component of impedance attributable to the shunt losses of the cable section are negligible for cable sections less than 50 km in length. However, earth fault resistance is related non linearly to the shunt component of a composite circuit. Therefore, shunt admittance should be considered when applying distance protection to composite distribution systems containing 'H' type cable sections exceeding 20 km in length, and earth fault resistance is likely. Traditionally, s.p.m. characteristics have been set to allow for the occurrence of fault resistance by reducing the setting angle by some predefined amount. It has been shown that for a composite circuit comprising a 50 km length of cable subject to an earth fault at the remote end of resistance 10.0Ω, that angular errors between s.p.m. impedance settings and impedance measurements inherently accounting for shunt admittance exist. These errors are attributable directly to neglecting shunt admittance in the s.p.m. setting calculation process.

A new impedance measuring algorithm, which allows for the effects of shunt admittance, is required. Such an algorithm is necessary if future microprocessor based distance protection is to be accurate when applied to power distribution composite circuits.

XI. ACKNOWLEDGMENTS

The authors would like to thank the University of Bath, GEC ALSTHOM T&D P&C, and EPSRC for the provision of facilities and support for this project. Further, thanks are extended to Mr. A Wallis, South Western Electricity Plc.

XII. REFERENCES

[1] R J Hewett & P J Moore, "Investigation into Distance Protection of a 33 kV Composite feeder using the EMTDC/PSCAD." 32nd Universities Power Engineering Conference, UMIST, Manchester, UK. 10th-12th September, 1997, pp279-282.

[2] C F Wagner & R D Evans,"Symmetrical Components," London: McGraw-Hill, 1933, p 218.

[3] L.Marti, "Simulation of Electromagnetic Transients in Underground cables Using the EMTP," in proceedings IEE International Conference on Advances in Power System Control, Operation and Management, December 1993, Honk Kong, pp 147-152.

[4] "PSCAD/EMTDC Version 2.00 User Manuals," Manitoba HVDC Research Centre, 1994.

[5] A M Gole et al,"A Graphical Electromagnetic Simulation Laboratory for Power Systems Engineering Programs." IEEE Trans PS, Vol 11, No. 2, May 1996, pp 599-606.

[6] PJ Moore & A T Johns,"Distance protection of Power Systems Using Digital Techniques," IEEIE Electrotechnology, October/November, 1990, pp 194-198.

[7] P J Moore,"Adaptive Digital Distance Protection," Phd Thesis, City University, London, April 1989.

[8] W.D. Stevenson,"Elements of Power System Analysis," 2nd ed. , London: McGraw - Hill, 1962, pp 114-132.

[9] GEC ALSTHOM Measurments Ltd, "Practical Relay Applications Guide," 1986.

Paper 3

Paper 301-033, entitled Novel Approach to High Impedance Earth Fault Discrimination on 33 kV Networks Containing Cable Sections , by R.J. Hewett, P.J. Moore, G. Weller (U.K.) has been accepted for presentation at the IASTED International Conference on Power and Energy Systems to be held November 8-10, 1999 at the Embassy Suites Hotel in Las Vegas, Nevada - USA.

Novel Approach to High Impedance Earth Fault Discrimination on 33 kV Networks Containing Cable Sections.

R J Hewett
University of Bath, UK.

P J Moore
University of Bath, UK.

G Weller
GEC ALSTHOM

ABSTRACT

Power distribution systems operating at 33 kV often contain both line and cable sections. Distance relay manufacturers are interested in the characteristics of these composite networks and their effect on accuracy of existing distance relay earth fault discrimination techniques. A symmetrical component based software network simulator has been developed and used to model typical three phase 33kV composite networks, enumerating system voltage and current data for all realistic operating conditions. The studies in this paper utilise this data, to investigate the accuracy of two existing earth fault discriminatory techniques and one novel approach taken by the authors.

Keywords : Protection, Earth Fault, Relay

1.0 INTRODUCTION

Distance protection offers the advantage of inherent back up for down stream protection units and negates the requirement for a communication link. Multi function microprocessor based relaying platforms surpass their electromechanical predecessors by offering increased reliability, lower maintenance requirements, and reduced cost. Power system owners and operators are under increasing pressure to operate systems efficiently and reliably often subject to stringent penalties should system failure occur.

A typical operating voltage for distribution circuits in the UK is 33kV. Environmental pressures or the requirement to infiltrate heavily populated areas mean such circuits frequently include underground cable sections - and are hence composite in nature.

Distance relay manufacturers are interested in the classification of the unique characteristics of such networks and the accuracy of the currently available earth fault discrimination techniques when applied to them.

Fault path resistance and its effect on the accuracy of earth fault elements has previously been investigated by many authors [1]. The significant shunt losses inherent in power cables and the effect of such losses on the accuracy of impedance measurement under high impedance earth fault conditions has yet to be investigated.

Recently, the authors have developed a new impedance measuring algorithm that models a protected network in terms of both its series and shunt parameters. As a part of this work a symmetrical component based software network simulator has been developed based on a steady state phasor model of system current and voltage vectors. This software package has been used to model a 33kV composite network subject to various earth faults and enumerate voltage and current for all realistic values of cable and line lengths, fault position, fault path resistance, remote end load and source impedance.

This paper initially describes the power distribution circuits used in the work and the maximum and minimum values of operating parameters. A brief outline of the simulation technique and software used precedes an overview of the three earth fault discriminating techniques used. Results obtained from the application of a traditional earth fault relay element utilising both a quadrilateral and self polarised mho characteristic are presented. Instances of inaccuracies in impedance measurement and fault discrimination are identified. Results obtained using the new impedance measuring algorithm combined with a modified quadrilateral tripping characteristic developed by the authors show improved accuracy in zone one earth fault discrimination.

2.0 POWER DISTRIBUTION CIRCUITS

2.1 Circuit Construction

The circuit constructions chosen for this work are the flat three wire Copper (Cu) stranded 0.2 Sq. inch cross sectional area (CSA) line supported on wood poles and a 3 core, Cu, round 0.3 Sq. inch CSA, 'H'type, 'screened' cable. Electrical parameters per km length are given in table A1 in Appendix 1.

The physical construction of the line chosen may be considered typical but many different types of cable can be found within modern power distribution networks.

2.2 Distribution Power Cables

A multitude of factors may influence the type of cable used. Historically in the UK the 3 core 'H' variety has been commonly used. Named after its inventor M Hostchstader , the cable consists of three screened conductors encapsulated within a medium impregnated non- draining paper insulation, in turn encapsulated within a common sheath. It offers good flexibility and reliability [2].

Other cable varieties exist. One such cable is the 'HSL' 3 core which is similar in construction to the 'H' variety but utilises a separate earthed sheath for each insulated phase conductor. The three sheaths are encapsulated within a common sheath applied for mechanical protection.

Single core cables may also be used in three phase systems. Utilising one cable for each phase they may be laid

in individual trenches or in a trefoil arrangement in one trench.

Each of these cable types require particular models to represent them in software based power system simulation programs. Currently cable modeling has its roots firmly set in the world of modeling overhead lines [3]. The physical construction of 'H' type cable lends its self to suitably accurate modeling, mainly because the equivalent star capacitance quoted by manufactures reflects the actual shunt capacitance between each phase conductor and its earthed screen [4]. Coupled with the common use of such cables in UK distribution power systems 'H' type cable has been selected for the studies in this paper.

3.0 CIRCUIT CONNECTIVITY.

Figure 1 presents the schematic of the composite power distribution system simulated in this work and is typical of a 33kV radial type feeder supplying a primary substation or a major industrial consumer of power. The feeder comprises two sections of cable and line connected in series - this being the minimum required to represent a composite network. Present on the cable to line termination pole would normally be some form of lightening surge divertors which are omitted in the network simulation. The circuit is three phase and the remote end load may be representative of the maximum demand of a primary sub station or the peak demand of a heavy industrial user.

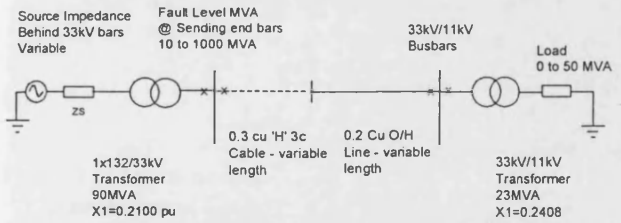

Figure 1: Basic schematic of Simulated 33kV Distribution Feeder.

There are a multitude of parameters which may vary in the distribution network of figure 1. Sending end bars short circuit fault levels, cable and line lengths, system loading and fault types must all be considered when assembling a typical representative model. The variables change between maximum and minimum values. Typical values are summarised in table A2 in Appendix 2.

Automated simulation studies which utilise the power system modeling software described in section 4.0 below have been used to enumerate sending end bus bar three phase voltage and current phasors for all operating parameters as described by table A2. These voltage and current signals are applied to the three earth fault discriminatory techniques described in section 5.0 and Appendix A3. Results are shown in section 7.0.

4.0 STEADY STATE DISTRIBUTED PARAMETER BASED POWER SYSTEM SIMULATOR.

For reasons of brevity an outline only of the simulation technique is presented here.

Reference to figure 2 shows a single line representation of a pre-fault circuit(a), a post fault circuit(b), and a final solution circuit(c) all of which are three phase. Circuit (c) shows Vs and Is ,the three phase voltage and current, at the sending end bus bar of the earth faulted circuit.

The pre-fault circuit is solved in the frequency domain for a single fundamental power system frequency , for example 50.0 Hz. The pre-fault voltages Vff and currents Iff at the fault point are calculated. Additionally, the sending and receiving end current phasors (Is and Ir) are also calculated for this pre- fault circuit. Pre-fault sending end voltage and current values Vsp and Isp are thus determined.

The post fault circuit (b) removes the voltage source and determines a single matrix representation of the parallel circuit seen from the fault point. For a single 'a' phase to earth fault the 'a' phase of the circuit is injected at the fault point with a voltage equal and opposite to Vff. Note , the inclusion of fault resistance, Rf, in the equivalent matrix. The sending end voltage and current dVs and dIs are found. These quantities represent the change in the voltage and current values between the faulted and pre faulted circuits.

Figure 2(c) shows the final solution circuit. The actual sending end voltage and current matrices Vs and Is are found simply using the pre and post fault data described above and the following equations,

$$Vs = Vsp + dVs \quad (1)$$

$$Is = Isp + dIs \quad (2)$$

The voltage and current matrices supply three software distance relay earth fault element simulations described in section 5.0.

5.0 DISTANCE RELAY EARTH FAULT ELEMENT SIMULATIONS

Elements implementing typical self polarised mho (SPM) and quadrilateral (QUAD) based tripping characteristics have been simulated in addition to the new technique proposed by the authors. The new earth fault discrimination technique is described briefly below.

5.1 New Hyperbolic Distributed Parameter Based Relaying Algorithm

5.1.1 Fundamental Theory

Utilising the theory of Wedephol[5] a power system may be modeled by distributed parameters and in turn these parameters can be used to represent network sections with two port networks [6]. Such circuit representation inherently represents the series and shunt parameters of a network. Detail of the calculation of the ABCD hyperbolic parameters may be found in reference[7]. The system is assumed ideally transposed.

5.1.2 Scope for Use in Zonal Distance Protection Discrimination.

Utilising this approach and considering the diagram of figure 3 from a knowledge of power system electrical parameters per km length and the sending end voltage and current values a set of 'virtual terminals' may be established at a predefined point distance X from the sending end bars. Setting X equal to 80% of total section length replicates the classic 'zone one' reach point of a distance protection relay. For reasons of clarity the circuit depicted comprises one section , however this section may be composite in nature.

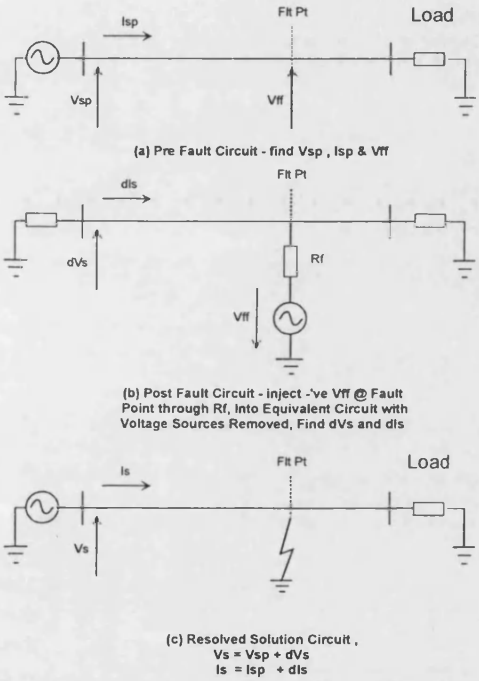

Figure 2 : Diagrammatic Representation of the Three Phase Superimposed Circuit Theory Used in Steady State Distributed Parameter Simulation Software.

A relay installed at busbar S measuring three phase voltage and current and utilising an algorithm which implements the theory of section 5.1.1, can thus calculate the voltage and current signals at the 80% reach point. Knowledge of the three phase voltage and current signals at each end of zone one and the hyperbolic circuit representation inherently accounting for a system series and shunt parameters provides sufficient information to allow a new basis for zone one earth fault discrimination .

With respect to figure 3 consider a notional single 'a' phase to 'earth' fault of zero Ohms resistance at the reach point (flta). The 'a' phase voltage at the fault point (Vfa) will theoretically equal zero. The sketch graph of figure 3 shows the voltage profile over the circuits zone one length.

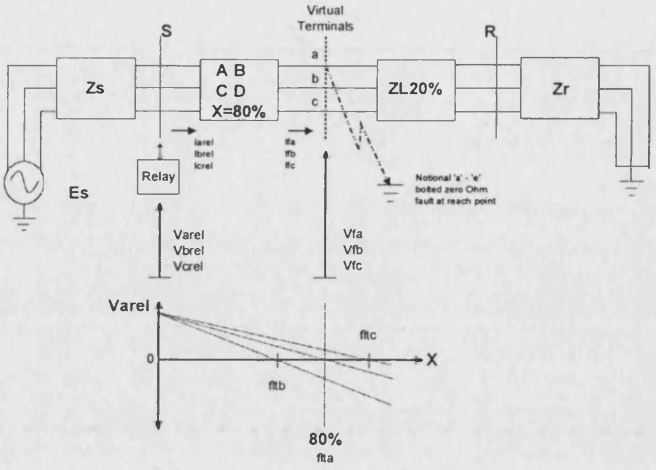

Figure 3 : Application of Hyperbolic Parameter Circuit Representation to Zone One Distance Protection Relaying.

In this case the faulted 'a' phase impedance calculated at the fault point (Vfa / Ifa = Zfa) will be zero. If however the same fault were to occur either behind or beyond the reach point (fltb or fltc respectively) then performing a Vfa / Ifa calculation will now yield some value of impedance Zfa. The sign of the imaginary component of this complex impedance can be used to indicate an earth fault as being behind or beyond the pre defined reach point. i.e. using the equation,

$$Zfa = \frac{Vfa}{Ifa} = Rrp + jXrp \qquad (3)$$

Thus a basis for discriminating an in or out of zone zero Ohm single phase to earth fault exists. Table 1 summarises the discrimination criteria.

Table 1 : Reach Point Earth Fault Discrimination Criteria

Reach Point Impedance Quadriture Component	Discrimination Meaning
- jXrp	In Zone
jXrp = 0	On Reach Point
+jXrp	Out of Zone

5.1.3 Proof of Reach Point Discrimination Accuracy

The accuracy of the criteria summarised in table 1 can be demonstrated for a typical 33 kV composite power distribution feeder.

Consider the feeder of figure 1 with cable and line sections of 20km length. The source bars have a three phase short circuit level of 250 MVA and a three phase inductive load of 0.8 p.f. lagging is connected at the remote end. A plot of Xrp for a bolted 'a' phase to earth fault applied between 50% and 100% is shown in figure 4. Xrp can be seen as equaling zero for an earth fault at the reach point

(80%). For faults beyond the reach point (80 to 100%) Xrp becomes a positive value. For those earth faults occurring behind the same reach point Xrp becomes a negative value. In this instance a simple test for the sign of Xrp can be used for 'in' or 'out' of zone discrimination. Exhaustive testing proved this to be true for a zero Ohm single phase to earth fault and all realistic combinations of circuit operating parameters and lengths.

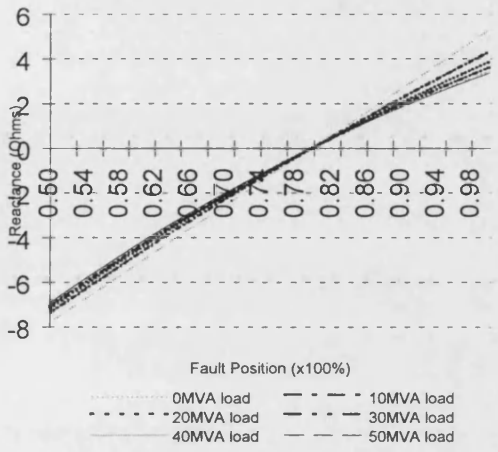

Figure 4 : Plot of Xrp v's Fault Position. Src Bars SCL=250MVA , Composite Circuit (20km cable+20km line), Varying Loads @30Degs PF Angle Lagging. Fault= 'a' - 'earth' of 0.0 Ohms Impedance.

5.1.4 Effect of Fault Resistance and Remote End Load Characteristics on Reach Point Discrimination Accuracy.

In practice faults on overhead line sections often result in arcs which posses resistance of some value. Further more, steel work , cast iron cable termination boxes and line supports represent significant resistance to the flow of fault current to earth. Cables due to their construction and the fact that they are buried below ground do not support significant values of fault path resistance[8]. Composite networks contain overhead line sections which may be subject to the occurrence of high impedance earth faults.

For a network on load and subject to a high impedance earth fault a parallel circuit will be formed between fault path impedance and the remote end load. An estimation of the pre- fault load must be made in order for this parallel circuit to be resolved and the effect of remote end load to be removed. In this manner the Xrp polarity criteria maintains accuracy under high impedance earth fault conditions.

The theory of symmetrical components provides a solution in that

$$Z11 = V11 / I11 \qquad (4)$$

where Z11 , V11 and I11 are positive phase sequence values for the circuits 'a' phase say. For the case of an 'a' - 'earth' fault on a three phase network V11 and I11 may be replaced by the 'a' phase voltage Va and Ia as calculated at the virtual terminals.

Expressing Z11 as the 'a' phase admittance *Yl* then during pre-fault,

$$Yl = Ira / Vra \qquad (5)$$

and post fault .....

$$Yra = Ira / Vra - Yl \qquad (6)$$

Yra is then the fault path admittance which when expressed as an impedance and for a high resistance earth fault at the reach point is

$$Zfa = 1 / Yfa = Rrp + jXrp \qquad (7)$$

Now even under high impedance earth fault conditions the tripping criteria summarised in table 1 remains valid, the effect of remote end load having been approximated and removed.

6.0 IMPLEMENTATION OF EARTH DISCRIMINATION USING A QUADRILATERAL CHARACTERISTIC

The new earth fault discriminatory methodology presented above has been implemented via a quadrilateral characteristic. Shown in figure 5.

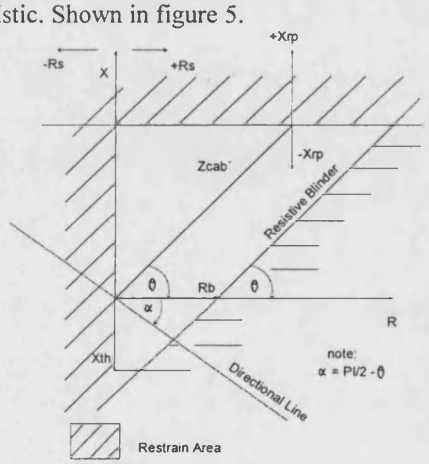

Figure 5: Earth Fault Element Quadrilateral Tripping Criteria.

The top reactance line is defined by the polarity of Xrp.

For the bottom and left hand trip boundaries the sending end impedance must be found using equation,

$$Zsa = \frac{Vsa}{Isa} = Rs + jXs \qquad (8)$$

The left hand boundary is defined by,

$$Rs \geq 0 \qquad (9)$$

To define the the bottom of the characteristic and provide directionality a reactance threshold value *Xth* is required. Such a value may be formed using the following equation.

$$Xth = Rb \tan\alpha \qquad (10)$$

Rb represents a resistive blinder value that must be defined in commissioning and

$$\alpha = (\Pi / 2) - \theta \qquad (11)$$

where θ represents the characteristic impedance angle of the protected feeder - again defined during commissioning.

A possible in zone event would be indicated by the condition

$$Xs \geq Xth \qquad (12)$$

Such a definition allows those earth faults occurring close in to the relay to be detected.

Note also that neither equation (3) or (10) require any form of earth fault compensation of the measured or calculated phase currents. The characteristic of the network in terms of zero and positive phase sequence parameters and thus the characteristic of the earth return path are pre-defined within the two port network ABCD parameter hyperbolic representation.

The right hand resistive boundary of the characteristic has been defined using a user input value of resistance. A possible in zone event occurs when

$$Rrp \leq Rb \qquad (13)$$

7.0 PERFORMANCE ASSESSMENT AND RESULTS.

Two composite circuits have been chosen to demonstrate the discrimination accuracy of the new earth fault relaying element (ABCD). These results have been compared with that yielded by two other traditionally used earth fault relaying techniques, namely the self polarised mho (SPM) and the quadrilateral (QUAD). These are

7.1 Short Composite

The circuit comprises 10km of cable and 20km of line.

7.2 Long Composite

The circuit comprises 60km of cable and 20km of line. The cable length may seem excessive but there instances such as the 56 km Isles of Scilly submarine 33 kV cable link in the UK - which justify this investigation.

7.3 Test Routines

In all cases sending end bar short circuit level is 250MVA, resistive blinders are set to 80.0 Ohms and various remote end loads are applied. Earth faults of fault path resistance values between 0.0 and 200.0 Ohms are automatically applied at incremental fault positions between 10 and 180% of feeder lengths.

For each of the two circuits the resistive reach point trip boundary for the SPM, QUAD and ABCD earth fault elements were recorded and are shown in figures 6 and 7 respectively.

8.0 DISCUSSION.

8.1 Short Composite Circuit Results

Figure 6(a) shows the reach point performance for the circuit on no load. The SPM exhibits poor performance for high impedance earth faults. The QUAD exhibits significant overreach which increases as fault path resistance increases. At it's worst the overreach is 120% of zone one length. this phenomena was discussed at length in a previous paper by the authors[4]. The QUAD eventually cuts off when fault path resistance approaches 100 Ohms. Thus, some discrepancy in resistive blinder performance is revealed. The ABCD earth fault element exhibits good resistive coverage up to its 80.0 Ohm resistive cut off.

Figures 6(b),(c),(d), show the reach point boundary for three cases of differing remote end maximum load. It can be seen that the QUAD exhibits poor performance. Significant under reach is now evident while the ABCD element exhibits good resistive coverage up to its blinder setting. In the worst case figure 6(d) the ABCD element suffers 4% overreach at fault path resistance value 79.0 ohms. For the same fault conditions the QUAD suffers 60% under reach and clearly performs comparatively poorly. In all three cases the SPM performs poorly in terms of resistive coverage as would be expected.

8.2 Long Composite Circuit

Figure 7 shows the resistive coverage trip boundaries but for the longer composite circuit which includes 60km of cable. Again the SPM performs poorly. Figure 7(a) shows the QUAD element overreaching considerably at 180% of the protected section length for an earth fault path resistance of 76.0 Ohms. The ABCD element clearly maintains reach point accuracy for all fault path resistance values up to it's maximum resistive blinder setting.

For the same network but subject to increasing remote end load levels, the ABCD element returns predictable performance, suffering in the worst case an 8% overreach at a 55.0 Ohm fault path resistance(figure 7(d)). The QUAD moves from the overreaching observed on no load to under reaching for a 30MVA remote end load. Here the under reach is approximately 10% of section length, for a fault path resistance close to the cut off setting of 80 Ohms. Attention is drawn to the unpredictable nature of the QUAD elements resistive blinder.

9.0 CONCLUSIONS

A novel approach to the discrimination of zone one high impedance earth faults on composite distribution circuits has been devised. Based on a hyperbolic distributed parameter model of the protected network to its 80% reach point, improved accuracy in reach point discrimination over two existing distance protection earth fault elements has been shown.

The new method accounts for the shunt losses of cable sections and for the more complex zero sequence characteristics of a composite network. Hence, a more accurate representation of the nature of the earth return path is made than would be effected by a traditional quadrilateral characteristic relying on earth fault compensation.

The quadrilateral characteristic which is often regarded as providing improved coverage for high impedance single

phase to earth faults has been shown to be inaccurate when applied to certain composite distribution networks. Depending upon circuit lengths and loading conditions a traditional quadrilateral characteristic has been shown to suffer significant under or over reach.

As would be expected the self polarised mho tripping characteristic has been shown to be completely inaccurate in terms of high impedance earth fault coverage unless modification effecting an opening out along the resistive axis of the impedance plain is applied i.e partial or full cross polarisation.

The new earth fault element described in this work has been shown to exhibit improved accuracy and more predictable performance in discriminating high impedance earth faults.

10.0 FUTURE WORK

Work conducted recently has incorporated the new earth fault element into a transient based software test harness. Tests conducted have shown acceptable operating times in terms of zone one earth fault and phase fault discrimination.

Also development work to modify the approach for accuracy under double end in feed situations has been completed.

A more in depth explanation of the development of a complete software prototype relay including phase elements, transient testing, and its application to systems subject to double end in feed will follow in a future publication.

11.0 REFERENCES

[1] GEC Alsthom Measurements Ltd, 'Protective Relays Application Guide', pp 190-191

[2] Barnes C C, 'Power Cables - Their Design and Installation', London, Chapman and Hall, 1966, pp2-7

[3] Marti L, ' Simulation of Electromagnetic Transients in Underground Cables Using the EMTP', IEE 2nd Int Conf on Advances in Power System Operation and Control, Operation and Management , Dec 1993, Honk Kong, pp 147-152.

[4] Hewett R J *et al*, 'Investigation into Impedance Measurement of Composite Power Distribution Feeders, Using the EMTDC', EMPD98, 3-4 March 1998, Singapore.

[5] Wedepohl LM, ' Application of Matrix Methods to the Solution of Travelling Wave Phenomena in Polyphase Systems', Proc. IEE, 1963,**110**,(2),pp 2200-2212.

[6] Stevenson W D , 'Elements of Power System Analysis', New York, McGraw Hill, pp114-131.

[7] Johns A T *et al*, ' New Technique for the Accurate Location of Earth Faults on Transmission Lines', IEE Proc Pow-Gener,Transm.Distrib.,Vol.142,No.2,pp119-127, March 1995.

[8] Elkateb M M, ' Improving Distance Protection for Underground Cables', Electrical review Vol.202, No.19, pp 43-45 ,19 May 1978.

12.0 APPENDICES

Appendix A1: Table A1

Parameter	Units	Line	Cable
PPS ac Resistance	Ω / km	0.136	0.093
PPS Reactance	Ω / km	0.348	0.099
ZPS ac Resistance	Ω / km	0.475	0.325
ZPS Reactance	Ω / km	1.217	0.346
ChargingCurrent(Ichg)	A/ km/ph	0.063	2.45
Equiv'StarCapacitance	μ F / km	0.011	0.405
Shunt Admittance	μMhos/ km/ph	3.30	127.23

Appendix A2 : Table A2

Parameter	Units	Min	Max
Sending end Bars Fault level	MVA	10.0	1000.0
Remote End Load	MVA	0.0	40.0
Remote End PF Angle	Degrees	-30.0	-
Section 1 Length	km	0.0	100.0
Section 2 Length	km	0.0	100.0
Fault Path Resistance	Ω	0.0	200.0
Fault Location.	%length	10.0	180.0

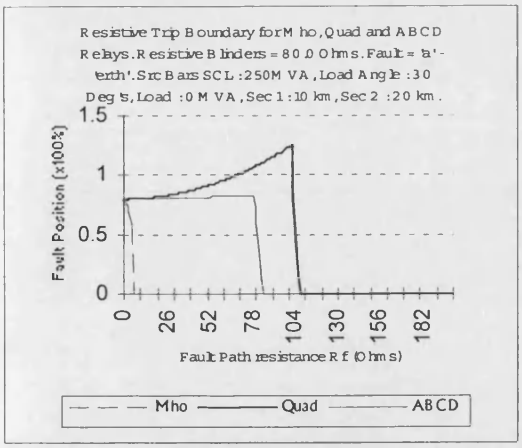

Figure 6(a)

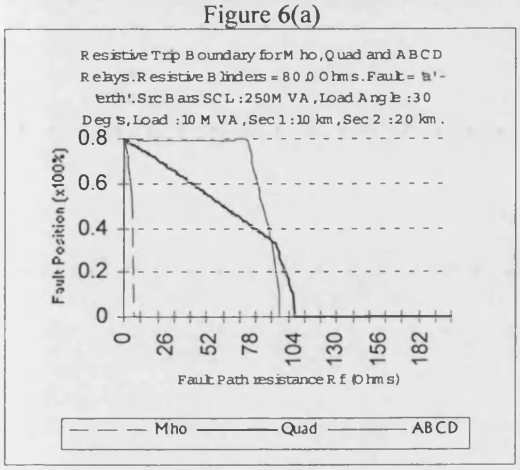

Figure 6(b)

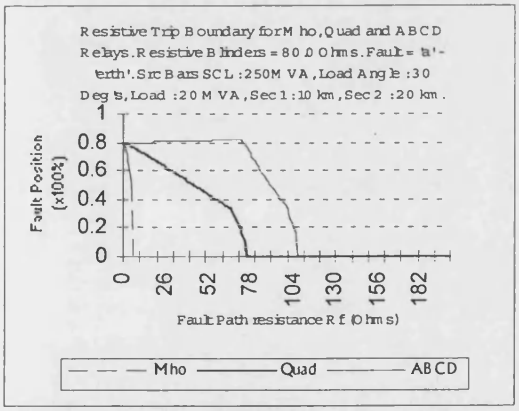

Figure 6(c)

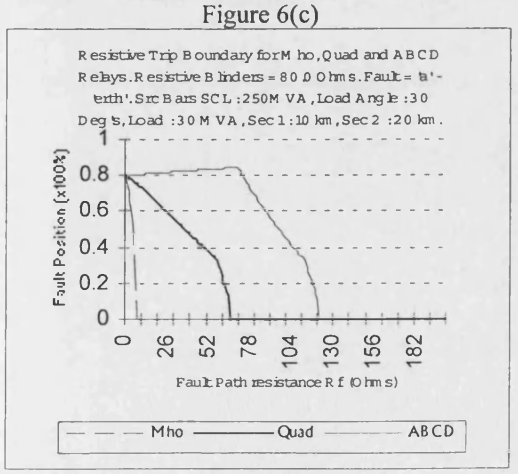

Figure 6(d)

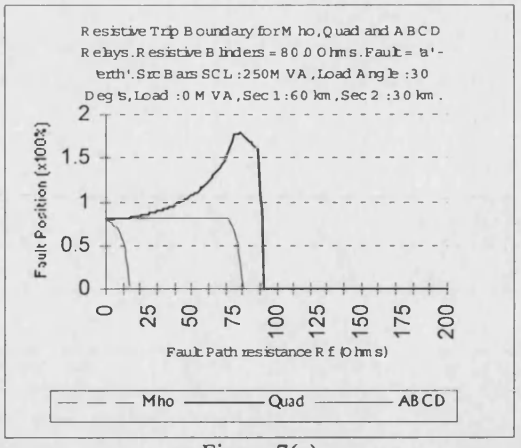

Figure 7(a)

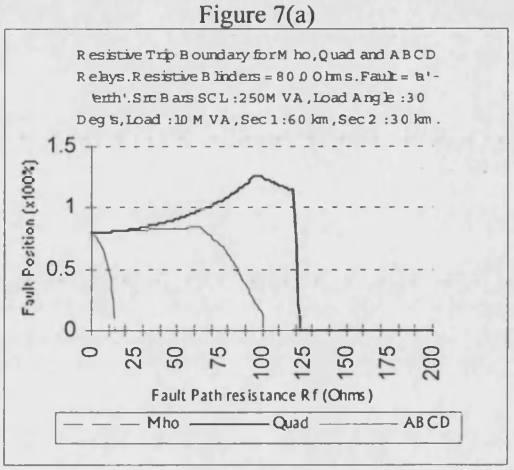

Figure 7(b)

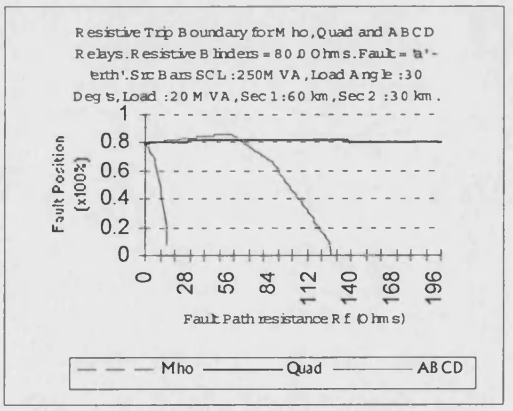

Figure 7(c)

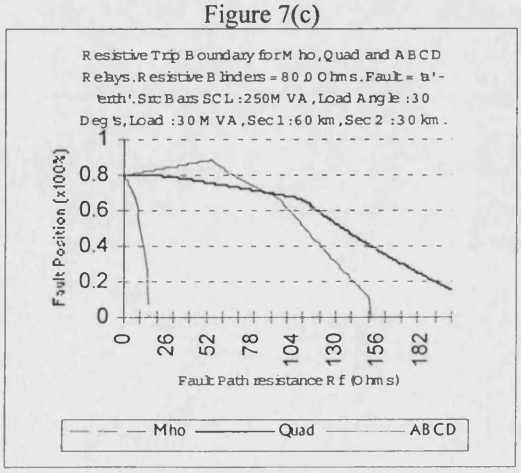

Figure 7(d)